NASA Technical Memorandum 4353

First International Microgravity Laboratory Experiment Descriptions

First Edition

FEBRUARY 1992

NASA

NASA Technical Memorandum 4353

First International Microgravity Laboratory Experiment Descriptions

First Edition

Edited by
Teresa Y. Miller
George C. Marshall Space Flight Center
Marshall Space Flight Center. Alabama

National Aeronautics and
Space Administration

Office of Management

Scientific and Technical
Information Program

1992

FOREWORD

The First International Microgravity Laboratory (IML) is the initial mission in a series of international missions with payloads dedicated to life sciences and microgravity science research. The primary objective of the IML mission is: to conduct science and technology investigations that require the low-gravity environment of space, with emphasis on experiments that study the effects of microgravity on materials and processes and living organisms. The International Microgravity Laboratory is a cooperative effort which involves six space research organizations; The National Aeronautics and Space Administration, NASA; European Space Agency, ESA; Canadian Space Agency, CSA; West German Research and Development Institute for Air and Spacecraft, DLR; French National Center for Space Studies, CNES; and the Japanese National Development Agency, NASDA--and more than 200 scientists from 14 countries.

The management of the IML program is directed by NASA Headquarter's Office of Space Science and Applications with R. Wayne Ritchie serving as Program Manager and Ronald J. White as Program Scientist for the IML-1 mission. The IML-1 mission is managed by the Marshall Space Flight Center, Huntsville, Alabama. Robert McBrayer and Robert Snyder are designated Mission Manager and Mission Scientist, respectively.

IML-1 is currently scheduled for launch from the Kennedy Space Center aboard the Orbiter Discovery. The mission is planned for a duration of 7 days at an orbital altitude of 160 n.mi. and an inclination of 57.5°. Science operations for the mission will be directed from the Payload Operations and Control Center at Marshall Space Flight Center.

The crew complement for IML-1 will consist of seven members; a flight crew composed of the commander, pilot, and a mission specialist, and a payload crew consisting of two mission specialists and two payload specialists. The mission specialists are career astronauts with backgrounds in science and engineering who will perform some aspects of the scientific investigations in addition to their responsibilities for operating specific Spacelab systems. The payload specialists are scientists chosen by NASA based on recommendations from the Investigators Working Group (IWG), the scientists whose experiments comprise the IML-1 payload. One payload specialist will possess expertise in the life sciences; the other payload specialist will have a background in materials science. Where possible crew activities will be scheduled such that critical facets of the scientific investigations can be performed by the crew member most knowledgable in that area.

Currently, the IML-1 payload complement includes 16 major payload elements, 7 life sciences experiments, and 9 materials science investigations, primarily maintained within the Spacelab module as shown in Figures 1 - 4. The protein crystal growth experiments, however, are contained in thermally-stabilized refrigerator/incubator modules housed in the shuttle mid-deck.

Table 1 provides a list of the payload elements categorized by experiment number and discipline, and contains other pertinent information such as the experiment title, experiment acronym, principal investigator, and sponsoring country. Comparable information pertaining to the individual Biorack experiments is contained in Table 2. The Co-Investigators for each experiment are listed in the Appendix to this document.

The life science experiments encompass a diverse group of biological investigations such as human physiology, plant physiology and morphology, reproductive and developmental biology, and cellular secretion, growth, and differentiation. These experiments are designed to evaluate specific effects of the space environment, such as radiation and microgravity, on biological systems. In addition to providing fundamental information necessary to understanding basic biological phenomena, many of these studies will have direct application in improving the health and well-being of astronauts.

The microgravity science experiments are designed to utilize the unique microgravity environment of space for processing materials and for investigating physical phenomena impacted by such gravity-related effects as buoyancy, sedimentation, and convection. The IML-1 microgravity science investigations include crystal growth studies, physical characterization of the Spacelab environment, and critical fluid measurements. These experiments have a wide range of applications in areas such as the pharmaceutical and biotechnology industries, metallurgy, infrared detector technology, and superconductivity, and in providing basic information necessary to understanding specific physical phenomena occurring both on Earth and in space.

In addition to the experiment payload, the IML-1 mission will support two additional payload elements, the IMAX filming of selected space scenes and the Space Acceleration Measurement System (SAMS). Although both of these elements are assigned experiment numbers, because of their nature neither activity possesses a Principal Investigator or is accorded a vote in the Investigators Working Group. The IMAX effort is a collaboration between NASA, the Smithsonian Institution, and the Lockheed Corporation with the specific purpose of documenting significant Spacelab activities and disseminating information concerning these activities and their results. The SAMS payload element was developed to monitor and record accelerations occurring in the Spacelab module in support of the Microgravity Vestibular Investigations (MVI) and Fluids Experiment System (FES) experiments. The data from this system will be used to determine the impact of accelerations on sensitive experiments.

TABLE 1. IML-1 Payload Elements

Discipline	Experiment Number	Title	Acronym	PI Name/Country
Life Sciences	6-IML-1	Gravitational Plant Physiology Facility	GPPF	
		-Gravity Sensor Threshold	GTHRES	Brown/USA
		-Response to Light Stimulation	FOTRAN	Heathcote/USA
	*7-IML-1	Biorack	BR	Brillouet (project scientist)
	8-IML-1	Space Physiology Experiments	SPE	
		-Energy Expenditure in Space Flight	EES	Parsons/Canada
		-Phase Partitioning Experiment	PPE	Brooks/Canada
		-Back Pain in Astronauts	BPA	Wing/Canada
		-Measurement of Venous Compliance	MVC	Thirsk/Canada
		-Positional and Spontaneous Nystagmus	PSN	McClure/Canada
		-Space Adaptation Syndrome Experiments	SASE	Watt/Canada
	10-IML-1	Microgravity Vestibular Investigations	MVI	Reschke/USA
	14-IML-1	Biostack	BSK	Bücker/Germany
	15-IML-1	Mental Workload and Performance Experiment	MWPE	Alexander/USA
	16-IML-1	Radiation Monitoring Container/Device	RMCD	Nagaoka/Japan
Microgravity Science	2-IML-1	Fluids Experiment System Study of Solution Crystal Growth in Low Gravity	FES	Lal/USA
		An Optical Study of Grain Formation		McCay/USA
	3-IML-1	Vapor Crystal Growth Studies of Single Mercury Iodide Crystals	VCGS	van den Berg/USA
	4-IML-1	Mercury Iodide Nucleation and Crystal Growth in Vapor Phase	MICC	Cadoret/France
	5-IML-1	Protein Crystal Growth	PCG	Bugg/USA
	12-IML-1	IMAX Camera	IMAX	
	13-IML-1	Organic Crystal Growth Experiment Facility	OCGP	Kanbayshi/Japan
	17-IML-1	Space Acceleration Measurement System	SAMS	
	18-IML-1	Cryostat	CRY	Littke/Germany Waggoner/Germany McPherson/USA
	19-IML-1	Critical Point Facility	CPF	Beysens/France Michels/The Netherlands Wilkinson/USA

*See Table 2 for Biorack experiment list.

TABLE 2. 7-IML-1 Biorack Experiments List

Experiment Title	Acronym	PI Name/Country
Genetic and Molecular Dosimetry of HZE Radiation	RADIAT	Nelson/USA
Microgravitational Effects on Chromosome Behavior	YEAST	Bruschi/USA
Chondrogenesis in Micromass Cultures of Embryonic Mouse Limb Mesenchymal Cells Exposed to Microgravity	CELLS	Duke/USA
Effect of Microgravity and Mechanical Stimulation on the In Vitro Mineralization and Resorption of Fetal Mouse Long Bones	BONES	Veldhuijzen/The Netherlands
The Role of Gravity in the Establishment of the Dorso-Ventral Axis in the Amphibian Embryo	EGGS	Ubbels/The Netherlands
Effect of Space Environment on the Development and of Aging Drosophilia Melanogaster	FLY	Marco/Spain
Effect of Microgravity Environment on Cell Wall Regeneration, Cell Divisions, Growth, and Differentiation of Plants From Protoplasts	PROTO	Rasmussen/ Denmark
Embryogenesis and Organogenesis of Carausius Morosus Under Space Flight Conditions	MOROSUS	Bücker/Germany
Dosimetric Mapping Inside Biorack	DOSIMTR	Reitz/Germany
Growth and Sporulation in Bacillus Subtilis Under Microgravity	SPORES	Mennigmann/ Germany
Friend Leukemia Virus Transformed Cells Exposed to Microgravity in the Presence of DMSO	FRIEND	Cogoli/Switzerland
Proliferation and Performance of Hybridoma Cells in Microgravity	HYBRID	Cogoli/Switzerland
Dynamic Cell Culture System	CULTURE	Cogoli/Switzerland
Growth, Differentiation and Development of Arabidopsis Thaliana under Microgravity Conditions	SHOOTS	Maher/UK Briarty/UK
Transmission of Gravistimulus in the Statocyte of the Lentil Root	ROOTS	Perbal/France
Gravity Related Behavior of the Acellular Slime Mold Physarum Polycephalum	SLIME	Block/Germany
Studies on Penetration of Antibiotic in Bacterial Cells in Space Conditions	ANTIO	Tixador/France

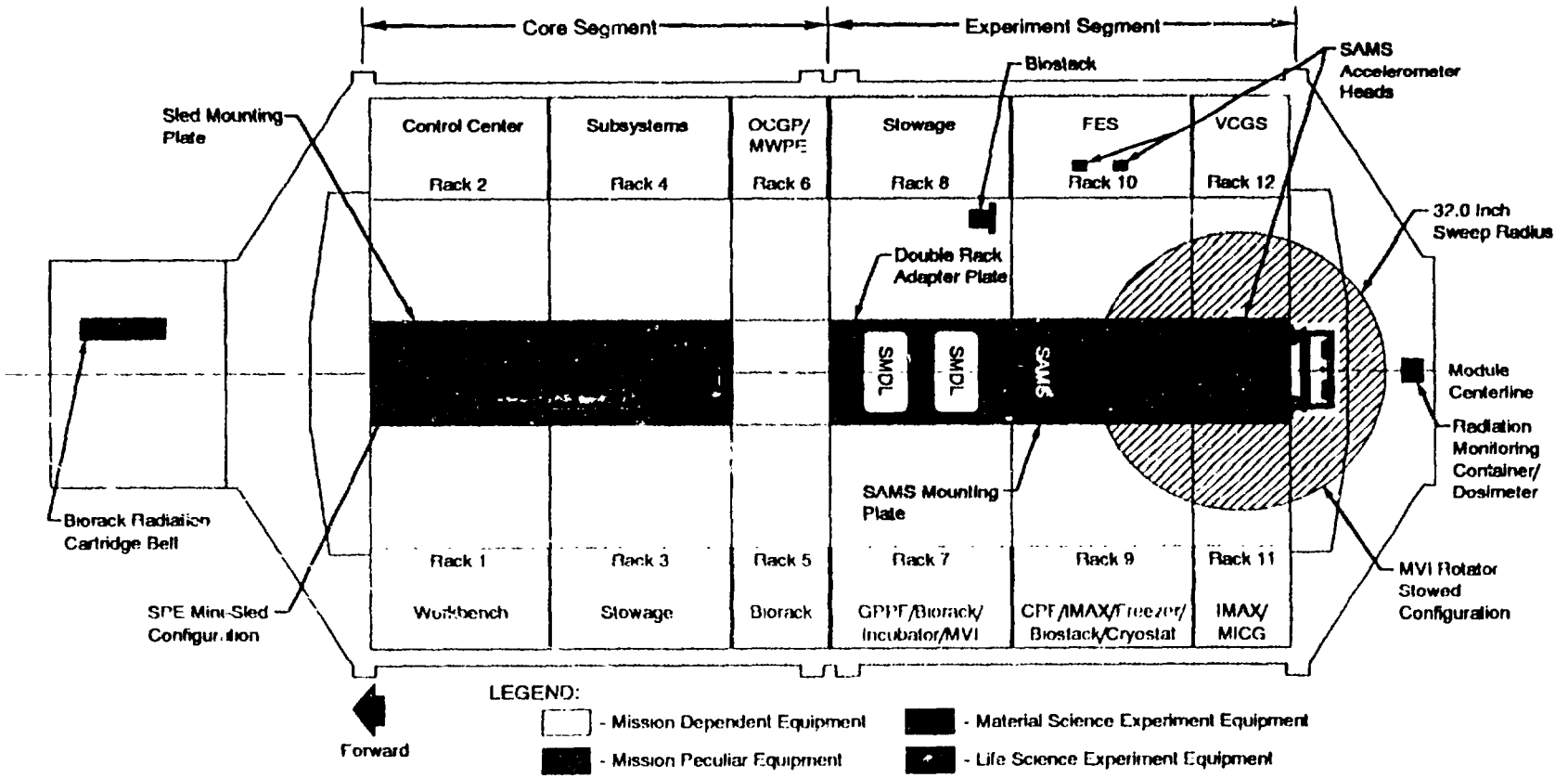

Fig. 1. IML-1 CENTER AISLE CONFIGURATION

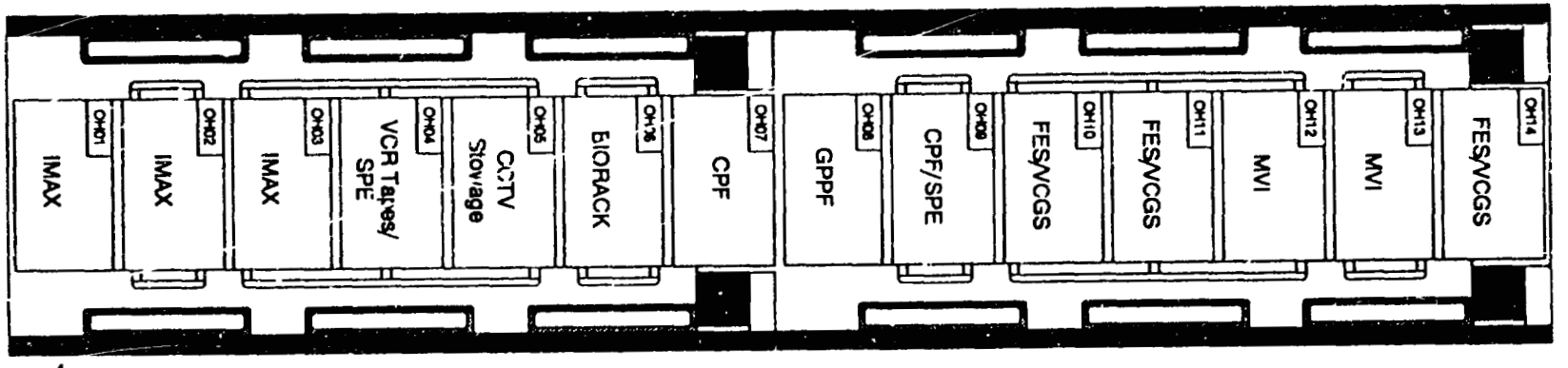

LEGEND:

- Material Science Experiment Equipment
- Life Science Experiment Equipment
- Mission Dependent Equipment

Fig. 2. IML-1 MODULE CONFIGURATION (OVERHEAD)

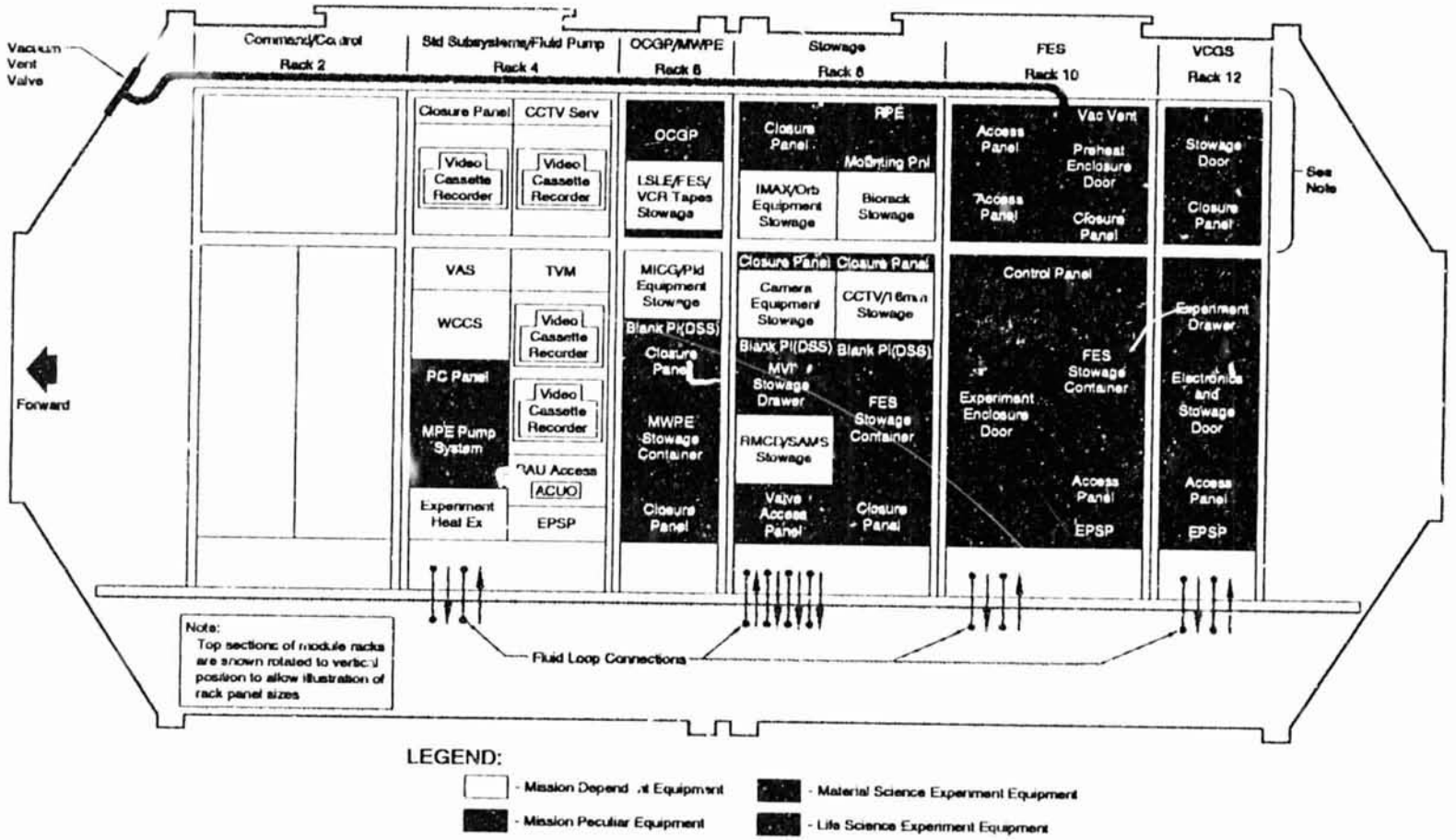

Fig. 3. IML-1 MODULE CONFIGURATION (STARBOARD SIDE)

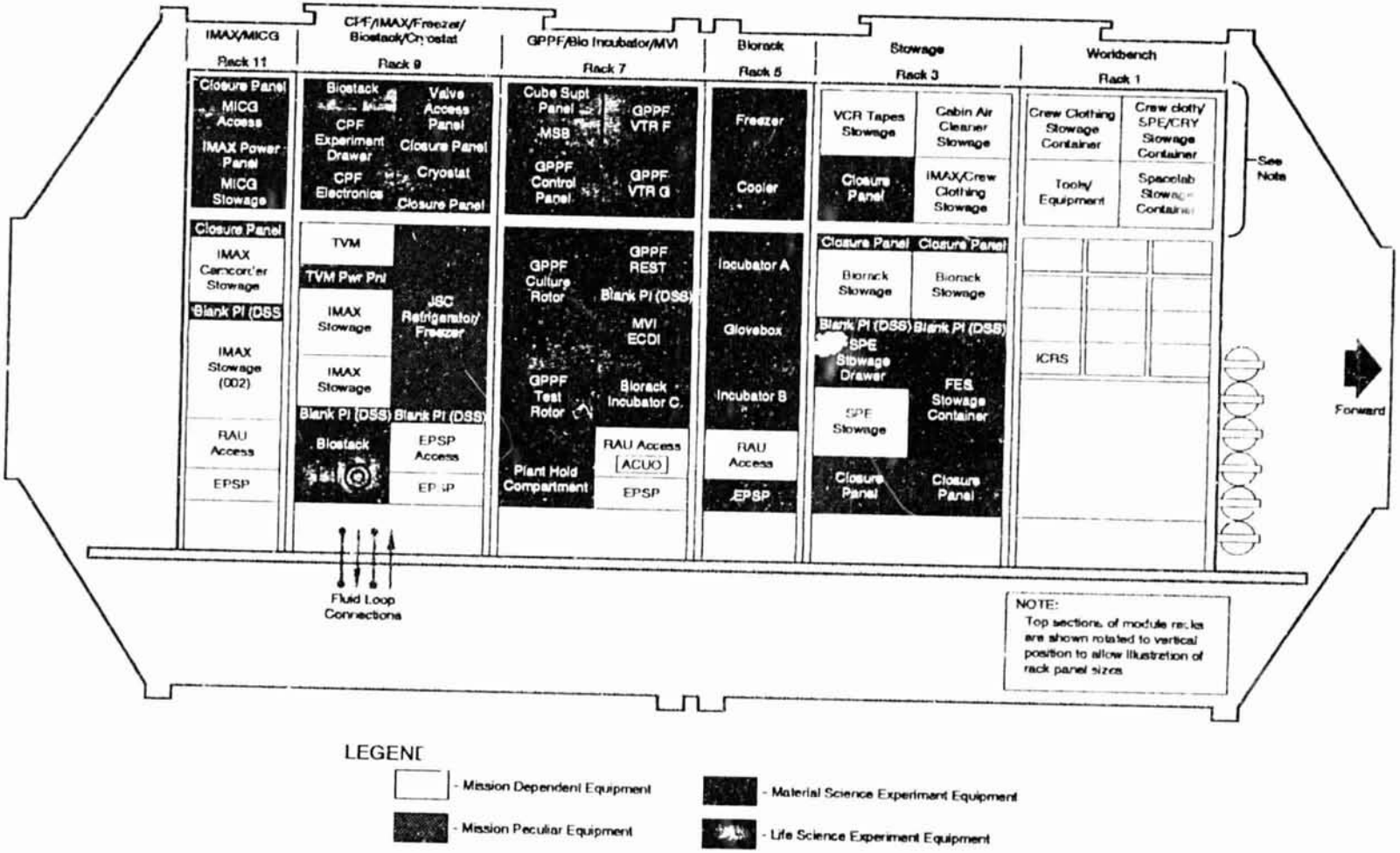

Fig. 4. IML-1 MODULE CONFIGURATION (PORT SIDE)

TABLE OF CONTENTS

TABLE OF CONTENTS (Continued)

TABLE OF CONTENTS (Concluded)

SECTION I

LIFE SCIENCES

N92-23601

GRAVITROPIC RESPONSES OF PLANTS IN THE ABSENCE OF A COMPLICATING G-FORCE (6-IML-1)

Allan H. Brown
University City Science Center
and
University of Pennsylvania
Philadelphia, PA USA

ABSTRACT

On the Earth it is patently impossible to measure any organism's tropistic, physiologic, or morphogenic reactions to environmental stimuli without taking into account our planet's gravitational influence on the time course of the test subject's response. It follows that all published reports of quantitative measurements of such responses must have been contaminated by an additional gravity dependent component which probably was not trivial. Our research effort, here referred to by its NASA acronym, GTHRES, has, as its principal scientific objective, the acquisition of experimental data from tests in a microgravity environment that will address a number of basic questions about plants' gravitropic responses to the perception of transversely applied g forces in the hypogravity range, from essentially zero to unit g. Comparable tests on Earth but in the same flight hardware, referred to the Gravitational Plant Physiology Facility (GPPF), will provide 1 g data for various useful comparisons. Four specific scientific questions will be addressed.

Scientific Background

For approximately a century, responses of plants to the environmental influence of Earth's gravity have been a major area of study by plant physiologists, so much so that, until recently, nearly all authors of textbooks on plant physiology have felt an obligation to retell two stories of cornerstone research in this field: (1) the discovery by late 19th century microscopists of easily sedimentable organelles, usually amyloplasts, in highly localized regions of most (not all) plant shoots and roots, and (2) how the first plant hormone was discovered during that period in which biochemistry in the modern sense was emerging. If these deserve to be called cornerstones, they should be related in some way but, even today, how they are part of the same stimulus/response mechanism is not well understood. The plant does not easily give up the secrets of its living machinery about which physiologists have been learning bit by bit with ever more potent investigative tools. We still have a long way to go. Nevertheless, there are some things we believe we understand well enough to use as a guide to what scientific questions most need answers.

We believe it is important that, in the tips of shoots and roots, there are special cells called statocytes which contain plastids, often about 40% more dense than typical values for

cytoplasm, and also a cytolymph whose viscosity often appears to be lower than average. Accordingly, sedimentation of the plastids, interpreted as passive stratification, may be achieved usually within tens of seconds or a very few minutes. We also find it easy to believe (perhaps only for want of a more attractive concept) that the plant's principal g-sensing organ is this small group of statocytes with their mobile amyloplasts and that the g-detection mechanism begins with the sedimentation of those plastids. Even though there are examples of plants whose cells contain no such starch filled amyloplasts nor any other structures capable of rapid sedimentation, the wide occurrence of "typical" statocytes in higher plants is compelling evidence that they are often--some would like to say always--involved in the process of detection of the g force vector direction. Whether or not the same process serves also to detect the intensity of that g force remains an open question. However, within the past decade, the plant science community has been in the process of restructuring its favorite basic theory of the mechanism of plant gravitropism. Newer experimental and theoretical contributions attribute tropistic bending of plant shoots, after a gravitropic stimulus, chiefly to altered local control of the shoot bending (Firn and Digby, 1977; Trewavas, 1981; Trewavas, 1982); local control resides in the region of maximual organ bending--not exclusively in the shoot tip region. This amounts to a fundamental revision of the classical model of plant gravitropism. It makes the results of GTHRES more relevant and especially more timely.

Gravitational plant physiologists are much less certain about how sedimentation of dense organelles leads to the intricate transduction of gravitational information into some biologically meaningful change in the organ's physical or biochemical machinery. We do not know what accounts for the storage of this environmental information with the plant. Nor do we understand in detail how that initiates a differential growth response that ultimately becomes evident as an adjustment of the growth direction patently appropriate as a gravitropic response.

Even to begin to answer such simple questions requires quantitative knowledge about the patterns of the stimulus/response process in suitable test plant material. For GTHRES we are using Avena sativa, undoubtedly the most popular test species for work in this field. The Avena coleoptile does not have a complete monopoly on the attention of plant gravitational physiologists but it has been the test organ of choice more often than any other for the better part of a century.

As science and technology have brought forth new investigative tools that seem to offer unique advantages for unlocking plants' secrets, these have been applied first to describe better the salient phenomena with improved clarity or precision or in new ways. No doubt this always will be true in principle. In the early exploratory stage of research on a new phenomenon its careful and quantitative description is essential. In studies of a familiar phenomenon by a new method which promises acquisition of a new kind of information the same is true. Whatever may follow must be based on earlier, careful, quantitative, descriptive investigations. Now that space flight has enabled scientists to record the gravitational behavior of plants in the absence of a complicating g force, it has become highly relevant to reexamine most basic plant responses in a satellite's microgravity environment. GTHRES is such a study.

Scientific Questions

The most basic questions relating to how plants detect and exploit gravity usually have been simple. The answers may lead to the construction of and testing of theories that could account for important pieces of that admittedly still baffling puzzle, gravitropism. Some of these basic questions are:

1. What is the plant's threshold of detection of a gravitational (or inertial) force? Some theories about the detection mechanism could be tested by such quantitative information. Also, the simple but very important matter of specifying the maximal g force to be deemed experimentally acceptable in Earth orbiting microgravity laboratories depends on it.

2. What is the plant's sensitivity to increments of g force above threshold? The concept of sensitivity, S, is defined by the ratio of incremental response of the test system to the increment of additional stimulus, in our case g. We need to measure sensitivity throughout a wide range of g forces, beginning, of course, as close as possible to zero g. Is S constant or does it change with increasing g? Is the response linear or is it better modelled by some other mathematical function? The answers will be important for our improved understanding of gravitropism.

3. Over what range does the Reciprocity Rule (g x t = k) hold and why? When Blaauw (1908) determined that a plant's tropistic response to light was related to both intensity and duration of the illumination exposure, he found that the product relationship (intensity x exposure time) for a given measured response was constant when the values for I and t varied in reciprocal manner over several orders of magnitude of either variable. This is now referred to by the shorthand description, I x t Law, Reciprocity Rule, or in other contexts as the Weber-Fechner Law, which states that sensation is a linear function of the logarithm of the stimulus.

Blaauw's student, C. J. Rutten-Pekelharing (1910), examined the comparable relationship between g force intensity (centripetal force) and exposure duration. She found the I x t Law held over a 65-fold range of either variable.

Because there now exists a relatively detailed theory for primary photochemical processes, we can say that one might have predicted that an I x t Law would be obeyed by plants' photic responses, but we have no such detailed theory for plants' gravitropic responses. Their obedience to an analogous g x t Law is not intuitively predictable and the range over which it may apply remains a question for empirical research.

Somewhat comparable data are available from human acceleration studies from which a g x t Law can be described; this hominid version of the plants' Reciprocity Rule holds over about a 10-fold range for man's detection of vertical (Y axis) acceleration (Jones and Young,

1978). There is no obvious theoretical reason why the Law should hold for plants over an even wider g-range or even why it should apply at all.

In its application to plant gravitropism, a valid Reciprocity Rule has a special importance because published data from several laboratories, all using the same grass species, Avena sativa, are not in good agreement or the shortest time the seedlings can be exposed to a transverse, unit g force field and still exhibit a detectable gravitropic response (Johnsson, 1965; Gordon and Shen-Miller, 1966; Shen-Miller et al., 1968; Pickard, 1973; Johnsson and Pickard, 1979). This measure, the minimal application time for a stimulus to elicit a just detectable response, often is referred to as "Presentation Time" (Pt) or "Minimal Presentation Time" (MPT). Generally, MPT is understood to refer specifically to stimulation by a unit g force whether gravitational or inertial (centripetal). However, the disagreement between results from different laboratories almost certainly is related to differences in methodology which implicitly involve assumptions about the wide range of applicability of the Reciprocity Rule and of the necessity to extrapolate plotted data beyond the range of the measured data points.

The above three basic questions, among others, have repeatly been drivers for biophysical research on plant responses to gravity throughout the present century. But all experiments had to be performed against a unit g background of Earth's gravity. To describe the way a plant's g sensing/response mechanisms work, an experimenter really should be able to vary gravity over its full range of biological interest, say from zero to a few g's above unity. Hypogravity ($0 < g < 1$) probably is the most interesting part of the dynamic range and, if it remains inaccessible, the experimenter is in somewhat the same situation as a hypothetical student of photometry who needs to calibrate a light meter but cannot use a dark room.

4. Is the clinostat environment the functional equivalent of space flight with respect to plants' gravitropic responses?

In the absence of any access to true hypogravity, especially zero gravity, plant physiologists have had to settle for simulations of the real thing by rotating their test subjects on clinostats. But only recently has it been possible to compare the performance of plants on clinostats with those in microgravity. Very few such comparisons have been made but the results so far have not been such as to bolster confidence in efficacy of clinostatting as a hypogravity simulation. Plants' responses to microgravity differed from those of plants on clinostats in the case of the leaf epinastic reaction (Brown et al., 1974) and in the case of hypocotyl circumnutation (Brown and Chapman, 1984). Since the validity of the clinostat as a simulator of hypogravity now can be examined on a varity of biological test systems, we can include this fourth question which may be answered by a space test of the clinorotation procedure so widely used for simulating the condition of weightlessness.

Experimental Approach

The GTHRES experiment (Figure 1), now planned for launch on the first International Microgravity Laboratory Mission (IML-1), will address in some measure all four of the

scientific questions explained above. However, principal emphasis will focus on determination of the plants' g force detection threshold, hence the NASA acronym G THRESHold. Avena seedlings will be grown on 1 g centrifuges in Spacelab until they are at the optimal growth stage for responding to a g force in the direction transverse to the coleoptile axis. Up to 18 seedlings at a time will be stimulated by a centripetal g-pulse which will be varied from set to set over a range of both g forces (0.1 - 1.0 g) and pulse durations (2 min - 2 hr) in various combinations. A maximum of 20 g-pulse combinations will be possible. After completion of a given g-pulse the responding plants will be monitored by time lapse video imagery. Tropistic responses will be followed for several hours. The time lapse response data will be stored on video tapes to be analyzed after landing. The plants will be grown, stimulated, and their responses completed in darkness. (The video monitoring radiation will be confined to a very narrow wavelength band centered at 890 nm.)

Flight Hardware

The apparatus, which was delivered to NASA for various kinds of qualification tests in January of 1986, simultaneously supports two quite different experiments. In addition to GTHRES, which is concerned with how oat seedlings respond to various g forces, there is another experiment, labelled FOTRAN (an acronym for phototropic transients), in which sets of wheat seedlings will be illuminated laterally by variable "doses" of blue light and the kinetics of their responses will be recorded by time lapse video cinematography. The data obtained from these stimulus/response episodes of FOTRAN also will be stored on video tapes. There are two tape recorders, one for each experiment, however, both recorders will record data from both experiments, a redundancy that is prudent and comforting. Figure 2 shows the essential features of the GTHRES plus FOTRAN hardware which NASA refers to as GPPF (Gravitational Plant Physiology Facility). Figure 3 shows a diagram of the containers (CUBES) that will house GTHRES seedlings. Cubes can easily be attached to (and detached from) the GTHRES ROTORS (centrifuges) for germination and early seedling growth at 1 g. Also, by repositioning a cube, the vector application of a test g-force can be made to act transverse to the seedling axis thereby delivering quantitatively specific g information to which the seedlings will be seen to react.

Possible Applications for Information to be Derived from the GTHRES Experiment

The scientific motivation for GTHRES is to understand better how plants detect, process, and respond to susception of gravitational or inertial forces. Quantitative descriptions of gravitropic responses to a range of intensities and duration of g stimulations probably are the most basic information our science needs to even begin to speculate on biophysical/biochemical mechanism(s). It seems extremely unlikely that such knowledge will never have important practical applications. But for now such "spin-offs" are quite unpredictable. How long will it take to identify applications? How important will they be? If we know the answers, GTHRES would not be a basic science experiment; it would be better classified as applied science. This does not imply invidious comparison of basic versus applied science. It is to recognize that all applied science depends on past scientific achievements, on

an enormous fund of information from which specific pieces can be selected to guide directed experimentation or development focused on a material goal. GTHRES results will become a unique part of that fund of information--new knowledge gained by a new method.

If asked to speculate, we might suggest one area of applied research or bioengineering where quantitative empirical information that could be derived from GTHRES results possibly will have some application to a NASA program. This relates to growing plants in large habitats: stations in Earth orbit, on journeys to explore Mars or other distant objects in our solar system, or on a lunar base--all being applications where a gravity force other than unit g prevails. If plants are to be used for atmosphere regeneration and/or food production in space habitats at microgravity or at any other g condition much less than unity, information on how plants grow and respond to g stimulations in hypogravic conditions may be relevant for planning culture systems to support space agriculture. Sober judgement may lead to the conclusion that such speculation is outrageous and we agree, however, it might be correct.

References

Blaauw, A. H., 1908: "Onderzoekingen omtrent de betrekking tusschhenlichstarkte en belichtrugstijd bij phototropische krommingen van keimplantjes van Avena sativa," Zittingversag van de K Akad van Wet, Amsterdam.

Brown, A. H., Chapman, D. K., and Liu, S.W.W., 1974: "A comparison of leaf epinasty induced by weightlessness or clinostat rotation," Bioscience **24**, 230-232.

Brown, A. H. and Chapman, D. K., 1984: "A test to verify the Biocompatibility of a method for plant culture in a Microgravity Environment," *Annals of Botany* **54** (Supplement 3), 19-31.

Firn, R. D., and Digby, J., 1977: "The role of the peripheral cell layers in the geotropic curvature of sunflower hypocotyls: a new model of shoot geotropism," Australian J. of Plant Physiol. **4**, 337-347.

Gordon, S. A., and Shen-Miller, J., 1966: "On the thresholds of gravitational force perception by plants," in Life Science and Space Research IV, A. H. Brown and M. Florkin, eds., Spartan Books, Washington, D.C.

Jones, G. M., and Young, L. R., 1978: "Subjective detection of vertical acceleration: a velocity-dependent response?" Acta Otolarngol **85**, 45-53.

Johnsson, A., 1965: "Investigation of the Reciprocity Rule by means of Geotropic and Geoelectric measurements," Physiol. Plantarum **18**, 945-967.

Johnsson, A., and Pickard, B. G., 1979: "The threshold stimulus for geotropism," Physiol. Plant **45**, 315-319.

Pickard, B. G., 1973: "Geotropic response patterns of the Avena coleoptile," Can. J. Bot. **51**, 1023-1027.

Rutten-Pekelharing, C J., 1910: "Untersuchunger uber die Perzeption des Schwerkraftreizes," Rec. Trav. Bot. Neerl. **7**, 241-348.

Shen-Miller, J. et al., 1968: "Thresholds for georesponse to acceleration in gravity-compensated Avena seedlings," Plant Physiol. **43**, 338-344.

Trewavas, A. J., 1981: "How do plant growth substances work?" Plant Cell and Environ. **4**, 203-228.

Trewavas, A. J., 1982: "Growth substance sensitivity: the limiting factor in plant development," Physiol. Plantarum **55**, 60-72.

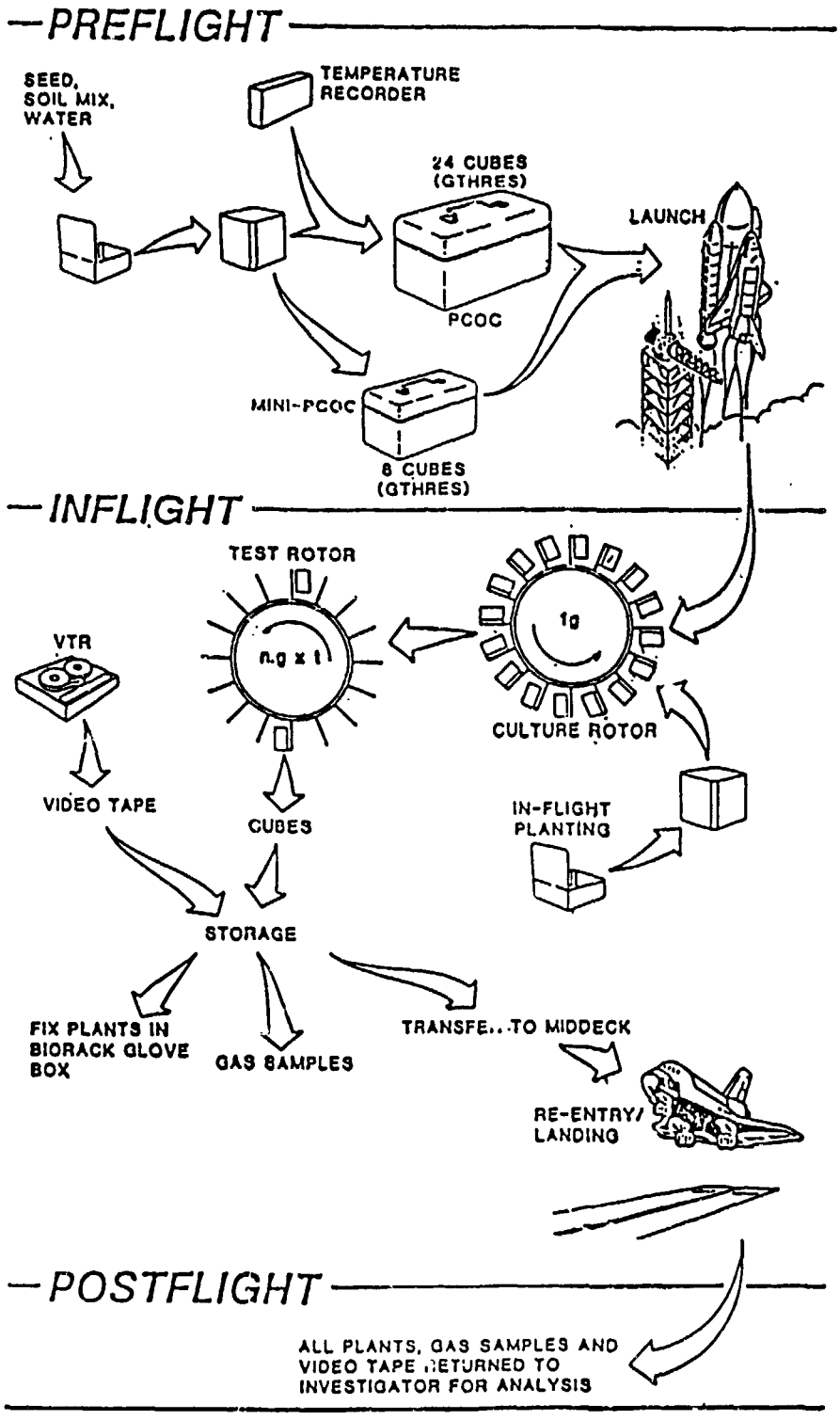

Figure 1. GTHRES Experiment Schematic.

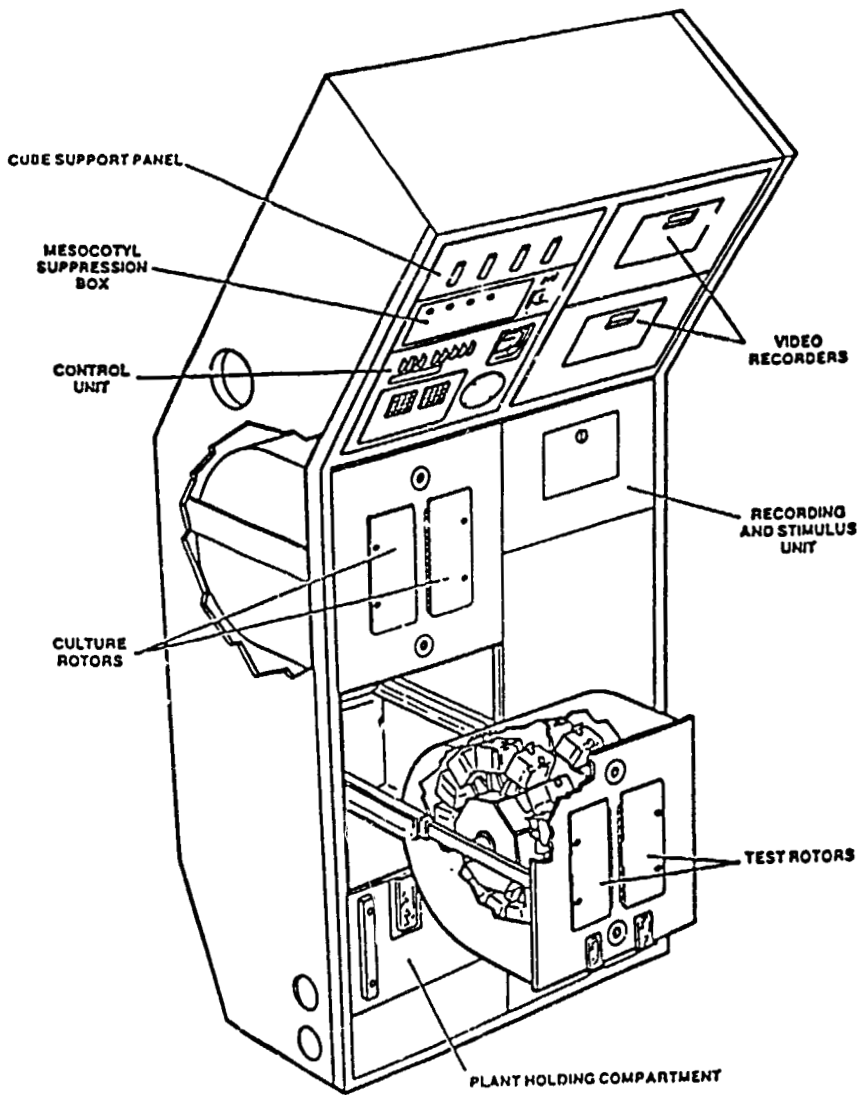

Figure 2. Gravitational Plant Physiology Facility.

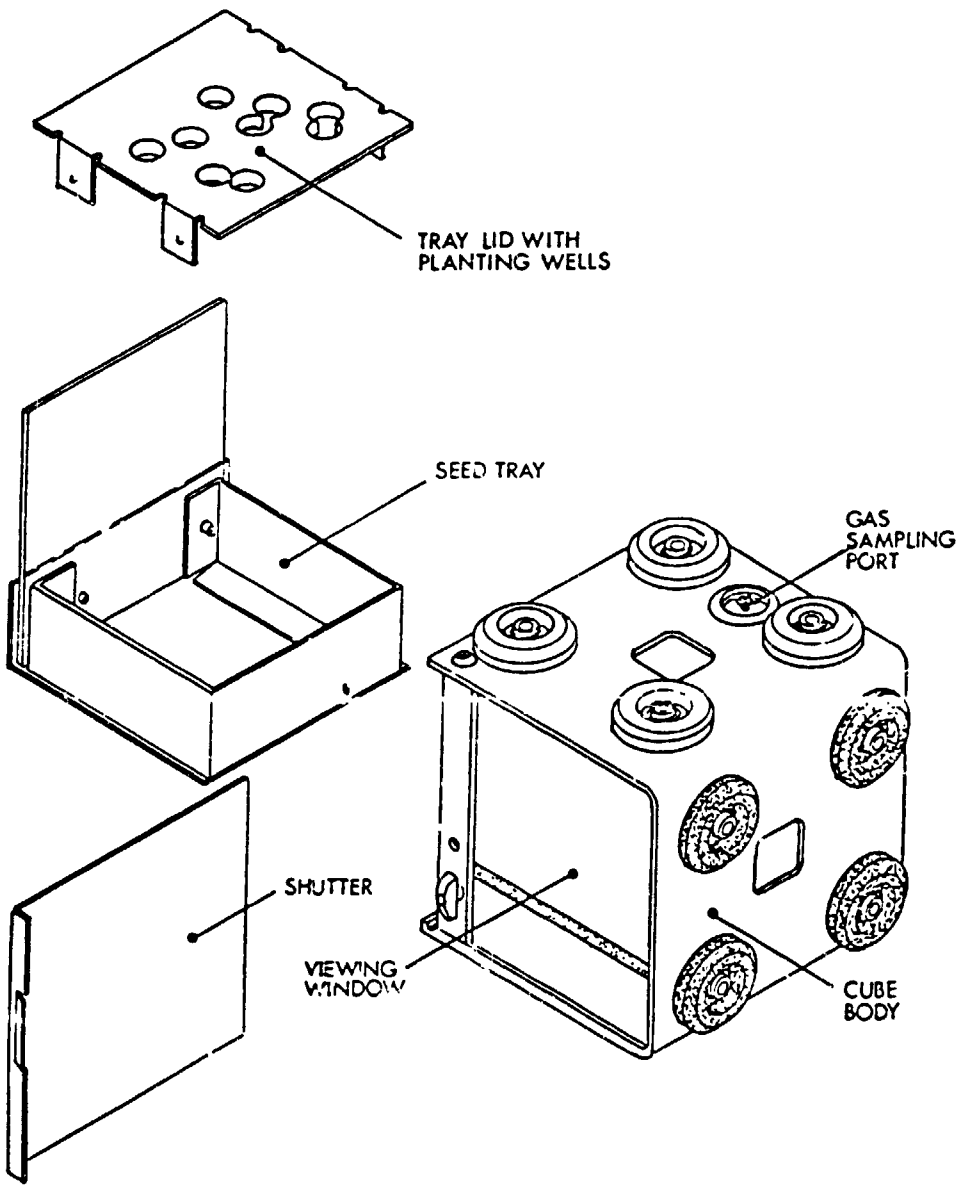

Figure 3. Exploded View of GTHRES Plant Cube.

N92-23602

A SPACEFLIGHT EXPERIMENT TO INVESTIGATE THE EFFECTS OF A RANGE OF UNILATERAL BLUE LIGHT PHOTOTROPIC STIMULATIONS ON THE MOVEMENTS OF WHEAT COLEOPTILES (6-IML-1)

David G. Heathcote
University City Science Center
Philadelphia, PA USA

Introduction

In 1978, in response to an announcement of opportunity by NASA, two independant groups proposed related investigations to study the response of seedling plants to photostimulations at microgravity. The two groups were led by A. H. Brown at the University of Pennsylvania at Philadelphia, and the author, then at University College, Cardiff. Cooperative effort between the two groups led to the development of a spaceflight experiment now known by its NASA acronym, FOTRAN. The purpose of this paper is to outline the scientific objectives behind the experiment and to give a brief description of the spaceflight equipment and the experimental procedures developed to accomplish the aims of the experiment. By reference to the results of ground-based studies the likely scientific returns of the FOTRAN experiment will be assessed.

The experiment is designed to investigate the effects of a range of blue light stimulations on the movements of wheat coleoptiles at zero-g. The seedlings will be dark-grown, and their movements assessed from infrared time-lapse video recordings made during flight. The photostimulus may be expected to modulate circumnutations of the coleoptiles, by synchronizing, initiating or amplifying these rhythmic movements, and to initiate the classic phototropic response.

Circumnutations are rhythmic movements shown by growing plant seedlings, which have been thought to be gravity-dependant by some authors (e.g., Gradmann, 1921; Israelsson and Johnsson, 1967), and autonomous by others (e.g., Darwin and Darwin, 1981; Heathcote, 1977). These rival theories were tested on the first Spacelab flight. The results from this investigation were extremely interesting, showing persistence of circumnutation under low gravity, but with reduced amplitude, and increased frequency (Brown et al., 1988). The SL-1 results were not predicted by either theory, and the FOTRAN experiment will provide the first opportunity to confirm these early findings.

The phototropic response is one of the two major systems found in higher plants which control the direction of growth. As such is of great importance to successful plant development. The other important control is the response of the plant to gravity via the gravitropic mechanism. Whilst it is a simple matter to investigate the gravitropic responses of plants in isolation by working in the dark or using suitable safelights, it is difficult to

investigate phototropic responses free from the influence of gravity. Once a phototropic curvature is initiated, a change in the orientation of the gravity sensing system relative to the gravity vector is an inevitable consequence. This change elicits the gravitropic response mechanism, resulting in an antagonistic curvature, tending to reduce or remove the initial phototropic curvature. The response to a brief, laterally applied light stimulus is therefore a curvature towards the light source, followed by a gravitropic counter-response bringing the plant back towards the original orientation. The position taken by a plant in response to a prolonged lateral light exposure will be some resultant of the opposing light and gravity effects. In dark-grown oat coleoptiles, the phototropic influence predominates (Pickard et al., 1969), whereas in etiolated cress hypocotyls the situation is reversed, with the gravitropic response being more important (Hart and MacDonald, 1981).

The FOTRAN experiment will also provide an opportunity to observe the movements that occur after the development of a phototropic curvature. In many cases of curved plants, a straightening reaction, sometimes known as autotropism, is observed. There have been suggestions - and refutations - that this autotropic reaction is gravity-based. The time lapse records of the seedlings to be obtained during the FOTRAN experiment will be of sufficient duration after the photostimulus to determine if a straightening of the photo-induced curvature does occur at 0 g.

There are two ways in which the influence of gravity on the physiological responses of plants can be nullified; by conducting the experiments at near zero gravity on an orbital space-craft, and by the use of clinostat devices as gravity compensators. The former approach is effective in reducing the mass acceleration forces acting on the plants to about 10^{-4} g, but is expensive, time consuming, and as events involving the loss of the shuttle Challenger have amply demonstrated, subject to unpredictable delays. The clinostat approach, first devised by Sachs (1882), aims to nullify the effect of gravity by compensation, rather than elimination, by utilizing devices in which plants are rotated about a horizontal axis. This rotation produces a situation in which the gravitational force acting on the plant integrated over time sums to zero. The technique is open to criticism (Brown, 1979; Brown et al., 1976). Clinostat rotation has been shown to give rise to developmental artefacts (Zimmermann, 1927; Hoshizaki and Hamner, 1962; Clifford 1979). Root growth, respiration rate and sensitivity to subsequent gravistimulation are all increased in clinostated oat seedlings (Dedolph, 1967). Moreover, in the few studies in which it has been possible to compare the effects of clinostat rotation with those of true microgravity obtained during space-flight experiments, there have been significant differences between plant responses seen on the clinostat and in orbital microgravity (Brown et al., 1974, 1976; Brown 1979; Brown and Chapman, 1984). Interestingly, in some cases, the effects of true microgravity have been intermediate between the responses seen at 1 g and during clinostat simulation. It is clear, therefore, that the clinostat provides only a rough simulation of the effect of true microgravity on the physiology of the plants: there is no substitute for experiments on board orbiting craft in seeking to understand plant responses to low gravity conditions.

The FOTRAN experiment utilizes components of the Gravitational Plant Physiology Facility (GPPF) which enables plants to be grown to a suitable developmental stage under artificial 1 g conditions and allows time lapse video records of plant movements (occurring at microgravity) before and after the application of controlled duration blue light photo-stimulations. Post-flight analysis of the video tape will enable analyses of circumnutation, phototropic and autotropic responses to be made.

By utilizing a range of photostimulus durations, the experiment will undertake an assessment of the dose response relationships of phototropism under orbital low gravity conditions. The complex nature of the relationship between total incident photon flux and the plant curvature that results from the stimulation has been the subject of discussion for many years (see for example, Blaauw and Blaauw-Jansen, 1970; Dennison, 1979; Steyer, 1967). Essentially, rather than observing an increase in the resulting curvature with increasing photon dose up to a saturation level as might be predicted, the large majority of investigators report a dip in the response curve at around 100 $J.m^{-2}$ for a wide variety of plant seedling shoots. In the case of Avena, this dip is manifested as a negative response - a curvature away from the stimulus source, but in the majority of species studied this dip region (often referred to as the System II response) is characterized by lesser magnitudes of positive response than shown at lower (System I) or higher (System III) doses. A full discussion of the complexities of the phototropic response curve is out of place here, but the FOTRAN experiment will utilize stimulus doses that cover the range between the System I curvature region (equivalent to a stimulus duration of 3 seconds to the equipment's photostimulus source) and the system III region produced by just over 30 minutes exposure. Thus the experiment will explore the effects of zero-gravity exposure over a representative portion of the effective phototropic dose range.

Materials and Methods

Plant Material and Experiment Protocol. In phototropic research, the Avena coleoptile system has become well-established. However, this seedling requires red-light pre-treatment to suppress the development of the mesocotyl, which otherwise interferes with measurements of curvature, etc. The provision of red light suppression is likely to be complicated within the time and other constraints of the space flight experiment. It was therefore decided to use wheat seedlings, in which the mesocotyl is genetically suppressed to avoid this difficulty. Seed of Triticum aestivum cv Broom are obtained periodically from Nickersons (RPF) Ltd., Rothwell, Lincolnshire, U.K. and stored at 8 °C until used. The seed is screened for obvious defects and seeds weighing between 30.1 and 40.0 mg selected for use. For the flight experiment, four batches of four growth containers holding six seeds each will be planted on the ground before the flight, and it is planned that a further batch of four containers will be planted in flight. The planting protocol for the ground batches is described below; in flight planting is modified as appropriate.

Samples of selected seeds are surface sterilized by immersion in a 2% solution of sodium hypochlorite for 2 minutes and then rinsed in running tap water before air drying under

a laminar flow hood. A commercial soil mix (Promix 50% peat, 50% vermiculite) at a relative water content of 150% of the soil mix dry weight is packed into the seed trays, and the tray lids fitted. Using a dibble, the seeds are positioned in the wells in the seed tray covers to orient the seed so that the emerging coleoptile is centrally placed in each well, and that the long axis of the eliptical cross section of the developing coleoptile is orientated at right angles to the direction of the photostimulus beam. Thus the resulting phototropic curvature will occur in a plane at right angles to the plane of the two vascular strands. This orientation is optimal for phototropic curvature (Pickard et al., 1969). The seeds are covered with soil mix, with the seed lying just below the surface. The seed trays are positioned in the growth containers ("cubes", described below), the shutters fitted, and the assembled containers placed in an incubator maintained at 22.5 ± 1 °C to allow germination to proceed until some 15 hours before launch. At this time, the 16 planted cubes, together with planted cubes for the GTHRES experiment, are transferred to a plant carry-on container (PCOC) in which they are transported to the shuttle, and stowed in a middeck stowage locker. The vertical orientation of the developing seeds will be carefully maintained during this transfer, and the orientation of the PCOC within the locker is also arranged such that the launch g forces will also act in the normal, "soil down" direction.

On orbit, after the activation of the Spacelab systems, the crew will transfer the seedling containers (in the PCOC) into Spacelab and transfer each cube into a GPPF unit (the culture rotor - described below) where they are maintained at a constant temperature (22.5 °C) and an artificial 1 g centrifugal field until 75 hours after imbibition. At this stage each batch of seed (in their light-tight cubes) are transferred by the crew to the GPPF REST unit (see below). In this unit, the coleoptiles are recorded on time lapse video using physiologically inactive IR illumination for a 5 hour period and then subjected to photostimulations of predetermined duration under the control of the GPPL control unit microprocessor. The seedlings are recorded on video tape for a further 7 hours. At the end of this period, the seedlings in the REST are replaced by a fresh 75-hour old batch from the culture rotor, and the experiment sequence repeated. The seedlings that were removed from the REST are transferred to the Biorack Glove Box where gas samples from the cube interiors are taken for later analysis and a sample of the coleoptiles are chemically fixed. The experimental sequence is repeated for a total of five batches of four cubes, each cube receiving an independantly controlled photostimulus. Thus a total of 20 different photostimulus doses (including zero dose) can be programmed into the experiment. The photostimuli are of constant intensity and programmed duration; light doses ranging from 0.34 $J.m^{-2}$ (1.15 $umol.m^{-2}$) to 113.9 $J.m^{-2}$ (380 $umol.m^{-2}$) will be given. The stimulus doses will be achieved by varying the duration of exposure from 3 to 999 s at a constant intensity of 0.114 $W.m^{-2}$ (0.38 $umol.m^{-2}.s^{-1}$) and occur at a seedling age of 80 hours after imbibition. In practice, a replication scheme will be used which will ensure the optimal coverage of regions of interest in the dose response curve.

Some limited video downlink for the data has been negotiated with the mission managers during the early part of the flight experiment. This data will be analyzed in near real time on the ground to enable us to fine tune the stimuli given later in the mission if this seems desirable. An outline schematic of the experiment flow is shown in Figure 1.

GPPF Hardware

The Gravitational Plant Physiology Facility is a collection of interconnected and interdependant units which occupy the major portion of a Spacelab double rack. The equipment layout is shown in Figure 2 which identifies the major components.

GPPF was developed for NASA Ames Research Center at the University of Pennsylvania and the University City Science Center, Philadelphia. The items required by the FOTRAN experiment are detailed below.

Control Unit. The control unit regulates all GPPF hardware functions. It contains the switches and circuit breakers for all other components and houses a microprocessor and associated I/O boards which together control the automatic sequencing of major parts of the experiment protocol, and measures and regulates temperature, motor speeds and the photostimulus durations required by the experiment. The control panel is fitted with a keypad, a 24 character display and a small video monitor which are used by the crew to interact with the experiment. In addition the unit controls timelapse video recording operations, activating video cameras, recorders, and video switches and resolving conflicts between the needs of the two GPPL experiments. It organizes data from the variety of sensors present in each unit into a data stream which is patched into the Spacelab data stream for down-linking to the ground. This data enables the functioning of the hardware to be monitored on the ground. In addition to experimental and environmental data, information is available on individual key and switch depressions, door openings, etc. to enable the experiment team on the ground to monitor the crew activities associated with the experiment.

Plant Growth Containers (Cubes). Each growth container (Figure 3) consists of a black anodized aluminum body 70 x 65 x 65 mm fitted with two acrylic plastic viewing windows on opposite faces. These windows are made from an infrared pass filter material (pass > 800 nm) and are completely light-tight to wavelengths that are physiologically active, and thus can be handled in normal lighting conditions. In the flight experiment infrared sensitive video cameras will be used for data recording. A seed tray (50 x 55 x 20 mm) fabricated from anodized aluminum fits into this body. A seed tray lid, also of anodized aluminum, completely encloses the soil mix except for six planting wells of 8 mm diameter. The planting wells are positioned to ensure that seedlings do not coincide on the photographic image, and do not shade each other from the stimulus light source. To the front face of the seed tray is fitted a clear acrylic window that forms the sixth face of the cubical assembly and allows entry of the photostimulus light beam. During the early growth of the seedlings, this window is covered by an anodized black aluminum shutter. A gas sampling septum, used to monitor the atmosphere within the container, is fitted to the main body. The complete assembly is not gas-tight, but diffusive gas exchange is restricted, which might lead to physiologically-significant accumulations of ethylene within the container.

Culture Rotor. The two culture rotors are small centrifuge devices which can hold eight cubes each. They are controlled to provide 1 g force at the level of the tray lids (soil surface). The centrifuge radius is 220 mm at this point. The rotor housing is temperature controlled to 22.5 °C. Cubes are placed on the rotors during the early stages of growth in orbit to provide an environment in which normal development can be orientated by the g vector to ensure that the coleoptiles will be in a suitable position for recording and photostimulating.

Recording and Stimulus Chamber (REST). The REST is the key GPPF component for the FOTRAN experiment. In this compartment (Figure 4) four plant containers can be attached to four independently-controlled light sources which provide the blue-light photostimuli. The containers are positioned between an infrared back light source (mounted in the REST compartment door) and an infrared-sensitive video camera. The camera takes images of the coleoptiles as shadowgraphs through the cubes' IR filter windows at 10 minute intervals throughout the activation of the REST unit. The cube shutters are removed only after the cubes are fully inserted into the REST unit; plush fabric seals prevent stray light leaks from entering the cubes and causing unintentional photostimulations. The REST light sources are shown in Figure 5. A Tungsten-filament bulb with a compact filament configuration which approximates a point source (type L2110, 4V, 1.1 Amp; Gilway Technical Lamp Co., Woburn, MA., U.S.A.) is situated, with the filament normal to the optical axis, at the focus of an acrylic fresnel lens (Lectric Lites Co., Fort Worth, TX, type no. 15, 80 mm focal length) to provide a collimated beam at the photostimulus window of the seedling container. Between the bulb and the lens is positioned a two-element filter, consisting of a clear lexan (polycarbonate) disc and a blue glass filter type 5433 (Corning, NY) which restricts the wavelength of the stimulus light to a band between 400 and 525 nm. The lexan filter element is included as a safety feature required for the flight hardware and also improves the cutoff below 400 nm. Within the cone of light passing the filter elements, but outside the beam reaching the plants, is a photoresistive sensor which is used to monitor the bulb output during a photostimulus. The output of the stimulus sources is 0.114 $W.m^{-2}$, 0.38 $umol.m^{-2}$, s^{-1}, measured on the optical axis at the plant position (using a type LI-188B Integrating Quantum/Radiometer/Photometer and sensor heads type LI-190SEB and LI-190SB; Li-Cor, Lincoln, NE). The spectral distribution of the source is as shown in Figure 6, obtained using an Isco type SR spectroradiometer (Instrumentation Specialties Co., Lincoln, NE). The emission corresponds closely with the known visible light action spectra for grass coleoptile phototropism (e.g., Thimann and Curry, 1960).

Plant Holding Compartment. This unit is a temperature controlled drawer, which is used for temporary storage of plant cubes, gas sampling syringes, etc.

Ground-Based Results. Two major studies have been undertaken using the FOTRAN experiment protocols and plant material. One of these (Heathcote and Bircher, 1987) used a purpose built clinostat holding replicas of relevent portions of the GPPF REST hardware to simulate microgravity conditions. One g data were also collected using the same apparatus with the clinostat axis in a vertical orientation, both rotational (to replicate clinostat vibrations, which might produce artefactual results) and in a non-rotating mode. In the other study, the "Investigator Ground Studies" (IGS), the experiments were conducted in the actual flight

hardware at Ames Research Center. In this case, only 1 g data were collected, since simulating low gravity is impractical with the rack mounted FORTAN experiment.

Data from these two sources are combined in Figure 7. In all cases, the phototropic response is quantified as the angular response 100 minutes after the onset of stimulation. In Figure 8, the time course of five individual coleoptiles responding to a 3 second photostimulus during IGS is shown.

Discussion. The Investigator Ground Studies provided an opportunity to test out, under realistic conditions, the operation of the flight hardware, and to assess the quality of the data to be expected from the experiment. Experience was gained both in the operation of the equipment and in the techniques for data reduction required to handle the large quantity of raw data produced by the FOTRAN operations. The individual plant responses, as exemplified by the data given in Figure 8, give confidence that the response patterns of growing coleoptiles are not significantly affected by the environment provided by the flight hardware, at least at 1 g. The data are of sufficient quality that confident assessment of the responses of individual plants in terms of phototropism and circumnutation can be made. The differences between the 1 g data collected on the clinostat and the flight hardware (during IGS) are statistically insignificant, whereas the data obtained during gravity compensation on the horizontally-rotating clinostat show highly significant deviations from 1 g behavior (Figure 7). This demonstrates the adequacy of the measurement precision and the replication levels determined for the FOTRAN flight experiment, and gives a high level of confidence in the ability of the FOTRAN hardware and experimental protocol to provide the desired scientific returns.

Despite the much delayed launch of the FOTRAN experiment, the scientific questions posed remain relevant, and a successful flight of GPPF and FOTRAN on IML-1 is eagerly awaited.

References

Brown, A. H.: 1979, The Physiologist **22**, Suppl., S15-18.
Brown, A. H., and Chapman, D. K.: 1984, Science **225** 230-232.
Brown, A. H., and Chapman, D. K.: 1988, in press.
Brown, A. H., Chapman, D.,K., and Lui, S.W.W.: 1974, Bioscience **24**, 518-520.
Brown, A. H., Dahl, A. O., and Chapman, D. K.: 1976, Plant Physiol. **58**, 127-130.
Blaauw, O. H., and Blaauw-Jansen, G.: 1970, Acta Bot. Neerl. **19**, 755-763.
Clifford, P. E.: 1979, Z. Pflanzenphysiol. **95**, 465-469.
Darwin, C., and Darwin, F.: 1981, The Power of Movement in Plants.
Dedolph, R.R.: 1967, In: COSPAR Life Sciences Space Research **5**, 217-228.
Dennison, D. S.: 1979, Encyclopedia of Plant Physiology, NS **7**, 506-566.
Gradmann, H.: 1921, Jb. Wiss. Bot. **60**, 97-201.
Heathcote, D.: 1977, Life Sciences Research in Space, ESA SP-130, pp. 195-201.
Heathcote, D., and Bircher, B. W.: 1987, Planta **170**, 249-256.
Hoshizaki, T., and Hamner, K. C.: 1962, Plant Physiol. **37**, 453-459.
Israelsson, D., and Johnsson, A.: 1967, Physiol. Plant **20**, 957-976.
Pickard, B. G., Dutson, K., Harrison, V., and Donegan, E.: 1969, Planta **88**, 1-33.
Sachs, J.: 1882, Arb. Bot. Inst. Wurzburg **2**, 209-225.
Steyer, B.: 1967, Planta **77**, 277-286.
Thimann, K. V., and Curry, G. M.: 1960, In: Comparative Biochemistry: A Comparative Treatise, Vol. 1, Sources of Free Energy, Florkin, M. and Mason, H. S. (eds.), pp. 243-309, New York, Academic Press.
Zimmermann, W.: 1927, Jarb. Wiss. Bot. **66**, 631-677.

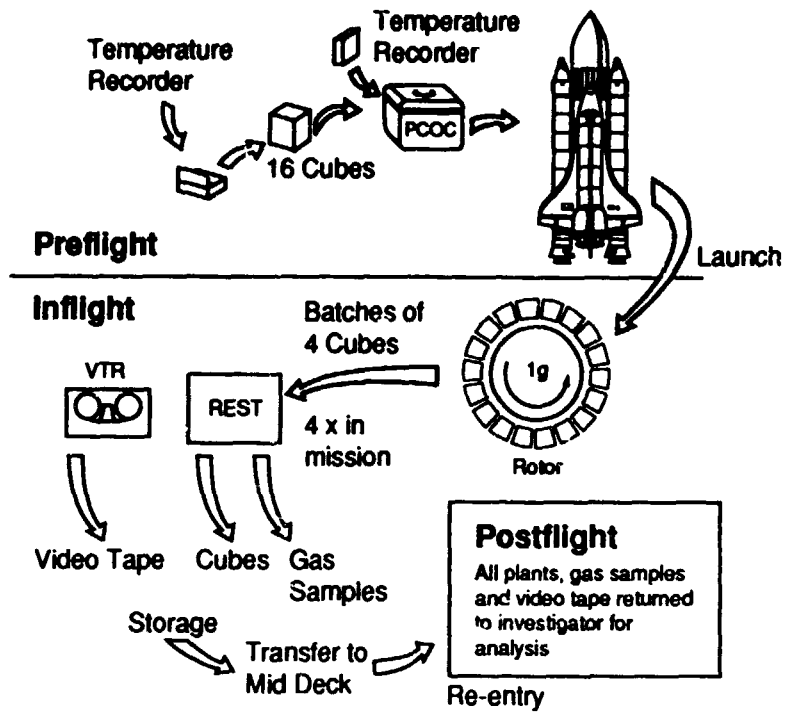

Figure 1. A schematic of the FOTRAN experiment flow. Note that the inflight planting of a fifth set of four cubes is not included.

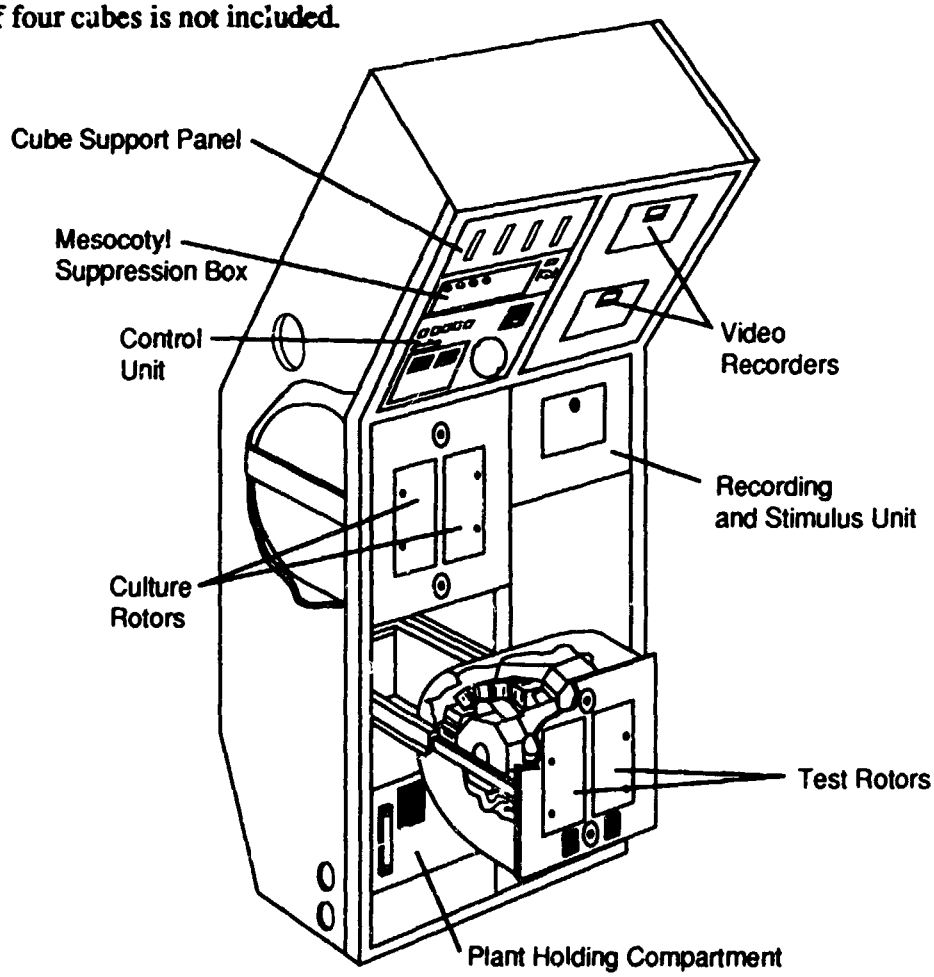

Figure 2. The layout of the Gravitational Plant Physiology Facility in a Spacelab double rack.

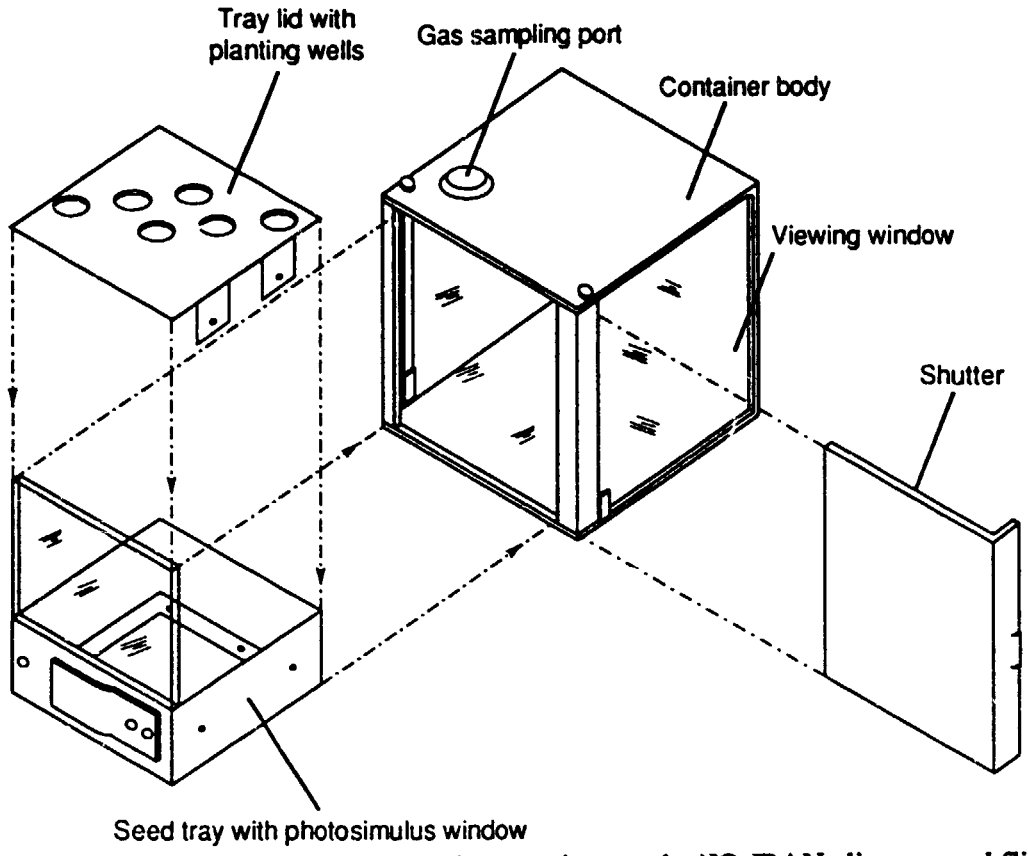

Figure 3. Dose/response curves for wheat phototropism on the FOTRAN clinostat and flight hardware.

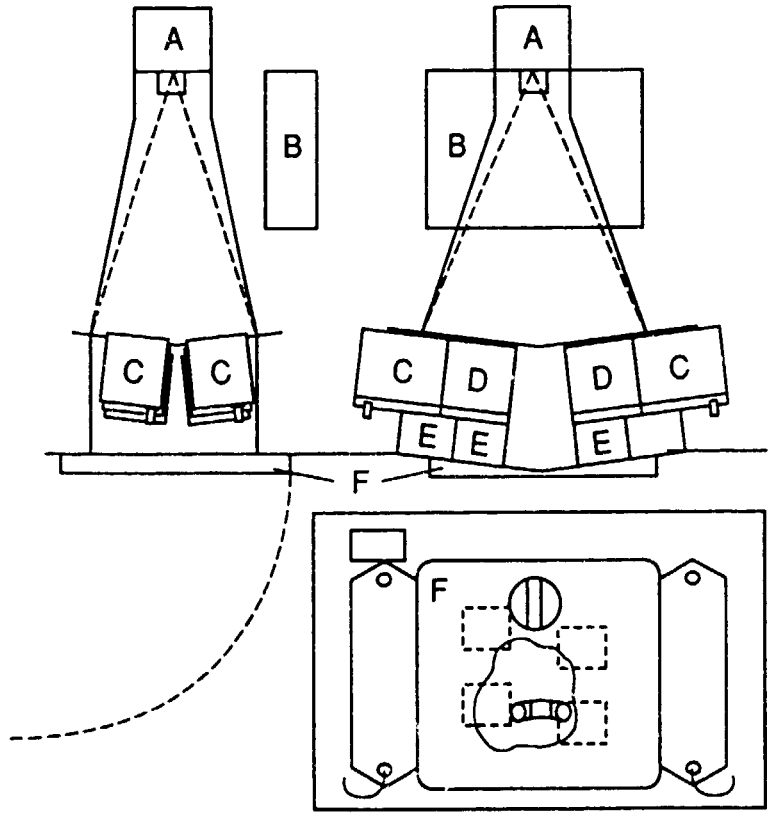

Figure 4. Schematic of the REST unit showing A, IR sensitive camera; B, camera electronics; C, stimulus source; D, plant container; E, IR back-light source; F, unit door.

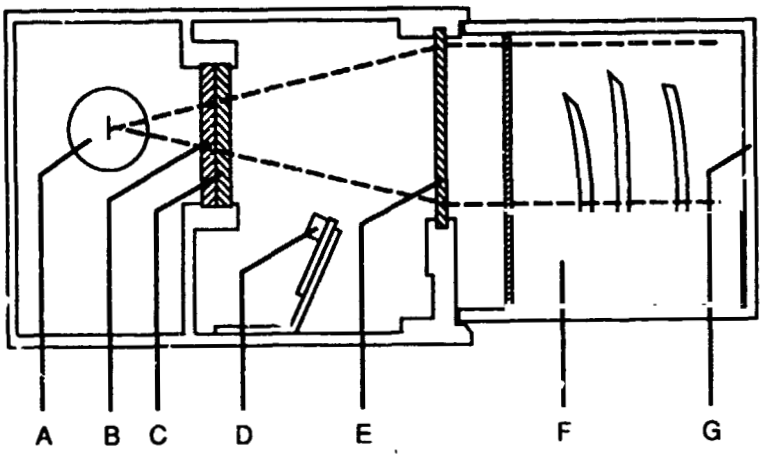

Figure 5. Section through the stimulus light source with growth container in position. A, Tungsten-filament bulb; B, lexan filter element; C, Corning blue glass filter, type 5433; D, photoresistor; E, Fresnel lens; F, seed tray with photostimulus window; G, growth-container body.

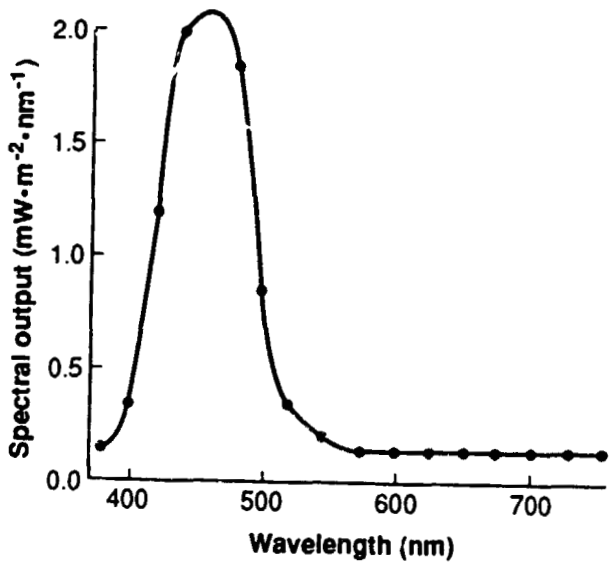

Figure 6. Spectral distribution of the light output of the stimulus light sources. The curve is fitted using a quasi-cubic splines technique.

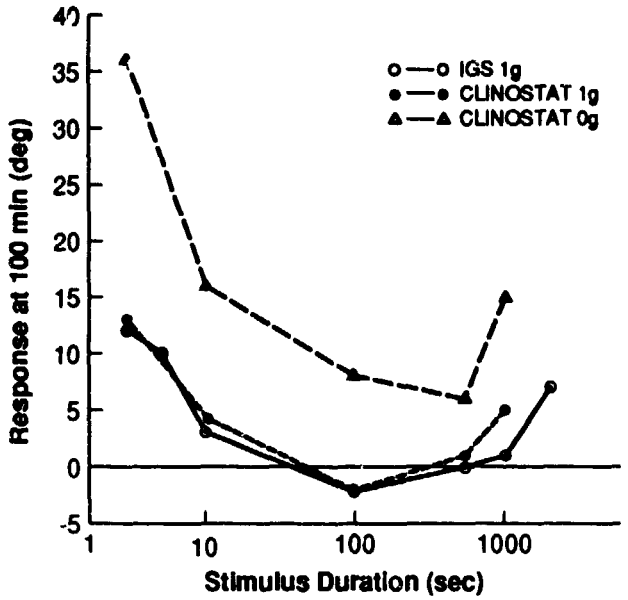

Figure 7. Dose/response curves for wheat phototropism on the FOTRAN clinostat and flight hardware.

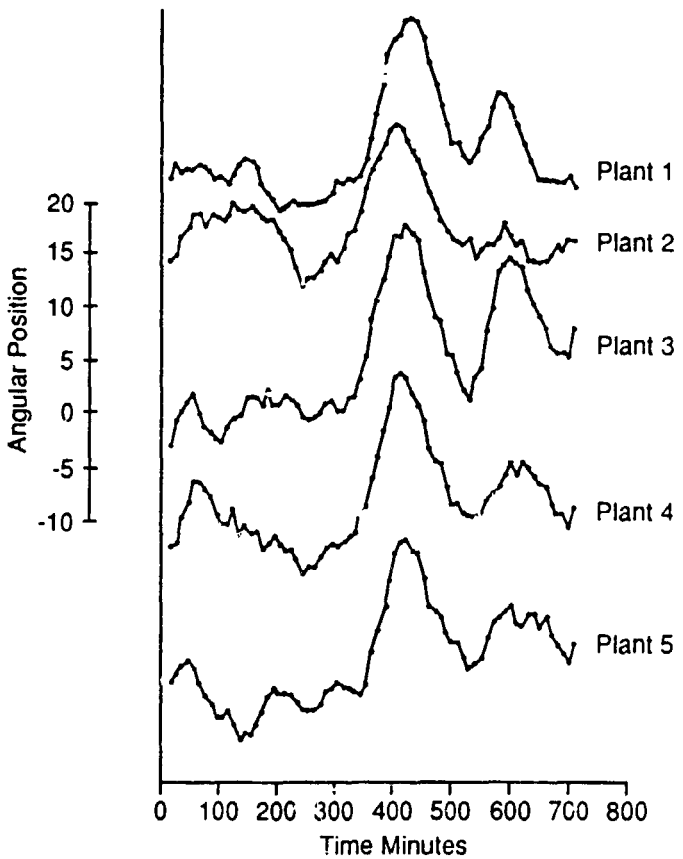

Figure 8. The individual time courses of the movements and phototropic response of five coleoptiles exposed to 3 sec photostimuli at 300 minutes.

N92-23603

GENETIC AND MOLECULAR DOSIMETRY OF HZE RADIATION (7-IML-1)

Gregory A. Nelson
Jet Propulsion Laboratory
Pasadena, CA USA

The Space Radiation Environment

Astronauts are routinely exposed to radiation at levels which exceed those experienced on the ground. These exposures may place them at higher risk for certain biological lesions such as cataracts, mutations, and cancers. The space radiation environment is extremely complex. It varies substantially both spatially and temporally. The radiation is a mixed field of UV, X-ray, and gamma ray photons, electrons, protons, neutrons, and atomic nuclei (cosmic rays or HZE particles). The sources of these species are the Sun and various galactic sources and these species are degraded or modified by spacecraft shielding to present a mixed field to targets inside. Trapped radiation belts of protons, electrons, and HZE particles also encircle the Earth and reach low altitudes over the South Atlantic Ocean. The radiation present in space is delivered at a relatively low dose rate, a feature which is known to alter the magnitude of effects. Finally, recent results from the D1 Spacelab mission indicate that a synergistic interaction of microgravity and radiation occurs in larvae of [illegible]. All of these features combine to make understanding the space radiation environment's biological effects a complex problem which needs solution in order to guarantee the health and safety of spaceflight crews and passengers.

Objectives

The objectives of the current study are to determine the kinetics of production and to characterize the unique aspects of genetic and developmental lesion induced in animal cells by radiation present in the space environment. Special attention is given to heavy charged particles. The organism Caenorhabditis elegans, a simple nematode, is used as a model system for a coordinated set of ground-based and flight experiments.

C. elegans as a Model System

C. elegans is a small, free-living soil nematode which reproduces as a self-fertilizing hermaphrodite or by mating with males. It is a small, transparent animal of maximum size 1 mm which feeds on E. coli bacteria in the laboratory. Figure 1 illustrates adult hermaphrodites as seen by bright field microscopy. Although small, it possesses all of the major organ systems and tissues found in other animals including mammals. Its transparency has allowed developmental studies on individual cells and it is one of two animals (the other a near relative) for which the entire cell lineage from fertilized egg to adult has been described. C. elegans has precisely 1031 somatic cells as an adult and 546 cells as a newly hatched larva. The location,

origin, identity and (at least broadly) the function of each cell has now been described. For heavy ion radiobiology experiments the discrete cell number means that experiments may be conducted on precise cellular in vivo. The development of certain adult structures from individual larval cells provides an amplification mechanism for detecting radiation damage. Since development is mosaic in C. elegans each cell develops independently of its neighbors.

The life cycle of C. elegans is short. Three days after fertilization an animal begins to lay its own eggs, up to 300 per individual. This life span is highly temperature dependent with a maximum fertile temperature (chronic exposure) of 26° and a lower survival limit of about 2 °C . The optimum growth rate and fertility is obtained at 20 - 22 °C. A reversible arrest in development occurs upon lowering animals to temperatures between 2 and 12 °C. C. elegans has the ability to adapt to drought, winter and flooding of soil by entering a dormant state called the dauer larva. This state can be brought about experimentally by slow starvation of a culture. In the dauer larva state an animal does not feed and may be maintained for at least 60 to 90 days. Normal development is resumed upon restoring the animal to its food supply. For the IML-1 flight, most worms will be flown as dauer larvae to minimize handling and physiological requirements. They will be reactivated post-flight for analysis.

Beginning in 1974, genetic studies with C. elegans broadened and became more sophisticated. To date, 920 genes and 320 chromosome rearrangements have been described and mapped and the majority of the genome has been cloned. Mutations affecting a wide variety of developmental processes and cell types are known. Phenotypes include: body shape and size (dumpy, long, blistered, roller mutants), cell division patterns (lineage mutants), muscle and nerve function (uncoordinated mutants), radiation sensitivity (radiation sensitive mutants), lethality due to absence of an essential gene function (lethal mutants) and others.

Ground Studies

Cosmic rays (HZE particles) can be simulated by the use of beams of accelerated charged particles. The Lawrence Berkeley Laboratory's BEVALAC accelerator is used for studies which investigate production of a variety of genetic and developmental lesions as a function of particle parameters such as charge, mass, velocity, LET (Linear Energy Transfer) and fluence. Ionizing photons from ^{60}Co as well as 254 nm UV photons are employed to determine cellular responses and to investigate their repair systems. Studies with neutrons are conducted at the Argonne National Laboratory's JANUS reactor. These basic research studies serve as baseline data for in situ measurements to be carried out in space. Strains of nematodes with enhanced sensitivities to radiation have been developed and their responses to radiations of various qualities are being characterized.

It is not technically feasible to produce a radiation field on the ground which simulates the situation in orbit. Particle accelerators produce unidirectional monoenergetic beams of particles and have substantial time limitations for ion switching and tuning which precludes

multi-species particle beams. Neutrons, bremsstrahlung, protons and modifications of fields by spacecraft shielding materials present further problems for simulation. No single ground facility can produce this mixed field so synergistic effects of the components and of gravity must be measured in situ during spaceflight. The ground based series of experiments using precisely controlled single sources of radiation provide an interpretive framework based on conditions where energy, charge, fluence and other parameters are accurately known.

By using appropriately constructed, genetically marked strains of worms, it is possible to search for mutants in large genetically defined regions or for mutations in particular genes. Special strains of worms are being used to isolate mutations in: (1) a set of about 400 essential genes utilizing a balancer chromosome (eT1 (III;V)) to control an autosomal region, and (2) a single gene, unc-22, which can be analyzed by molecular techniques. A variety of such mutants have been generated in ground controls using gamma rays, heavy ion beams, and neutrons to provide the baseline for the mixed radiation field in space.

To monitor normal chromosome behavior and cell reproduction, animals "marked" with dumpy and uncoordinated mutations are used in growing populations to monitor meiosis and recombination. Reproduction and development are assayed by self-fertilization in hermaphrodites and successful mating is assayed by the inclusion of males with hermaphrodites. Anatomical abnormalities in gonads, muscles, and intestine are detected by light microscope examination of fixed, stained animals.

Flight Experiment Design

The IML-1 nematode experiment will employ the Biorack multifunctional biology facility which provides an incubator at 22 °C with 1 x G centrifuge controls and cold storage at 5 °C. Two configurations of hardware will be employed in the RADIAT Biorack experiment. These will be placed in Biorack "Type I" and "Type II" experiment containers and incubated in several locations within the Biorack system as well as in the Spacelab tunnel in order to vary temperature, shielding and the force of gravity. Figure 2 summarizes the flight hardware configuration.

Measuring the Effects of Average Radiation Eleven Type I containers will be used to maintain worms in both the dauer larva state and as actively developing animals. Two containers will be placed at 5 °C, four will be incubated at 22 °C (two in the 1 x G centrifuge and 2 at 0 x G) and five will be placed in a cloth "cartridge belt" attached to the forward Spacelab connecting tunnel. The latter location is chosen as a minimum shielding location at ambient temperature (18 - 25 °C) which is monitored by the ambient temperature recorder (ATR) contained in the belt. Inside the Type I containers are four or eight lexan tubes stoppered with silicone rubber plugs containing the nematodes. Each Type I also contains two CR-39 polycarbonate nuclear track detectors or three laminated stacks oriented along x, y, and z axes, and a set of thermoluminescence detectors (TLDs) to map the local radiation environment. Most tubes will contain 1 ml of a suspension of 10,000 - 40,000 larvae in buffer and 1 ml of

air. Dauer larvae will be activated after landing and processed to obtain mutants induced by the mixed radiation field.

In several tubes placed on the centrifuge and inside the 22 °C incubator, small growing populations of worms will be inoculated to measure the effect of gravity on growth and development of genetically marked animals over multiple generations. Genetic marking of strains will allow three generations to be distinguished and permit abnormalities in meiosis and recombination to be directly measured. Mating, fertilization, and the developmental switch from the dauer state to the normal larval state will also be assessed. In these developmental studies only the average radiation environment will be correlated with lesions in nematodes.

Measuring the Effect of Specific Events. Two Type II containers will be incubated in the Biorack cooler at 5 °C. This temperature is required for immobilization of animals in a stiff agarose gel matrix. In these studies an attempt will be made to correlate individual HZE "hits" with particular worms in order to establish how particle parameters correlate with mutation structure. Inside each Type II container are housed four stacks of seven "nematode assemblies." Each "assembly" is composed of the following layers from bottom to top: (1) a polycarbonate support with holes for air exchange and corner fittings for assembly, (2) a nitrocellulose filter onto which 10,000 dauer larvae per cm^2 are filtered onto a monolayer and immobilized with a 1 mm thick layer of 4% agarose gel, (3) a 10 micron teflon separator membrane, and (4) a set of one or two CR-39 nuclear track detector foils each 600 microns thick. These are assembled and registration marker holes are bored at the corners for alignment of layers. During post flight, the CR-39 layers are removed and chemically "etched" by Prof. Eugene Benton at University of San Francisco to develop latent HZE particle tracks. The track geometry is calculated using a computerized microscope image analysis system, and the projected coordinates of each track in the nematode monolayer are determined. The nematodes associated with sets of tracks are removed for analysis from the immobilizing gel by means of a punch mounted on a micrometer stage. In this way "hit" animals may be distinguished from unhit animals analogous to the "Biostack" series of experiments flown on previous spaceflights.

Dosimetric mapping of several locations within Biorack and Spacelab will be provided by summing the results of track detectors and TLDs within the various components of the experiment. Together with experiments operated by European and Japanese investigators, a rather complete picture of the radiation environment within Spacelab should emerge.

In-flight operations consist of unpacking Type I and Type II containers from middeck passive thermal control units and mounting them in their incubation locations as soon as possible after orbit is achieved. Restowage at the latest practical time will maximize radiation exposure time in low shielding areas.

Summary

The RADIAT experiment on Biorack will attempt to describe the production of mutations and developmental defects in a simple animal due to interactions with various components of space radiation. Several shielding environments will be sampled and controls for the effects of gravity will be employed. Mutations due to an average mixed radiation field as well as those due to single identified ions will be processed to characterize potentially unique structures of lesions induced in the space environment. If development is normal in microgravity, this will also be the first time a multicellular organism will have completed multiple life cycles in space.

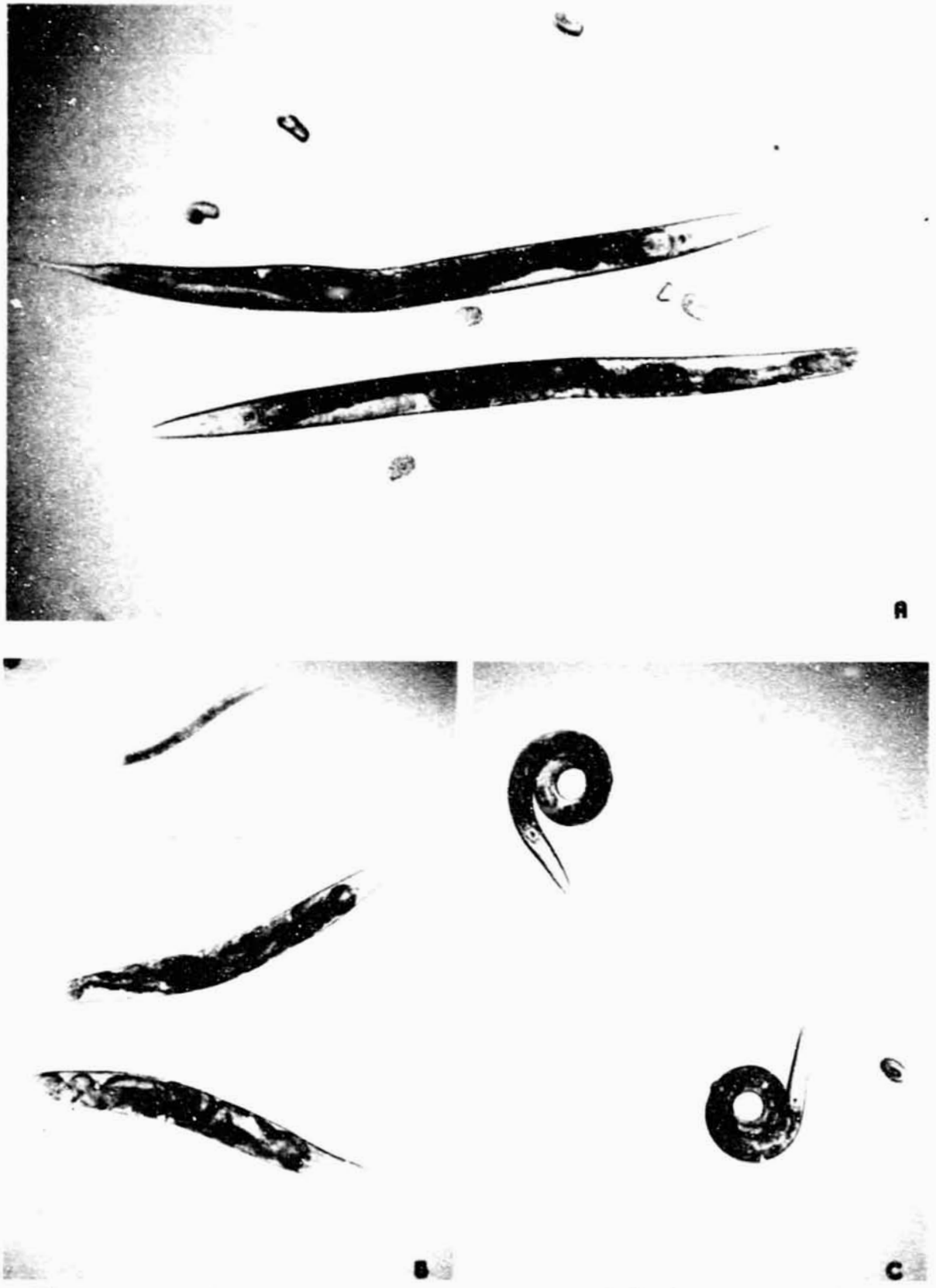

Figure 1. Adult C. elegans hermaphrodites seen by bright field microscopy. Panel A shows two Wild-type animals. Panel B illustrates the phenotype of a Dumpy mutant. Panel C illustrates an Uncoordinated mutan. which coils.

IML-1 Nematode Radiation Experiment

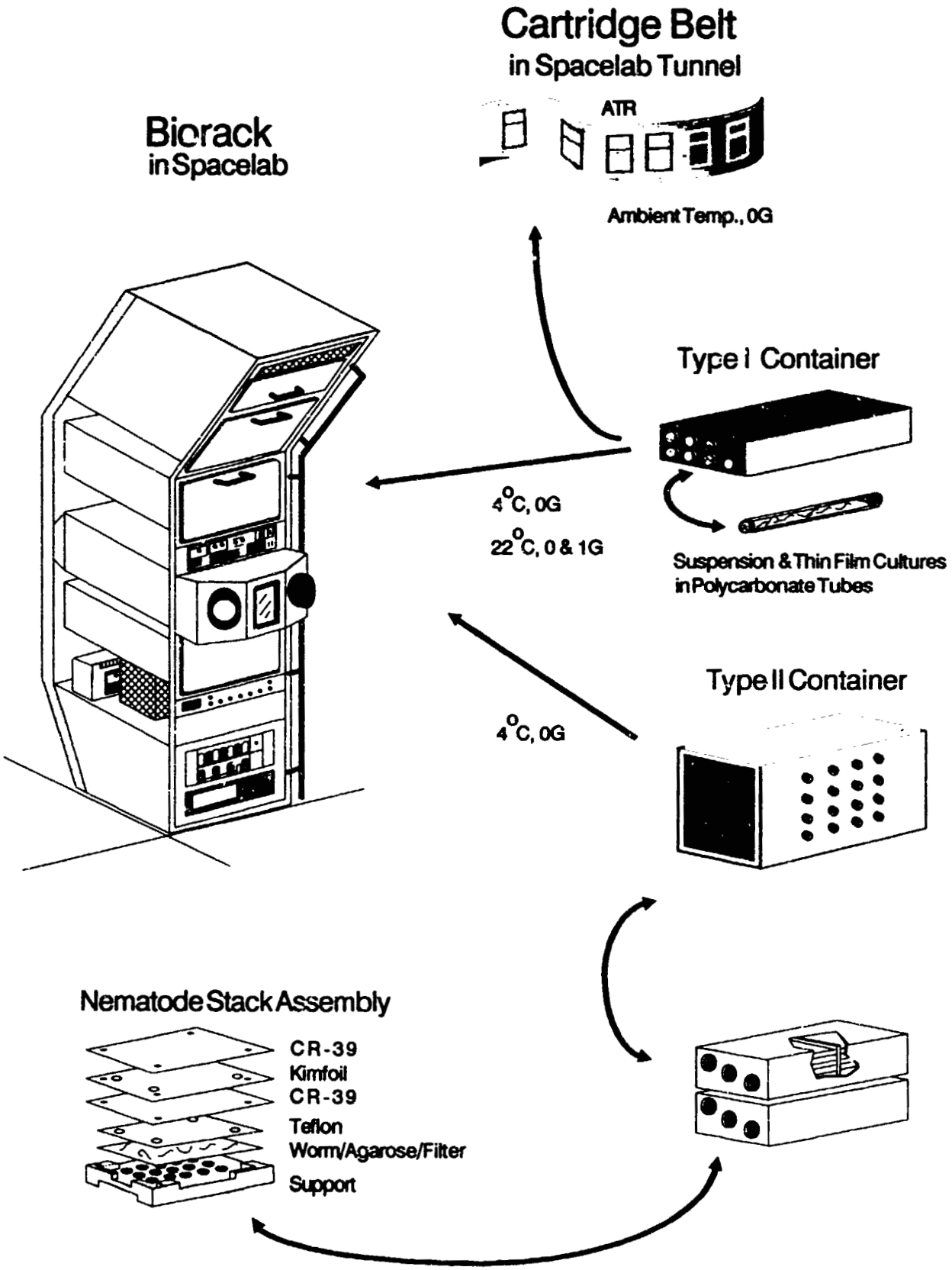

Figure 2. Schematic of hardware configuration and placement of samples in Spacelab.

N92-23604

MICROGRAVITATIONAL EFFECTS ON CHROMOSOME BEHAVIOR (7-IML-1)

Carlo Bruschi
International Center for Genetic Engineering and Biotechnology
Trieste, Italy

Background

It has been demonstrated in many different biological organisms that the two major space-related phenomenon - microgravity and radiation - have measured effects on genetic structures (DNA and chromosomes). Microgravity alters metaphase plate spindle formation and thereby alters chromosome structure and segregation during mitosis (identical cell division). Radiation can act at the molecular level producing changes in DNA structure, which is monitored in cells undergoing meiosis (reduction cell division). Microgravity and radiation effects are monitored separately in the same organism by measuring genetic damage during mitosis and meiosis.

To accomplish this, the common yeast Saccharomyces cerevisiae is used because it is capable of undergoing both meiosis and mitosis and therefore one can monitor frequencies of chromosomal loss and structural deformities and DNA mutation rates with a resolution impossible in higher organisms.

The yeast cultures are maintained at 1 g and 0 g in Biorack during flight. During four periods inflight, half of the yeast cultures are fixed with glutaraldehyde for postflight ultrastructural analysis of mitotic and meiotic cells. The other cultures will remain living in the Biorack and return refrigerated for postflight genetic analyses.

The cultures are maintained in separate sealed culture chambers. Each double chamber has two culture wells designated for a solid medium reservoir for yeast growth. Four of the double chambers are contained in a tray that fits into the Type I/O container (Figure 1). The chambers can be opened to access the cultures for preflight preparation and postflight analyses. Each culture well consists of a lexan chamber fitted with a moveable piston, both with a molecular layer of silicone to ease piston raising and lowering during fixation operations. The bottom plate made of polystyrene has two grooved circular areas into which lexan rings fit; the well thus created contains 300 µl of solid agar medium upon which the yeast is deposited. The bottom plate with media and yeast screws into the upper chamber (Figure 2). Prior to fixation, the piston is pushed down with a syringe-type ventilation tool to vent the air inside the chamber. The fixative is then injected through the piston with a hypodermic syringe.

Eight Type I/O containers with live yeast cultures will be flown, four wild-type to be grown at 22 °C and four containing temperature-sensitive mutant yeast grown at 36 °C. Half of these containers are placed on the 1-G centrifuges as inflight 1-G controls; the other half

of these containers are placed on the l-G centrifuges as inflight l-G controls; the other half remain static during flight. Four other Type I/O containers are used as a depository for the fixed culture chambers. These four containers are each initially fitted with two dummy culture chambers to replace the chambers removed from the containers on the centrifuge to balance it. Four additional Type I/O containers are each filled with two 3 cc and one 2 cc syringes, shown in Figure 3. A dummy Type I/O is used as a balance for the centrifuge when removing the cultures for fixation in the glovebox; living yeast cultures remain inside the incubators during the entire flight.

Experiment Containment and Handling. The eight Type I/O containers with yeast are stowed in one of the 5 °C PTCUs in the middeck during launch. The four Type I/Os containing fixative syringes are stowed in the 10 °C PTCU. The ventilation tool, syringe plungers, and dummy Type I/O containers are stowed in the Biorack stowage inside Spacelab.

Following Biorack activiation, the four mutant yeast containers are transferred to the 36 °C incubator, two at zero and two on the l-g centrifuge. The four wild-type yeast containers are transferred exactly the same way into the 22 °C incubator. The four fixative containers are transferred to the 4 °C cooler.

At each of four times during flight at 2-hour centers, one double chamber from each of four cultures is fixed: one at 22°C l G, one at 22° 0 G, one at 36° l G, and one at 36° 0g. The cultures are fixed inside the glovebox using the ventilation tool, fixative syringes, and syringe plunger. Each chamber receives 1.0 cc of glutaraldehyde. The fixed cultures are placed in one of the recipient Type I/O containers and stowed in the +4 °C cooler. Empty containers that originally contained fixative syringes are stowed in Biorack stowage. When the fourth fixation operation is complete, half of the total 64 living yeast cultures will have been fixed. The other cultures are allowed to grow undisturbed during the mission. Just before the Biorack is unloaded, the living cultures are transferred to the 4 °C cooler. The remaining four empty Type I/O containers inside the incubators are transferred to Biorack stowage.

At the end of the mission, the eight Type I/O containers in the 4 °C cooler are transferred to one of the 5 °C PTCUs and placed in the middeck for re-entry. The ventilation tool, syringe plunger, and dummy containers remain in Spacelab stowage.

At least to levels of containment are provided for the glutaraldehyde fixative at all times. The concentration and volume of glutaraldehyde in each syringe is 2.2% in either 3 ml or 2 ml syringes. Table 1 contains a description of the biological specimen and chemicals used for this investigation.

Objectives

The effects of the two major space-related conditions, microgravity and radiation, on the maintenance and transmission of genetic information have been partially documented in many organisms. Specifically, (1) microgravity acts at the chromosomal level, primarily on the structure and segregation of chromosomes, in producing major abberations such as deletions, breaks, nondisjunction, and chromosome loss and (2) to a lesser degree, cosmic radiation appears to affect the genic level, producing point mutations and DNA damage. To distinguish between the effects from microgravity and from radiation, it is necessary to monitor both mitotic and meiotic genetic damage in the same organism. The yeast Saccharomyces cerevisiae is used to monitor at high resolution the frequency of chromosome loss, nondisjunction, intergenic recombination, and gene mutation in mitotic and meiotic cells, to a degree impossible in other organisms. Because the yeast chromosomes are small, sensitive measurements can be made that can be extrapolated to higher organisms and man. The objectives of the research are (1) to quantitate the effects of microgravity and its synergism with cosmic radiation on chromosomal integrity and transmission during mitosis and meiosis, (2) to discriminate between chromosomal processes sensitive to microgravity and/or radiation during mitosis and meiosis, and (3) to relate these findings to anomalous mitotic mating type switching and ascosporogenesis following meiosis.

MAJOR HARDWARE

- Yeast culture chambers
- Type I containers
- Fixative syringes
- Biorack Facility (ESTEC)

TABLE 1. Definition of Biological Specimen and Related Chemicals

Type	Amount/Number	Remarks
Biological Specimen		
Saccharomyces cerevisiae (Common Brewer's Yeast)	2-6 x 10^7cells/colony; total of 1 x 10^8 cells/well 8 culture wells/Type I/O container	
Liquid Culture Medium		
N/A		
Solid Culture Medium		
YPD Medium	300 microliters/well - 9.6 ml total	4 Type I/O
SP-III Medium (Sporulation Medium)	300 microliters/well - 9.6 ml total	4 Type I/O
Other Special Chemicals		
Glutaraldehyde with Sorenson's Buffer	2.2% by volume 32 ml total stored in 4 Type I/O Each Type I/O has two 3 cc syringes and one 2 cc syringe (8 cc/Type I/O)	1 ml injected into each of 32 wells. Final concentration is same.

Preservation

One half of the samples are fixed; one half remain living. All samples are returned at +5 °C.

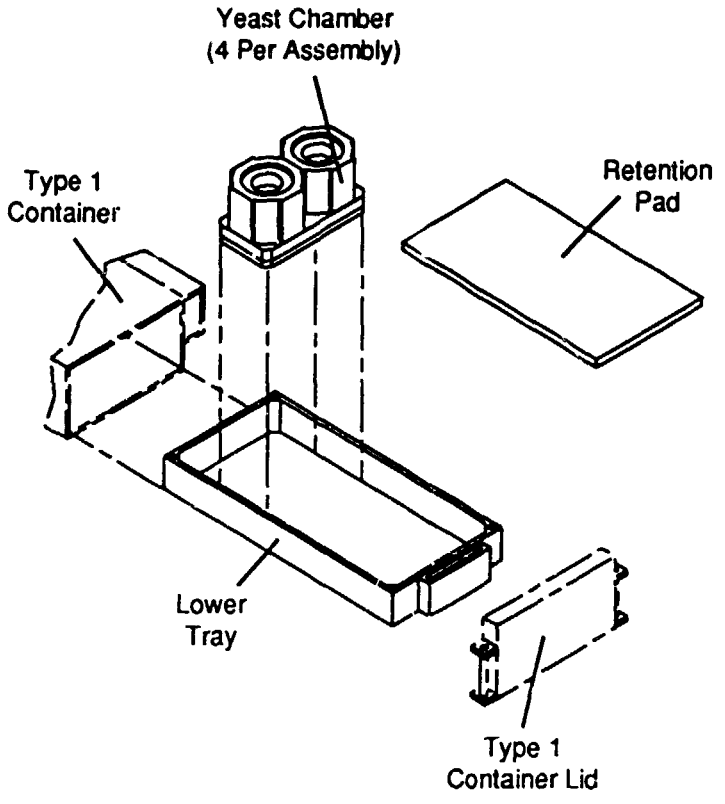

Figure 1. Yeast Culture Experiment Assembly.

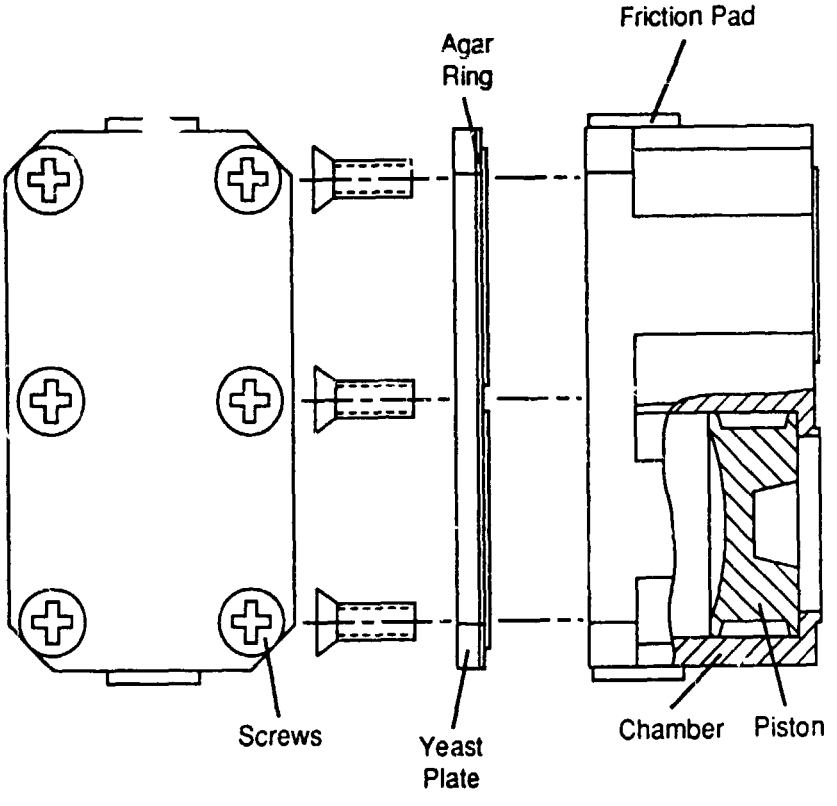

Figure 2. Yeast Culture Chamber.

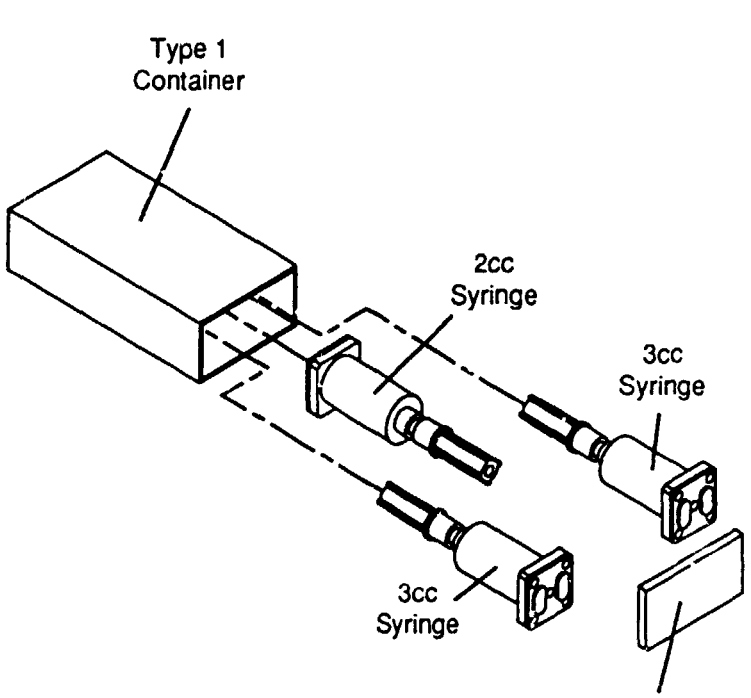

Figure 3. Fixative Syringes.

N92-23605

CHONDROGENESIS IN MICROMASS CULTURES OF EMBRYONIC MOUSE LIMB MESENCHYMAL CELLS EXPOSED TO MICROGRAVITY (7-IML-1)

Jackie Duke
University of Texas Health Science Center
Dental Branch/Dental Science Institute
Houston, TX USA

A basic question in space biology is whether changes in gravity (Δg) are perceived at the cellular level. Previous studies with a variety of cells have shown that this is the case (Table 1), but to date the response of skeletal cells has not been examined, even though the skeleton is sensitive to gravitational changes. The objective of the CELLS experiment is to examine the effect of microgravity in vitro on a skeletal cell known to be sensitive to gravitational changes both in vivo and in vitro--the mammalian chondrocyte (Table 2).

TABLE 1. Effects of Δg on Cells

Cells	Effect
WI-38 fibroblasts on Skylab 3	Consumed 18% less glucose
Paramecium aurelia	Proliferation increased by μg; decreased by 2 g
Paramecium tetraurelia	Cell volume and cell growth rate are increased in μg
Lymphocytes	5 X increase in interferon production in μg. Mitogen activation increased at 2,4,10 g; decreased by exposure to actual or simulated μg
HeLa cells, chicken embryo fibroblasts, Sarcoma Gallieri cells (rat), Friend leukemia virus-transformed cells	Increased proliferation at 10 g
Rat pituitary cells	Decreased growth hormone release in μg
Escherichia coli	Higher proliferation, increased resistance to antibiotics, and 3-4 X more frequent gene transfer in μg

TABLE 2: Effects of Δg on Chondrocytes

Early ossification of femoral heads of centrifuged rats
Delayed mineralization and abnormal collagen formation in growth plates of rats flown on Cosmos 1129
Changes in height and altered matrix in growth plates of rats flown on Spacelab 3, Cosmos 1887, and Cosmos 2044
Lack of fracture repair in fibulae of rats flown on Cosmos 2044

In the CELLS experiment, cell suspensions are prepared from limb buds of 12 day embryonic mice, and cells are inoculated into the hardware at high densities which promote cartilage differentiation. The well characterized micromass system reflects changes in chondrogenesis occurring in vivo due to mutations or exposure to teratogens, so results of this experiment should be indicative of how in vivo limb development might be affected by microgravity. When studies of early limb development begin, whether on extended shuttle missions or on Space Station Freedom, in vitro studies will have to be carried out as well as in vivo ones in order to determine if the observed effects are due to a direct action of gravity on the developing skeleton, or indirect, due to maternal changes.

The cell culture hardware for the CELLS experiment represents a significant advance in the ability to grow cells in space. The main unit of the CELLS hardware is a cell culture chamber with two non-communicating wells. Within each chamber is a "blister" or "bubble" of a gas exchange material (Silastic) which expands as medium is added and collapses as medium is removed. Four of these culture units (eight wells) fit into each Type I container. Injections for medium removal or additions are made with a hypodermic needle through the gasket between the chamber and the bottom plate. A deflector ring in the bottom of the chamber is designed to prevent forces produced during medium injection and withdrawal from dislodging the cells.

Initial injections for cell culture (4×10^5 cells/20 µl drop) are made using a Stepper syringe, which is inserted through the gasket and through a silicon plug in the deflector ring into the center of the chamber. After a 2 hour attachment period, 1.8 ml of medium is added, filling the Silastic bubble. Large air bubbles are removed, and four of the BEXs (Bubble Exchange unit) are placed in each Type I container, and then in a refrigerator and slowly cooled to 5 °C. For flight, cultures will be placed in 4 °C PTCUs and put into stowage on the middeck. Also in middeck stowage will be 40, 5 ml syringes with medium at ambient temperature, and 30 syringes with fixatives (20, 3 cc with 1% glutaraldehyde; 10, 2 cc with 1%

formalin in 95% ethanol) at 4 °C. Empty syringes for removal and freezing of used medium will be in Biorack ambient stowage.

On orbit, cultures will be placed in the Biorack incubator and the fixative and medium will be placed in the cooler. The first medium change takes place at L + 15 hours. Additional medium changes occur at 26 ± 2 hour intervals. One Type I container from 1 g and one from μg will be fixed at each medium change, and refrigerated until recovery. Postflight, chondrogenesis will be assessed in a number of ways:

1. Alcian-blue stained regions: Cultures will be stained with alcian blue at low pH, which is specific for cartilage. Measurements will include total cartilage area and number and size of cartilage nodules.

2. Immunological assays: Formalin-fixed cultures will be embedded in Lowicryl, sectioned, and stained with an indirect method to detect collagen types. Antibodies against the following will be used:

Type I collagen:	Non cartilage collagen. Should be in cell layers between nodules.
Type II collagen:	Cartilage type collagen. Abundant in nodules.
Type X collagen:	Associated with cartilage hypertrophy.
Cartilage proteoglycan:	Affects collagen aggregation; hydration of proteoglycen important in cartilage functions.

3. SEM and TEM: Morphometric techniques will be used to assess cell-cell, cell-matrix, and matrix-matrix interactions including collagen fibril length and width, and proteoglycan granule size and distribution. Intracellularly, markers of chondrocyte differentiation and cell activity will be assessed: nucleocytoplasmic ratio, number and size of Golgi vesicles and of RER cisternae, and mitochondrial distribution.

4. Medium analysis: Medium will be analyzed by ELISA to detect levels of collagen types and of proteoglycans. Glucose levels will be assessed by a colorimetric test.

The CELLS experiment will be the first culture of skeletal cells to be flown in space, and the first in which daily medium changes are to be made. The successful completion of this experiment will significantly advance our knowledge of how cells respond to μg, and will expand our capability of culturing cells in space. Because of the presence of a 1-g centrifuge, and because the system is amenable to both centrifugation and clinostating, the CELLS experiment is also likely to show how centrifugation may be used to predict μg results and whether or not the clinostat is a good model of μg.

In addition, biomedical problems, such as bone loss and decreased red cell volume, could be due to a general μg effect on differentiation, including processes such as hematopoiesis, wound healing, immunological function, recruitment of osteoblasts, and fracture repair. Effects on cartilage formation are particularly relevant in the last case since a cartilage callus stage is involved.

ORIGINAL PAGE
BLACK AND WHITE PHOTOGRAPH

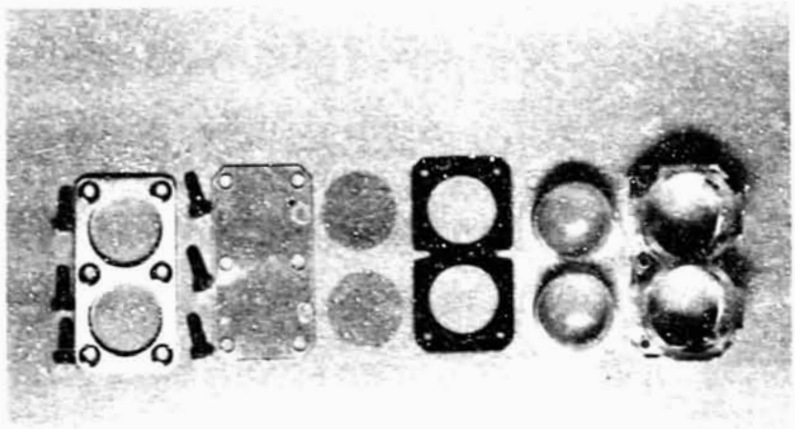

A

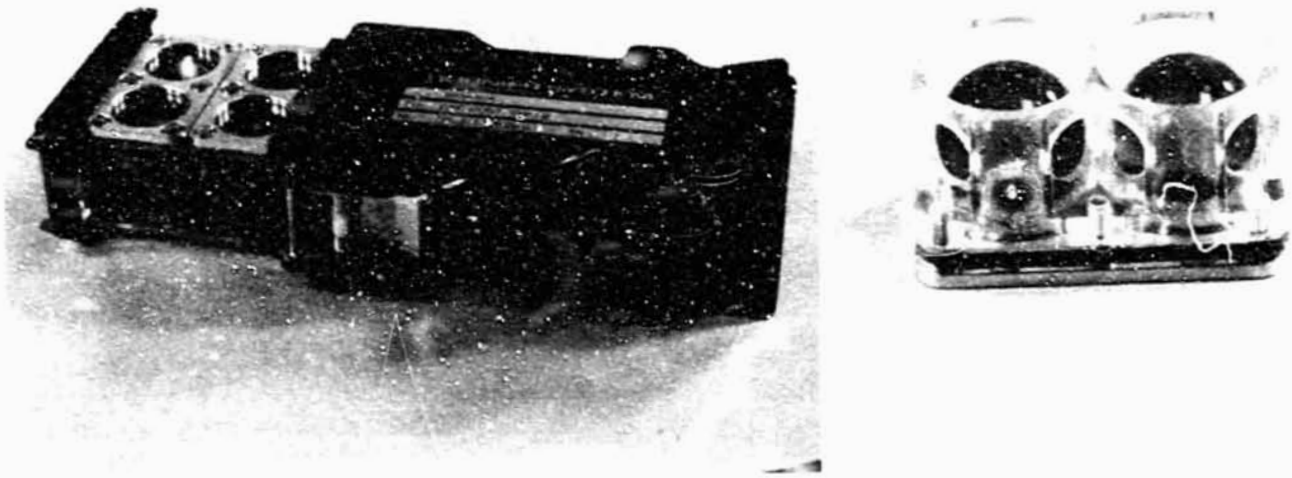

B

Figure 1. A. BEX Components: Chamber, "Double Bubble," Gasket, Coverslips, Bottom Plate, Reinforcing Plate, Screws. B. BEX's in Type I. Insert, One Unit.

Figure 2. Transmission electron microscopy photograph of chrondrocytes in the flight hardware--exhibiting the typical rounded chronodrocyte profile, numerous mitochrondria and expanded RER, and intercellular matrix of collagen and proteoglycan.

N92-23606

EFFECT OF MICROGRAVITY AND MECHANICAL STIMULATION ON THE IN VITRO MINERALIZATION AND RESORPTION OF FETAL MOUSE LONG BONES (7-IML-1)

J. Paul Veldhuijzen
Acta-Vrije Universiteit
Dept. of Oral Cell Biology
Amsterdam, The Netherlands

Mechanical forces play an important role in the differentiation, growth, and (re)modeling of skeletal tissues. An increase in the normal loading pattern of the skeleton leads to an increase in bone mass. An overall decrease in the functional load exerted on the skeleton produces mineral loss and osteoporosis. However, the responses of the skeletal tissue cells to various loading conditions are still largely unresolved, as is the mechanism of the cellular response to a changed mechanic l environment. Using an in vitro approach we hope to avoid some problems encountered in the use of in vivo animal and man models, which have been extensively used in the past.

In a number of experiments we have demonstrated that 16 and 17 day old fetal mouse long bone rudiments (metatarsalia), cultured in a liquid culture medium, are very suitable to study mineralization and resorption, respectively. We have also demonstrated that under hydrostatic compression (130 mbar above ambient, achieved by compressing the gas phase above the culture medium) mineralization is increased, while resorption is decreased. Culture of long bone rudiments under non-compressed control conditions can be regarded as a situation of partial unloading, showing some phenomena of a disuse situation.

Under microgravity conditions, responses of osteoblasts and chondrocytes (involved in mineralization) and osteoclasts (involved in mineral resorption), to culture with and without compression, may be much more outspoken. This will have advantages for the study and the interpretation of the role of cellular events in the process of mineralization and resorption of developing skeletal tissues under various loading conditions.

Experiment "BONES" is carried out in four Type I/O and four type I/E containers. All containers have a one way ball valve in the small side (Figure 1). This valve is used to flush the containers at the beginning of the experiment and after 2 days, using a special gas mixture (5% CO_2 in air). The use of this gas mixture is required because the tissue culture medium is buffered with Na-bicarbonate. The gas mixture is carried in a pressure bottle of 150 ml, pressurized at 80 bar (Figure 4). The gas flow is regulated with a micrometer valve, while a safety valve (set at 1 bar) protects the container. The containers accommodate hardware modified from the French "ANTIBIO" experiment of Dr. Tixador (Toulouse). There are holes in the cover plates and the sides to ensure good gas exchange during flushing (Figure 2). The

permeable polyethylene culture bags (Figure 3; developed by the group of Dr. Tixador) filled with 700 µl medium, including 10% rat serum. In containers used for biochemical studies, the culture bags contain a glass ampulla with radioactive labels (45Ca and 32P). By turning the metal splines (just visible through the culture bags in Figure 3) using a hexagonal key this ampulla is broken and the content is released into the culture bag at the beginning of the experiment. In containers used for histological studies, the glass ampulla contains a fixative; this ampulla is broken at the end of the 4 day experiment.

To study the effect of increased compression on the skeletal tissue cells, Type I/E containers are pressurized. These containers have 12 culture bags (instead of the 16 in the type I/O containers) because part of the room in the hardware is occupied by a pressure sensor and electronics to measure the pressure during pressurization and during the actual experiment (Figures 2 and 3). The pressure is monitored using the PROD (Pressure Read-Out Device) which is attached to the container (Figure 4). The PROD is connected on one side to the electrical connector of the type I/E container and on the other side to the data and power lines of Biorack. During pressurization successive red LED's (four) and one yellow LED indicate under pressure. A green LED indicates the correct pressure of 130 mbar. Over pressure is indicated with a yellow and one final red LED. Each successive LED indicates a 5 mbar change in pressure. Pressure read-out starts at 100 mbar. Since the containers are pressurized at ambient (22 °C) and the closed containers are then placed in the 36 °C incubator, the electronics inside the containers compensate for this temperature difference. The green LED indicates that at ambient temperature a pressure is reached, which, when the container is placed in the incubator, will increase by the temperature difference until the experimental pressure reaches 130 mbar.

All eight containers are kept at ambient temperatures in the middeck between hand over and activation of Biorack, to minimize biological activity prior to microgravity conditions. In containers used for biochemical experiments glass ampulla containing the radioactive labels are broken. All containers are flushed, and four are pressurized. Placing the containers in the 36 C incubator initiates normal biological activity. After 2 days all containers are flushed again, and four containers are again pressurized. After the 4 day experimental period, containers for biochemical purposes are placed in the freezer (- 15 °C) to stop biological activity. In containers for histological purposes the glass ampulla with the fixative are broken, and these containers are then placed in the cooler (+4 °C).

Figure 1. Type I/E container (with the electrical connector in the lid), showing the one way ball valve in the small side. This valve is used during flushing and pressurization.

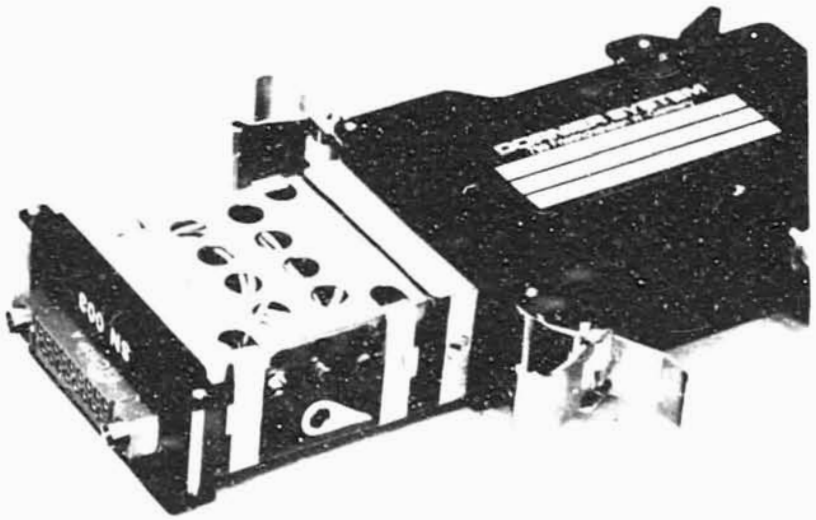

Figure 2. Opened Type I/E container with the typical hardware to accommodate the culture bags. Holes are present in coverplates and sides to ensure good gas exchange. Through the holes in the top left one fourth part of the hardware, the electronics are partly visible.

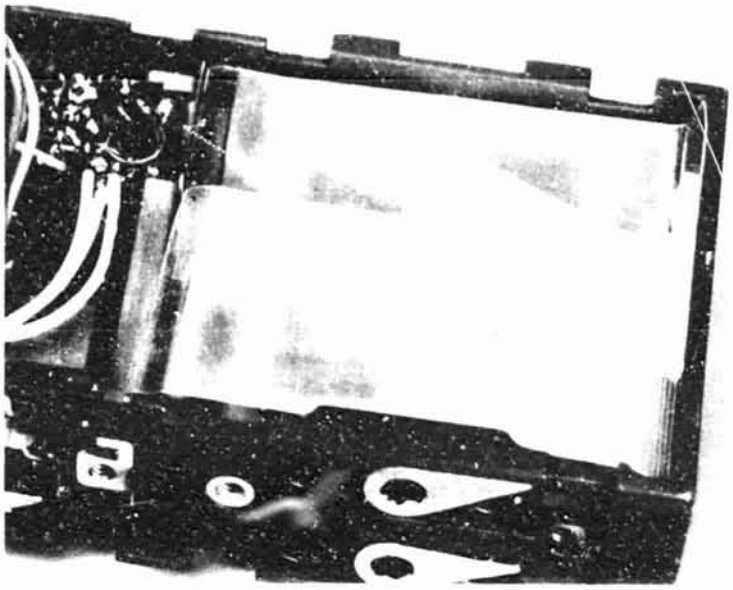

Figure 3. View of hardware with the cover plates removed. Two culture bags, including a glass ampulla are visible on the right side. In the upper left part of the hardware the pressure sensor can be seen, with parts of the electronic components. In the side the hexagonal holes, used to turn the metal splines (visible through the culture bags!), are shown.

Figure 4. The pressure bottle (with micrometer valve and safety valve) is connected to a Type I/E container. On top of the container the PROD is attached. The PROD is connected to the containers with a flat electrical connector. The other electrical connector is used to connect the PROD with data and power lines of Biorack

"EGGS" - THE ROLE OF GRAVITY IN THE ESTABLISHMENT OF THE DORSO-VENTRAL AXIS IN THE AMPHIBIAN EMBRYO (7-IML-1)

Geertje A. Ubbels
Hubrecht Laboratory
Netherlands Institute for Developmental Biology
Utrecht, The Netherlands

In this experiment we intend to fertilize frog (Xenopus laevis) eggs under microgravity, to perform histological fixations at two different programmed times, and after return to Earth, to determine whether timing and pattern of egg cleavages and axis formation are normal. Because of the limited viability of the gametes, this experiment will be the very first to be activated in the Biorack.

In growing ovarian frog eggs the various yolk components are formed in a characteristic pattern. This pattern is independent of gravity and is maintained by the cytoskeleton, a network of molecular fibrils. The mature unfertilized eggs of anuran amphibians are radially symmetrical about an "animal-vegetal" polar axis, which becomes vertical upon fertilization and which initially roughly foreshadows the head-tail axis of the embryo.

Sperm penetration causes an asymmetric contraction of the animal pigment cap and starts a cytoplasmic rearrangement, setting up a second "dorsal-ventral" axis and thus determining the ultimate bilaterally symmetrical structure of the embryo. The side of sperm entry becomes the ventral side in the majority of cases observed. Although the sperm, through its interaction with the egg's cytoskeleton, is the primary cue for this polarization, additional factors are involved as well.

Gravity may well be such a factor, since egg rotation and centrifugation experiments on the uncleaved Xenopus laevis egg show that the cueing action of the sperm may be overridden by gravity and the centrifugal force, respectively. This suggests that in normal development gravity cooperates with the sperm in the establishment of dorso-ventral polarity. Logically only an experiment under microgravity conditions can prove this definitively. This will be tested by a study of egg fertilization and development under microgravity conditions and under 1-g conditions on one of the 1-g centrifuges aboard. A similar experiment will be performed simultaneously on Earth.

The housing of the experiment specimens and chemicals consists of a cylinder block (AEC - Automatic Experiment Container), equipped with spring-loaded pistons for sequential operation (Figure 1). The pistons are initially restrained by nylon threads surrounded by heater wires. These wires heat up when a current is supplied and this breaks the nylon threads, thus

releasing the pistons. The movement of the pistons causes fluids to be transferred from one cylinder to another. Non- return valves are incorporated at all but one of the cylinder interfaces to prevent uncontrolled mixing of the fluids. Only the egg cylinder connects freely with the testis cylinder (both contain initially an identical medium) and through this, some of the fixative will slightly fix the remaining part of the testis. The experiment cycle is controlled by a microprocessor, which activates the heater wires for release of the pistons at pre-selected times during the flight.

Eggs and testes are brought up separately (late access) at 10 °C, recovered from dormant conditions and mixed automatically, as early as possible in flight, at 22 °C. Samples of fertilized eggs are fixed at two different stages of development with either a solution of glutaraldehyde or with a compound fixative, Bouin d'Hollande. These fixatives are contained separately in a membrane compartment inside the G-compartment (Figure 1).

Such a separate block assembly (AEC) is contained in each of six Type 1/E containers, which are stowed in a 10 °C PTCU middeck locker during the launch. Following Biorack-activation, the six containers are transferred to the 22 °C incubator, four on the static rack and two on one of the 1-g centrifuges. Inside the incubator, the containers are electrically connected for automatic fertilization of the eggs and the histological fixation at the third cleavage and gasurula stages.

To avoid excessive heating of the biological materials by the microprocessor after performance of fertilization, the experiment modules will be temporarily parked in electrically inactivated positions, also in incubator A (22 °C), and only be electrically activated at the proper times for histological fixations, when the Payload Specialist will plug them in for a few seconds. The experiment modules with the fixed biological materials are subsequently removed from incubator A, and after inspection in the glove box, inserted in a middeck locker at 10 °C, where they will be kept until the end of the mission.

This experiment is very similar to an experiment previously flown in Biorack on the Spacelab D1 mission which, however, failed because of some hardware malfunctions and biological problems. The design and operation of the experiment for the IML-1 mission are similar to those during the D1 mission, except for the use of two different histological fixatives, and minor hardware changes. The fixative is now contained in an elastic membrane (see Figure 1), closed by a perspex disk at the side of the bottom plate. A perspex ring on the top side guides the plunger, and the fixative is pressed out near the bottom plate. This extra containment avoids the possibility of the eggs being poisoned before they are fertilized.

The modifications have been tested repeatedly, using flight-type manually operated laboratory modules. The most convincing tests were two experiments performed in real Space, in the SOUNDING ROCKETS TEXUS-17 (1988) and MASER-3 (1989), launched from Kiruna (North Sweden).

In both missions eight containers, manufactured with the modifications, were loaded with biological material and flown as part of the Payload, while another eight similar containers were activated as controls on Earth. Both times, all sixteen containers performed flawlessly, electronically as well as mechanically, and there was no leakage. The vibrations and accelerations during the launch of a sounding rocket are more intense than those which the containers should sustain during the launch of the space shuttle.

The biological results of the two sounding rocket experiments were interesting and promising for longer-lasting Space experiments on Xenopus development, since Xenopus eggs were successfully fertilized for the first time in Space during the TEXUS-17 flight on May 2, 1988. The fertilization rate was high. This result was repeated during the MASER-3 Mission, when two pilot experiments were also included. The latter showed that newly fertilized Xenopus eggs can stand reentry perturbations. However, they developed abnormally. Although an additional control experiment made it less likely that this was the result of reentry perturbations, only a longer period of development under microgravity can reveal whether this abnormal development is the result of the fertilization and a few minutes of development under microgravity. This may be checked during the IML-1 mission, by making a pilot experiment in a slightly modified manually operated flight module-type experiment container. Compared to the Sounding Rocket experiments, the IML-1 experiment has the disadvantage of a relatively long period of "late access" (more than 14.5 hours), reducing the viability of the eggs.

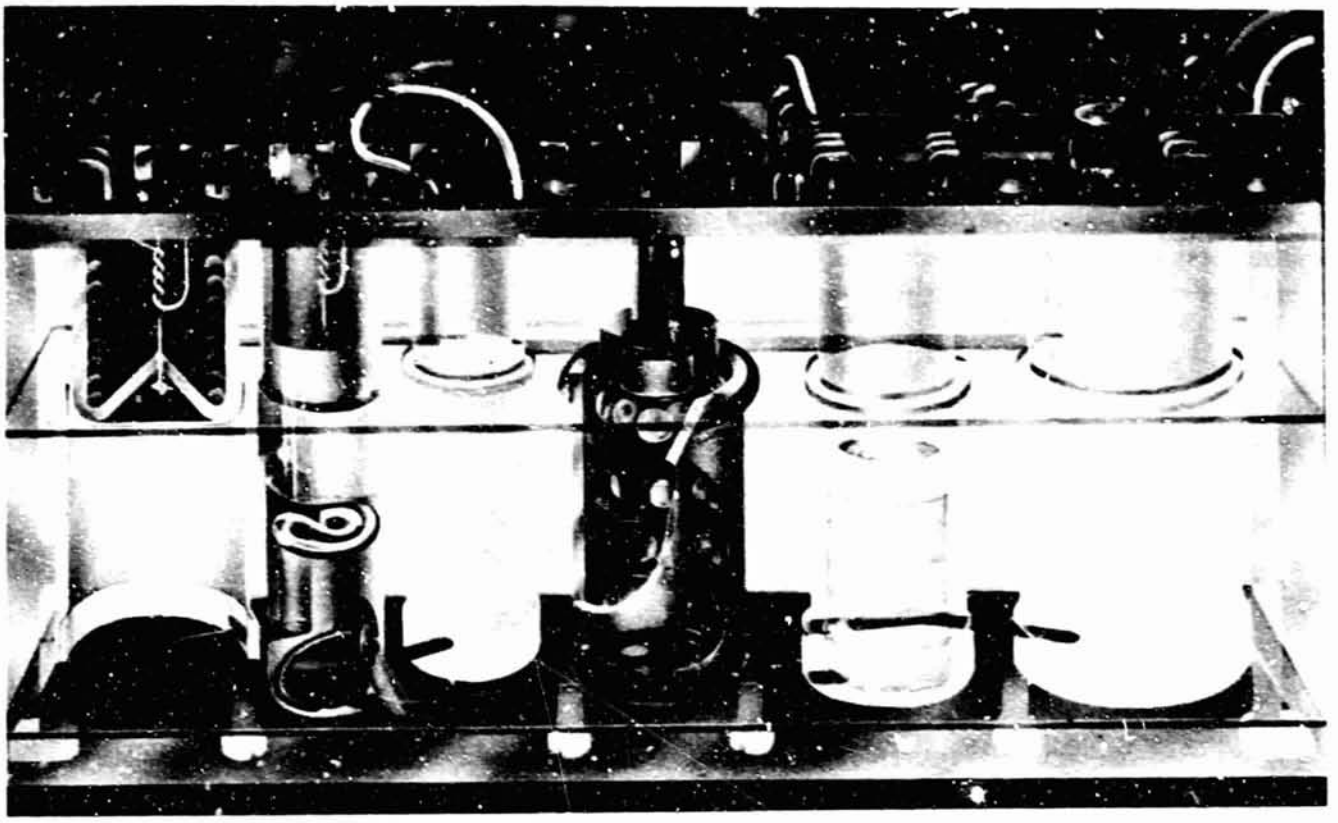

A T R E G M

Figure 1. The modified experiment container, shown twice the actual size, designed for the IML-1 mission (a perspex block, 79.5 x 19.0 x 33.1 mm) with electronics mounted on top (overall height, with electronics: about 40 mm). Activation of the plungers occurs when a signal from the microprocessor heats the wires and burns the nylon thread. The six compartments contain (in order of operation):

T. 0.7 ml full-strength MMR with one testis. Upon activation of the crusher in this compartment the testis is punctured and sperm is released. After release of the crusher, the volume in T is 0.4 ml.

A. 1.5 ml 10% MMR. Activation of the plunger in A pushes the fluid to the testis compartment (T). Thus, fluid from T is pushed through a channel in the bottom plate into the egg compartment (E). Fluid from E is pushed away through a channel between the two halves of the perspex block into the now available space above the plunger in A. The sperm is mobilized through dilution of the full-strength MMR. (Note nylon thread and wire heater above the plunger and rolling sleeve below.)

R. 0.6 ml 10% MMR. Activation of the plunger pushes buffer solution via T into the egg compartment E.

M. 2.0 ml 25% MMR. Activation of the plunger in M replaces sperm by fresh culture medium, in which the embryos will develop until the time of fixation.

Figure 1 (Concluded)

G. The G compartment (1.0 ml) holds a cylindrical elastic bag containing 0.24 ml 25% MMR, with 7% glutaraldehyde, closed with a perspex disk (extra T perspex containment). Activation of the plunger in G presses the glutaraldehyde out into the E compartment. The biological material is then fixed and stays in the fixative until the experiment containers are opened after the mission.

E. 0.9 ml full strength MMR with 2 groups of 15 eggs each from 2 different females, separated by a vinathene sieve and 2 rings. (Note: this figure indicates 5 layers of eggs, which will not be the case in the IML-1 experiment.) A temperature sensor is mounted above the egg cylinder.

Standard composition of full-strength MMR: 100 mM NaCl, 2 mM KCl, 1 mM $MgSO_4$, 2 mM $CaCl_2$, 5 mM Na-Hepes buffer, 0.1 mM EDTA; osmolarity: 230 m Osm, pH 7.8. The solutions in the A, R, and M cylinders will be saturated with oxygen at room temperature, just before filling and immediately before the bottom plate is closed.

N92-23608

THE EFFECT OF SPACE ENVIRONMENT ON THE DEVELOPMENT AND AGING OF DROSOPHILA MELANOGASTER (7-IML-1)

Roberto Marco
Department of Biochemistry UAM/Institute of Biomedical Investigations CSIC
Madrid, Spain

Experiment Description

The objective of this proposal is to repeat the experiment performed in the Biorack during the Spacelab D1 mission flown in November 1985. In this experiment, several quantitative differences were noted between the Drosophila maintained in space in containers under microgravity conditions, and the ones housed in the 1-g centrifuge and the parallel ground control: (a) there is a stimulation of the rate of oogenesis, (b) there is an impairment in embryonic development reflected in a delay and/or inhibition in larval hatching, and (c) the Drosphila males which had been exposed continuously to microgravity during the D1 mission showed an accelerated aging process, with a shortening in their life spans. In IML-1, the same experiment will be repeated, modified in such a way that complementary evidence will be obtained, namely, the embryos from different egg laying periods during the flight will be left to develop in the same conditions in which they have been maintained, i.e., in microgravity and/or 1-g centrifuge, to monitor whether the effects detected in the initial 24 hour of development, i.e., during embryonic development, are also visible or even more apparent at later stages of development. In addition, flies recovered from the experiment will be used to study their aging response. In this way more information will be gathered on the processes affected by microgravity in complex organisms.

This experiment involves the study of the development of eggs of the fly Drosophila exposed to microgravity. It is presumed that oogenesis, rather than further states of embryonic development, is sensitive to gravity. This hypothesis will be tested by collecting eggs layed at specific times inflight and postflight from flies exposed to 0 g and 1 g. This portion of the experiment is a repetition of an earlier experiment flown in Biorack during the Spacelab D1 mission. An added feature of the experiment for the IML-1 mission is to study the effect of microgravity on the life span of Drosophila male flies.

The flies are housed in subcontainers. One container fits inside each of eight Type I/O containers. Four of the Type I/O containers each contains a group of 60 adult male flies and no ... nale flies. These flies are used for the aging study. Two of the Type I/O containers hold mixed flies and two of the Type I/O containers hold male flies under 0-g conditions. The flies in the other four Type I/O containers are maintained under 1-g conditions.

Each subcontainer has a slot through which feeding/egg collecting trays are exchanged. These trays are shallow containers coated with agar containing a fly nutrient (yeast extract and sucrose). Eggs are laid on the surface of the agar.

The feeding/egg collecting trays are exchanged by removing the fly subcontainer from the Type I/O container and inserting a new tray into the slot opening on one side of the subcontainer. This action causes the old tray to be pushed out of the subcontainer through the slot opening on the other side (see Figure 1). The trays have the same dimensions as the slot openings. The flies are prevented from escaping since there is no opening of the subcontainer at any time during operation.

Six new trays are contained in each of the nine Type I/O containers. The trays are held in a frame that fits inside each Type I/O container. The Type I/O containers with mixed flies will receive a new tray each day on orbit. The Type I/O containers with male flies will only receive a new tray every other day. After exchange, the old trays are stored in the same frame and Type I/O container from which the new trays were obtained. The contents of the old trays are then frozen for postflight analysis.

On one day of the mission, the trays in the Type I/O containers with mixed flies will be exchanged twice. Each of the resulting old trays from the second exchange is stored in a special incubation subcontainer that contains additional agar media. This is to allow the eggs on these trays more time to develop. One incubation subcontainer is fitted inside each of four Type I/O containers.

Upon recovery the different trays will be studied to verify the compatibility of Drosophilia development with microgravity conditions, scoring any embryonic anomalies that may appear. In particular in this experiment, the group of containers in which embryos and larvae are allowed to further develop in space will show the significance and the extent of the delay observed in the previous Spacelab D1 mission.

Furthermore, the adults recovered from flight and those emerged from the last group of trays, i.e., from the embryos laid in the shuttle before landing, will be studied with respect to their aging response.

Figure 1. Exchange of the Feeding/Collecting Trays of Fly Subcontainer.

EFFECT OF MICROGRAVITY ENVIRONMENT ON CELL WALL REGENERATION, CELL DIVISIONS, GROWTH, AND DIFFERENTIATION OF PLANTS FROM PROTOPLASTS (7-IML-1)

Ole Rasmussen
University of Aarhus
Denmark

With future biological experiments in space in mind, it is essential to obtain information on the effects of gravity on basic cell biological processes such as growth, division, and differentiation.

Plant protoplasts represent a good model for the study of cell growth and differentiation. Results from the Spacelab D1 mission with cultures of different unicellular organisms strongly suggest that weightlessness may affect cell proliferation and development.

Protoplasts are naked plant cells where the cell walls have been removed by enzymatic digestion. Protoplasts are surrounded only by a plasmamembrane and represent therefore a very sensitive system for reception of outer stimuli such as gravity.

Plant cells are totipotent: i.e., it is possible to regenerate intact plants from protoplast cultures. The primary goal of this project is to investigate if microgravity has any influence on growth and differentiation of protoplasts. Formation of new cell walls on rapeseed protoplasts takes place within the first 24 hours after isolation. Cell divisions can be observed after 2-4 days and formation of cell aggregates after 5- 7 days. Therefore, it is possible during the 7 day IML-1 mission to investigate if cell wall formation, cell division, and cell differentiation are influenced by microgravity.

Protoplasts of rapeseed and carrot will be prepared shortly before launch and injected into 0.6 ml polyethylene bags. Eight bags are placed in an aluminum block inside the ESA Type I container. The containers are placed at 4 °C in PTCU's and transferred to orbiter mid-deck. At 4 °C all cell processes are slowed down, including cell wall formation. Latest access to the shuttle will be 12 hours before launch.

In orbit the containers will be transferred from the PTC box to the 22 °C Biorack incubator. The installation of a 1-g centrifuge in Biorack will make it possible to distinguish between effects of near weightlessness (ca 10^{-3} g) and effects caused by cosmic radiation and other space flight factors including vibrations. Parallel control experiments will be carried out on the ground.

According to a preplanned time schedule samples of protoplasts will be investigated during the mission by the crew. By use of a hypodermic syringe and needle inserted through the septum, aliquots of the protoplast samples will be removed and loaded on microscope slides with prefixed coverslips. Microscopic examinations will be carried out and typical developmental cell stages will be recorded and photographed using a Pentax camera. The rest of the sample will be fixed by glutaraldehyde and kept in the cooler for ultrastructural analysis after retrieval.

After landing non-fixed samples will be transferred to new growth medium and subcultured for the purpose of regenerating whole plants.

The hardware for our IML-1 Biorack experiment is shown on Figures 1 and 2.

The flexible plastic bags allow sample removal and the consequent change in volume, without the need to allow the entry of contaminating air.

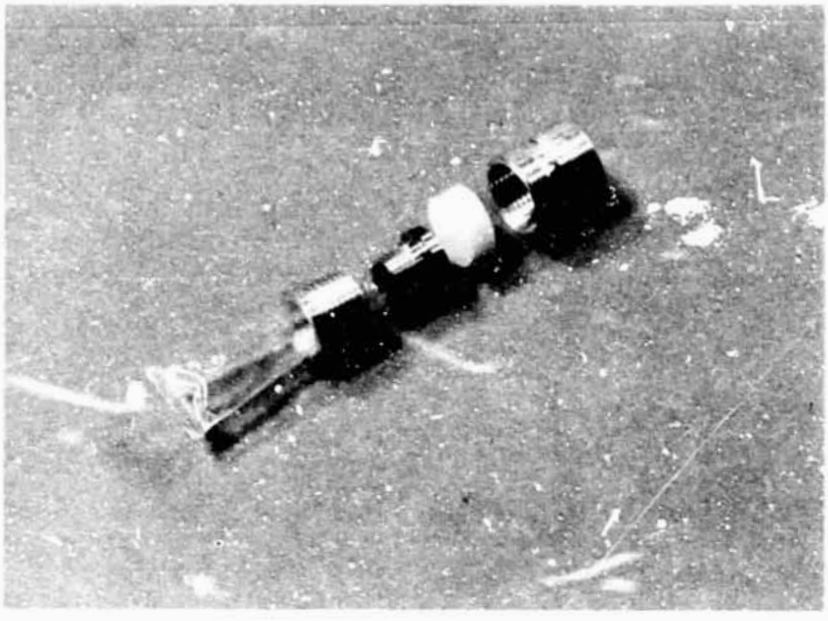

Figure 1. A Protoplast Culture Chamber Assembly.

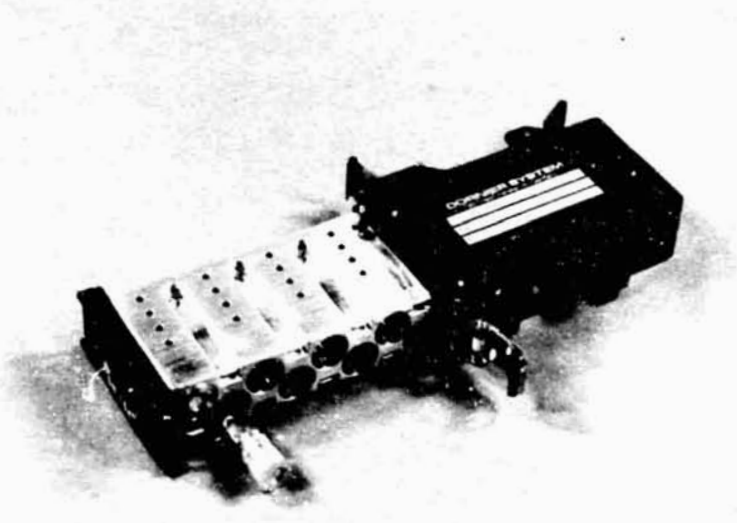

Figure 2. Culture Chamber Holder for Typ I Container.

N92-23610

EMBRYOGENESIS AND ORGANOGENESIS OF CARAUSIUS MOROSUS UNDER SPACE FLIGHT CONDITIONS (7-IML-1)

D. H. Bücker
Institute for Aerospace Medicine
DLR
Cologne, Germany

The experiment is part of a radiobiological space research program to obtain experimental data on the biological effectiveness of the structured component of cosmic radiation during spaceflight. Such data are required as basic information for a quantitative assessment of the potential hazard of these particles to man or any biological specimen in space, especially during future long-duration or repeated spaceflights.

In this proposed experiment, Carausius morosus embryos of different ages will develop under spaceflight conditions. The experiment is designed to determine especially the influence of galactic heavy ions of very high energy deposition in microgravity on developmental processes of different radiation sensitivity and regenerative capacity. Layers of Carausius morosus eggs (each layer accommodates a certain development stage I-V) are sandwiched between different track detectors (cellulose nitrate, CR39). This method allows the localization of the trajectory of each heavy ion in the biological layer and the identification of the site of penetration inside the egg.

From the physical radiation data, obtained by the adjacent track detectors and integrating dosimeters, information on charge and energy of the respective particles and on the composition and intensity of the background radiation will be obtained.

The evaluation of the previous Carausius experiments has shown that:

(1) Hits by single heavy ions caused body anomalies, if applied during stages of organogenesis, and were responsible for late effects, such as retarded growth after hatching.

(2) Microgravity led to disturbances of early embryogenesis resulting in reduced hatching rates.

(3) Combined action of heavy ions and microgravity aggravated the damage to early embryogenesis.

(4) In all stages of development, a hit of heavy ion under microgravity conditions, resulted in an unexpectedly high frequency of abnomal larvae.

Postflight analysis will again include analysis of hatching frequency, growth kinetics, vitality, frequency of anomalies, male:female ratio, and genetic changes in the progeny. Results in these topics obtained so far should be extended and improved. In addition, biological investigations of the observed body anomalies and the brain are planned. In case of irradiation, the brain tissue runs the highest risk from expsoure during the period of development between the third and eighth week.

The experiment uses a standard Biorack Type II experiment container. Several holes of 1 mm diameter will be drilled through the container walls to provide adequate air exchange with the environment. The experiment will be placed into the 22 °C incubator of the Biorack.

N92-23611

DOSIMETRIC MAPPING INSIDE BIORACK (7-IML-1)

G. Reitz
Institute for Aerospace Medicine
DLR
Cologne, Germany

Spacelab experiments are done in an environment with electromagnetic radiation, charged particles, and secondary radiation. This flux is not constant but changes with spacecraft inclination and altitude, solar activity, and the Earth's magnetic field. Moreover, the shielding of the spacecraft is only approximately known and depends on the payload and its arrangement.

This experiment documents the radiation environment inside Biorack and compares it to theoretical predictions. Other experiments inside Biorack need this information to determine whether changes to samples are caused by radiation or microgravity.

Dosimetric stacks, each with 20 to 100 sheets of plastic detector foils (cellulose nitrate, Lexan, and CR39) and nuclear emulsions of different radiation sensitivity are packed together with Thermoluminescence dosimeters (TLD) inside Type I containers. Crew members place two stacks in the 37 °C incubator and four in the 36 °C incubator, two of which are placed on the 1-g centrifuge. Two stacks are located in a stowage position at ambient temperature.

After the mission, the plastic detectors are etched and the nuclear emulsions are developed similar to photographic emulsions. The traces as a result of the interaction of heavy ions with matter can then be evaluated under a microscope. The number, charge, and the energy of the particles will be determined. From the TLD readings, the absorbed dose of the low-LET components (electromagnetic radiation, electrons, and protons) will be received.

During the Spacelab D1 mission, similar detectors recorded an average dose equivalent of 0.5 mSv a day. Doses in the 22 °C incubator were slightly higher than those in the 37 °C incubator. The heavy ion flux was shown to vary even in a single Spacelab rack up to a factor of 2. These results clearly show that for experiments which are critical to radiation effects it is necessary to measure radiation fields as close as possible to biological specimen.

N92-23612

GROWTH AND SPORULATION OF BACILLUS SUBTILIS UNDER MICROGRAVITY (7-IML-1)

Horst-Dieter Mennigmann
Institute of Microbiology
University of Frankfurt
Frankfurt/Main, Germany

The experiment is aimed at measuring growth and sporulation of Bacillus subtilis under microgravity.

Bacteria are simple unicellular organisms which (with exceptions)

- show no differentiation
- can live in simple liquid media where they
- grow fast (doubling time of 30 minutes or less) and
- reach high titers (10^8/ml or more).

Higher organisms exhibit so-called differentiation into cells and tissues with special functions; most bacteria do not. However, some bacteria under given circumstances (e.g., exhaustion of the growth medium) wrap up part of their cellular content into special structures ("spores") which are surrounded by a very rigid envelope - a process ("sporulation") considered to represent a simple (model) type of differentiation. Bacillus subtilis is one such type of a bacterium that can sporulate.

Thus, Bacillus subtilis is an organism well suited to study such fundamental processes of life as growth and differentiation under microgravity. The hardware for this experiment consists of a culture chamber (15 ml) made from titanium and closed by a membrane permeable for gases but not for water. Two variants of this basic structure have been built which fit into the standard Biorack container types I and II, respectively.

In the latter case next to the aforementioned main chamber, but separated by pistons, there are four side chambers: two with pistons to be operated manually by the astronaut for inoculating a few spores to start and to finally add antibiotics to halt metabolism, respectively; and two with motor-driven ones for samples to be taken in between, and to be fixed, without agitating the culture. Growth of the bacteria will be monitored by continuously measuring the optical density with a built-in miniaturized photometer. Other parameters (viability, sporulation, fine structure, size distribution of cells and spores, growth kinetics, etc.) will be measured on the fixed samples and on those where metabolism was temporarily halted, respectively.

In the former case all operations will be performed manually. Half of these smaller containers will be kept stationary while the others will be placed on a 1-g reference centrifuge. This should make it possible to distinguish between gravity effects and others (e.g., mission parameters, radiation).

This experiment to some extent is a repeat of an experiment flown in Biorack on the Spacelab D1 Mission. This previous one revealed that Bacillus subtilis in low Earth orbit starts to grow earlier, grows faster, yields a higher final number of cells, and shows a reduced tendency to sporulate. Unfortunately, due to an interruption in the communication line the experimental part "type I container" was stopped prematurely so that a proper control is missing. Nevertheless, from the former experiment sufficient results and experience was gained to warrant, for the present experiment, some minor modifications in both the experimental sequence and the hardware.

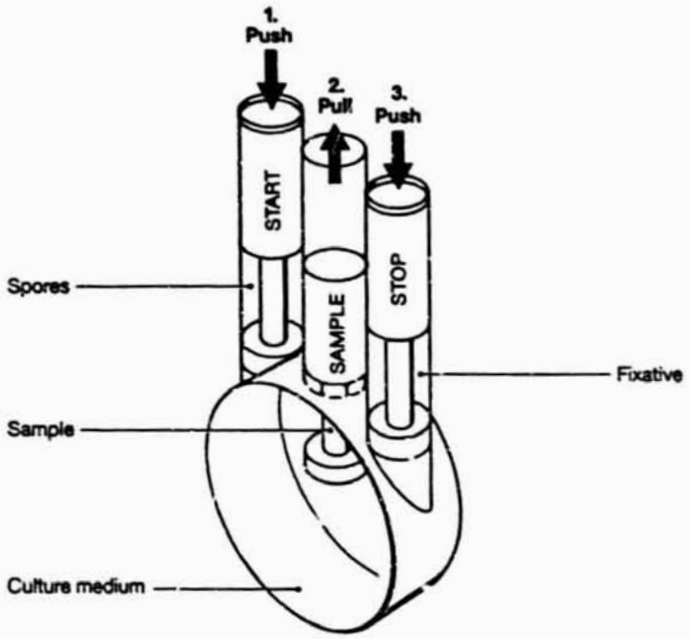

A

B

Figure 1. Experimental unit type I. (a) Basic functions; (b) experimental unit (lower left) and container (upper right). The culture chamber proper is covered from both sides by a foil permeable for gases only and which, for protection, is covered by a perforated metal plate.

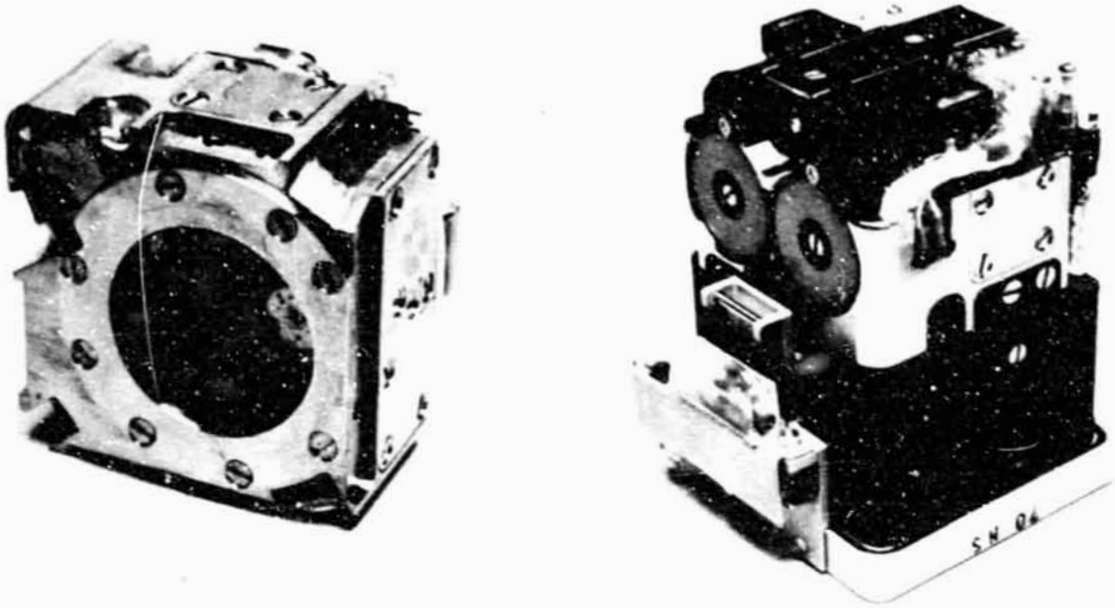

a b

c

Figure 2. Experimental unitType II. The upper shiny part of the experimental unit (a) contains the culture chamber proper, some details of which can be seen in (b); the lower black part houses the electronics. The whole unit is covered by a container (c), the holes in which are, like the culture chamber, covered by a foil permeable only for gases.

N92-23713

FRIEND LEUKEMIA VIRUS TRANSFORMED CELLS EXPOSED TO MICROGRAVITY IN THE PRESENCE OF DMSO (7-IML-1)

Augusto Cogoli
ETH Institute of Biotechnology
Zurich, Switzerland

Experiment Description

This experiment is one of three Biorack experiments being flown on the IML-1 mission as part of an investigation to study cell proliferation and performance in space. The purpose of this particular experiment is to study the adaptation of living cells to microgravity.

Friend cells are murine, virus-induced, erythroleukemic cells. Under normal conditions, only 1% or 2% of the cells are hemoglobin-positive. However, in the presence of dimethylsufoxide (DMSO) (1%) the population of hemoglobin-positive cells rises to 96% within 3 days. Therefore the in vitro transformation of Friend cells by DMSO is a good model for the study of cell differentiation and protein biosynthesis. Since previous experiments in space have shown that important cell functions such as mitosis and biosynthesis are altered under microgravity conditions, it is of great interest to extend these investigations on the adaptation of cells to a change of the gravitational environment to other systems like Friend cells. Cultures of cells will be prepared shortly before launch. Once in space, transformation will be induced by injection of DMSO. One set of cultures will be chemically fixed with glutaraldehyde for electron microscopic investigations; another set will be preserved for determining the amount of hemoglobin produced and the extend of cell proliferation.

Four Type I/O containers are filled with Friend cell cultures. One Type I/O container is filled with eight fixative syringes while another is filled with eight DMSO syringes. The experiment is initiated by the injection of DMSO into each of the Friend cell cultures. Following initiation, the cultures are incubated at +37 °C. Half of the cultures are maintained under 0-g conditions during incubation while the other half are maintained under 1-g conditions. After approximately 6 days of incubation, half of the cultures are fixed by the injection of glutaraldehyde. The fixed cultures are then transferred back into the +37 °C Incubator, together with the unfixed cultures. All four containers will remain there until Biorack unloading.

The Friend cell cultures are maintained in culture blocks, as shown in Figure 1. Two culture blocks fit inside a Type I/O container. Each culture block has a movable piston with a built-in septum. The DMSO and the fixative are injected into the cultures using pre-filled hypodermic syringes that are inserted through the septum in each culture block.

Experiment Containment and Handling

The five Type I/O containers that contain the Friend cell cultures and the fixative syringes are stowed in one of the ambient stowage inserts on the middeck during launch. The sixth container, which contains the DMSO syringes, is stowed in Spacelab stowage.

Following Biorack activation, the four containers that contain the cell cultures are transferred to the +37 °C incubator, two of them on the static rack and two on one of the l-g centrifuges. The container filled with fixative syringes is transferred to Biorack stowage in Spacelab.

The experiment is initiated by bringing the four Type I/O containers with cell cultures into the glove-box and injecting DMSO into each of the cultures blocks using the DMSO syringes. The four containers are then returned to their original positions in the + 37 °C incubator.

After approximately 6 days of incubation, two containers (one 0-g and one l-g) with cell cultures are again brought back to the glove box. The cultures are fixed. This operation is performed by injecting the fixative into the culture blocks using the fixative syringes. The containers with the fixed cultures are then transferred back into the +37 °C incubator together with the unfixed cultures. All four containers will remain inside incubator until unloading. At the end of the mission, the four containers in the +37 °C incubator are transferred to one of the ambient stowage inserts on the middeck for re-entry. The empty Type I/O containers that originally held the fixative and DMSO inducer are left in Biorack stowage.

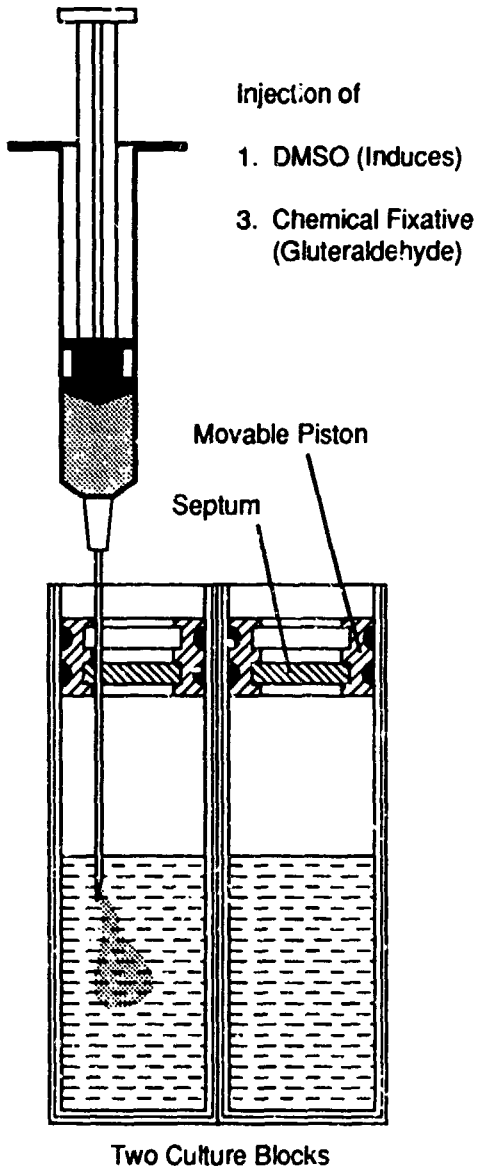

Figure 1. Friend Cell Culture Blocks.

N92-23614

PROLIFERATION AND PERFORMANCE OF HYBRIDOMA CELLS IN MICROGRAVITY (7-IML-1)

Augusto Cogoli
ETH Institute of Biotechnology
Zurich, Switzerland

This experiment is one of three Biorack experiments being flown in the IML-1 mission as part of an investigation to study cell proliferation and performance in space. The purpose of this particular experiment is to study how cell performance (biosynthesis and secretion) is altered by altered gravity conditions. Hybridoma cells are obtained by fusion of an activated B-lymphocyte with a myeloma cell. Activated B-lymphocytes, derived from a human or an animal, carry the information required to produce antibodies of a certain specificity and can survive only a few days in culture. Myeloma cells are tumor cells which can grow indefinitely in culture. Therefore, the product of the fusion is an immortal cell line capable of producing homogeneous antibodies (monoclonal antibodies). Today's technology permits one to derive hybridomas secreting antibodies against any natural or artificial antigen. The Hybridoma cell cultures are divided into two equal groups. One group is incubated for 2 days and the other group is incubated for 4 days. At pre-selected times during incubation, a label, Thymidine, is injected into the cultures in each group. When incubation is completed for the first group, DMSO is injected into cultures in that group and then those cultures are frozen. When the incubation period is completed for the second group, DMSO is injected into those cultures and they, in turn, are frozen. Half of the cultures in each group are maintained under 0-g conditions during incubation. The cultures in the other half are maintained under 1-g conditions. DMSO is used as a cryopreservative at a final concentration of 10%.

The Hybridoma cell cultures are maintained in culture blocks that are identical to those used for the Friend cell culture experiment. Two culture blocks fit inside a Type I/O container, as shown in Figure 1. Each culture block has a movable piston with a built-in septum. The label and DMSO are injected into the culture using pre-filled hypodermic syringes that are inserted through the septum in each culture block.

Four Type I/O containers are filled with Hybridoma cell cultures. Another Type I/O container is filled with eight label syringes. The DMSO is contained in eight syringes that are contained in a fabric pouch. Finally, a dummy Type I/O container is used to keep the 1-g centrifuge in balance when one of the two containers with 1-g cultures is removed.

Experiment Containment and Handling

The five Type I/O containers that contain the Hybridoma cell cultures and label syringes are stowed in one of the ambient stowage inserts on the middeck during launch. The fabric

pouch with the DMSO syringes and the dummy Type I/O container are stowed in Biorack stowage in Spacelab.

Following Biorack activation, the four containers with the cell cultures are transferred to the + 37 °C incubator. After 42 hours of incubation, 2 containers are transferred to the glove box and their cultures labelled using the label syringes. Then they are returned to their original 37 °C positions. After 6 hours of incubation with the label, the containers are returned to the glove box and DMSO is injected into each culture block using the DMSO syringes. The two containers are then transferred to the -15 °C LSLE freezer in Spacelab. DMSO is used as a cryopreservative at a final concentration of 10%.

The process is then repeated for the two containers that have remained in incubation during the first 4 days. After 88 hours of incubation for these containers, they are brought into the glove box and the label is injected into each of the culture blocks using the label syringes. These containers are then returned to their original positions in the 37 °C incubator. After 6 hours of incubation with the label, these containers are returned to the glove box and DMSO is injected into each culture block using the DMSO syringes. The two containers are then transferred to the -15 °C LSLE freezer in Spacelab.

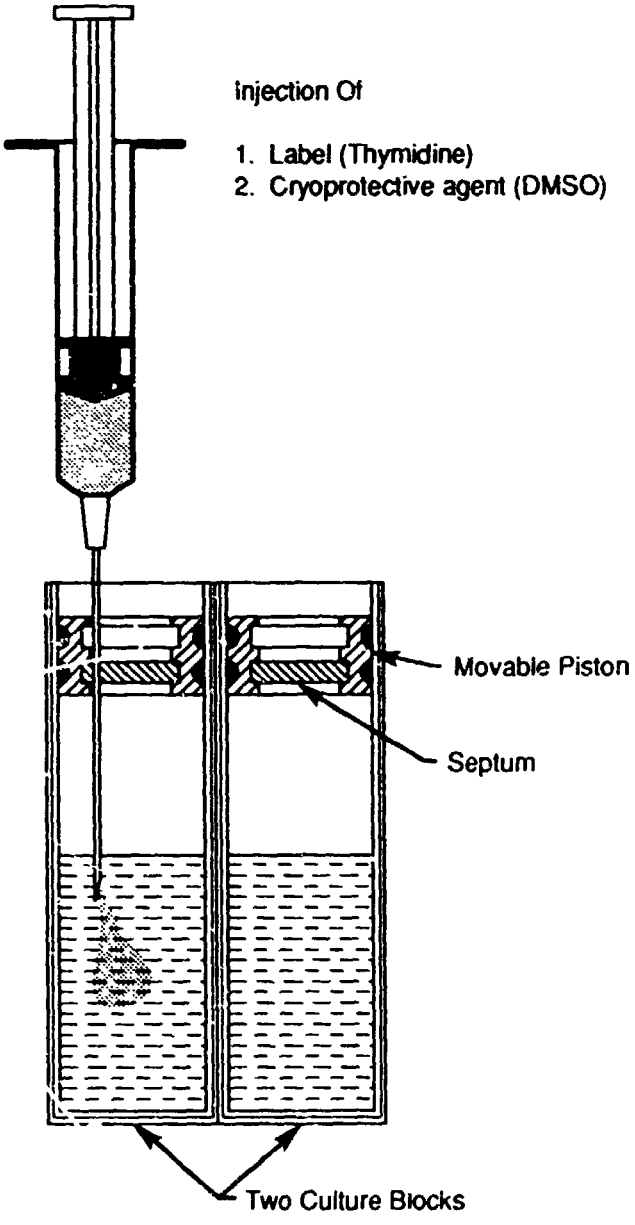

Figure 1. Hybridoma Cell Culture Blocks.

N92-23615

DYNAMIC CELL CULTURE SYSTEM
(7-IML-1)

Augusto Cogoli
ETH Institute of Biotechnology
Zurich, Switzerland

Experiment Description

This experiment is one of three Biorack experiments being flown on the IML-1 mission as part of an investigation studying cell proliferation and performance in space. One of the objectives of this investigation is to assess the potential benefits of bioprocessing in space with the ultimate goal of developing a Bioreactor for continuous cell cultures in space. This experiment will test the operation of an automated culture chamber that was designed for use in a Bioreactor in space.

A Bioreactor for processing in space will consist of many single pieces of hardware. One of the most critical pieces is the culture chamber. Moreover, since a Bioreactor is a complex instrument, any device capable of simplifying the system is welcome. The device to be tested is called the Dynamic Cell Culture System (DCCS). It is a simple device for cell cultures in which media are renewed or chemicals are injected automatically, by means of osmotic pumps.

For the first test in space, a well known cell line, Syrian Hamster Kidney Cells, has been selected. This cell line is dependent on a surface to grow on. This requirement is met by the introduction of microcarriers consisting of collagen-coated, dextran beads.

This experiment uses four Type I/O experiment containers. One DCCS unit which contains a culture chamber with renewal of medium and a second culture chamber without a medium supply fits in each container. Two DCCS units are maintained under 0-g conditions during the on-orbit period. The other two units are maintained under 1-g conditions on a 1-g centrifuge. A DCCS unit is illustrated in Figure 1.

The four Type I/O containers are stowed in one of the ambient stowage inserts on the middeck during launch. Following Biorack activation, the four containers are transferred to the +37 °C incubator, with two containers on the static shelf and the other two containers on one of the 1-g centrifuges. Near the end of the mission, the four containers will be transferred to the glove box and the osmotic pump shut down in each container. Two containers are then returned to the +37 °C incubator, the remaining two to the +4 °C cooler. At the end of the mission, the two cooled containers are transferred to one of the +5 °C PTCUs on the middeck; the remaining two are placed in one of the ambient stowage inserts on the middeck for re-entry.

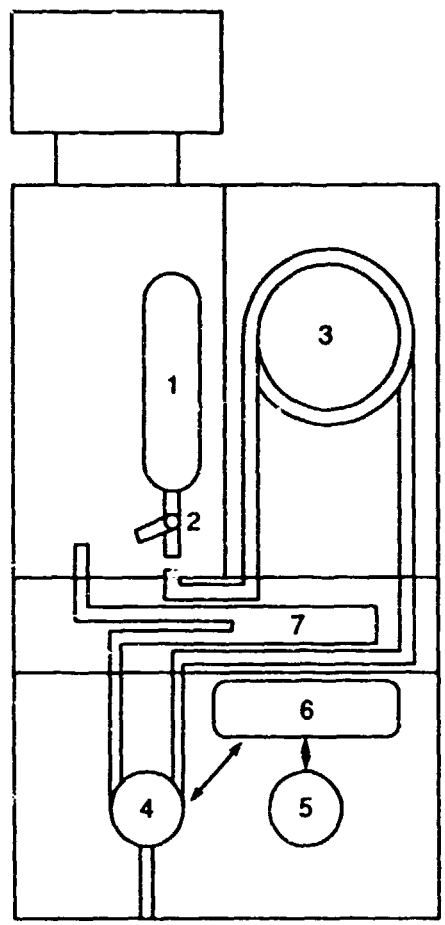

1 Osmotic Pump
2 Valve
3 Medium Reservoir
4 Active Chamber
5 Batch Chamber
6 Gas Chamber
7 Waste Reservoir

Figure 1. Dynamic Cell Culture Chamber.

N92-23616

GROWTH, DIFFERENTIATION AND DEVELOPMENT OF ARABIODOPSIS THALIANA UNDER MICROGRAVITY CONDITIONS (7-IML-1)

E. P. Maher
The Open University in Scotland
United Kingdom

L. G. Briarty
Department of Botany, University of Nottingham
United Kingdom

A number of aspects of cellular development and differentiation are known to be influenced when organisms are grown under microgravity conditions. In the case of plants, their overall behavior may be modified, as well as there being perceptible differences in the structure of individual cells. The aim of this experiment, or rather set of experiments since it covers a range of different observations, will be to quantify the structural and behavioral changes taking place in germinating seeds of the small plant Arabidopsis thaliana.

The protocol to be used will involve germination of the seeds in orbit, and then their growth will be followed by fixing and photographing samples of microgravity-grown and 1-g control seedlings at intervals over 4 days. The different studies which will then be performed can be classified in relation to the parts of the plant involved.

The first study will be an examination of the ultrastructure of the root statocytes, the cells containing gravity sensors, to determine whether their development proceeds normally under microgravity conditions; this is essential before any more ambitious experiments on graviresponse can be contemplated. The effects of growth in microgravity on the polarity of the statocytes, and on the structure, orientation, and distribution of their amyloplasts will be investigated. The provision of a 1-g centrifuge on the Biorack enables this to be done under carefully controlled conditions.

A second study will examine the differences in root and shoot development and orientation between normal wild type seedlings and those of an agravitropic mutant (aux-1), one which does not respond normally to gravity. Will the normal seedlings in microgravity behave like agravitropic mutants at 1 g?

A third set of observations will be made on the structural changes occurring during reserve breakdown and utilization in the cells of the cotyledons, the storage organs of the seed. Under normal circumstances these change from being lipid and protein-filled organs to become green and leaf-like. This is a development sequence which is fairly well understood, and it will serve as a model for study of the effects of microgravity on a complex sequence of processes.

Quantitative stereological analysis of cell shape, structure, and content, and a study of cytoskeleton organization, will allow a stage by stage comparison of development in 1 g and microgravity conditions.

The fourth part of the work will be an examination of the statocytes present in the shoot and their development in microgravity. These are organs which have received less investigation than root statocytes, and comparison of the development and organization of the two homologous organs should be of value.

The final, and perhaps the simplest part of the study, will provide an answer to the debated question of whether the formation of the hypocotyl hook in seedlings is gravity-dependent. Agravitropic mutants do not form normal hypocotyl hooks when grown at 1 g.

These are studies which have developed from ground-based research on agravitropic mutants and on normal seed formation and development. However, the overall objectives of the work are to determine what might be the long-term effects of microgravity on the growth of plants. This, in turn, is of utmost importance if plants are to be used as elements of closed or semi-closed life-support systems of the sort which will be essential for long-term spaceflight.

The part of the experiment to be carried out in orbit consists of the germination of the seeds by adding water to them, then their subsequent growth and fixation at intervals, with some samples being kept in microgravity conditions while others are maintained on a 1-g control centrifuge in the Biorack. A repeat of all the procedures will be carried out under identical conditions on the ground to provide a further control.

All the manipulations will be carried out with the plants in growth chambers 18 x 20 x 30 mm, two of which fit into a Biorack Type I container (Figures 1 and 2). The growth chamber is a simple closed container with a transparent lid, and with a silicone rubber septum at each end. The seeds are launched glued to a porous substrate with a plant gum (Figure 3), there being 13 seeds of the wild type and 12 of the mutant in each chamber. Growth is started, probably on day 4 of the mission, by injecting a measured amount of water through one of the growth chamber septa with a syringe. The water is absorbed into the substrate and into the seeds, and the gum retaining them is dissolved. For germination to occur these seeds require a light stimulus, and so after they have imbibed water for 12 hours, the growth chambers are placed under the Biorack lamp for 30 minutes (Figure 4). The growth chambers are replaced in their Biorack containers, four in the Biorack 22° incubator in microgravity and two on the 1-g control centrifuge.

Fifty hours after initial hydration, the first samples are taken. Two growth chambers from microgravity and one from the 1-g centrifuge are removed to the Biorack glove box. They are photographed in stereo, and then each is filled with fixative by injection from a demountable, glutaraldehyde-filled syringe (Figure 5) through the septa, the displaced air and any excess fixative being retained in an empty syringe. (The syringes are stored in a separate Type II container.) The growth chambers are re-photographed, and are then placed in storage at 5

degrees where they are retained until recovery after landing. This sequence is repeated a further three times at 15 hour intervals giving a total of four sets of samples.

On return of the samples to the investigators they will immediately be processed for light and electron microscopy so that they can be returned to the home laboratories in a stable form for subsequent analysis. The stereoscopic photographs will be used for the identification of individual seedlings, as well as giving data on their morphology during growth.

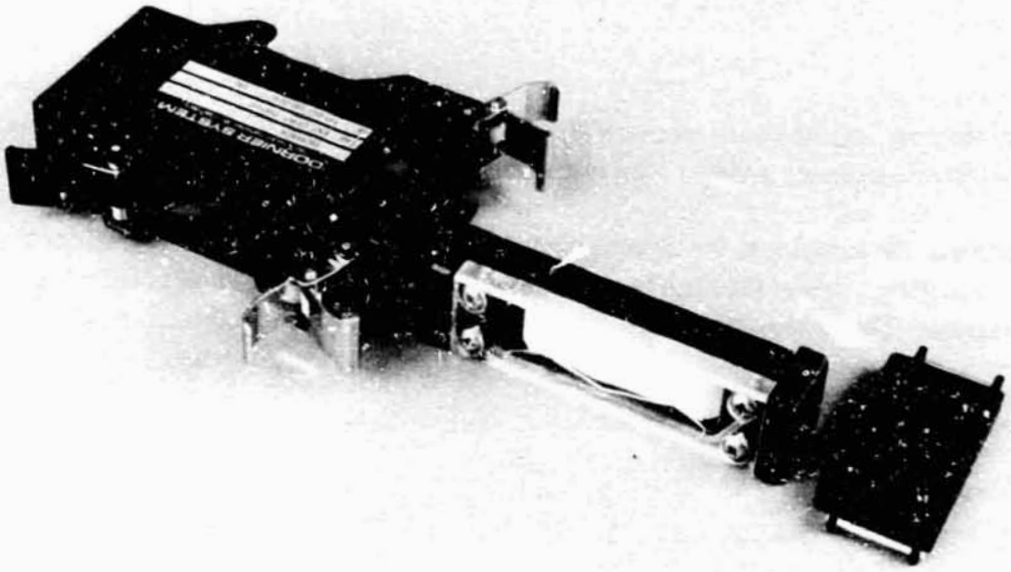

Figure 1. A growth chamber for experiment SHOOTS together with a Biorack container.

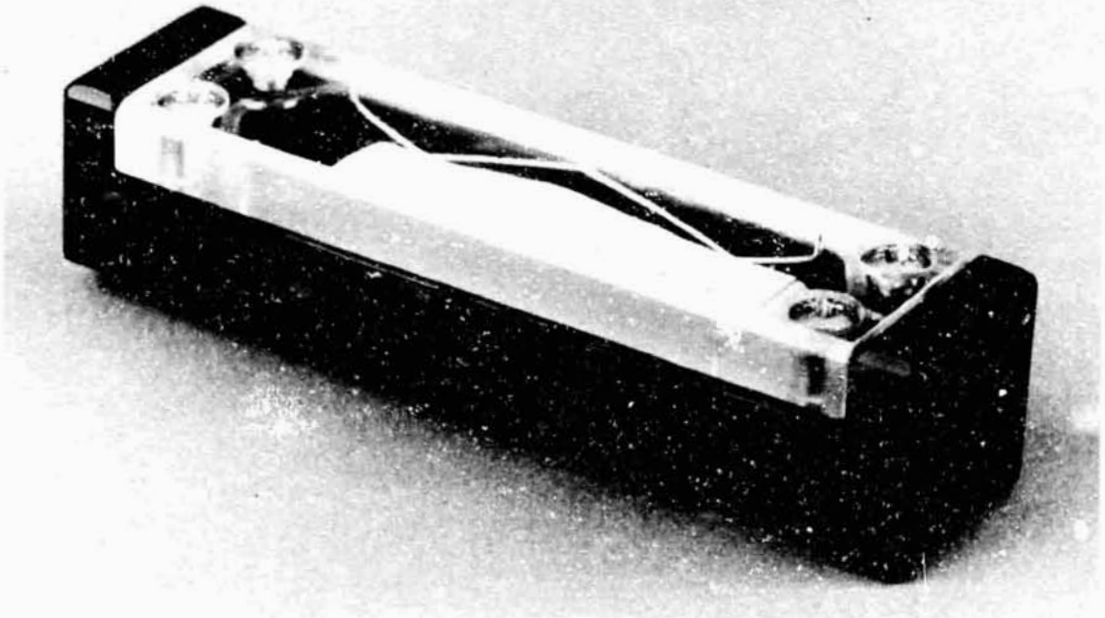

Figure 2. A SHOOTS growth chamber; the seeds can just be seen, lying along the centre line.

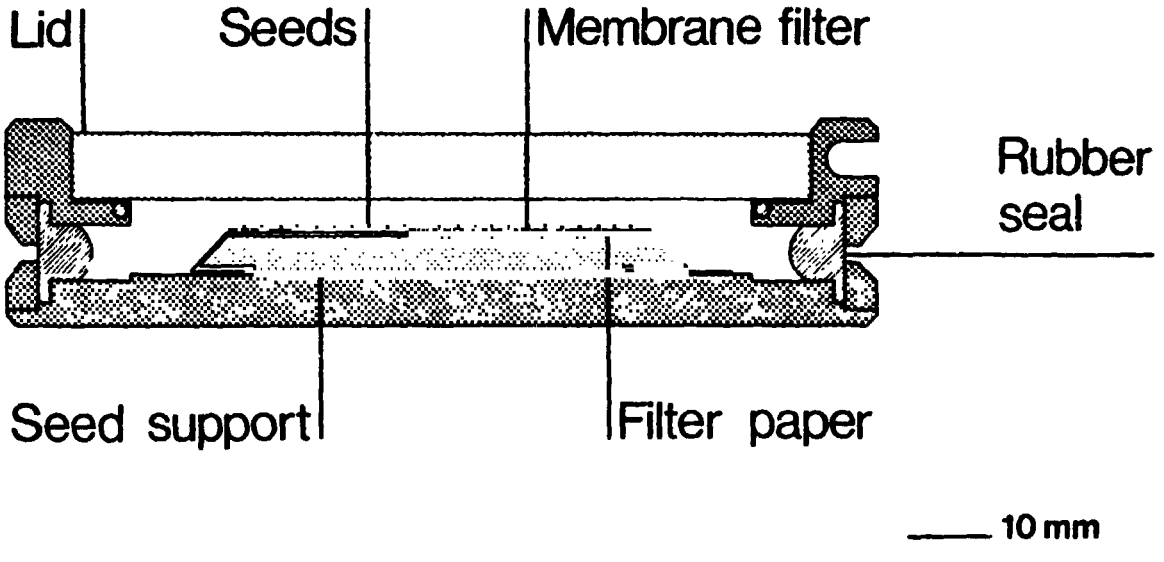

Figure 3. Section through an assembled SHOOTS growth chamber showing the positions of the seeds on their support, and the rubber seals through which liquids are introduced.

IML–1 Biorack Experiment SHOOTS

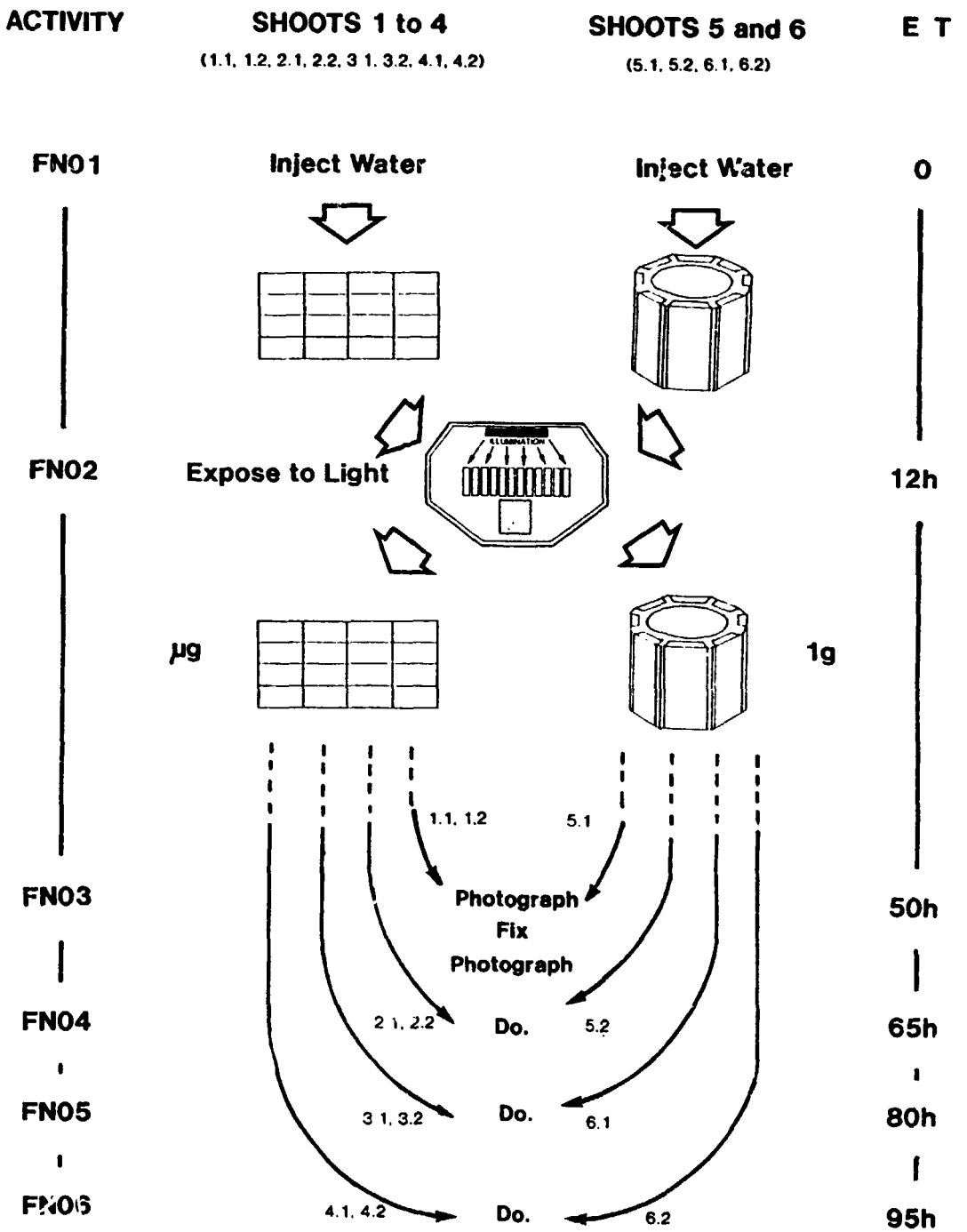

Figure 4. Sequence of activities carried out for experiment SHOOTS. The numbers (e.g., 1.1, 2.1) identify individual growth chambers.

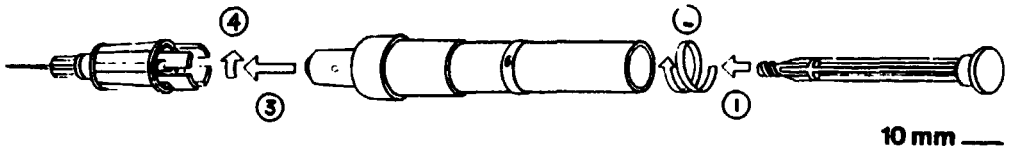

Figure 5. The components of the syringe used for fixative injection. The numbers indicate the order of assembly.

N92-23617

TRANSMISSION OF GRAVISTIMULUS IN THE STATOCYTE OF THE LENTIL ROOT (7-IML-1)

Gerald Perbal
Universite Pierre et Marie Currie
Paris, France

When a primary root is not correctly oriented with respect to gravity, it bends in order to reorient its extremity in the direction of the g vector. The cells (statocytes) responsible for gravisensing in roots are located in the center of the cap. Statocytes show a polarization of their organelles, the nucleus being situated near the proximal wall, whereas the amyloplasts (statoliths) are sedimented on large aggregates of endoplasmic reticulum at the distal pole. It is generally accepted that amyloplasts are responsible for gravisensing and that their sedimentation is necessary to trigger the gravitropic response.

The relative density of starch is greater than that of the surrounding cytoplasm and the amyloplasts therefore move in the statocytes when the root is subjected to a change in orientation: when the root is placed horizontally, the amyloplasts sediment along the longitudinal wall, but do not touch the plasma membrane. The nature of the cellular structure that plays the role of the transducer of the action of these organelles is still controversial.

The aim of this Biorack experiment is to determine the presentation time (minimum stimulation period to provoke a slight but significant response) of gravireaction of lentil roots cultivated in microgravity for 27 hours.

The location of the statoliths in the statocytes will be analyzed in parallel in order to find the cell structure (endoplasmic reticulum, microtubules, plasma membrane) which can transmit the physical effect of the pressure of the statoliths into a biochemical factor leading to an asymmetrical production or release of the inhibitor which is reponsible for the gravitropic response.

Seeds of Lens culinaris will be used because of their small size, the homogeneity of their germination and, in particular, because they are very sensitive to gravistimulus.

The dry seeds, with their coat removed in order to facilitate root growth, will be placed in small growth chamber (Figs. 1 and 2). The minicontainers consist of a transparent cover and a metal partition with holes punched into it to allow hydration of the cellulose sponge. The seeds will be held in place on the sponge by means of a metal bar and will be oriented so that the roots would grow in the direction of the main axis of the chamber

The experiment will be activated by injecting water into the sponge through one of the two entry tubes (Fig. 3) by means of a syringe with a special cap coupled to the chamber. Two

minicontainers will be then placed together on a metal holder and inserted into a type I container (Fig. 4) which will be in turn inserted into the 22 °C Biorack incubator.

The first sample will be fixed by glutaraldehyde just after the stimulation period (5, 10, 15, 25, 40 and 60 min). To do this, the crew will introduce the minicontainer in a special device and the glutaraldehyde will be injected into the minicontainers by means of a spring-driven piston. Excess pressure will be avoided by pushing air and water out of the minicontainer onto the top of the piston.

The second sample will be placed in front of a camera in order to follow the gravitropic reaction of roots. Time lapse photography will make it possible to calculate the kinetics of the gravicurvature as a function of the duration of the stimulation.

The nature of the cellular structure responsible for the transduction of the pressure of amyloplasts into an asymmetrical signal will be determined.

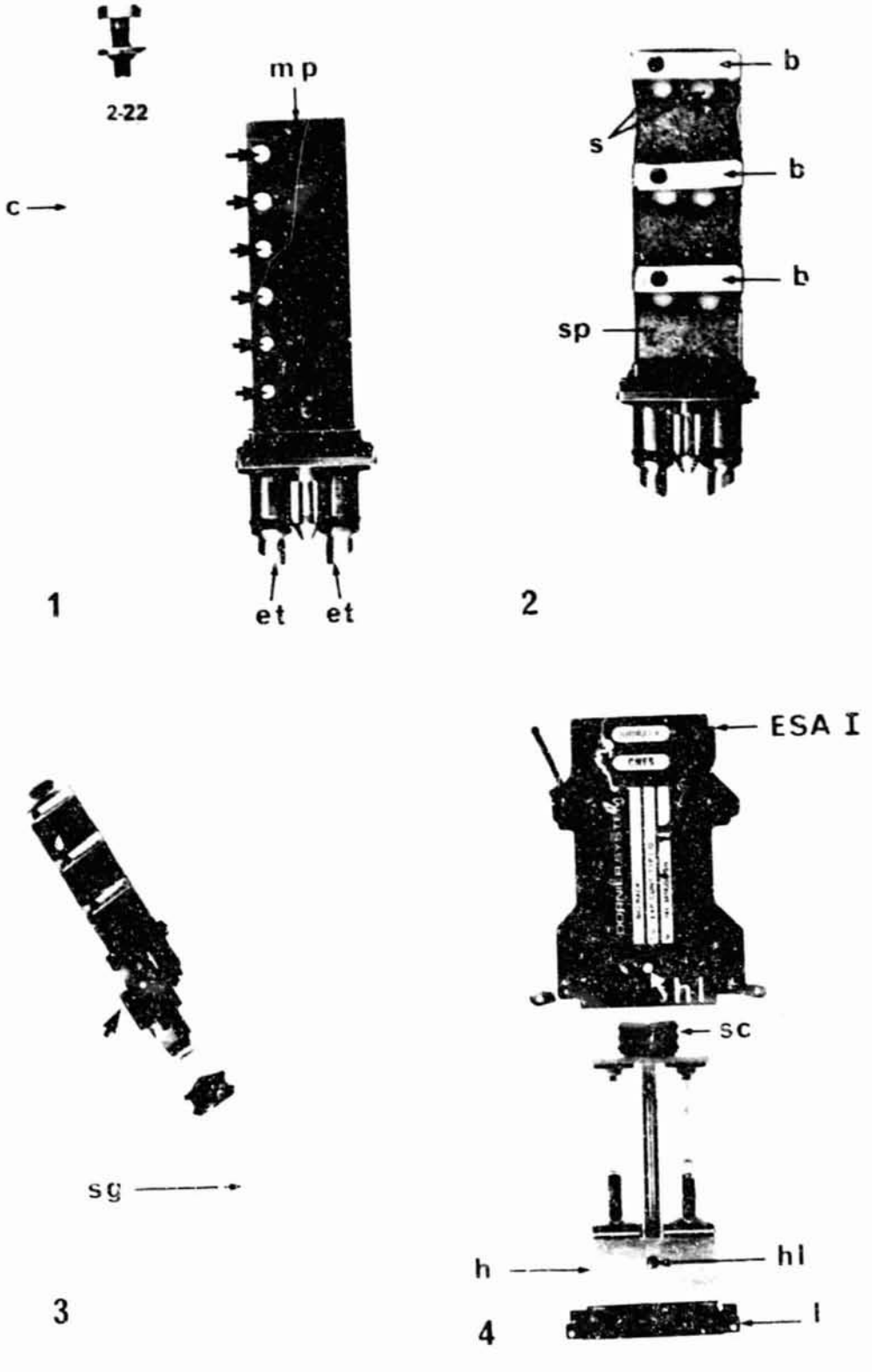

Figures 1 and 2. Minicontainers. b, metal bars; c, cover; et, entry tube; mp, metal partition; s, seed; sp, cellulose sponge.

Figure 3. Hydration of a minicontainer. sg, syringe, arrow, special cap.

Figure 4. ESA Type I container with two minicontainers. h, holder; hl, hole; l, lid; sc, screw.

N92-23618

GRAVITY RELATED BEHAVIOR OF THE ACELLULAR SLIME MOLD PHYSARUM POLYCEPHALUM (7-IML-1)

I. Block
DLR, Germany

Gravitational biology investigates the influence of gravity on living organisms. One approach is to look for the effects the absence of gravity has on cells, plants, and animals. This will promote the understanding of conditions a human being is exposed to during long-term space flights; simultaneously, gravitational biology contributes to the general understanding of life. The investigation of free living single cells, especially of those having no specialized structures for the perception of gravity (gravireceptors), but nevertheless performing a clear orientation reaction towards gravity (geotaxis), will clarify the question of a general gravisensitivity of cells.

The objective of the present experiment is to investigate the effect of near weightlessness (0 g) on a single cell. The test object is the acellular slime mold Physarum polycephalum (Figure 1). This cell of variable size (in the experiment about 1 cm in diameter) is composed of a network of protoplasmic strands which perform rhythmic contractions in the minute range. These contractions of the strands' ectoplasmic walls generate the force to drive the vigorous shuttle streaming of fluid protoplasm inside the strands (hydrostatic pressure flow). A net transport of protoplasm in one direction determines the direction of the cell's locomotion. External stimuli may influence, via changes of the contraction rhythm, the cell's locomotion itself. In this way gravity modifies the contraction rhythm of the strands, the streaming velocity of protoplasm in the strands, and the direction of locomotion of the whole slime mold (geotaxis).

These effects of gravity on the contraction rhythm and on the streaming velocity were demonstrated in previously conducted experiments involving a single 180°-horizontal turn in the Earth's gravity field, the simulation of the weightless condition on the fast-rotating clinostat, and real near weightlessness during the Spacelab D1 Mission (only one experiment): the contraction rhythm always responds with a transient increase in frequency. Thereafter the slime mold adapts to the new conditions by a backregulation to the initial values. The streaming velocity shows a more permanent response: during 0-g conditions it is increased. The IML-1 mission gives the opportunity to verify and improve these results and to perform a statistical evaluation of the data obtained (parts 1 and 4 of the experiment).

The other parts of the experiment will address the major question of how this cell, which does not possess any specialized gravireceptors, gets the information about the direction of the gravity vector. The basis of this approach is the photoreaction of the slime mold which it performs upon illumination with white and blue-green light. The light induces a transient decrease in contraction frequency, which is quite the opposite response as induced by a

gra stimulus. Apart from that, both light and gravireactions not only follow the same time pattern but are followed by similar backregulations to the initial values. In the flown experiment we expect indications concerning the mechanisms involved in g-perception and regulation from the simultaneous as well as from the subsequent initiations of the two reactions (parts 2 and 3 of the experiment, respectively). Results of previously conducted ground-based experiments are pointing to the involvement of mitochondria, which not only provide the energy necessary for the contractions, but which also play an important role in the regulation of the contraction rhythm and they might even be the g-receptors themselves. The role of the mitochondria in the generation of the contraction rhythm is speculative, but perhaps also here some enzyme will be identified as being the "oscillophore", as is the case for glycolysis. Oscillophores may be the basics for biological-including circadian-rhythms.

The hardware for this experiment includes four standard ESA Biorack Type I containers, each containing two small culture chambers made of aluminum (64 x 20 x 9.5 mm) in which the slime molds are cultivated (Figure 2). Each chamber has two glass windows, one red and one clear, the latter covered with a removable red transparent tape as a protection against light of the shorter wavelengths.

The experiment will be performed in the Biorack glove box using the improved ESA Biorack light microscope, which in its original configuration was flown in the Spacelab D1 Mission. It is now a real multi-purpose research microscope (Figure 3), providing the light intensity necessary for a reliable performance of the photoreaction part of the experiment. Incorporated into one of the microscope's binocular eyepieces is a photo-diode light measurement system to record changes in light transmission resulting from the rhythmic contractions of the strands. Moreover, the microscope is fitted with a Sony video camera to allow a simultaneous recording of the streaming velocity of protoplasm in the strands.

Experiment Procedure: Shortly before launch the Type I containers will be placed in the 10 °C PTCU and loaded into the middeck of the shuttle. In-flight an experiment session will be initiated by transferring two Type I containers to a 1-g centrifuge located in the Biorack incubator A (22 °C). After about 5 hours, the light-microscope assembly will be installed in the Biorack glove box. The following typical experiment session will be composed of four parts:

(1) Measurement of the 0-g reaction (repetition of the D1 experiment): it is intended to increase the amount of data to allow a statistical evaluation. Two culture chambers will be transferred from the 1-g centrifuge to the glove box, where one chamber will be put aside for the third part of the experiment and the other chamber will be inserted in the microscope. There the slime mold's response to the 1-g to 0-g transition will be recorded.

(2) Photoreaction measurement with simultaneous induction of the 0 g and light reactions: Another culture chamber will be taken from the centrifuge and, immediately before its insertion in the microscope, its red-light protection filter will be removed to allow the light stimulation of the slime mold.

(3) Photoreaction measurement of the 0 g-adapted slime mold, which had remained in the glove box since the first part of the session.

(4) Measurement of the 0 g-adapted slime mold without light stimulation: to be performed after the reattachment of the red-light protection filter to the chamber already observed in part 3.

The 2-hour experiment session will be closed by returning the culture chambers to the Type I containers and these to the 10 °C PTCU. The microscope will be stowed in the Biorack overhead stowage container.

As a control a parallel experiment session will be run simultaneously to the space experiment in the ground laboratory at the KSC.

In conclusion, the investigation aims at improving our knowledge of a general gravisensitivity of cells and additional information is expected on the mechanisms involved in g-perception and regulation.

ORIGINAL PAGE
BLACK AND WHITE PHOTOGRAPH

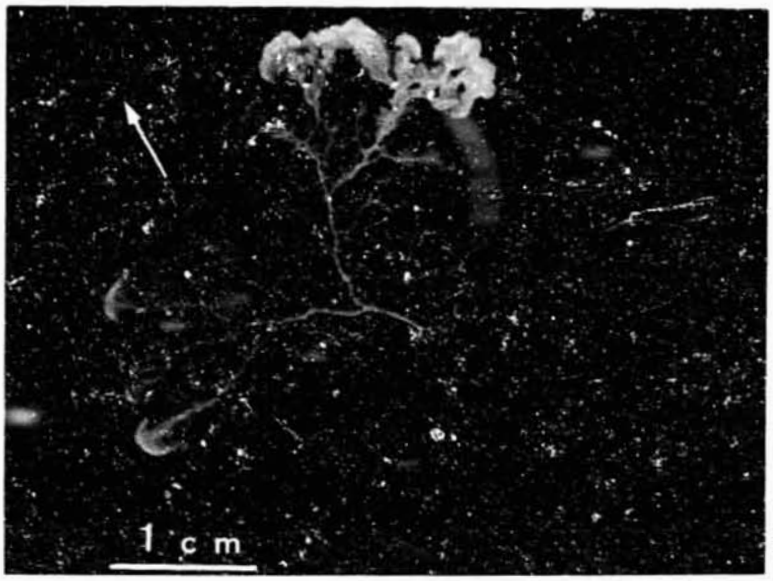

Figure 1. The acellular slime mold Physarum polycephalum showing the network of strands and the leading front zones (above and left). The direction of locomotion of the cell is indicated by the white arrow.

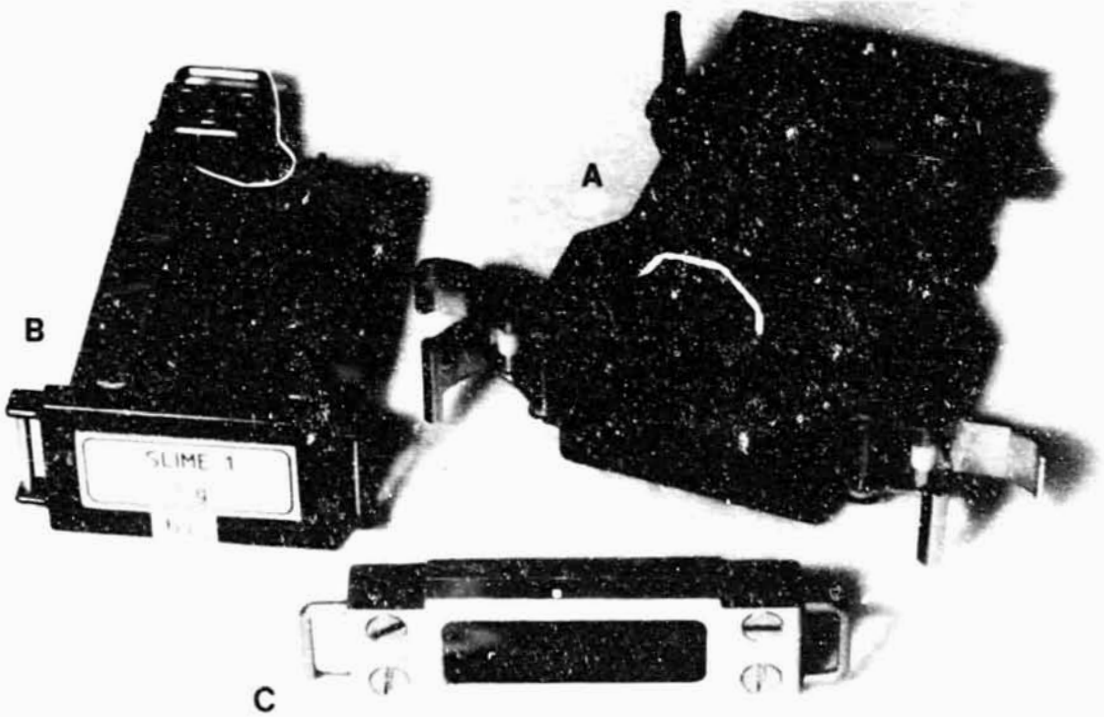

Figure 2. Hardware for the experiment (already used in D1): (A) Type I container, (B) holder for two culture chambers, and (C) culture chamber.

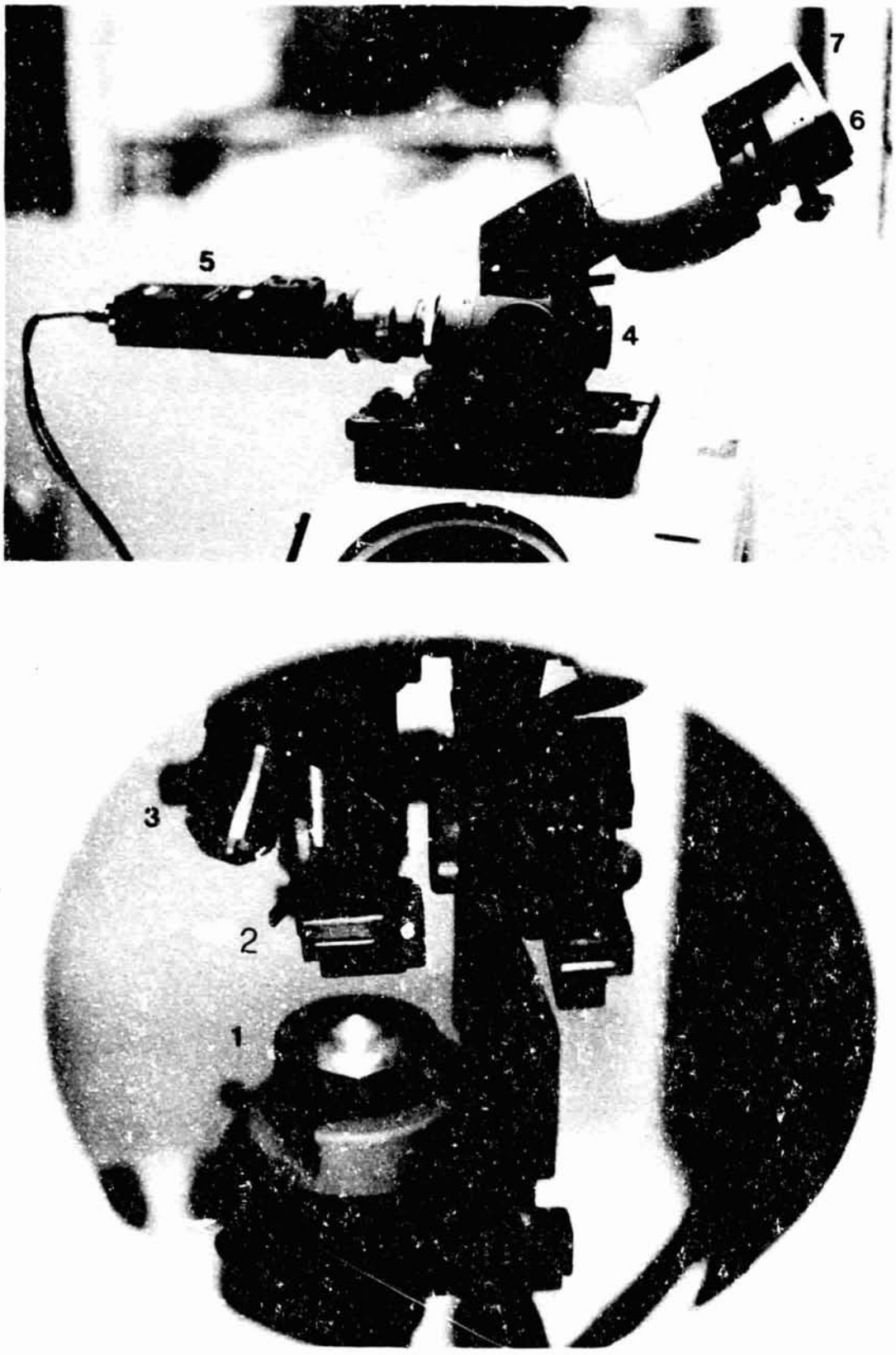

Figure 3. The ESA Biorack light microscope (breadboard) to be used in two Biorack experiments. Description starting below: (1) condensor, (2) sample holder with inserted culture chamber, (3) objectives, (4) beam splitter, (5) video camera, (6) eyepiece, (7) photo-diode assembly

N92-23619

STUDIES ON PENETRATION OF ANTIBIOTIC IN BACTERIAL CELLS IN SPACE CONDITIONS (7-IML-1)

R. Tixador
Universite Paul Sabatier
Toulouse, France

The first space microbiology experiment was made over 20 years ago by Y. Gagarine who carried an E. coli culture on the first manned flight aboard Vostok I. This was followed by several other biological experiments performed over the next few years on either manned or unmanned flights.

In the early days, these simple experiments did not produce spectacular results. In fact, the investigators only reported the results of post-flight investigations carried out on micro-organism subcultures after recovery. The findings are often difficult to explain, not only because the investigations were not carried out in flight but also, in many cases, because of poorly controlled experimental condition. One of the first space microbiological experiments of real interest was performed by R. Staehle. During the Skylab 2 and 4 missions, he studied the behavior of several bacteria in space, particularly the growth of colonies, the mutation rates and the morphological characteristics of Bacillus subtilis, Bacillus mycoides, and E. coli. Only Bacillus subtilis developed in flight and revealed marked changes in the morphology of colonies in the space samples. On the other hand, modifications of antibiotics sensitivity were observed for several antibiotics in post-flight tests.

Another very interesting microbiological experiment was carried out by G.R. Taylor and S.N. Zaloguev during the American/Soviet joint manned flight, the Apollo-Soyuz Test Project (ASTP). They took microflora samples from various parts of the astronauts bodies, before, during, and after flight. The main aim of this experiment, jointly conducted by American and Soviet scientists, was to study a possible bacterial transfer in the confined environment of a spacecraft. Other complementary experiments were also performed, on bacterial samples collected during the pre-flight, in-flight, and post-flight phases and tested after the flight with a number of antibiotics. The results showed that bacteria collected inflight presented a higher resistance to antibiotics than samples collected during the pre- and post-flight phases.

Other results showed a stimulating effect induced by space flight in several microorganisms. V.A. Kordium observed that the growth rate of Proteus vulgaris cultivated aboard Salyut 6 was strongly stimulated. A similar phenomenon was reported by H. Planel on Paramecium tetraurelia cultivated aboard Salyut 6 in experiments Cytos 1 and Cytos M, and by G. Richoilley on the same protozoan during the D1 mission. This increase in the growth rate observed in flight, is also described by D. Mergenhagen on Chlamydomonas reinhardii and by D.

Me nigmann on Bacillus subtilis also during the D1 mission. Moreover, R.A. Mattoni also reported a stimulation of the Salmonella proliferation developed aboard the second Biosatellite.

On the other hand, the Cytos 2 experiment was performed aboard Salyut 7 in order to test the antibiotic sensitivity of bacteria cultivated in vitro in space. An increase of the Minimal Inhibitory Concentration (MIC) in the inflight cultures, that is, an increase of the antibiotic resistance was observed (R. Tixador); complementary studies of the ultrastructure showed a thickening of the cell envelope (L. Lapchine).

In order to confirm the results of the Cytos 2 experiment, we performed the ANTIBIO experiment during the D1 mission to try to differentiate, by means of the 1-g centrifuge in the Biorack, between the biological effects of cosmic rays and those caused by microgravity conditions. The originality of this experiment was in the fact that it is also designed to test the antibiotic sensitivity of bacteria cultivated in vitro during the orbital phase of the flight.

The results show an increase in resistance to Colistin in in-flight bacteria. The MIC is practically double in the in-flight cultures: 2 µ/ml for in-flight cultures and 1 µ/ml for the ground-based control cultures.

A cell count of living bacteria in the cultures containing the different Colistin concentrations showed a significant difference between the cultures developed during space flight and the ground-based control cultures.

The comparison between the 1-g and 0-g in-flight cultures show similar behavior for the two sets. Nevertheless, a small difference between the two sets of ground based control cultures was noted. The cultures developed on the ground centrifuge (1.4 g) present a slight decrease in comparison with the cultures developed in the static rack (1 g).

In order to approach the mechanisms of the increase of antibiotic resistance on bacteria cultivated in vitro in space we have proposed the study on penetration of antibiotics in bacterial cells in space conditions. This experiment (AO-BR- IML1-23F) was selected for IML 1 mission.

1. Biological material

- Bacterial strain:
  E. coli ATCC 25922

- Compound of culture medium:

$SO_4(NH_4)_2$	2 g
PO_4H_2K	0.117 g
PO_4HNa_2	3.272 g
$C_6H_{12}O_6$	5 g
H_2Od Q.S.	1000 ml
Yeast extract	0.5 g
pH	7 6

- Antibiotic:
  Dihydrostreptomycin 3H

2. Packaging of cultures

The culture chambers used will be similar to the plastic bags previously described by R. Tixador et al. and used in previous experiments. Each culture chamber contains 0.7 ml of culture medium with Dihydrostreptomycin 3H at a subinhibitory concentration of 2 µ g/ml and a glass ampoule filled with the bacterial suspension (Figure 1).

The glass ampoules will be filled under pressure with an overnight bacterial culture diluted in physiological water. The concentration of this suspension will be determined so as to obtain an inoculum of 2.5×10^5 bacterial/ml at the inoculation of the culture. The filled culture chambers will be welded in sterile conditions and placed by layers of four in a mechanical device which will be fitted into a Biorack Type 1 experiment container. The ampoules will be broken by the astronaut thus provoking the inoculation of cultures (Figs. 2 and 3).

The containers will be placed respectively on a static rack and on the 1-g centrifuge.

3. Pre-experiment preparation

The antibiotic Dihydrostreptomycin 3H and E. coli bacteria will be prepared and tested just before this experiment (Figure 4).

4. Experiment (Figure 5)

Four sets of identical cultures will be placed respectively:

In-flight: on 0-g static rack

on 1-g centrifuge.

In the ground-based Biorack

synchronous experiment

The containers will be maintained at a low temperature of +4 °C until the active phase of the experiment.

The start of the active phase will be initiated when the cultures will be inoculated by breaking the ampoules. They will then be placed in the incubator at 37 °C (± 1 °C).

At regular intervals, a set of cultures will be picked from the incubator and stored at 4 °C in the cooler in order to stop the bacterial development.

5 Post-flight phase (Figure 6)

After landing the biological material will be recovered and treated immediately for the laboratory investigations (radioactive measurement, electron microscopy, cell count, etc.).

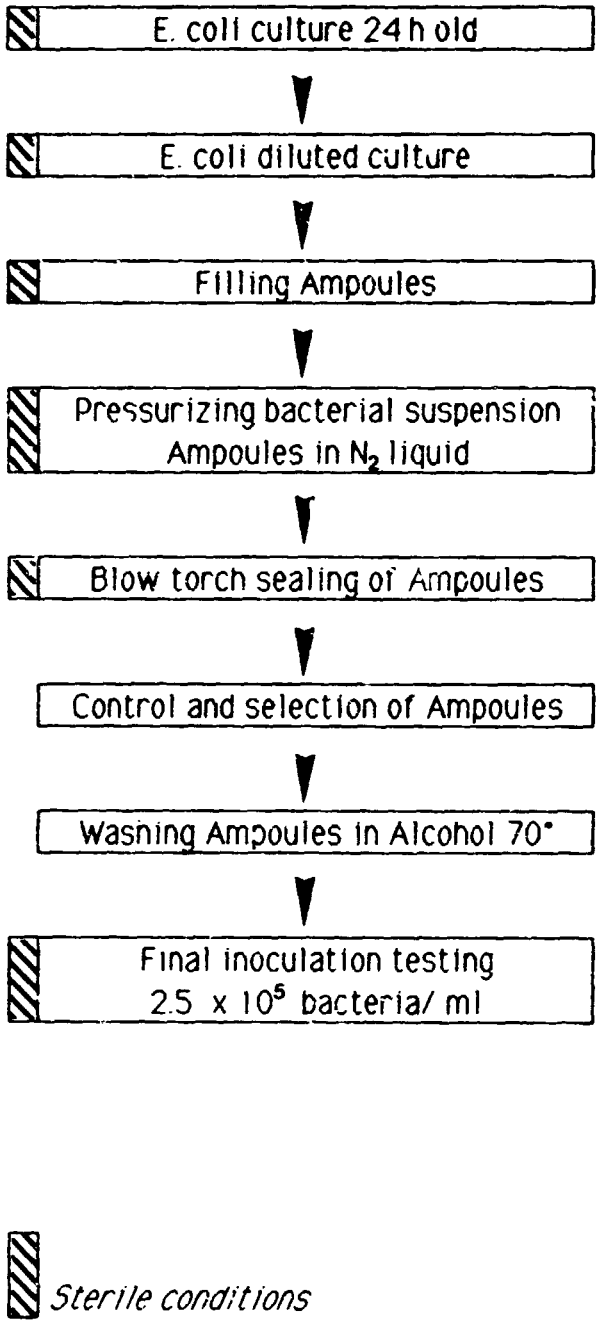

Figure 1. Bacteria Suspension Procedure.

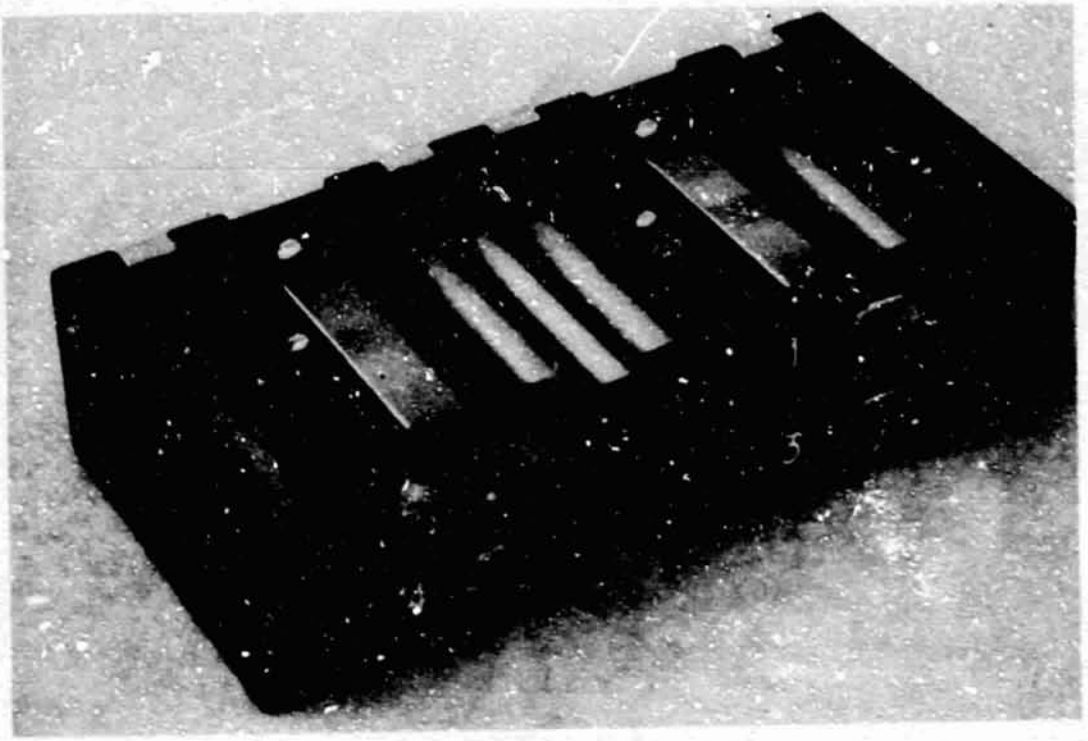

Figure 2. Experiment Hardware.

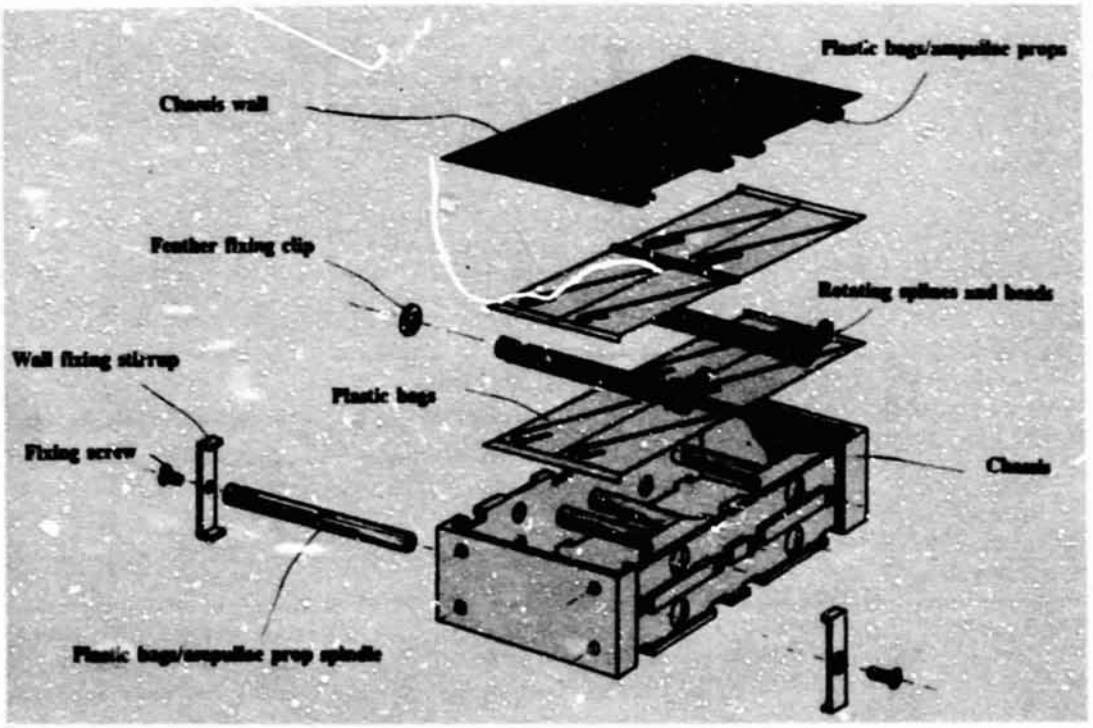

Figure 3. Cutaway of the Hardware with Cultures Chambers.

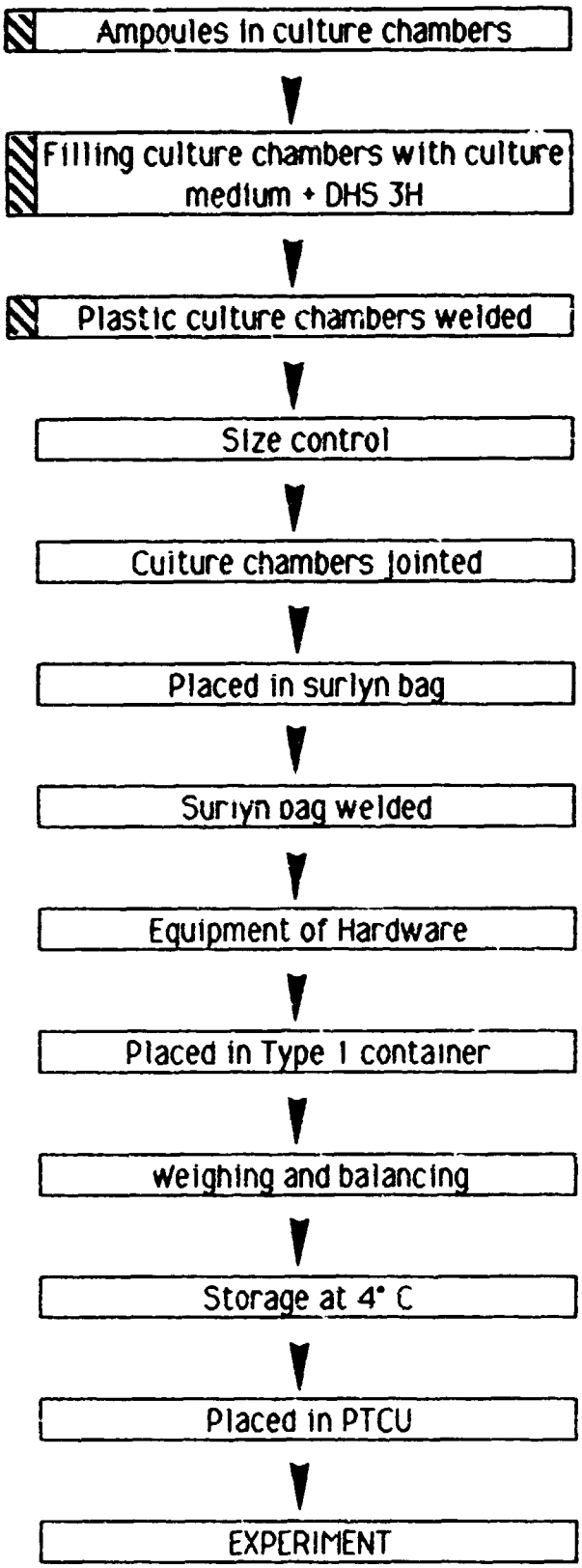

Figure 4. Pre-Launch Preparation.

IN FLIGHT AND GROUND BASED CONTROL

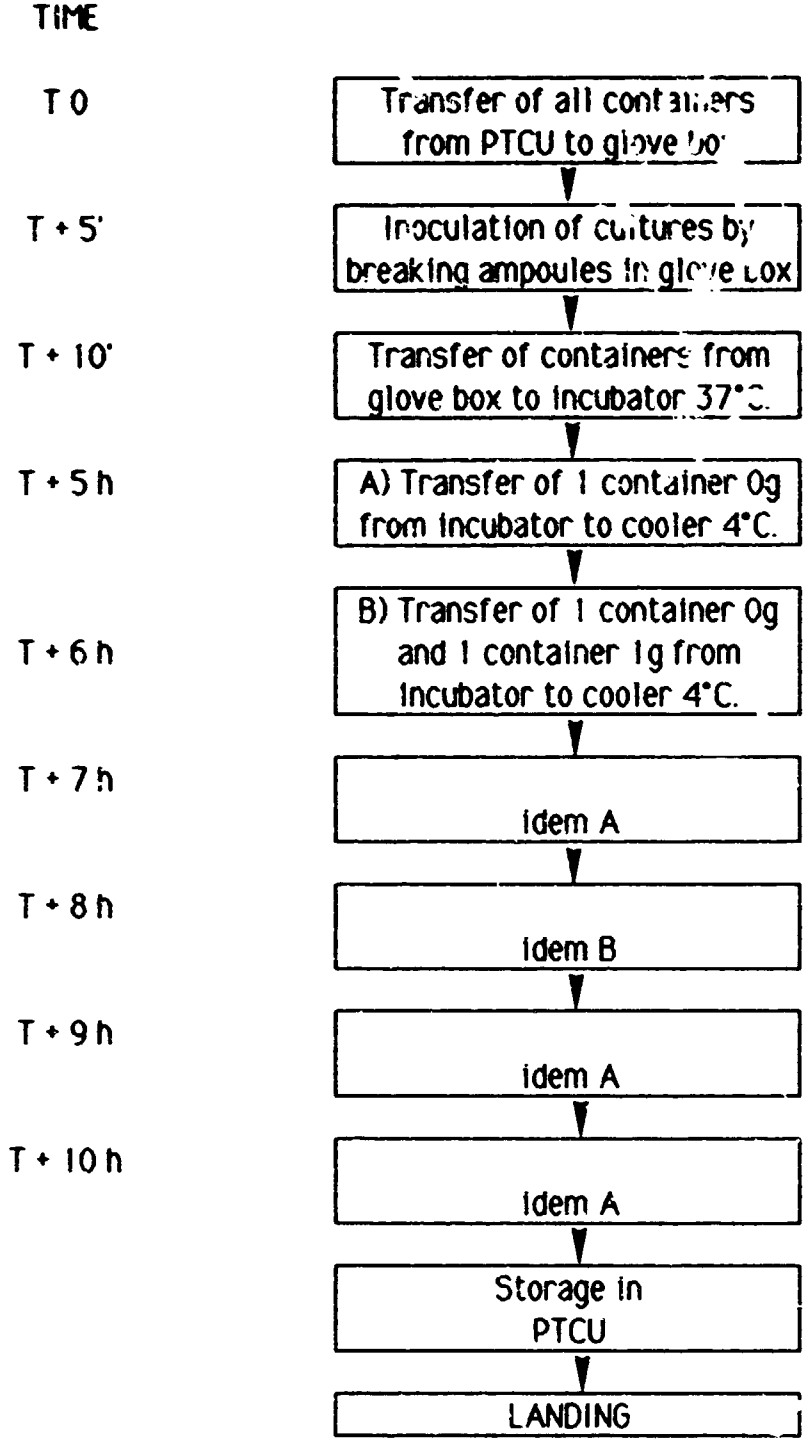

Figure 5. Active Phase.

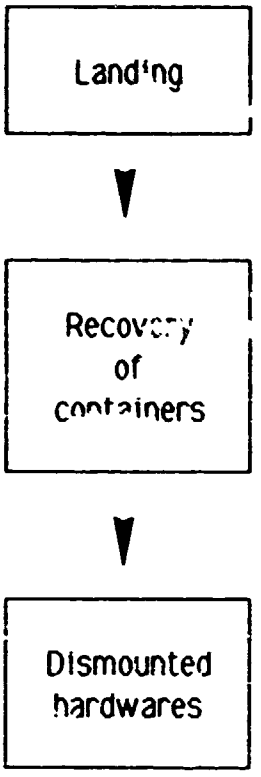

Post flight analysis

* Electron microscopy
* Radioactivity measurement
* Cell count
* Morphometry

Figure 6. Post-Flight Phase.

Space Physiology Experiments (SPE)

The Canadian Space Agency has coordinated the preparations for a set of experiments by Canadian Principal Investigators and their colleagues. Dr. Alan Mortimer, Chief of Space Life Sciences for the Canadian Space Agency, serves as SPE Mission Scientist and Mr. Bruce Aikenhead, Director General of the Canadian Astronaut Program, is listed by NASA/MSFC as the SPE Payload Element Developer.

The development of these experiments has been supported by the Canadian Space Agency, the National Research Council of Canada, the Medical Research Council of Canada, and the Canadian Defence and Civil Institute of Environmental Medicine (DCIEM). The investigators are also grateful to the NASA Johnson Space Center for the loan of certain items of flight-qualified equipment.

Most of the Space Physiology Experiments will study various aspects of the response of the human body to the weightless condition encountered in space flight and one experiment examines the physics of the separation of immiscible liquids in the absence of gravity in anticipation of an application to the separation of biological substances.

N92-23620

ENERGY EXPENDITURE IN SPACE FLIGHT (DOUBLY LABELLED WATER METHOD) (8-IML-1)

Howard G. Parsons
The University of Calgary
Calgary, Alberta, Canada

Precise measurements of energy expended by crew members during space flight are expected to become more important as the planned duration of space flights increases. The nutritional resources to be stowed onboard for crews whose missions may last several months must be predicted accurately. The objective of the Energy Expenditure in Space Flight (EES) experiment is to demonstrate and evaluate the doubly-labelled water method of measuring the energy expended by crew members during approximately 7 days in microgravity.

The doubly labelled water technique, which the Principal Investigator and his colleagues use in hospital care for patients, determines carbon dioxide production which is then used to calculate energy expenditure.

The method relies on the equilibrium between oxygen in respiratory carbon dioxide and the oxygen in body water. Because of this equilibrium, the kinetics of water turnover and respiration are interdependent.

Under normal conditions man contains small but significant amounts of deuterium and oxygen 18. Deuterium is eliminated from the body as water while oxygen 18 is eliminated as water and carbon dioxide. The difference between the turnover rates in the two isotopes is proportional to the carbon dioxide production. Deliberately enriching the total body water with both of these isotopes (in the form of an administered dose of doubly labelled water, $D_2{}^{18}O$) allows the isotope turnovers to be accurately measured in urine, plasma, or saliva samples. The samples are taken to the laboratory for analysis using an ion-ratio mass spectrometer.

The method is useful because it is relatively non-invasive, can provide long term measurements of energy expenditure (weeks), and is accurate to within 6% of indirect calorimetry in humans. The isotopes are stable and are non-radioactive.

The administration of the labelled water can also be used to measure total body water by application of the dilution principle. Body composition can then be calculated from the total body water and the body mass. Knowledge of body composition is itself useful and, in addition, changes in body composition over a period of time when energy intake is known can be related back to energy expenditure.

For the IML-1 EES experiment, the subject's baseline isotopic composition will be measured using pre-launch urine samples obtained daily during the week before launch.

Precise doses of heavy water to be ingested by two subjects in flight will have been prepared and placed in 30 ml syringes to facilitate oral administration. The first dose will be taken at the beginning of the second flight day. Urine samples will be collected approximately 3 hours and 6 hours following ingestion and daily thereafter. A second dose will be taken immediately following landing and urine samples will be collected 3 and 6 hours later.

The urine samples and samples of shuttle galley water will be stowed and recovered post-landing for transfer to the University of Calgary for analysis.

A third crew member, who will not receive the heavy water dose, will serve as a control subject.

Subjects will also be required to provide food and fluid intake records for the immediate pre-flight period as well as during the mission. These will be analyzed for water content and nutritional composition (primarily energy). Samples will also be obtained of tap water at the pre-flight crew quarters and of any other significant water sources, including beverages, for later isotope analysis.

Pre-flight and post-flight height and weight data will be obtained for each subject.

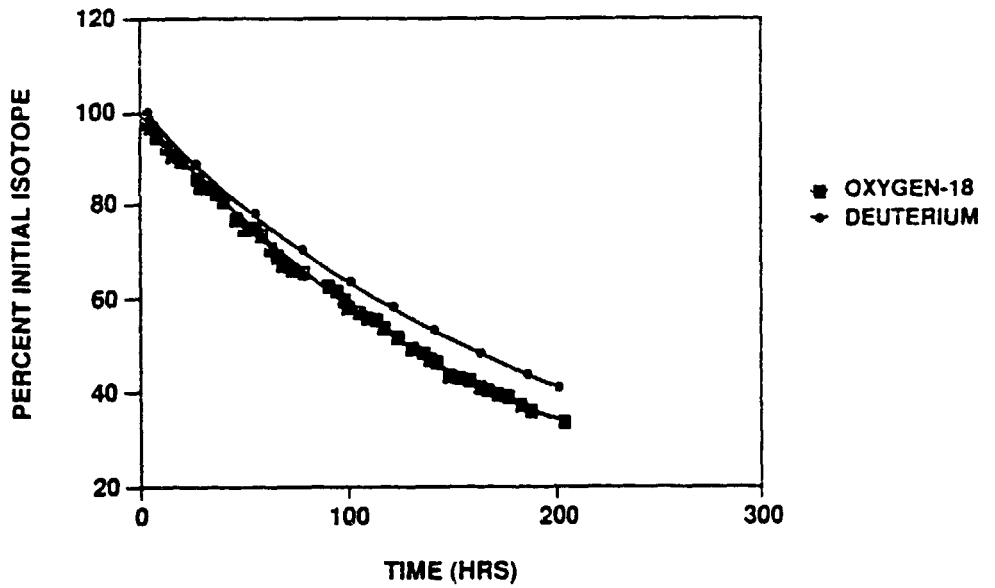

Figure 1. Isotope Elimination.

N92-23621

PHASE PARTITIONING EXPERIMENT
(8-IML-1)

Donald E. Brooks
University of British Columbia
Vancouver, British Columbia, Canada

Phase partitioning is a method of separating biological cells and macromolecules via their differential distribution in two phase aqueous polymer solutions. The ultimate goal of the experiment is to test the hypothesis that the efficiency of separation of closely related cell types, by partitioning in immiscible aqueous phases, will be enhanced in the non-convective environment provided by space. Before a cell separation experiment can be performed, the demixing of immiscible aqueous polymer solutions must be understood and controlled in order to optimize the experimental conditions for a cell separation experiment in the future. The present Phase Partitioning Experiment (PPE) is the third in a series, the first two having been flown on STS 51-D in April 1985 and STS 26 in October 1988. In those experiments the immiscible aqueous phases demixed spontaneously at different rates, the final disposition being one in which the phase which wetted the container wall surrounded the second phase which formed an "egg yolk" in the center of the chamber.

Since the location of the demixed phases must be controlled if cells are to be isolated from each phase, one of the concerns of the present experiment is to attempt to control this localization, as well as to affect the rate of demixing, by applying weak electric fields to the systems as they demix following manual agitation. The wetting of the walls in the upper and lower halves of the chambers will also be modified by chemically coating them so that each half will be wet by a different phase. The principle of electric field assisted demixing has been demonstrated on KC-135 flights, and in the laboratory in extremely dilute emulsions of one phase in the other. In the latter case it has been shown that drops of one phase suspended in the other have electrophoretic mobilities which increase as a function of droplet size and differ in sign depending on which is the continuous phase. Hence, an electric field should drive phases of the two types in opposite directions, thus generating demixing. Because of the complexity of the systems we have no way of predicting the demixing rates or the stability of the process in equal volume mixtures of the two phases. One goal of the present experiment, therefore, is to obtain baseline data on electric field-associated effects on demixing and on the stability of the interface between the phases in the presence of electric fields.

The data obtained in the experiment consists of a photographic record of the samples as a function of time after mixing in the presence and absence of electric fields, the magnitudes of the currents drawn in each chamber and the sample temperature. In addition, the isolated samples will be returned for chemical analysis. Demixing kinetics will be determined by subjecting the photographs to a two-dimensional Fourier analysis to obtain the dominant length scale as a function of time.

The PPE experiment apparatus (Figure 1) consists of two linked units, the Separation Unit (SU) and the Power and Control Unit (PCU). The SU contains six pyrex glass chambers, each of which is equipped with electrodes at either end through which the electric field is applied. The electrodes are composed of reversible Ag/AgC1 pairs which pass current without producing gas provided sufficient AgC1 coating is electrolytically applied before or during the experiment. The field strengths involved are extremely low, the currents never exceeding 10 ma per chamber. These currents correspond to electric fields of the order of 0.7 V/cm for a typical two phase mixture. The aqueous polymer solutions themselves consist of buffered solutions of dextran and polyethylene glycol (PEG), the PEG-rich phase being dyed blue. They have flown on two previous flights and are completely non-toxic.

The phases are mixed by manually shaking the SU, each chamber being equipped with a mixing ball which emulsifies the samples. Electric current for each chamber is supplied via a cable originating from the PCU. The PCU is entirely self-contained, power being supplied by a battery pack within it. The PCU contains circuitry and controls for applying currents of various levels in each chamber, for automatically re-plating electrodes between runs (if necessary), for recording the time elapsed in either mode and for displaying the temperature in one of the chambers as detected by a thermocouple counted behind one electrode.

Photography of the state of the liquid samples is carried out using the shuttle-supplied photoflood light box as an illumination source. The SU is mounted in a cradle attached to the bottom of the PCU and the light box is located behind the SU. The PCU/SU and the light box are mounted via dovetail joints on a bracket permanently fixed to a Spacelab rack panel. Two 35 mm cameras are mounted on support arms which extend out from the mounting bracket to allow photography of the six back lit sample chambers by one and recording of the numerical data from a digital display on the front of the PCU by the other.

When separation (partitioning) of the phases is completed, the "upper" and "lower" halves of each chamber can be displaced horizontally, isolating each half and allowing the contents of the two halves of the chamber to be analyzed upon completion of the mission. Since the samples will consist of equal volumes of each phase, if localization by electric fields and wetting is complete each isolated half chamber should contain a single phase.

The PCU and SU are stowed in a locker for launch and landing. On Mission Day 4 the SU is taken from the middeck locker, shaken repeatedly to thoroughly mix all systems, and fixed along with the PCU on the mounting bracket in the Spacelab until the demixing experiment is to be performed. At that time, the cameras are mounted and the state of the systems photographed before mixing. Various electric field magnitudes are applied to the six chambers to examine the stability of a pre-formed interface to electric fields. The field direction is then reversed for an equal length of time to attempt to re-stabilize the interface. The SU is next unmated from the PCU, shaken thoroughly, replaced in its bracket and the systems photographed at intervals for 20 minutes with no applied electric fields. The SU is then again unmated from the PCU, the systems mixed thoroughly, the SU remounted, the electric fields turned on, and the systems photographed at intervals for 20 minutes with the electric field on and less frequently for another

60 minutes with the fields off to allow observation of the effects of applied fields and of any spontaneous re-equillibration which may occur on their removal. Finally, the contents of the top and bottom chamber halves are isolated by rotating the transport knob on the SU, the SU photographed a final time, and the apparatus re-stowed.

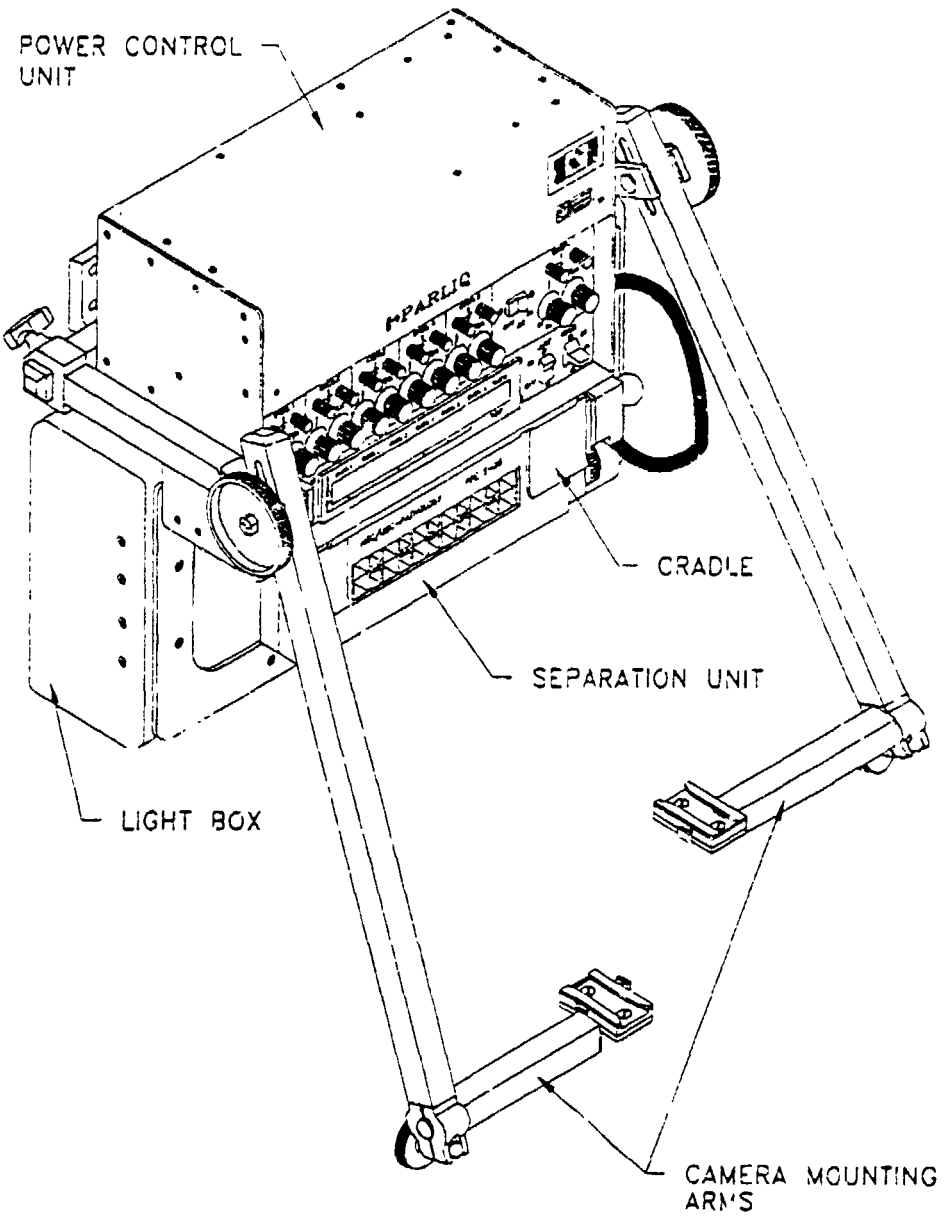

Figure 1. Phase Partitioning Experiment Apparatus.

N92-23622

BACK PAIN IN ASTRONAUTS
(8-IML-1)

P. C. Wing
University Hospital, Shaughnessy Site
Vancouver, Canada

Background

A NASA review of Flight Medicine Clinic data on 58 astronauts produced information about the incidence but not the severity of the back pain problem. According to NASA's figures, approximately 68% of astronauts reported back pain during space flight. The pain is present during rest periods and may interfere with sleep. There is no indication that the pain persists post-flight.

As a preliminary study for IML-1 experiment, a pain diagram was used to elicit information about the incidence and severity of back pain experienced by 20 payload specialists on 22 shuttle flights (one PS flew on three missions) from 1983 to 1986. There were 18 responses from 17 PSs (one PS provided information about two missions). Thirteen PSs (72%) reported experiencing some degree of b. . pain, ranging from dull (can be ignored) to severe, making concentration difficult. For the majority, the pain was dull in nature, and did not interfere with work or concentration. For some, the pain abated after only a few minutes; for others, the pain persisted for the entire duration of the flight.

The back pain problem may be related to the height increase known to occur during space flight. An increase in height of up to 7.0 cm was reported on two American space flights, including the Apollo-Soyuz mission. A small increase in height was reported in the first 2 to 3 days, with a major change of a further 4-5 cm occurring between days 6 and 9. The Soviets have reported that the height increase is maintained for the duration of extended Space Station (MIR) missions and may even persist on return to Earth's gravity. Since the normal unfolding of the spinal cord with forward flexion would allow it to extend by only 4.5 to 5.6 cm (10% of its length), we can extrapolate that the spinal cord is under traction even in a neutral position at microgravity.

It is logical to assume that the majority, if not all, of the height increase during space flight occurs in the vertebral column since the spine consists of 23 or 24 disc spaces, each with the potential to expand by several millimeters. The height increase is 2 to 3 times greater than that known to occur with diurnal variation in healthy young adults (average 2 cm).

The spine is made up of multiple "vertebral motion segments," consisting of the disc, the adjacent vertebral bodies, and the facet joints. Normally, tension and pressure in the intervertebral discs are a balance of several factors: gravity, muscle tone, tissue tension, and osmotic pressure. An imbalance in these factors will lead to a change in disc configuration and

thus a change in spine configuration. Exposure to prolonged microgravity may set off a chain of events. An increase in disc water content with increased intradiscal pressure and disc height; flattening of the normal thoracic kyphos, and if the facet joints do not open up, an increase in the lumbar lordosis, and traction on the facets. Back pain may result from tension on the annulus, posterior longitudinal ligaments, facet capsule and/or ligamentum flavum, and from muscle spasm. Increased disc height may also lead to spinal cord disproportion, resulting in traction on either the spinal cord, the anterior or posterior primary rami of the spinal nerves, and/or the peripheral nerves. Any of the structures in the back, other than the insensitive nucleus pulposus and spinal cord, are possible sources of the back pain reported during space flight.

The purpose of the IML-1 study is to investigate the pattern and severity or intensity of back pain experienced by astronauts, to determine whether there is a correlation between back pain and the reported height increase of up to 7.0 cm, and to document changes in range of motion and spinal contour.

The objectives of the Back Pain in Astronauts (BPA) experiment are thus to document (1) the pain pattern and severity experienced by astronauts, (2) the rate of change of height, (3) the changes in spine shape and length, and (4) the changes in range of motion of the spine and legs using stereophotogrammetry, direct height measurement, pain questionnaires, and pain drawings. The experiment will provide the first documentation of changes in spinal contour, range of motion, and pain pattern related to height increase during space flight.

Because we are interested in the changes in the spinal column, but can only photograph the skin, the crew member's back is marked with reference points along the scapulae, down the spinal column, and over the iliac crests. Using foot restraints when necessary, the crew member assumes a series of positions, a neutral "standing" posture, spinal flexion, spinal extension, spinal rotation (left and right), free float, femoral stretch, and straight leg raise.

The subject is photographed with two 35 mm cameras mounted on a stereo camera bar 3 meters from the subject. The cameras are precisely aligned with targets mounted on the bulkhead behind the subject. These targets are used for calibration and as reference points. When the subject is positioned correctly, the stereo cameras are triggered simultaneously by a hand-held infrared shutter relese. Post-flight the pairs of photographs are placed in a stereoplotter, a special instrument that generates a three-dimensional image from photo pairs. Very precise measurements can be made from the 3D image. The measurements from the stereophotographs will allow investigators to evaluate changes in height, spinal shape, and range of motion.

The changes in spinal shape and mobility, as determined by stereophotography, will be correlated with any back pain experienced. The pattern of the pain, its intensity, the time of maximal discomfort, and methods used to ease the pain are recorded on a daily pain questionnaire. Height, measured directly, is also recorded daily on the pain questionnaire.

By interpreting the photographs and correlating the results with the subject's pain pattern, investigators may be able to elucidate the cause of the back pain and recommend ways to prevent or alleviate it.

MEASUREMENT OF VENOUS COMPLIANCE
(8-IML-1)

R. B. Thirsk
Canadian Space Agency
Ottawa, Ontario, Canada

One physiological consequence of living and working in space is cardiovascular deconditioning. During spaceflight, an astronaut's cardiovascular system is altered such that it has a decreased tolerance to a gravitational force field. Upon return to Earth, an unprotected astronaut may then experience symptoms of orthostatic intolerence such as fatigue, lightheadedness, "gray-out" or fainting. There are several conjectured causes of this phenomenon but the primary cause is believed to be an inflight loss of intravascular and extracellular fluid volume. Fortunately, countermeasures such as saline rehydration and the use of antigravity suits exist to minimize the symptoms and assist the astronaut's readaptation back to the terrestrial environment.

The prime objective of this IML-1 investigation is to measure the bulk compliance (i.e., the distensibility) of the veins in the lower leg before, during, and after spaceflight. It is of particular interest whether venous compliance over the range of both positive and negative transmural pressures (i.e., various states of venous distention and collapse) changes throughout the duration of spaceflight. Information concerning the occurrence and character of compliance changes could have implications on the design of improved antigravity suits and further the understanding of inflight and postflight venous hemodynamics.

During the mission, the bulk venous compliance of the right lower leg of three crew members will be measured using an ultrasonic limb plethysmograph and two large compression cuffs that will encircle the thigh and calf. Inflation of the two cuffs in turn will alter the transmural pressure in the underlying veins and cause them to dilate or collapse. The plethysmograph will measure and record the ensuing changes in lower leg volume. Measurements will be made on each participating crew member on two occasions during the flight as well as twice before and three times after the mission.

The second objective of this IML-1 investigation is to evaluate an experimental antigravity suit system which has been designed to counteract the deleterious cardiovascular effects of long duration spaceflight. This suit system has been developed at the National Research Council of Canada in Ottawa and at the Defense and Civil Institute of Environmental Medicine (DCIEM) in Toronto. The suit has a total of eleven pressure bladders and is able to apply three hybrid modes of pressurization to the subject's legs and lower abdomen: (i) graded: a graduated pressure is applied uniformly in time to the legs and lower abdomen, (ii) sequential: a lengthening zone of external pressure moves in a wave-like manner from the ankle to the abdomen, or (iii) graded-sequential: a combination of (i) and (ii). These modes of pressurization

to have been investigated during a series of ground-based human centrifuge experiments and tilt table experiments at DCIEM in an effort to optimize a returned astronaut's central blood volume, and arterial blood pressure.

Soon after the IML-1 mission returns to Earth, one of the crewmembers will don the experimental antigravity suit. The suit will be evaluated under three conditions: (i) no suit pressurization, (ii) the pressurization format of a conventional antigravity suit, and (iii) predetermined hybrid pressurization formats. The basis of the evaluation will be by physiological measurement of the cardiovascular system as well as crew member comments.

N92-23624

POSITIONAL AND SPONTANEOUS NYSTAGMUS
(8-IML-1)

Joseph McClure
The University of Western Ontario
London, Ontario, Canada

Nystagmus is an involuntary oscillation of the eyes with a slow eye movement in one direction and a compensatory quick eye movement in the opposite direction to return the eyes to their original position. The slow phase of nystagmus is often generated by asymmetry in the peripheral vestibular system, and generally nystagmus in the horizontal direction dominates although vertical and rotary nystagmus can be seen in certain pathological situations.

Peripheral spontaneous nystagmus has been defined as nystagmus that has a direction-fixed slow phase and beats with about the same slow phase velocity in all head positions. Spontaneous nystagmus is generally accepted as a manifestation of an inherent asymmetry in the peripheral vestibular system. Such asymmetry is generally secondary to neural disorders of the inner ear such as labyrinthitis, Meniere's disease, acoustic neuroma, etc.

If nystagmus is present that changes magnitude or direction of the slow phase velocity with change of head position relative to the force of gravity, then the nystagmus is defined as a positional nystagmus. It has been implied in the literature that positional and spontaneous nystagmus do not occur simultaneously. It is our impression that positional and spontaneous nystagmus can occur simultaneously as independent phenomena and that the slow phase velocity components of the nystagmus generated in each case are additive.

Peripheral spontaneous nystagmus is an important clinical parameter since it is a measure of asymmetry in the peripheral vestibular system caused by disease. We have always assumed that any nystagmus observed in a neutral position relative to the force of gravity (i.e., sitting, supine, etc.) represents the component of spontaneous nystagmus. The only way to validate this assumption is to eliminate the positional nystagmus via the weightless environment and observe for any residual spontaneous nystagmus.

Many normal subjects have low intensity spontaneous and/or positional nystagmus with eyes closed that can be measured with electro-oculography (EOG). The experimental conditions can be attained by measuring nytstagmus while performing positional tests on appropriate subjects before, during, and after space flight.

Data for the PSN experiment will be collected in conjunction with the Space Adaptation Syndrome Experiment (SASE). At one point in SASE, the subject is seated stationary on the sled with horizontal EOG electrodes applied. Horizontal nystagmus data will be collected with

the head in a neutral position and with the head tilted to the extreme right and left lateral positions.

This relatively simple experiment should help to answer the question as to whether spontaneous nystagmus and positional nystagmus are superimposed and, as well, determine whether nystagmus observed in a neutral position reflects the spontaneous component.

N92-23625

SPACE ADAPTATION SYNDROME EXPERIMENTS
(8-IML-1)

D. Watt
McGill University
Montreal, Quebec, Canada

This set of seven experiments will study adaptation of the human nervous system to weightlessness, with particular emphasis on the vestibular and proprioceptive systems.

Sled/H-Reflex Experiment

The absence of gravity must cause human otolith organ function to be altered significantly. These changes should be reflected in modified vestibulospinal reflexes. In this experiment, subjects will be exposed to sinusoidal linear motion as a stimulus to the otolith organs. H-reflex testing will be used to detect resulting modulation of spinal cord excitability. This approach will make it possible to determine how vestibulospinal reflex function changes during and after exposure to weightlessness (even if those changes are subthreshold), free of contamination by voluntary motor activity.

Wearing ear plugs and a blindfold to eliminate sound and visual cues, a test subject for the Sled Experiment is strapped into a seat on a device called the mini-sled (Figure 1). The seat slides gently back and forth along two rails for a maximum distance of 100 cm (40 in.) to provide a linear acceleration stimulus to the otolith organs. The test subject is further outfitted with electrodes that stimulate reflexive muscle responses in the leg. One electrode placed behind the subject's knee applies small electric shocks to the leg, and electrodes placed over the calf muscles record the responses. Acting through usual reflex pathways, the acceleration stimulus to the inner ear changes the response to the electrical shocks in the leg, and thus, it is possible to measure otolith activity in an alert human being with a functional vestibular system. To study the two independent receptors that make up each otolith organ, the subject is accelerated back and forth while seated upright and while positioned on the back.

A computer records all results during the experiment, and the data are analyzed after landing. If the nervous system learns to reinterpret the modified sensory information from the otoliths, acceleration stimuli to the inner ear should continue to influence the response recorded in the leg. If the nervous system learns to ignore that information, the variation in leg responses should gradually disappear.

Rotation/VOR Gain Experiment

There are several reasons why the vestibulo-ocular reflex (VOR) and other components of gaze control may be abnormal in weightlessness. These abnormalities could be an underlying

cause of the Space Adaptation Syndrome since an unstable retinal image usually leads to motion sickness. Subjects will use self-generated head movements to stimulate their semi-circular canals. Eye and head rotations will be measured and the gain of the VOR calculated. The subjects will also perform a gaze refixation task to evaluate eye-head coordination in weightlessness.

Strapped into the stationary mini-sled seat, the test subject wears electrodes and measuring devices that record head and eye movements (Figure 2). In the first test, the crew member looks at a target, closes the eyes, rotates the head to the side while trying to keep the eyes pointed at the unseen target, and then opens the eyes. The effectiveness of the vestibulo-ocular reflex is determined by how close the subject's gaze is to the target when the eyes are opened. In a complementary test, the subject, with eyes closed, oscillates the head from side to side or up and down while trying to keep gazing at an imaginary fixed target. The subject's ability to keep the eyes pointed at the target is a measure of the reflex effectiveness. Finally, the subject is asked to move the head and eyes as necessary to look at a spot of light which reappears in different locations on a screen.

In this experiment. all results are recorded on an analog tape and analyzed after flight.

Visual Stimulator Experiment

Subjects exposed to steady rotation of their visual field experience an illusion of self-motion known as circularvection. There is now evidence that in the absence of a gravitational reference, the phenomenon is enhanced as visual inputs become relatively more important than vestibular inputs. This experiment builds on the previous studies of Young and should lead to increased understanding of this important mechanism whereby the nervous system compensates for disrupted vestibular function in space.

The subject on the stationary seat of the mini-sled faces a dome-shaped, randomly patterned rotating visual field with its rim 2 inches ahead of his eyes. This position leaves a narrow rim of the outside world still visible around the periphery of the dome, which has been found to enhance the circularvection illusion, and to simplify the tracking task. The stimulus will consist of constant speed rotation of the device at 30, 45, or 60 degrees per second, in one direction or the other, for about 40 seconds. During the application of the visual stimulus, the subject will develop a feeling of self-rotation, accompanied by apparent rotation of the small part of the outside world which he can see in his peripheral vision, beyond the d rim. The subject's task will be to rotate a crank attached to a 360 degree precision po ometer, matching crank angular velocity to the apparent rotation velocity of the outside world.

A computer will monitor and record both dome speed and crank speed and the strength of circularvection will be calculated by comparing these signals.

Proprioception (Relaxed) Experiment

Anecdotal reports and the results of previous flight experiments provide a body of evidence suggesting that proprioception is degraded in weightlessness.

In this experiment, an observer moves the head, arm, or leg of a blindfolded test subject, who remains passive during the movements (Figure 4). The observer bends the joint first to a reference angle and then to a slightly different angle. The subject must determine whether the second angle is larger or smaller than the reference angle, then move the joint and finally set it back to the second angle. A goniometer measures the actual angles which are recorded by computer.

The methods used will allow the determination of proprioceptive thresholds, and should detect interactions occurring between the proprioceptive, vestibular, and motor systems, during and after prolonged exposure to weightlessness.

Proprioception (Active) Experiment

There appears to be an unusual degree of loss of sense of orientation and of perception of body image in the absence of both gravity and vision. Body image perception seems to improve following active muscular contractions. Using a pointer similar to a flashlight, the subject will point at a series of memorized targets during a prolonged absence of vision (Figure 5). A second crew member records how closely the light beam comes to each target. This test is repeated with the subject's eyes closed only during the extension, pointing, and retraction of the arm. This will make it possible to separate errors caused by degraded proprioceptive ability from those resulting from a distorted image of the outside world. This should determine if the perceptual errors are the result of faulty sensory inputs or if they have a more complex cause.

Proprioception (Illusions) Experiment

Some crewmembers from previous space flight missions have described illusions in which hopping up and down resulted in a feeling of the floor moving up and down like a trampoline underneath them. This could be the result of inappropriate motor commands, incorrect sensory feedback, or modified interactions between the two. In this experiment, subjects will perform several types of rhythmical motor activity, note any resulting proprioceptive illusions, and determine the effects of vision and tactile inputs on these illusions (Figure 6).

Tactile Acuity Experiment

During prolonged space flight, as unloaded intervertebral discs expand, astronauts become several centimeters longer. This could lead to pressure blocks of nerve roots. In this experiment, tactile acuity will be measured in one finger and one toe with the aid of metal blocks having surfaces on which parallel ridges are spaced increasingly close together (Figure 7). The subject is required to distinguish by touch alone the direction of the unseen ridges.

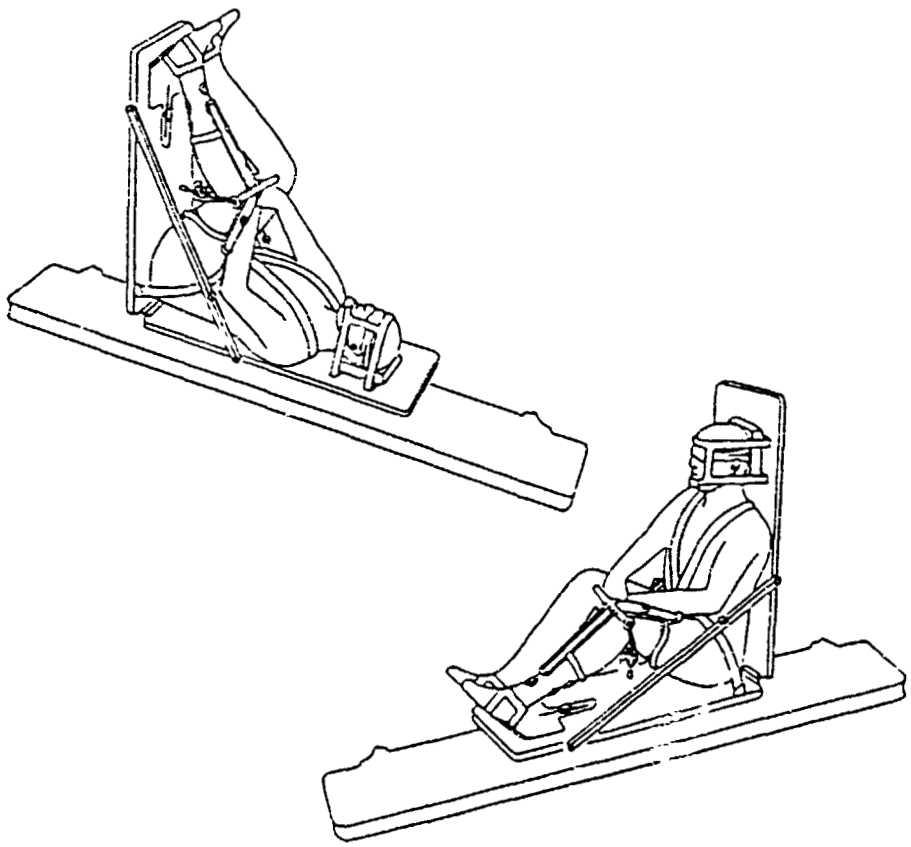

Figure 1. SLED/H-Reflex Experiment.

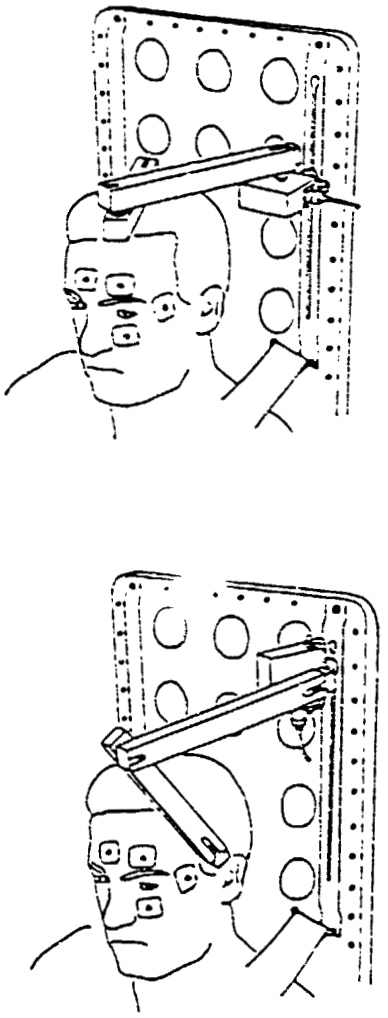

Figure 2. Rotation/VOR Gain Experiment.

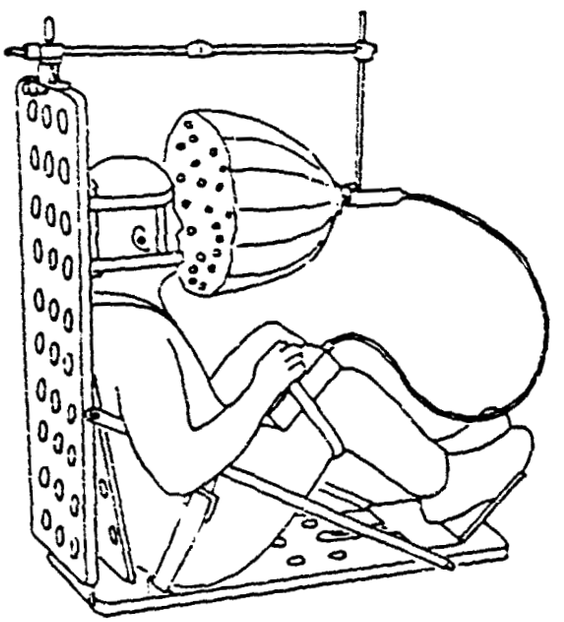

Figure 3. Visual Stimulator Experiment.

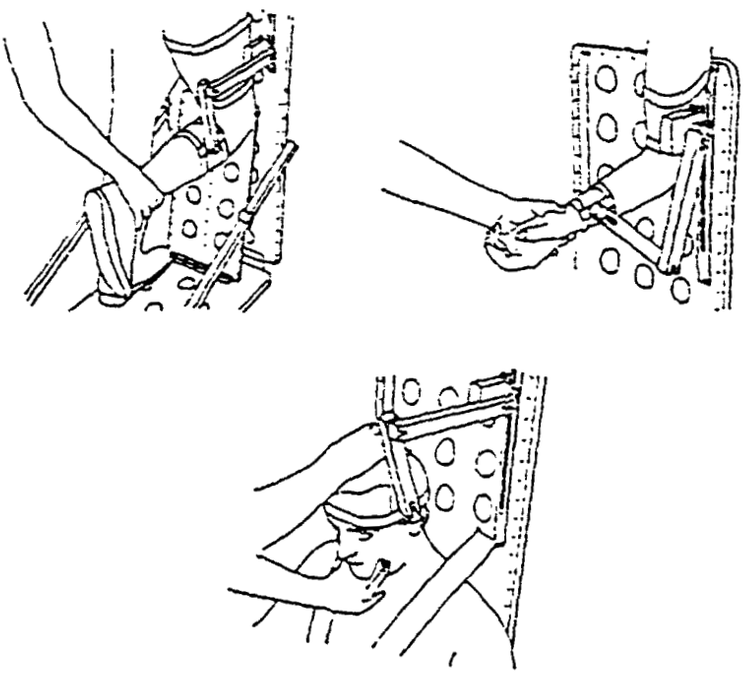

Figure 4. Proprioception (Relaxed) Experiment.

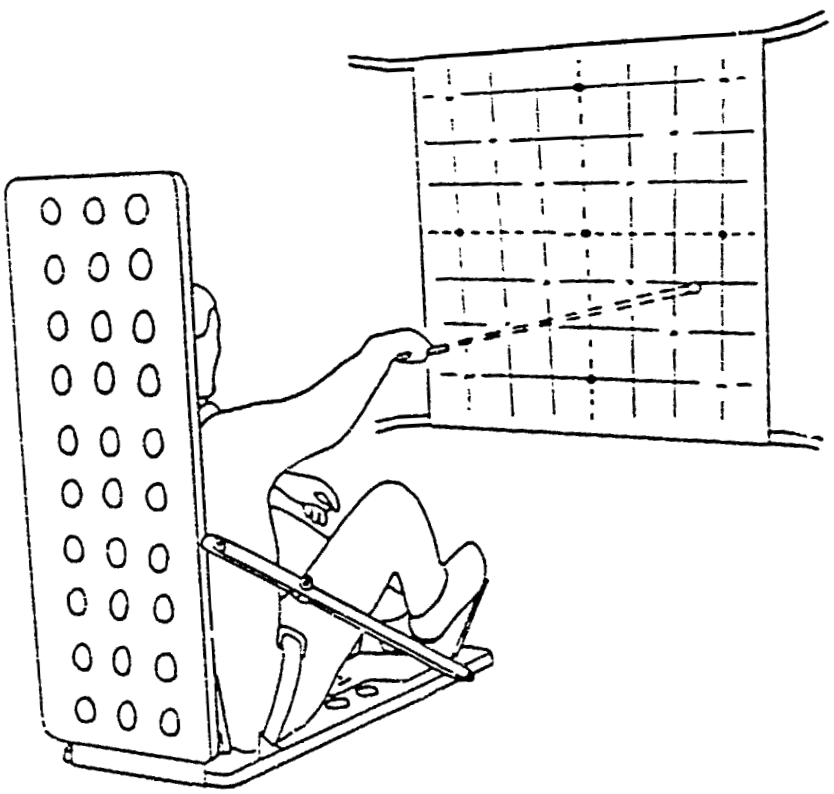

Figure 5. Proprioception (Active) Experiment.

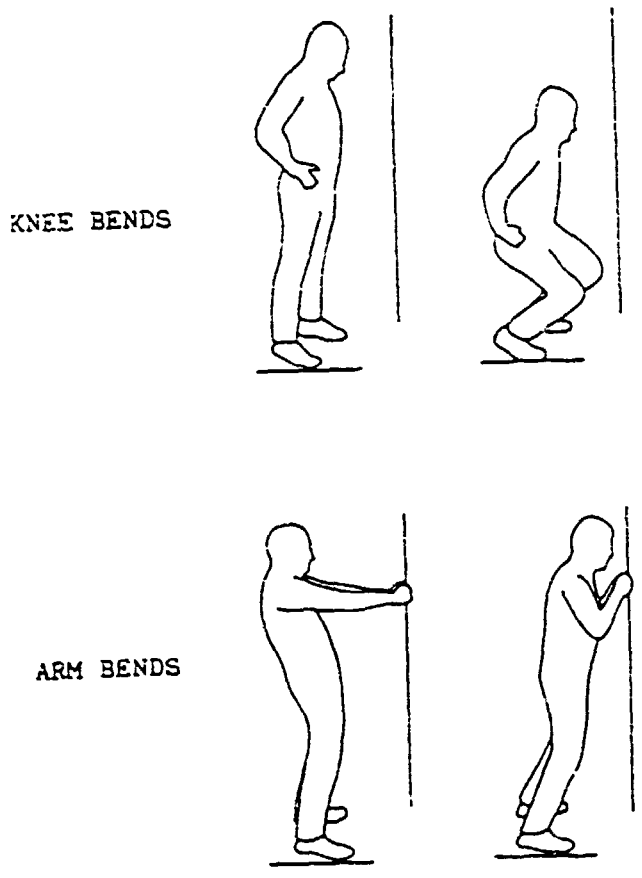

Figure 6. Proprioception (Illusions) Experiment.

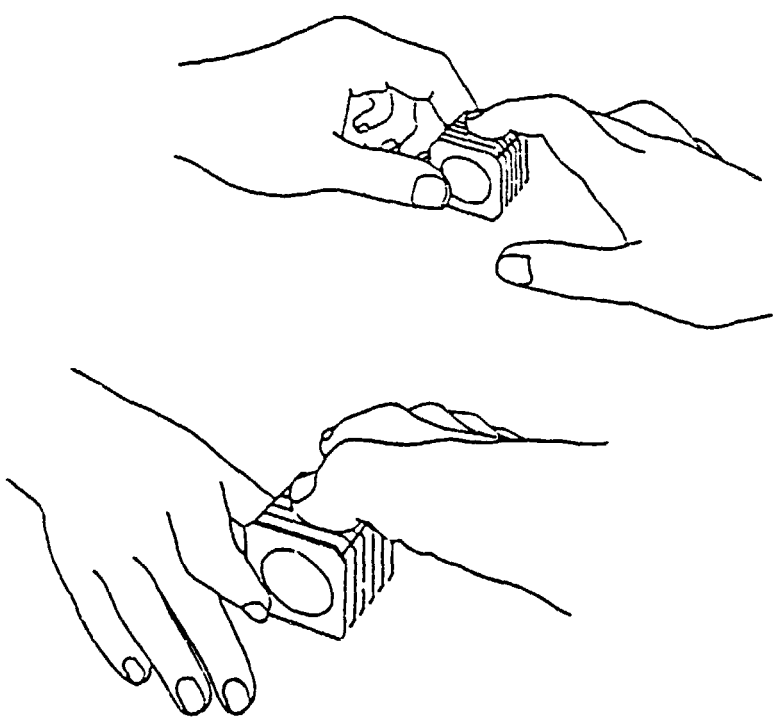

Figure 7. Tactile Acuity Experiment.

N92-23626

MICROGRAVITY VESTIBULAR INVESTIGATIONS (10-IML-1)

Millard F. Reschke
NASA, Johnson Space Center
Houston, TX

Our perception of how we are oriented in space is dependent on the interaction of virtually every sensory system. For example, to move about in our environment we integrate inputs in our brain from visual, haptic (kinesthetic, proprioceptive, and cutaneous), auditory systems, and labyrinths. In addition to this multimodal system for orientation, our expectations about the direction and speed of our chosen movement are also important. Changes in our environment and the way we interact with the new stimuli will result in a different interpretation by the nervous system of the incoming sensory information. We will adapt to the change in appropriate ways. Because our orientation system is adaptable and complex, it is often difficult to trace a response or change in behavior to any one source of information in this synergistic orientation system. However, with a carefully designed investigation, it is possible to measure signals at the appropriate level of response (both electrophysiological and perceptual) and determine the effect that stimulus rearrangement has on our sense of orientation. The environment of orbital flight represents the stimulus arrangement that is our immediate concern. The Microgravity Vestibular Investigations (MVI) represent a group of experiments designed to investigate the effects of orbital flight and a return to Earth on our orientation system.

All of our tests are based on a fundamental chain of ideas. In orbit, the absence of an effective gravity vector in the "freefall" environment of the orbiting craft creates the requirement for adaptive changes in sensorimotor and perceptual systems that on Earth subserve the voluntary and reflexive control of eye, head, and body motion relative to the Earth. Interactions between the vestibular, visual, and proprioceptor systems are necessary for these control functions. Adaptive change in the motion control functions of these sensorimotor systems provokes motion sickness. Space sickness is a particular form of motion sickness. A functional vestibular system is apparently necessary for motion sickness. Therefore, measures of perceptual and sensorimotor reactions to stimuli involving interactions between vestibular, visual, and proprioceptive systems at selected times before, during, and after space flight will provide measures of changes that are an integral part (part and parcel) of the adaptive process.

The favorable consequences to the astronaut of the adaptive changes are improved efficiency and abatement of sickness associated with head and body movement during the orbital mission. The price for these improvements on orbit is maladaptive perceptual and sensorimotor reactions during return to Earth and during readaptation to Earth. The threats posed by maladaptive perceptual and sensorimotor reactions are at least as great as those posed by the discomfort of space motion sickness. Advancement of knowledge of mechanisms of adaptation to "environmental" change in the acceleration field is of profound importance to all NASA

mission, present and future. Any future knowledge gained in neurophysiological mechanisms of the adaptive process will achieve holistic functional significance only when tied to solid facts on the perceptual and sensorimotor reactions to measured stimulation of the orientation sensors before, during, and after orbital missions. The Microgravity Vestibular Investigations project is an effort to provide these fundamental facts.

Premise

The basic premise of this investigation rests on four points:

1. There is a normal synergy or interaction in the vestibular system between activity arising in the semicircular canals, the otolith organs, the visual system, the somatosensory system, and probably other sensory systems. Through coordination of the many inputs, the sensation of movement and accuracy of compensatory responses to various states of motion is maintained. Integration of this sensory information may begin at the receptor level (i.e., in canal/otolith interaction) but most probably occurs mainly within the central nervous system.

2. Otolith input is altered during spaceflight. The phasic component of the otolith signal in response to linear acceleration during translation persists, but the static component is probably absent. Therefore, spontaneous activity from the otolith organs associated with signaling position in a gravitational field must be modified as a new set point is established.

3. Adaptation will occur in microgravity with corresponding modifications of sensory and motor reflexes until new and appropriate response patterns are established.

4. In the immediate postflight period, responses will reflect the nature and degree of the inflight adaptation.

Based on these four points, an inclusive hypothesis would suggest a modification of the normal synergy that exists to coordinate canal, otolith, proprioceptive, and other sensory input. This modification will be reflected in the compensatory eye movements and perceptual reports elicited by angular acceleration when that acceleration is either self-imposed or passively experienced on a rotator.

Vestibular Function

If a cat is dropped upside down, it will land right side up on all fours. If a new newborn infant is tilted backward, its eyes will roll downward so that its gaze remains fixed. If the reader shakes his head from side to side as he reads this overview, the print nonetheless stands still. Each of these effects represents a compensation for a disturbance to balance or orientation, and each is controlled in part by the sensory apparatus in the vestibule of the inner ear. While these responses are a part of our everyday lives, they are basically reflexive in nature and are seldom called to our attention. The vestibular system functions to stabilize gaze and ensure clear vision during head movements. Because head movements can be fast, the visual system, encumbered

by relatively slow retinal processing cannot act rapidly enough to produce compensatory eye movements that would maintain images steady on the retina. The vestibulo-ocular reflex (VOR), which depends upon the motion sensors of the labyrinthine semicircular canals and otolith receptors, produces promptly generated slow-phase eye movements that compensate for head rotation. Thus, a horizontal rotation of the head to the right produces an equal eye movement in the orbit to the left so that the sum movement (eye in space or gaze) does not change and the image of the world does not move on the retina. The VOR is not capable of maintaining an image on the retina during sustained rotation; therefore, there is a need for alternative means of image stabilization to supplement the fading vestibular response. The optokinetic system serves this function by taking over and maintaining compensatory slow-phase eye movements during sustained rotation when the labyrinthine signal declines.

EXPERIMENT DESCRIPTIONS

MVI is comprised of seven different experiments conducted on the IML-1 payload crewmembers. The experiments require the MVI Rotating Chair to provide stimulus in the subject's Yaw, Pitch or Roll planes. The experiments and the axes tested for each are:

Suppression of the Vestibulo-Ocular Reflex:	Yaw & Pitch
Semicircular Canal Dynamics:	Yaw, Pitch & Roll
Visual-Vestibular Interaction:	Yaw & Pitch
Per-Rotatory and Post-Rotatory Nystagmus:	Yaw, Pitch & Roll
Optokinetic Responses:	Yaw & Pitch
Sensory Perception Reporting:	Yaw, Pitch & Roll
Preflight and Postflight Testing:	Yaw, Pitch & Roll
	Dynamic Posture Test
	Positional Nystagmus

SUPPRESSION OF THE VESTIBULO-OCULAR REFLEX

Keeping the visual image of an object still while moving the head is critical for reading, for tasks requiring eye-hand coordination and possibly, for avoiding motion sickness. All the MVI experiments converge on answering questions of how processing of vestibular information

about head movements is affected by orbital flight, and this experiment's unique contribution is to study this in a particular visual context.

If the head is rotated and the eyes don't turn relative to the head, the visual image will sweep across the whole retina. This visual sweep and the vestibular signal from the rotation both elicit reflexes (the optokinetic reflex (OKR) and the VOR, respectively) driving the eyes opposite to the head movement. This keeps the eyes stationary relative to space and to the visual background. The OKR and the VOR are field-stabilizing reflexes. The eyes can also fixate on a small object of interest that is moving relative to the fixed background and follow it without moving the head (pursuit response), but in doing so optokinetic stimulation in the opposite direction is generated. For this experiment, the background is darkened to prevent optokinetic stimulation and a small target is fixed relative to the head as the subject is rotated. This situation allows us to study how the pursuit responses suppress the VOR.

There is evidence that vestibular processing is affected by transitions between a terrestrial gravitoinertial force background and the micro-gravitoinertial force environment of orbital flight. Thus, interactions between pursuit and vestibular eye movements may be altered during space shuttle missions. Deficits in visual and visuo-motor performance may occur, and their time course and extent may correlate with the occurrence of symptoms of space motion sickness.

Background

1. What is the evidence that the VOR and pursuit interact?

When we look at a moving object we usually do it by moving both the head and eyes. The process of turning the head in the direction of the object produces a vestibular stimulus which activates the VOR, holding the gaze stationary in space. It is unclear what cancels the VOR.

There are several possibilities for what the cancelling signal is. It could be the signal that drives pursuit eye movements, it could be a copy of the vestibular signal with the opposite sign gated by pursuit information, or it could be feedback from the neck. Evidence from lesions in humans and from the similarity between visual suppression of the VOR and visual pursuit suggests that the pursuit signal is the cancellation signal. For example, Halmagyi and Gresty (1979) have shown that patients with lesions that degrade pursuit also have deficits in the ability to cancel the VOR. In normal humans (Barnes, et al., 1978; Barnes, 1983) and monkeys (Lisberger and Fuchs, 1978), the ability to suppress the VOR diminishes at higher frequencies where the pursuit system also breaks down.

2. How do the VOR and pursuit contribute to suppression?

The VOR and visual pursuit interact during visual suppression of the VOR in ways that are predictable from their individual characteristics. Quantitative models covering the

behavior of each system and of the interaction between them will be presented in the next science orientation training tour.

The VOR is frequency dependent. The gain is higher and the phase angle between eye and head movements is smaller at higher frequencies. The pursuit system is also frequency dependent, its gain being lower and phase angle larger at higher frequencies. Figure 2 shows that when VOR gain (ratio of eye to head movement in the dark) is higher there is less suppression (the ratio of eye to head movement is higher when there is a head-fixed target).

When the gain of pursuit errors is large, suppression is poor (the relation of eye to head movement is large when there is a head-fixed target). Visual performance suffers when suppression is not achieved. The ability to read letters presented in an expected location - straight ahead of the head - is degraded at high frequencies of head oscillation, paralleling breakdown of suppression at high frequencies.

3. What affects the normal frequency dependence of suppression?

Anything that affects the VOR, pursuit, or the mechanism of interacting can affect visual suppression of the VOR. Consumption of alcohol interferes with the ability to pursue moving objects, and this manifests itself as a degradation in the ability to suppress. The effect of alcohol on pursuit and on suppression cuts across a range of frequencies. Blurred vision and decrements in visual recognition also occur.

Patients with peripheral vestibular injuries have impaired VOR function and impaired visual suppression of the VOR. These patients can stabilize their gaze fairly well during oscillation in full room illumination, but in the dark, the VOR and suppression are worse than in normals because the eye and head movements are out of phase.

Changes in the VOR that can affect suppression are not limited to changes in gain and phase. Some mechanisms subserving the VOR can affect the three dimensional organization of the VOR. Peterson, Baker and Wickland (1987) have exposed cats to conditions where oscillation of the head in yaw is coupled to vertical optokinetic stimulation. This brings about an adapted state of the VOR in which yaw head movements in the dark elicit pitch eye movements.

We have reason to believe the astronauts will experience a small degradation in visual suppression of the VOR upon insertion into orbit. There is no reason to expect the dynamics of pursuit to change as a function of gravitoinertial force level, but there is reason to suspect that the dynamics of the VOR will. Data from parabolic flight experiments (DiZio and Lackner, 1988), observations made before and after orbital flight (Oman and Kulbaski, 1988), and studies of cross coupling of optokinetic after-nystagmus (Raphan and Cohen, 1988) all point to a decrease in the time constant of decay of post-rotatory nystagmus after a transition from 1 g to 0 g in orbital flight. There is also ample evidence of an interaction between angular and linear acceleration in the VOR on Earth (cf. Benson, 1974 for a review).

Applying these data from the time domain to the frequency domain (assuming linearity) suggests that responses to low frequency oscillation will be altered initially in 0 g relative to 1 g. At 0.05 Hz, there should be an increase in the usual phase lead of the VOR and a small decrease in gain. It is clear that fixation suppression does not work by simple suppression of the VOR, so gravitoinertial force dependent changes in the VOR at low frequencies will probably produce gravitoinertial force dependent changes in suppression at low frequencies. Thus, a quantitative comparison of phase and gain of the visually suppressed and unsuppressed VOR at low frequencies is the most important potential contribution for this experiment.

Methods

This experiment will be conducted in both pitch and yaw axes. In pitch, oscillation will occur at two frequencies (0.05 and 1.25 Hz, each with 40/s peak velocity), and two visual conditions (in total darkness and with a head fixed target). In yaw, pseudorandom rotation (see Semicircular Canal Dynamics below) will be performed during both darkness and head-fixed target conditions. These conditions are shown schematically in Figure 3.

The main objective of data analysis will be to compare the velocity of eye movements and head movements. Head velocity is recorded and stored directly by monitoring chair velocity. Eye velocity must be derived from the eye position signals. Eye and head velocity will both be subjected to time series analysis and will be compared in terms of gain and phase. Difference in phase and gain across frequencies, visual conditions and rotation axes as a function of orbital flight will provide the evidence needed to test the hypotheses listed below.

Expected Results

1. There will be an increase in phase lead and a small reduction in gain of the VOR at low frequencies early in orbital flight relative to preflight.

2. The ability to fixate a head-fixed visual target during rotation will decrease at low but not high frequencies early in orbital flight relative to preflight. That is, the percent suppression will decrease.

3. Changes for the vertical VOR and for vertical suppression will be qualitatively similar but smaller.

4. It is unclear whether the VOR will return to its normal behavior during a space shuttle mission, but whether or not the VOR returns to normal during an extended period of exposure to weightlessness, visual suppression will return to normal. If the VOR does not return to normal and suppression does, it can be inferred that the pursuit system, or the way pursuit cancels the VOR, has changed.

5. There may be a correlation between the time course of adaptation of the VOR or suppression of the VOR and the severity of motion sickness symptoms inflight.

6. If adaptation of the VOR and its suppression occur after the initial inflight changes, there will be after-effects postflight.

References

Barnes GR, Benson AJ, Prior ARJ (1978). Visual-vestibular interaction in the control of eye movements. Aviat Space Environ Med, 4:558-564.

Barnes GR (1981). Visual-vestibular interaction in the coordination of eye and head movements. In: Fuchs & Becker (eds), Progress in Oculomotor Research, New York, Elsevier, 299-308.

Barnes GR (1984). The effects of ethyl alcohol on visual pursuit and suppression of the vestibulo-ocular reflex. In: J Stahle (ed), The Vestibular System. Fundamental and Clinical Observations. Almqvist & Wiksell, Uppsala. 161-166.

Benson AJ. Modification of the response to angular accelerations by linear accelerations. In: HH Kornhuber (ed), Handbook of Sensory Physiology, Vol. 6, Part II. Springer-Verlag, Berlin. 281-320.

DiZio P, Lackner JR (1988). The effects of gravitoinertial force level and head movements on post-rotational nystagmus and illusory after-rotation. Exp Brain Research, 70:485-495.

Halmagyi GM, Curthoys IS (1987). Human compensatory slow eye movements in the absence of vestibular function. In: MD Graham & SL Kemink (eds), The Vestibular System. Neurophysiologic and Clinical Research. Raven, New York, 471-479.

Halmagyi GM, Gresty MS (1979). Clinical signs of visual-vestibular interaction. J Neurol Neurosurg Psychiatry, 42:934-939.

Lisberger SG, Fuchs AF (1978). Role of primate flocculus during rapid behavioral modification of vestibulo-ocular reflex. I. Purkinje cell activity during visually guided horizontal smooth-pursuit eye movements and passive head rotation. J Neurophysiol, 41:733-763.

Oman CM, Kulbaski MI Space flight affects the 1 g post-rotatory vestibulo-ocular reflex. Paper presented at The Barany Society Symposium on Representation of Three Dimensional Space in the Vestibular, Oculomotor, and Visual Systems. Bologna, Italy, June 3, 1987.

Peterson BW, Baker JR, Wickland C (1987). Spatial properties of the vestibulo-ocular reflex before and after labyrinthine lesions. In: MD Graham & JL Kemink (eds), The Vestibular System. Neurophysiologic and Clinical Research. Raven, New York, 455-461.

Raphan T, Cohen B (1988). Organization principles of velocity storage in three dimensions: the effect of gravity on cross-coupling of optokinetic after-nystagmus. In: B Cohen and V Henn (eds), Representation of Three Dimensional Space in the Vestibular, Ocuiomotor and Visual Systems, New York Academy of Sciences, New York.

Wall C, Black FO (1984). Intersubject variability in VOR response to 0.005-1.0 Hz sinusoidal rotations. In: J Stahle (ed), The Vestibular System. Fundamental and Clinical Observations. Almqvist & Wiksell, Uppsala, 194-198.

SEMICIRCULAR CANAL DYNAMICS

The general premise for the MVI set of experiments is that all systems of the body will attempt to adapt to weightlessness in a way that will optimize performance in the new environment. This will occur in posture and the control of eye movements with corresponding modification of sensory and motor reflexes until new and appropriate response patterns are established. It is expected that the weighting of canal and otolith inputs to the system will change with time inflight and will be reflected in eye position responses. The pseudorandom rotation tests in this experiment are designed to measure the weighting of the canal inputs to control of direction of gaze. As discussed above, pseudorandom stimuli will be used in Yaw in darkness and with a head fixed target. This stimulus will also be used in Roll and in Pitch (as an alternate inflight procedure).

Background

Two major mathematical tools utilized by engineers and scientists to analyze dynamic systems are time domain methods represented by differential and difference equations and frequency domain methods represented by transform calculus.

The basic view of a gain-phase system analysis is illustrated in Figure 4. The features tend to be much the same for biological system with changes occurring in the shape of the curves.

The use of frequency domain analysis in engineering from electric circuits to mechanical devices and on to complex systems of components is pervasive. When feedback control is considered, the tool is used to predict the behavior of an open loop system after the control loop is closed. In biology, the method has been extensively used when system performance must be quantified and characterized completely. Human operator performance, particularly under conditions when the human operator is part of a larger system is sometimes quantified using frequency domain analysis. That way, the operator can be embedded into the overall analysis of system performance.

Sensory systems which bring the external world to consciousness, such as the visual system and the auditory system, have been subjected to forms of frequency analysis. An example in the visual system is the determination of the light modulation frequency at which rapid variations in light magnitude can no longer be observed. The auditory system utilizes frequency domain analysis to reduce complex sound to their components. Its nature, therefore, makes it a prime candidate for frequency domain analysis. Indeed this system may have the longest history in this field

Why Use this Analytical Tool?

The vestibular system contributes to two major control systems, the Vestibular Ocular Reflex (VOR) and the postural control system. The MVI experiments utilize these systems as windows into changes occurring in the nervous system as a result of extended exposure to weightlessness. The evidence is clear that frequency domain tools will deliver the information required from the investigations. We have had experience with the tools and there are ample reports in the literature to support these methods.

The VOR is a complex control system having a number of inputs and several tasks to perform toward the organism's function. The overall dynamics of the VOR can be broken down by stage. That is, the end organ, the several involved processing centers of the Central Nervous System (CNS), and the eye in its orbit.

Physical Dynamics

Cupular Movement - The fluid filled semicircular canal with its cupular obstruction can be characterized by an analysis of its physics at several levels of detail. The most intuitive is a underdamped second order differential equation having the characteristics of inertia (fluid mass), restoring force (cupular elasticity) and viscosity (fluid shear on the wall of the canal).

Eye Movements - The and the eye in its socket and there are dynamics which arise from the interactions of neural structures.

Neural Dynamics

The nervous system communicates over distances greater than a few hundred microns by discrete events called action potentials which are propagated undistorted using the metabolic energy of the brain. The view of the nervous system generally held by neurophysiologists engaged in research on control systems within the body is that signals being passed from place to place on neural pathways are encoded by rate of discharge. There are numerous details under this statement but the approximation is good to the first order. These discrete event signals interact and are modified near cell bodies in ways analogous to the changes which occur to electronic signals are modified in electronic systems by summing, filtering and re-routing. Thus

new dynamics are imposed by waystations of the nervous systems which do not have obvious physical substrates such as mass, friction, and potential energy storage. Moreover, large changes in this signal processing capability can occur as a result of the needs of the organism. Some of the dynamical components of the VOR nervous circuit are as follows:

First Order Fibers - Goldberg and Fernandez (1971; Fernandez et al., 1972) have recorded responses of first order vestibular neurons to various motion stimuli. Approximately, the observed dynamics reflect the displacement of the cupula within the semicircular canals for the rotation detection system and displacement of the otoconia with respect to the otolithic membrane in the linear motion detection system. As will be enumerated later, this detection reflects velocity of angular motion and acceleration in the otolithic system.

Integration - The fact that the first-order fibers deliver velocity information to the CNS and the major task of the eye movement system is to maintain positional stability, requires an integration of the velocity signal so that the ocular muscles will be driven by the proper signal. It is generally accepted that this integration is accomplished by neural circuits located in the brainstem.

Velocity Storage - For the angular motion system, the observed time constants for horizontal eye movements did not match the time constants observed in the above first-order fiber system. This discrepancy could not be accounted for in any other location than in the CNS. Further, the horizontal eye movement system has been observed to "forget" its motion state and come under control of another system. An example of the conditions for this is a change in the plane of rotation for the head. A simple dynamical system which could accomplish this is pole zero pair on the real axis which cancels out the original time constant of the canal system and establishes a longer time constant in its place. Since any such system must have internal memory states, it is convenient to provide these memory states with the facility to forget upon command from an outside influence. Thus, a single neural network provides the means to explain two experimental observations.

Choice of the Stimulus Signal

The enumeration below is a list of characteristics which are desirable in a stimulation signal.

Covers the frequency range - It is an imperative that the stimulus contain energy across the entire spectrum being considered for analysis. Energy outside the band of interest is wasted. When particular discrete frequencies are of interest, it is best to concentrate energy at those frequencies.

Use complex signals - Signals such as sinusoids allow a subject to anticipate the motion. Often this is desired but when the primitive portions of the system are the objects of the analysis,

the anticipation effect is confounding. Signals which change themselves at random or at least are too complex to be anticipated remove this effect.

Persistently exciting - It is better to pack as much energy into the stimulus as possible within certain limitations. It is important as well to have the energy of the signal spread over all the time allotted for the signal rather than being delivered in short intervals. This reduces the dynamic range of the excitation for the same total energy and therefore helps keep the signal within the linear range of the system under analysis.

Control start-up transients - A signal with large derivatives or even discontinuities any time in its duration introduces transients which may push the system outside its linear region of operation and therefore disturb the frequency analysis. Smooth start up is an important factor in this and when the stimulus is periodic, the end of the period should be continuous with the beginning.

Avoid interaction among frequency components - One of the tenants of linear systems theory is that different frequency components do not interact. In living systems, however, it is inevitable that harmonics and other interproducts will arise. A signal which avoids this or at least makes it detectable is desired.

The stimulus chosen for this experiment is the sum-of-sines pseudorandom periodic stimulus. It is closely related to the pseudorandom noise stimulus first used by O'Leary and Honrubia (1975) to identify neurophysiological systems. It satisfies the needs expressed above with few compromises. It is made up of a number of sine waves which may or may not be harmonically related. The stimulus we have chosen has components which are all harmonics of a fundamental which is missing from the series. Generally the phases of the components are random with respect to each other but some are chosen to meet the start-up smoothness criteria.

Complex - Above all, the sum-of-sines stimulus appears to the subject to be random. He will not be aware from cycle-to-cycle where in the stimulus he is and will not be able to anticipate the state of the chair motion more than a few hundred milliseconds ahead.

Initial conditions controlled - At the start of the stimulus, the chair will be at rest and will have zero acceleration. This condition provides for both a smooth start and stop and allows a seamless transition between periods.

Periodic - The signal is periodic, which carries with it the advantage that time to frequency conversion is most easily done utilizing discrete-time to discrete-frequency algorithms (FFT).

Relative Primes - The harmonics chosen are relative primes. This means that nonlinearities which generate harmonics and cross terms will not lay over each other and can therefore be measured and separated in the frequency domain from the principle components of

the response. The actual values of the primes chosen are based on an equal logarithmic frequency model.

Can be packed - Through the generation of several series all meeting the above criteria, special ones can be chosen which pack the most amount of energy into the smallest excursion. This helps keep the equipment in its proper operating range and also optimizes the persistently exciting requirement.

Methods

As illustrated in Figure 6, semicircular canal dynamics is studied in Yaw, Roll and Pitch planes using the pseudorandom stimulus described above. The data analysis will involve first deriving time domain data and then frequency domain data.

Eye velocity - A signal processing step is executed on the eye movement signal to remove the fast phase component of eye movement, leaving a slow phase which can be differenced to produce a sampled slow-phase velocity signal.

Accumulated eye position - By extrapolating the eye velocity signal over the fast phase components, an estimate is obtained of what the eye position would have been if the fast phase components had not reset the eye position.

Ocular Counterroll - With current technology, the only method of analysis for rotation of the eye in the X axis is by analysis of a video or photographic image of the eye. The MVI ground based equipment includes a device to convert video to eye movement data. As it stands, the method is very computer intensive and cannot be run in real time.

After the derived time domain data from above has been verified it will be converted to frequency domain information. The values of frequency which will be analyzed are locations of the signal energy, namely the harmonics of the fundamental which are in the sum-of-sines signal. These will be the records and charts from which the final conclusions of the research will be derived.

Gain and Phase vs. frequency - After the chair data and the eye movement data are converted to common units and transformed separately to the frequency domain, the transformed eye movement data will be divided by the transformed chair data. The result will be a complex sequence. Gain is derived from the complex series by taking the magnitude of each complex number, and phase is derived by taking the inverse tangent of each number.

Expected Results

Our expectation is that the VOR gain and phase as derived from the transfer function analysis will be modified, and these modifications are of central origin. Of particular interest will be the time course of the changes. It is expected that the changes from the baseline will take 3 to 6 days and recovery after landing will take somewhat less. In addition, the two axes which are commonly influenced by otolith inputs (Pitch and Roll) may be altered more than the Yaw axis which, in normal posture, operates independently of the otolithic system.

References:

Cohen, B., The Vestibulo-Ocular Reflex Arc, In The Handbook of Sensory Physiology Vol VI/1 H.H. Kornhuber (ed) pp 476-540, 1974.

Fernandez, C., J. M. Goldberg, and W. K. Abend, Response to Static Tilts of Peripheral Neurons Innervating Otolith Organs of the Squirrel Monkey, J. Neurophysiol. Vol. XXXV, #4, 1972.

Goldberg, J. M. and C. Fernandez, Physiology of Peripheral Neurons Innervating Semicircular Canals of the Squirrel Monkey. I. Resting Discharge and Response to Constant Angular Accelerations, J. Neurophysiol. Vol. XXXIV, #4, 1971.

Luenberger, David G. Introduction to Dynamic Systems- Theory, Models & Applications- Wiley, 1979.

O'Leary D. P. and V. Honrubia, On-Line Identification of Sensory Systems Using Pseudorandom Binary Noise Perturbations, Biophysical Journal, Vol 15, pp. 505-532, 1975.

Robinson, D. A., The Systems approach to the Oculomotor System, Vision Research, Vol. 26, pp. 91-99, 1986.

VISUAL-VESTIBULAR INTERACTION

This study will investigate the extent to which sinusoidal angular motion could modulate slow phase velocity of nystagmus elicited by optokinetic stimulus at constant velocity. Rotation in yaw combined with horizontal optokinetic nystagmus, and rotation in pitch combined with vertical optokinetic nystagmus will be investigated with two oscillations frequencies and one velocity of optokinetic stimulus. Rotation in darkness and optokinetic stimulus presented with the rotator in static position will be used as controls.

Background

In recent years, the interaction of optokinetic and vestibular stimuli on the slow-phase velocity (SPV) of nystagmus (Koenig, et al., 1978; Barnes, et al., 1978; Guedry, et al., 1978; Buizza, et al., 1980) and on the perception of body motion (Zacharias, 1977; Dichgans and Brandt, 1978) has gained increasing interest. The resulting research work has improved our understanding of how man compensates for a sensory deficit: there is no receptor signaling constant angular or linear body velocity. The adequate inputs to the semicircular canals are angular accelerations; and to the otoliths, linear accelerations. With vestibular stimuli of high frequency (sinusoidal stimulation above 0.1 Hz) this deficit is compensated for by the inertia of the cupula which integrates the acceleration to a velocity signal of the head in space (Fernandez and Goldberg, 1971). With lower frequencies of vestibular stimulation, the activity of an additional central integrator, presumably located in the vestibular nuclei storing the neuronal activity from the peripheral nerve, elicits a vestibulo-ocular reflex (VOR) in phase with head velocity (Buettner, et al., 1978).

In spite of its integrative properties, the vestibular system is not able to provide an adequate velocity signal during motion with constant angular velocity. In the presence of visual cues, this can be compensated for by the visual system. When the whole visual surround moves with uniform velocity, a sensation of self-motion is induced (circular vection) (Brandt, et al., 1973). The neurophysiological basis for this perception is a convergence of visual inputs on the premotor structures of the vestibular system (Henn, et al., 1974; Waespe and Henn, 1977).

Features common to VOR and optokinetic after-nystagmus (OKAN), as well as recordings from vestibular neurons during OKAN, indicate that the convergence of the two inputs has to be located at or prior to the level of the central integrator in the vestibular nuclei mentioned above (Raphan, et al., 1977, 1979). Thus OKAN and the prolongation of the peripheral time constant to that of the VOR could be accomplished by the same integrator.

Interaction of vestibular and optokinetic nystagmus under natural conditions was first demonstrated by Maurer (1935), who showed that optokinetic stimulation reduces post-rotatory nystagmus. Thus additional optokinetic stimulation results in a better correspondence of stimulus velocity and SPV of nystagmus than pure vestibular stimulation. Quantitative measurements of interaction lead to contradictory assumptions on how the outputs of the vestibular and optokinetic system are combined to yield a common SPV output. Allum, et al. (1976) suggested a variable gain in both the vestibular and the optokinetic system before their summation. Linear interaction was proposed by Robinson (1977) on the basis of the data from Waespe and Henn (1977) which suggested a switching between the vestibular and optokinetic input. Recently, Koenig, et al. (1978) found rather accurate linear interaction when the vestibular and optokinetic stimuli added. But when the vestibular stimulus was opposite to the optokinetic, SPV of the OKN was reduced more strongly than was expected on the basis of linear interaction. These data were used as the basis of a model of nonlinear interaction by Schmid, et al. (1980).

The basic advantage of the present experiment is that we use sinusoidal oscillations instead of a velocity step for the vestibular stimulus, combined with a unidirectional optokinetic stimulus. This makes it possible to measure, within the limited time frame imposed by the constraints of experimentation in space, the interaction when both stimuli are of same or opposite directions. In general, on ground, there is a very good correspondence of the SPV observed with pure optokinetic stimulation and the change in SPV by the additional vestibular stimulus (Koenig and Diehggns, 1982). Thus, the optokinetic reflexes, predominantly the pursuit system, modulate SPV in the same way during combined visual vestibular stimulation as during pure optokinetic stimulation. When the vestibular and optokinetic stimuli add, the retinal image motion helps to decrease the SPV (or to suppress the VOR) so that the eye velocity never exceeds the optokinetic stimulus velocity. When the two stimuli are in opposite directions, a fully compensatory SPV depends on the respective gain of both vestibular and pursuit systems.

Methods

Visual-vestibular interaction will be evaluated using the Helmet-mounted Optokinetic Stimulus (OKS) Module during sinusoidal oscillation. This module provides a moving visual field (black/red checkered pattern) which may be oriented to turn right to left, left to right, up to down, or down to up.

The OKN field direction will move horizontally (left to right or right to left) with the head in the yaw orientation and vertically (up to down or down to up) for the pitch head position. Data will be collected at 0.2 Hz and 0.8 Hz (same frequencies as SPE/SASE FO-2) for both yaw and pitch orientations. The peak velocity of both the optokinetic stimulation and rotator oscillation will be 40 deg/sec.

Figure 7 illustrates these conditions. The data analysis will essentially be the same as described above for the VOR suppression experiments.

Expected Results

1. Major changes should occur for visual vestibular interaction about pitch axis when compared to yaw axis because the synergy between canals and otoliths will be disrupted in free fall;

2. Adaptive changes should occur throughout the flight during visual vestibular interaction about pitch axis when both stimuli will be in the same direction. At the beginning of the flight SPV should be greater than the optokinetic stimulus velocity and the visual pattern should then appear moving in the opposite direction of its actual displacement. Then SPV should be fully compensatory given the development of the visual suppression of nystagmus throughout the flight.

3. The storage mechanism eliciting after-nystagmus will change its charge to a considerable extent in such as long intervals as 25 seconds. So, it should also be discharged at the end of the optokinetic stimulus, and the SPV during the following pure vestibular stimulation should change accordingly. It will be interesting to compare this effect throughout the adaptive process to the microgravity environment.

4. In addition, previous data on OKN and VOR in earlier space flights suggest that a direction-specific (downward) change in the SPV should occur during visual vestibular interaction in the vertical plane in a weightless environment. Indeed, previous studies have indicated that the asymmetry between upward and downward OKN is reversed during the first three days of spaceflight, and parabolic flight as well (Clment, et al., 1986; Clment and Berthoz, 1988). The beating field of vertical OKN and the vertical OKAN time constant are also affected. Then, changes in the vertical VOR as a function of angular acceleration and optokinetic stimulus are expected to occur in the direction of the observed reversal of OKN during orbital flight. It has been hypothesized that the suppression, during free-fall, of the antigravity tonic influence exerted by the otoliths, which tends to raise the body and to rotate upward the eyeball (upward drive) in order to compensate for the downward pull of gravity, would then facilitate eye movements directed downwards. Such an asymmetry should be exemplified during the visual vestibular interaction protocol.

References

Allum JHJ, Graf W, Dichgans J, Schmidt CL (1976) Visual-vestibular interactions in the vestibular nuclei of the goldfish. Exp Brain Res 26: 463-485

Barnes GR, Benson AJ, Prior ARJ (1978) Visual vestibular interaction in the control of eye movement. Aviat Space Environ med 49: 557-564

Brandt Th, Dichgans J, Koenig E (1973) Differential effects of central versus peripheral vision on egocentric and exocentric motion perception. Exp Brain Res 16: 476-491

Buettner UW, Buettner U, Henn V (1978) Transfer characteristics of neurons in vestibular nuclei of the alert monkey. J Neurophysiol 41: 1614-1628

Buizza A, Leger A, Droulez J, Berthoz A, Schmid R (1980) Influence of otolithic stimulation by horizontal linear acceleration on optokinetic nystagmus and visual motion perception. Exp Brain Res 39: 165-176

Clment G, Vieville T, Lestienne F, Berthoz A (1986) Adaptive modifications of gain asymmetry and beating field of vertical optokinetic nystagmus in microgravity. Neurosci Lett 63: 271-274

Clment G, Berthoz A (1988) Vestibulo-ocular reflex and optokinetic nystagmus in microgravity. Adv Oto-Rhino-Laryng 42, Karger, Basel (in press)

Dichgans J, Brandt Th (1978) Visual vestibular interaction: effects on self-motion perception and in postural control. In: Held R, Leibowitz H, Teuber HL (eds) Perception. Springer, Berlin Heidelberg New York (Handbook of sensory physiology, vol 8, pp 755-804)

Fernandez C, Goldberg JM (1971) Physiology of peripheral neurons innervating semicircular canals of the squirrel monkey. II. Response to sinusoidal stimulation and the dynamics of the peripheral vestibular system. J Neurophysiol 34: 661-675

Guedry FE, Lentz JM, Jell RM (1978) Visual vestibular interaction: influence of peripheral vision on suppression of the vestibular ocular reflex and visual acuity. WASA, NAMRL 1246

Henn V, Young LR, Finley C (1974) Vestibular nucleus units in alert monkeys are also influenced by moving visual fields. Brain Res 71: 144-149

Koenig E, Allum JHJ, Dichgans J (1978) Visual-vestibular interaction upon nystagmus slow phase velocity in man. Acta Oto-Laryngol 85: 397-410-

Koenig E, Dichgans J (1982) inear interaction of vestibular and optokinetic nystagmus. In: Roucoux A, Crommelinck M (eds) Physiological and pathological aspects of eye movements. Junk Publishers, The Hague Boston London, pp 271-280

Maurer OH (1935) Some neglected factors which influence the duration of post-rotational nystagmus. Acta Oto-Laryngol 22: 1-23

Raphan T, Cohen B, Matsuo V (1977) A velocity-storage mechanism responsible for optokinetic nystagmus, optokinetic after-nystagmus and vestibular nystagmus. Dev Neurosci 1: 37-47

Raphan T, Matsuo V, Cohen B (1979) Velocity storage in the vestibulo-ocular reflex arc. Exp Brain Res 35: 229-248

Robinson DA (1977) Linear addition of optokinetic and vestibular signals in the vestibular nucleus. Exp Brain Res 30: 447-450

Schmid R, Buizza A, Zambarbieri D (1980) A non-linear model for visual-vestibular interaction during body rotation in man. Biol Cybernetics 36: 143-151

Waespe W, Henn V (1977) Neuronal activity in the vestibular nuclei of the alert monkey during vestibular and optokinetic stimulation. Exp Brain Res 27: 523-538

Zacharias GL (1977) Motion sensation dependence on visual and vestibular cues. Ph. D. Thesis. MIT, Cambridge

OPTOKINETIC RESPONSES

As mentioned above, the vestibulo-ocular reflex is a mechanism for moving the eyes in response to movements of the head. The vestibular system in combination with the visual and proprioceptive systems maintains an approximate fixed gaze in space as we move about in the environment. This tends to keep images fixed on the retina so that we may see clearly. If we are to fully understand how space travel affects our ability to compensate for head movements, we must first have a fundamental understanding of the quantitative dynamical aspects of the VOR and how it interacts with other systems to implement compensation for motion. Over the last 12 years, considerable insight about the detailed dynamics of the VOR has come from modelling the VOR as a dynamical system and identifying a process in the central vestibular system which is responsible for "integrating" vestibular, visual, and proprioceptive information to generate compensatory eye movements. This process has been labelled a velocity storage integrator.

Background

When the head is rotated in the dark, slow phase eye velocity increases immediately to compensate for the rotation and then decays to zero as the rotation continues, called per-rotatory nystagmus. When the rotation is stopped, there is a reversal of slow phase eye velocity (post-rotatory nystagmus) into the anticompensatory direction which decays to zero with the same time course as the compensatory response during the rotation. An interesting observation is that the time course of the decaying velocity is generally two or three times as long as the change in activity seen in peripheral units in the eighth nerve. This indicated that some central storage mechanism was responsible for lengthening the time course of the response.

Another phenomenon having similar characteristics which also indicated that some central storage mechanism was responsible for generating the slow phase compensatory eye movements is observed after optokinetic stimulation. This is called optokinetic after-nystagmus (OKAN) When an optokinetic drum is rotated about a subject's yaw axis, the eyes follow the drum. When the lights are extinguished, the compensatory eye movements do not disappear immediately but continue, decaying with a time course similar to that of compensatory eye velocity during rotation. What is interesting is the fact that during OKN eye velocity builds up to a steady state value, while during rotation in dark eye velocity decays. In addition, the eye velocity during the OKAN is oppositely directed to that of the anticompensatory eye velocity when the subject is stopped after rotation. This indicates that the visual and vestibular systems complement each other during rotation in light and that the anticompensatory after-responses cancel each other when rotation is stopped. When the two are combined, one gets the appropriate compensatory response. When a subject is rotated in light, there is compensation throughout the period of rotation. When the subject is stopped, there is no anticompensatory response.

In summary, the vestibulo-ocular reflex responds with a gain close to one in the monkey, and has a time constant of about 12 to 15 seconds mainly attributed to velocity storage. Velocity storage is also activated by the visual system by full field optokinetic stimulation.

A key insight about the properties of the VOR which has been gained over the past decade has been the idea that the storage properties associated with both vestibulo-ocular compensation and optokinetic following are both mediated by a common mechanism that we have called the velocity storage integrator. The properties of the velocity storage integrator are such that it is capable of storing velocity information up to some saturation level and then it declines with increasing stimulus velocity.

While the studies on velocity storage for rotations about a vertical axis have elucidated the dynamical aspects of the VOR, the full functional significance of velocity storage in coordinating postural stability is only recently coming to light. An important discovery in the last few years has been the realization that velocity storage has a three dimensional structure and the profound effect that gravity has on the storage properties.

The model of visual-vestibular interaction about a vertical axis is shown in Figure 8A and forms the basis for the generalization to three dimensions. Vestibular nystagmus is generated by head velocity signal rh, which through the cupula dynamics generates the signal rv, that appears in semicircular canal afferents in the vestibular nerve. This information activates the integrator, as well as projecting around it, to form a component of the eye velocity command signal in the vestibular nuclei Vn. The time constant of the integrator is equal to 1/ho. OKN is initiated by the velocity signal ro generated by movement of the visual surround. From this signal is subtracted head velocity and eye velocity, whose sum is gaze velocity. This generates the retinal slip signal e. The slip signal can be extinguished by light switch L or transmitted centrally to two elements. One is the direct pathway that is responsible for rapid changes in eye velocity. It has been omitted so as to concentrate on those signals that converge onto the integrator and the vestibular nuclei. The second is a nonlinear function whose output activates the velocity storage integrator (visual coupling to the integrator). The suppression switch S in the model is utilized to discharge or 'dump' the integrator rapidly during visual or tilt suppression.

The three dimensional extension of the model is shown in Figure 8B. Head and surround velocity are transformed into canal based coordinates. Tcan is the transformation from head to canal coordinates and Dcan is the dynamic three dimensional transformation of the canals. Toto and Doto are the transformations that convert linear acceleration or changes in the position of the head with regard to gravity into the velocity command signals that drive the integrator during such motions as pitching while rotating (Raphan, et al., 1983) or off-vertical axis rotation (OVAR) (Raphan and Cohen, 1981; Cohen, et al., 1983). The canal excitation vector rc, is dynamically transformed into a signal, rv, representing the eight nerve canal excitation vector. The visual signal is also converted into canal coordinates by Tcan to generate a central representation of retinal slip in canal coordinates e. Both rv and e activate a multidimensional representation of velocity storage which combines with the direct vestibular pathway to generate eye velocity in canal coordinates. This representation of eye velocity is transformed back into

head coordinates by the transformation Tcan-1 to generate eye velocity in head coordinates which can combine with head and surround velocity. The three dimensional structure of the direct optokinetic pathway has been left out in order to concentrate on those parameters which couple to the velocity storage integrator.

The state of the integrator is the three dimensional vector x and is presumably encoded in the second order lateral, posterior and anterior canal oriented neurons in the vestibular nuclei. The vector e is the retinal slip, n(e) is a nonlinear matrix operator on the central representation of retinal slip, Go is the coupling matrix from the eighth nerve to the integrator and Ho is the matrix representing the dynamics associated with the integrator.

Gravity has a profound effect on the mathematical structure of the velocity storage integrator. When subjects are on their sides and receive optokinetic stimulation about their vertical axis, the velocity storage integrator is activated in such a way so as to produce optokinetic after-nystagmus which has a vertical component. The oblique optokinetic after-nystagmus that develops is more closely aligned with the spatial vertical. Some of the interesting aspects of the dynamics of this "cross-coupled" response are the following:

1. The time constant of the horizontal component is somewhat shortened.

2. The buildup and decay of the slow phase velocity in for the vertical component of nystagmus is asymmetrical and is consistent with the asymmetries and the dynamic properties of velocity storage when rotations are about the subjects' pitch axis with the subjects on their sides.

When subjects are upright receiving vertical optokinetic stimulation in the upward direction, the velocity storage integrator is activated in such a manner so as to produce OKAN which has a small time constant and little activation. When the head is tilted 90 deg., the level of OKAN is increased and the time constant is bigger. For vertical optokinetic stimulation in the downward direction, a similar change in the characteristics of the velocity storage integrator is observed. There is an increased level of OKAN with a longer time constant. There is also an asymmetry between upward and downward slow phase velocity. The upward slow phase velocity is stronger and has a longer time constant. Recently we have discovered that the asymmetry is modified by tilting the animal more than 90 deg, i.e., into the southern hemisphere, i.e., head down. This indicates that the asymmetries as well may be a function of gravity.

In summary, we have reviewed the dynamical behavior of the VOR and the optokinetic reflex and shown that both activate a central vestibular process called the velocity storage integrator. We have also shown that velocity storage has a three dimensional structure that is modified by gravity. The effects of the modification are changes in time constants and activation levels of horizontal and vertical compensatory eye velocity for different orientations of the head with regard to gravity. Humans also have velocity storage although it is weaker than storage in monkeys.

Methods

Horizontal and vertical optokinetic responses are recorded in the Yaw and Pitch orientations, respectively. As Figure 9 illustrates, this experiment will also be conducted with the crewmembers free-floating out of the Rotating Chair. Due to crew-time constraints, the free-floating portion of this experiment will be conducted only later in the flight on two of the four MVI subjects. While free-floating, oblique (30) optokinetic stimulation will be used in addition to horizontal and vertical. As an alternate procedure, the optokinetic responses will also be recoreded while the crewmembers tilt their heads laterally to one side. For each optokinetic stimlus run, three speeds are presented in succession (20, 60 and 40/sec) for 15 sec each in one direction, and then OKAN is recorded in darkness for 15 sec. The same stimulus is then presented in the opposite direction (i.e., 15 sec of 20/sec, 15 sec of 60 /sec, 15 sec of 40/sec, 15 sec of darkness).

Expected Results

The purpose of the MVI optokinetic experiments during the upcoming flight is to obtain information on the time constant of the velocity storage integrator in the absence of gravity when it is activated to produce horizontal and vertical OKAN. Some of the questions which we hope to answer are:

1. What is the relationship between the time constants of the velocity storage integrator before, during and after insertion into microgravity for horizontal and vertical nystagmus?

2. To what extent are the time constants in the various planes equalized in microgravity?

3. How will asymmetries in vertical storage be affected by space travel?

4. What is the time course of adaptation of the various time constants?

5. What effect does head tilt have on the optokinetic responses inflight?

References

Cohen B., Helwig D., Raphan T.: Baclofen and velocity storage: A model of the effects of the drug on the vestibulo-ocular reflex in the Rhesus monkey., J. Physiol. (Lond.), 393:703-725, 1987.

Cohen B., Henn V., Raphan T., Dennett D.: Velocity storage, nystagmus, and visual-vestibular interactions in humans. Annals of the New York Academy of Sciences, New York, Vol. 374, pp. 421-433, 1981.

Cohen B., Matsuo V., Raphan T.: Quantitative analysis of the velocity characteristics of optokinetic nystagmus and optokinetic after-nystagmus. J. Physiol. (Lond.) 270: 321-344 (1977).

Cohen B., Raphan T., Waespe W.: Floccular and Nodular control of the vestibuloocular reflex. In: The Vestibular System: Neurophysiologic and Clinical Research, (Malcolm D. Graham & John L. Kemink, eds.), Raven Press, New York, 1988.

Cohen B., Suzuki J.I., Raphan T.: Role of the otolith organs in generation of horizontal nystagmus: Effects of selective labyrinthine lesions. Brain Res. 276. 159-164, 1983.

Raphan T., Cohen B.: Multidimensional modelling of the vestibulo-ocular reflex. In: Adaptive Processes in Visual and Oculomotor Systems. (eds. E. Keller & D. Zee). Pergamon Press, Holland 1986.

Raphan T., Cohen B.: Organizational principles of velocity storage in three dimensions: The effect of gravity on cross-coupling of optokinetic after-nystagmus (OKAN) In: The Representation of Three Dimensional Space in the Vestibular, Oculomotor and Visual Systems, Ann. N.Y. Academy of Science (eds. B. Cohen & V. Henn), 545:74-92, 1988.

Raphan T., Cohen B.: The role of the integrator in modelling the visual-vestibular interaction. In: Models of Oculomotor Behavior and Control (ed. B. L. Zuber). CRC Press, West Palm Beach, Fla., pp. 91-109, 1981.

Raphan T., Cohen B.: Velocity storage and the ocular response to multidimensional vestibular stimuli. In: Berthoz, A. and Melvill-Jones, G. (eds.), Reviews in Oculomotor Research, Elsevier North Holland, pp. 123-143, 1985.

Raphan T., Cohen B., Suzuki J.I., Henn V.: Nystagmus generated by sinusoidal pitch while rotating. Brain Res. 276: 165-172, 1983.

Raphan T., Matsuo V., Cohen B.: Velocity storage in the vestibular-ocular reflex arc (VOR). Exp. Brain Res. 35:229-248 (1979).

Raphan T., Schnabolk C.: Modelling slow phase velocity generation during off-vertical axis rotation (OVAR). In: The Representation of Three Dimensional Space in the Vestibular, Oculomotor and Visual Systems, Ann. N.Y. Academy of Science (eds. B. Cohen & V. Henn), 545:29-50, 1988.

Sturm D., Raphan T.: Modelling the three dimensional structure of velocity storage in the vestibulo-ocular reflex. Proc. 14th Bioengineering Conf. (IEEE), 1988

Waespe W., Cohen B., Raphan T.: Dynamic modification of the vestibulo-ocular reflex by the nodulus and uvula. Science 228: 199-202, 1985.

Waespe W., Cohen B., Raphan T.: Effects of flocculectomy on vestibular and optokinetic nystagmus and unit activity in the vestibular nuclei. Adv Oto-Rhino-Laryng. 30: 226-229, 1983.

Waespe W., Cohen B., Raphan T.: Role of the flocculus and paraflocculus in optokinetic nystagmus and visual-vestibular interactions: Effects of lesions, Exp. Brain Res. 50:9-33, 1983.

PER-ROTATORY AND POST-ROTATORY NYSTAGMUS

This experiment is designed to test, with one minute long constant angular velocity rotation, the per-rotatory and post-rotatory nystagmus slow phase velocity decay profile dynamics in Yaw Pitch, and Roll. These angular acceleration impulses are used to examine indirect VOR pathway responses which were described in the Optokinetic Responses section above.

Background

When a human subject is rotated about an earth vertical axis for an extended period, nystagmus slow phase velocity decays from its initial value in quasi-exponential fashion with an apparent time constant on the order of 12 seconds. After several minutes of rotation, nystagmus disappears, and the subject is no longer aware of his rotation. If the rotation is then suddenly stopped, the subject immediately feels that he is rotating in the opposite direction, and exhibits the well-known phenomenon of post-rotatory nystagmus (PRN). The nystagmus beats in the opposite direction to that seen during the original turning period (the "per rotatory period"). The nystagmus slow phase velocity is initially equal to approximately 60 percent of the previous rotation rate, and then decays with an apparent time constant in a manner similar to the per rotatory response. This "impulse response" test paradigm is of particular utility in quantifying the characteristics of the human VOR, since the response dynamics are approximately linear (e.g., doubling the input doubles the response; responses can be predicted assuming superposition in time). Once the impulse response of the VOR is known for a given axis, if the VOR dynamics are linear, it is theoretically possible to predict the time course of nystagmus for any arbitrary input.

The per- and post-decay of nystagmus was for many years attributed solely to the semicircular canal cupula-endolymph dynamics, which are relatively linear, and believed independent of g. However, more recent experiments in animals have shown that the cupula-endolymph dynamics (as manifest in semicircular canal afferent neuron responses) have a shorter time constant (5-6 sec; Goldberg and Fernandez, 1971) than that manifest in PRN (Cohen, et al., 1977; Waespe et al., 1983). Investigators have postulated the existence of two parallel pathways from the vestibular periphery to the eye velocity input centers of the

oculomotor nuclei: one, the so called "direct VOR pathway", carries the 5-6 sec time constant semicircular canal afferent information. The second, an "indirect" pathway, passes through a "velocity storage" center with somewhat slower (approx 15-20 sec) dynamics, and which effectively integrates canal, otolith, optokinetic, and haptic inputs, and provides a second, augmenting oculomotor input which prolongs the PRN response, lengthening the "apparent time constant" of nystagmus decay. The PRN response decline - traditionally characterized by a single decaying exponential - is now seen as consisting of the sum of at least two decaying exponential terms. Although the anatomical site of the velocity storage mechanism has not yet been determined, the dynamics of the indirect pathway have been deduced using both vestibular and optokinetic inputs in the yaw and pitch axes. There is some evidence in animals that velocity storage mechanisms in the pitch axis have a longer time constant for pitch forward than for pitch back. Little is yet known concerning human velocity storage in roll. The yaw indirect velocity storage pathways in the human appear to saturate at relatively modest nystagmus slow phase velocities. Mathematical models for cupula/endolymph dynamics, afferent neuron transduction and encoding, direct VOR pathway and indirect VOR pathway velocity storage have been developed, and will be reviewed in the course of experiment training. It is clear that the traditional view of the human VOR as a "reflex" which exhibits linear system dynamics is correct only in a qualitative sense. Nonlinear models are required to accurately predict the time course of responses in many cases.

It is now thought that gravity dependent effects on angular VOR responses may be mediated via indirect VOR pathway mechanisms. Experiments have shown that the dynamics of post-rotatory nystagmus in animals and man is dependent on the orientation of the subject with respect to gravity. Khilov (1929) first demonstrated that the duration of PRN following a stopping stimulus was dependent upon the orientation of the head to gravity in the post-rotational period. The phenomenon was, e.g., confirmed by Koella (1947) in rabbits, and in humans by Correia and Guedry (1964), and also by Benson and Bodin (1966), who showed that if the body is kept in an erect position, the slow phase decays quasi-exponentially with a time constant of 10-12 seconds. However, if the subject's head is tilted in pitch or roll by 90 deg during this period of post-rotatory nystagmus, the magnitude of the slow phase is rapidly decreased, and time course of decay decreases as if the "apparent time constant" of decay had been reduced. If the head is then subsequently raised to the erect position, nystagmus strength and time constant are once again increased, although not to the level they would have had if the head tilt had not taken place. This phenomenon - sometimes termed "nystagmus dumping"- has been assumed to be mediated by the otolith organs, although the exact mechanism is subject to some debate. Possibly a "dump" of the putative integrator in the system takes place, triggered by a conflict between angular velocity storage integrator output (signalling, in effect, "I'm rotating about a horizontal axis") and gravireceptor information (signalling "no I'm not!").

There have been occasional anecdotal reports of oscillopsia (apparent motion of the seen world upon active head movement) from shuttle astronauts in flight. However, oscillopsia has not regularly been reported by participants in parabolic flight. Many have speculated that a change in VOR gain or time constants might be a contributing factor in the etiology of space motion sickness. Quantitative parabolic flight experiments using sinusoidal stimuli have

generally shown no consistent changes in medium frequency VOR gain (Jackson and Sears, 1966; Vesterhauge, et al., 1984). Experiments by DiZio, et al. (1987, 1989) have demonstrated that the apparent time constant of PRN in yaw and pitch is shortened during (but not after) acute exposure to weightlessness. Space shuttle experiments conducted to date using active head movements and sinusoidal stimuli generally support the view that there is no consistent change in gain in the yaw axis (Thornton, et al., 1985, STS-6-8; Watt, et al., 1985, STS 41-G), although one experimenter (Clement, et al., 1985) has observed a decreased gain early in the mission. Yaw axis post-rotatory nystagmus was monitored inflight in one crewmember on the SL-1 mission using a hand spun rotating chair; results indicate no change in gain and are suggestive of a shortened time constant in flight, but are not statistically conclusive. The nystagmus dumping phenomenon appeared present in flight, suggesting that the dumping phenomenon can be triggered by processes related to the active head movement, rather than by gravity per se.

Comparison of pre and postflight PRN among four Spacelab-1 and five D-1 astronauts (Oman and Kulbaski, 1988; Oman and Weigl, 1989) have shown a residual shortening of the apparent time constant during the first several days after return from week long flights, out no consistent change in the magnitude of the initial peak slow phase velocity response (see Figure 10). The effects were thus qualitatively similar to those observed by DiZio, et al in parabolic flight. Responses gradually returned to preflight norms during the first postflight week. Oman, et al. have speculated that as a consequence of the altered gravireceptive input in weightlessness, the CNS may reduce the vestibular component driving central velocity storage in favor of visual inputs. Confirmation of this hypothesis awaits the results of further PRN testing both on orbit and pre/postflight, and data on changes in the visually dependent response of the velocity storage system from simultaneous experiments on human optokinetic after-nystagmus.

Methods

As illustrated in Figure 11, time constants will be tested in the clockwise and counterclockwise directions, and in three axes - Yaw, Pitch, and Roll. The constant velocity per-rotatory period will be 60 sec in duration at a velocity of 120°/sec. These values were chosen to match those used in previous SL-1 and D-1 experiments. Acceleration and deceleration will be set at 120°/sec^2.

Horizontal, vertical, and torsional eye position data will be analyzed using software which includes routines for calibration, semi-automated detection and removal of nystagmus fast phases, and calculation of the time course of nystagmus slow phase velocity for each run. Data from individual runs will be ensemble averaged by crewmember, session, and rotation direction and examined for changes. At least two different approaches will be used for making "same or different" statistical comparisons. One approach involves fitting the slow phase velocity time series (either individual runs or ensemble averages) with a multi-parameter model for the VOR so as to parameterize the data. Computed parametric data will then be analyzed using traditional statistical methods (e.g., ANOVA, using SYSTAT). A second approach (Oman and Kulbaski, 1988) involves computing a chi square parameter for the sum of the squared differences between

two ensemble averaged time series, each normalized based on pooled variance estimate computed for each point in time. This method allows us to assess whether there is a statistically significant difference between any two mean SPV profiles (e.g., comparing preflight vs. inflight) without having to "force fit" any particular mathematical model to the time series data in order to parameterize it.

Expected Results

This protocol will be utilized to investigate the hypothesis that adaptation to weightlessness influences the dynamics of the "indirect" VOR pathway through the "velocity storage" system. Responses of this same pathway are also simultaneously under investigation using optokinetic stimulation (see above). We hypothesize that any g dependent changes in velocity storage pathway time constants or storage asymmetries will also be manifest in optokinetic responses.

References:

Benson A.J. and Bodin M.A. (1966) Aerospace Medicine 37:889.

Cohen B., Matsuo V. and Raphan T. (1977) Quantitative analysis of the velocity characteristics of optokinetic nystagmus and optokinetic after nystagmus. J. Physiol. Lond 270: 321-344

Correia M. and Guedry F.E. (1964) US Naval School of Aviation Medicine Report NAV SAM 905, Pensacola, FL.

DiZio P., Lackner J. and Evanoff J. (1987) The influence of gravitoinertial force level on oculomotor and perceptual responses to sudden stop stimulation. Aviation, Space. Envir. Med. 58: Suppl. A.

Goldberg J.M. and Fernandez C. (1971) Physiology of peripheral neurons innervating semicircular canals of the squirrel money. J. Neurophysiol. 34:635-684

Khilov K.L. (1929) Zh. ughn. nos. gorlov. Bolezn. 6:289-299.

Koella W. (1947) Helv. Physiol. Pharmacol. Acta 5:154-168.

Oman C.M. and Kulbaski M. (1988) Spaceflight affects the 1-g postrotatory vestibulo-ocular reflex. Adv. Oto-Rhino-Laryng. 42: 5-8

Oman C.M. and Weigl H. (1989) Postflight vestibulooculer reflex changes in Space Shuttle Spacelab D-1 crew. Abstract: 1989 meeting of the Aerospace Medical Association, May 7-11, Washington, DC

Raphan T. and Cohen B. (1988) Organizational principles of velocity storage in three dimensions. Ann. NY Acad. Sci. 545:74-92

Waespe W., Cohen B. and Raphan T. (1983) Role of the flocculus and paraflocculus in optokinetic nystagmus and visual vestibular interactions: effects of lesions. Exp. Brain Res 90:9-33

SENSORY PERCEPTION REPORTING

The vestibular system operates as a silent partner with other sesnses improving the efficiency of control of goal-directed head and body movement relative to the earth. Vestibular sensations do not reach conscious awareness as we skillfully move about. Vestibular sensations achieve conscious awareness only when they are "disorderly" in relation to concomitant information from other senses that participate in the voluntary control of head and body motion. The "dizziness" that accompanies vestibular disorders is usually poorly described because the perceptual event is characterized by the confusion and disturbance that comes from mixed signals among the various senses involved in the control of motion. Under the controlled conditions of MVI the crewmembers will be asked to report with this experiment whether their perceptions of particular motions in orbit are (1) different than they were on Earth and (2) are more (or less) confusing (or disturbing) than they were on Earth. This experiment is also designed to describe, quantify, and record any changes in symptoms of motion sickness which may occur during the flight. Although none of the features of this experiment are intended to induce motion sickness symptoms, the coincident occurrence of motion sickness and the nature and degree of symptoms are very important to the interpretation of data collected during the performance of the other MVI experiments. In addition, the use of any anti-motion sickness medication will be very important to the investigators in interpreting their data.

Background

Orientation illusions have been studied in parabolic and orbital flight. Theses studies indicate that when static visual cues to self orientation are "wrongly" interpreted by the brain, illusory perceptions of self-orientation with respect to the vehicle result. Attempts have been made to define the perceptual "rules" which the brain uses to identify objects and surfaces and to infer self-orientation. Reports from the crews of the D-1 and Spacelab-1 missions indicate that, when the identity of the subjective "floor" changes, it generally becomes that cabin surface which is closest to being beneath the observer's feet and parallel to the left/right head visual axis. Similarly, if an observer floated very close to a cabin surface with his body parallel to it, there was a tendency to perceive the surface as a subjective wall (even if it were actually a ceiling or floor). In other cases, a change in gaze angle or scene content was sufficient to trigger a change in subjective orientation. For example, if the observer simply viewed another person who was floating nearly horizontal or inverted with respect to the actual cabin floor, and if other visual

cues were ambiguous, the observer often suddenly felt that he himself was tilted and that the wall or ceiling of the vehicle closest to being in the direction of the seen person's feet was perceived as the subjective floor. Orientation illusions can often occur spontaneously in zero-g, but are also subject to volitional control. ("If I decide that I want to make the true floor a ceiling, suddenly it is.")

Another illusory phenomenon which occurs in parabolic and orbital flight is the Inversion Illusion - a feeling of somehow being continuously upside down while in weightless flight. Some crew members have been able to reverse or diminish the illusion by pulling themselves down into a seat. Another reported that he could reduce the paradoxical sensation only by looking at the reflection of his own face in a shaving mirror.

Other sensory perceptual distortions which have been observed by space crews during and/or after orbital flight include, among others, paradoxical motion, vection, and altered awareness of limb position. Some crewmembers have described, when during a deep knee bend with their feet affixed to the orbiter floor, a sensation of the floor coming up to meet them rather than their body lowering to the floor. Perceptions of the wall seemingly moving toward the observer rather than the observer's body moving toward the wall as he bent forward have also been reported.

The various illusory phenomena experienced in parabolic and orbital flight, both from the scientific objective of seeking to understand the integration and underlying mechanisms of the neurosensory system, as well as from the operational need to fully understand, and prevent if possible, the symptoms of space motion sickness, are important experiences to study and quantify.

Space motion sickness has been the most clinically significant phenomenon occurring during the first few days of space flight on the space shuttle. Symptoms of motion sickness in space were first reported by Soviet Cosmonaut Titov in 1961. During the United States Mercury and Gemini programs, no instances of space motion sickness were reported. However, during the Apollo program, 35 percent of crewmembers reported symptoms and during the three Skylab flights, 60 percent of the astronauts were affected by symptoms of motion sickness. We believe that this emergence of motion sickness symptoms was due to the ability of the crewmembers to move about within the spacecraft in the larger Apollo and Skylab vehicles, while during the Mercury and Gemini flights, very little movement was possible due to the confined quarters within these vehicles. The space shuttle has a relatively spacious flight deck and middeck, permitting crewmembers considerable freedom for head and body movements. When the Spacelab is flown in the payload bay, the room for movement is increased even more. Consequently, there is ample opportunity for visual and motion stimulation to occur.

Of the 85 crewmembers whose first space flight occurred during the first 24 shuttle flights, 67 percent reported some symptoms of motion sickness during the first 2 to 4 days. Their motion sickness experience included one or more of the following symptoms: headache, malaise, drowsiness, disequilibrium, lethargy, anorexia, stomach awareness, nausea, and

vomiting. Of these 67 percent with symptoms of space motion sickness, 26 (46%) were classified as mild, 20 (35%) were moderate, and 11 (19%) were severe. Although there is great individual variation, investigation of the motion sickness experienced during the shuttle flights has shown two "typical" patterns of symptom development. In the first pattern there is unmistakable and rapid onset of symptoms with, in an occasional case, an episode of vomiting occurring as early as 15 minutes after launch. Individuals with this pattern may have several episodes of vomiting, often without precedent nausea. They are likely to experience other symptoms as well with both gastrointestinal and central nervous system manifestations. In the second pattern of onset there is a more gradual development of symptoms often starting with a mild headache, anorexia and lethargy. These individuals may go on to vomiting, but usually not until the latter part of the first day in orbit. The type of symptom onset does not, however, seem to be predictive of either the overall severity or duration of symptoms. In both cases, movement of the head and/or body and unusual visual orientations are provocative and kept at a minimum by the affected crewmember. Movements in the pitch plane seem to be especially uncomfortable for some crewmembers. In addition, visual cues associated with being off-vertical with respect to the interior of the vehicle can be provocative and are avoided by the astronauts affected with motion sickness. In a few cases, no symptoms are experienced during the first day of flight, but then develop on the second flight day. Also, a few crewmembers who took an anti-motion sickness medication (Scop-Dex) during the first one or two days of flight did not develop any symptoms until after they stopped the medication.

A number of theories have been advanced to explain the cause of motion sickness. None has been successful, however, in fully explaining the underlying mechanisms involved in the development of motion sickness symptoms. The one factor which is a prerequisite for motion sickness to occur is an intact vestibular system coupled with the presence of real or apparent motion of the head and/or body. Thus the investigation of each of the hypotheses of this experiment is expected to shed some light on the underlying mechanisms which reach clinical expression in the experience of motion sickness, visual orientation illusions, and other sensory distortions.

Methods

Implementation of this experiment will require crewmembers to utilize a standardized Sensory Perception Questionnaire as a checklist for inflight reporting of any illusions or symptoms. The questionnaire has been assembled from previous questionnaires (ground-based, DSO-401, DSO-459, Spacelab 1, and D-1). There are three reporting timeframes for this experiment. (1) It is vital that the reporting of sensations, illusions, and symptoms be accomplished concurrently with the other MVI experiments inflight by means of a microcassette voice recorder. Dynamic changes in motion sickness symptomology will be recorded by describing specific symptoms and by using a subjective self rating of overall discomfort assigned a numerical score from 0 to 20 (1 being no symptoms, 20 being emesis). (2) The second reporting timeframe will be performed at the end of each test session and will allow the crewmember to reflect on comparisons across different runs and chair orientations. (3) The third

report will be recorded at the end of each shift, and the crewmembers will record motion sickness symptomology using both a checklist (Figure 12) and a timeline chart describing the timecourse of any symptoms using the 0-20 discomfort rating score (Figure 13).

PREFLIGHT AND POSTFLIGHT TESTING

The main objective of the preflight baseline data collection is to obtain normal one-g responses from each payload subject. These responses will serve as baseline criteria from which all in-flight adaptation and postflight readaptation will be evaluated. These tests involve nominal and alternate in-flight test objectives as well as the other pre/postflight functional objectives. The preflight sessions are performed at 130, 68, 30 and 15 days prior to launch.

In addition, the Launch-130 day session will be used as a control study to duplicate the early postflight test schedule (including other IML-1 experiment objectives) in order to identify what individual responses, if any, might change as a function of interactions across the different BDC tests or as a function of the repeated testing.

The postflight readaptation testing occurs on landing day within 1-2 hours, and is repeated on 1, 2, 5 and 7 days after the landing. In addition to the Pitch, Yaw and Roll experiments which are also performed inflight, the preflight and postflight testing includes testing for Positional Nystagmus and on a Dynamic Posture Platform.

POSITIONAL NYSTAGMUS TEST

The purpose of the positional nystagmus test is to determine whether or not a nystagmus results from a change in head or body position.

Depending upon the conditions of the test (eyes open, eyes closed, visual fixation, etc.), a positional nystagmus has been reported in as many as 50% of putatively normal subjects. This study is designed to determine the incidence of positional nystagmus in flight crews and relate these findings to other vestibular test results.

Background

The incidence and prevalence of positional nystagmus in the normal population has never been determined. Studies of so-called "normal" populations have been highly selected, and report an incidence of positional nystagmus ranging from about 25-50%.

Positional nystagmus associated with vestibular disturbances, on the other hand, can be as high as 100% in patients with benign paroxysmal positional nystagmus and vertigo, to a variable percentage in patients in various stages of compensation from unilateral or asymmetric bilateral

vestibular disturbances. There does not appear to be a consistent relationship defined between patients with a positional nystagmus and motion sickness.

Methods

This test will consist of horizontal and vertical EOG recordings, approximately 30 seconds in duration, obtained with the crewmember in each of the following positions: (1) upright, seated; (2) supine; (3) supine with head turned to the right; (4) supine with head turned to the left; (5) supine with head and neck extended over the edge of the examining table; (6) body and head turned to the right side with neck supported; and (7) body and head turned to the left side with neck supported. EOG responses will be recorded in each position with the crewmember's eyes open and closed in the dark. No visual targets will be provided, and tapping patterns will be employed as attention tasks (peak alertness is required). The test session will also include the Dix-Hallpike maneuver (1951), which consists of a rapid backward motion to a head-hanging and turned position.

Expected Results

Under normal circumstances, the vestibular system (both semicircular canals and otolith systems) responds only to angular and linear accelerations, respectively. The presence of a nystagmus in 1 g would suggest that the VOR is attempting to correct for an abnormal or inaccurately detected head acceleration.

DYNAMIC POSTURE TEST

The Dynamic Posture Test will be performed as a pre- and postflight study to determine the ability of subjects exposed to microgravity to interact visual, vestibular and proprioceptive sensory orientation references for control of upright stance before and after exposure to 0 g.

Postural instability on return to 1 g has been a consistent result of sustained exposure to microgravity. This study addresses the sensorimotor adaptive changes associated with control of upright posture upon return to earth following space flight.

Background

In a terrestrial environment, the vestibulo-spinal systems are organized to control center of force produced by the effects of gravity acceleration on the body center of mass over the foot supports when standing. When a human is introduced to 0 g, the forces acting upon the body center of mass change from primarily those produced by gravity to forces on the body resulting from active and passive body movements. Maintenance of head, body and eye stability under the two circumstances would require very different motor programs. Reprogramming of body

movements in space to maintain clear vision or to minimize center of mass movements would require disregarding otolith input references normally used as a reference to vertical. Upon re-entry to 1 g, re-establishment of preflight reflexes would be required in order to re-adapt to Earth vertical references provided by otolith responses to gravity.

The types of movements required to maintain distribution of the center of force over the feet during standing in normal subjects requires rotation around the ankle joints on a fixed surface, and hip movements if standing on a rail. In space, the hip movements would be the only body axial movement pattern which would be potentially effective in controlling body center of force. Consequently, upon return to Earth the subjects must switch from a "hip" synergy to an "ankle" synergy as they re-adapt to an Earth environment.

Methods

The Dynamic Posture Test is currently being used on Extended Duration Orbiter missions under a Detailed Secondary Objective (DSO 605). This test utilizes a modified posture platform (Equitest; Portland, OR) which consists of two sets of automated test procedures: movement coordination tests and sensory organization tests. During the movement coordination tests the platform will be suddenly translated forward or backward (by about 3 inches) or suddenly rotated toes-up or toes-down (by about 10 degrees) to perturb the subject's upright stance. The reflex responses to each of these sudden perturbations is monitored and recorded for a 2.5 second period. For the sensory organization tests, movements of the footplate or the visual surround or both will be referenced to the subjects postural sway and the responses for each sensory test will be recorded for 20 second periods.

In addition to the postural sway of the subject, the muscle activity from the legs will be measured using conventional electromyographic (EMG) techniques. The same electroding procedures decribed above for the EOG electrodes will be used for EMG as well, except that the electrode sites may be shaved if necessary to achieve acceptable electrode impedance. A safety harness is worn by the subject during this test and an operator's footswitch must be depressed throughout the test for it to be operational.

Expected Results

In one-G environments, the vestibulo-spinal systems are organized to control body center of mass over a support surface while resisting 1 g. In 0 g, these control systems must be reorganized to control inertial movements of the body center of mass.

EQUIPMENT DESCRIPTION

Figure 14 contains an experiment block diagram to define the MVI flight equipment and their interfaces. Below is a description of the main equipment components.

Experiment Control and Data Interface (ECDI)

The ECDI is a programmable microcomputer-based control center for the MVI experiment. The ECDI performs the following functions:

(1) acquisition of analog experiment sensor data (5 channels at 128 Hz and 8 channels at 32 Hz);

(2) data formatting and transmission over the Spacelab High Rate Multiplexor (HRM) and Closed Circuit Television (CCTV) systems;

(3) experiment stimulus hardware control via analog and/or digital means;

(4) experiment operation management via real time data displays and custom designed software.

Rotator

The experiment unique Rotator has been designed to mount and operate in the center aisle of the Spacelab. Operational safety requires a 32 inch sweep radius from the center axis of rotation. The Rotator is programmed to provide three types of velocity profiles (pseudorandom, step, and sinusoid).

Chair

A chair has been designed for MVI to improve the capability to accommodate all subject positions and restraint requirements. The subject's head is repositioned with respect to the axis of rotation by removing the entire chair from the rotator base and resecuring the chair to a different attachment point on a different side (i.e., no lateral head tilts are required). A trunnion design has been developed which will allow a secure attachment point to the rotator base but will also allow the operator to quickly change the subject/chair position. This chair repositioning method allows for subject rotation in the yaw, pitch and roll planes. The design requires that the subject's body be centered over the axis of rotation in the pitch and roll configurations, which means the head is slightly off-center resulting in eccentric rotation.

The Helmet Restraint Device attaches to the rotating chair and is used to fix the position of the subject's head relative to the rotational axes of the rotator by locking the helmet into a fixed position. The HRD has a quick-release attachment point to the top of the Helmet for subject ingress and egress. To accommodate subjects of various sizes, the HRD can be adjusted up and down along the chair frame by releasing two locking pins. Once adjusted to a comfortable position for the subject, the HRD is locked into place by engaging the HRD locking pins in indexing holes in the chair frame.

Helmet Interface Box (HIB)

The Helmet Interface Box mounts on the MVI rotator/chair assembly and provides:

(1) the interface and controlling circuitry for devices used on the MVI Helmet.

(2) data communication circuitry for transmitting experiment sensor data to the ECDI and digital command signals from the ECDI.

The HIB contains the LSLE Electro-oculographic Signal Conditioners, which are lightweight, miniaturized, battery operated electronic systems capable of detecting and amplifying the EOG potentials generated by the human eye. Each unit has two amplifier channels such that both left-right (horizontal) and up-down (vertical) eye positions are detected.

Helmet Assembly and Modules

The MVI subject will wear a lightweight Helmet Assembly which provides for:

(1) interchangeable mounting of visual stimulus modules and a video recording module;

(2) hard mounting of head acceleration sensors;

(3) total restraint of the subject's head relative to the rotational axes.

Throughout the many experiments, the helmet can be used in free head movements or constrained in the Helmet Restraint Device on the chair.

The Helmet contains earphones for communication from the operator and auditory stimulus cues (e.g., an oscillating tone or white noise). Two visors on the Helmet move independently and have a bayonet mount for the three different Helmet Modules.

The Camera Module contains a miniature CCD video camera and an infrared illumination source which are positioned with respect to the subject's eye to record eye movements. The illumination intensity of the IR source is by computer control from the ECDI.

The LED Module houses an array of five LEDs used for eye movement calibrations. The center LED is also used as a fixation target during some portions of the MVI experiment. Digital command signals from the ECDI control the timing and sequence of the LEDs.

The Monocular Optokinetic Stimulus (OKS) Module contains a variable speed/direction DC motor-driven checkerboard pattern to provide a moving visual display in front of the eye. The pattern can be reoriented by 90 deg to alternate between horizontal and vertical planes with respect to the subject. The speed, direction (CW or CCW) and pattern illumination are controlled by software in the ECDI.

INFLIGHT PROCEDURE DESCRIPTION

The MVI rotator experiments have been grouped for timeline efficiency into three timeline models or Functional Objectives, or FOs (Pitch, Yaw and Roll). The Pitch FO includes all of the previously described protocols that require pitch rotation. Similarly, FO-2 Yaw and FO-4 Roll test the subject in the yaw and roll orientations. In FO-3 OKAN, the subject is free-floating out of the chair with a visual stimulus provided by the OKS module connected to the MVI helmet. In addition to these timeline models, FO-5 SPR involves the subject's monitoring of sensory perceptions. Other FOs have been developed for experiment setup and system testing, subject preparation, subject/operator handover, and experiment stowage.

MVI is timelined to be performed by all four payload crewmembers on the Pitch, Yaw and SPR procedures. The Roll is only scheduled to be performed by one crewmember, and OKAN by two crewmembers. The goal is to obtain early, mid and late measurements of the Pitch and Yaw procedures to define the inflight adaption time course.and correlate this with the postflight readaptation time constants as well. Figure 15 illustrates when the measurements occur relative to the hypothesized adaptation curves. Due to crew time constraints, the Roll and OKAN measurements are limited to the steady-state late mission part of the adaptation curves.

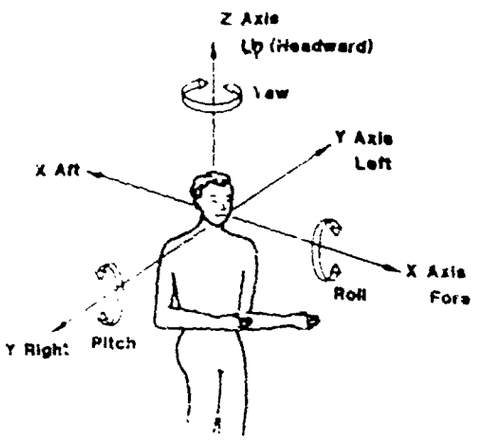

Figure 1. Illustration of Rotational Axis Frame of Reference.

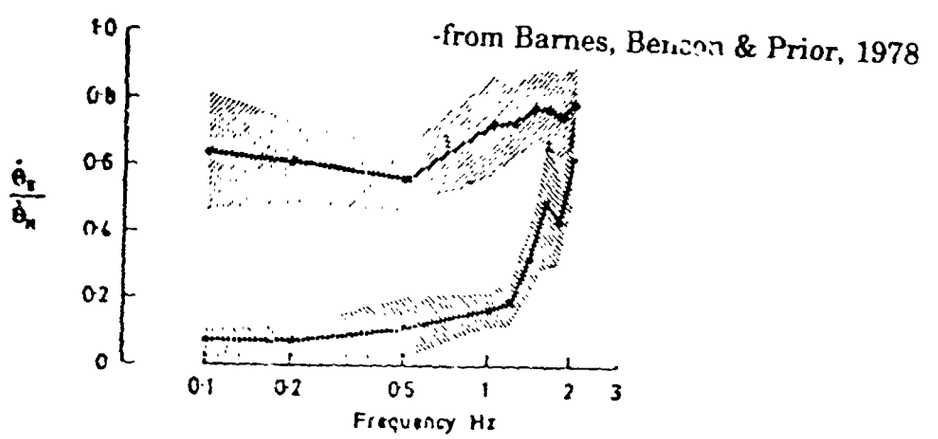

Figure 2. Comparison of the VOR and visual suppression of the VOR in humans. The upper curve shows the ratio of eye velocity relative to the head velocity (VOR gain) in the dark. The lower curve represents the same ratio when a head fixed target is present.

ROTATIONAL AXES

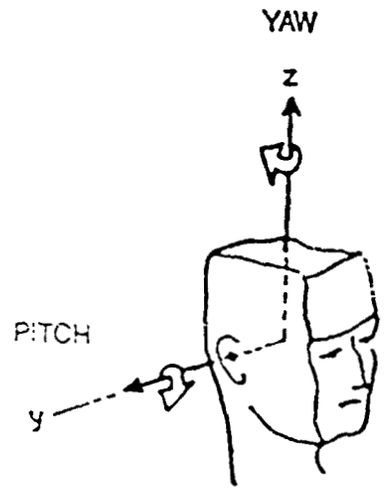

EYE MOVEMENT RESPONSES

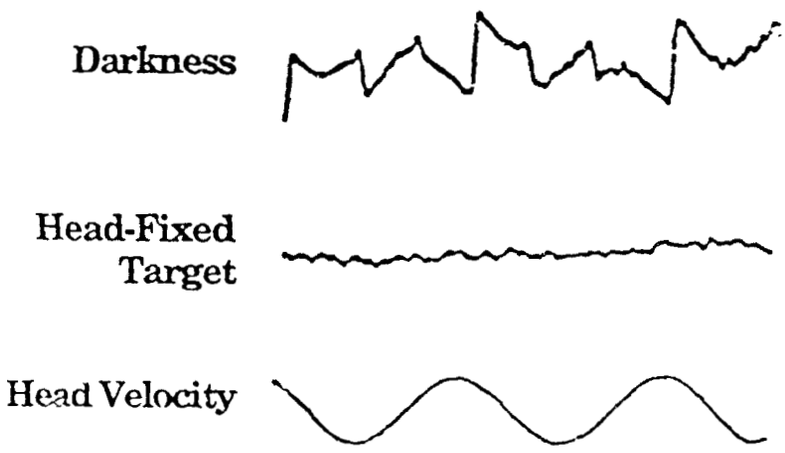

STIMULUS CONDITIONS

Visual Conditions	Pitch Rotation	Yaw Rotation
Darkness	Sinusoids (0.05 & 1.25 Hz)	Sinusoids (0.05 & 1.25 Hz) Pseudorandom (0.02 - 1.39 Hz)
Head-Fixed Target	Sinusoids (0.05 & 1.25 Hz)	Pseudorandom (0.02 - 1.39 Hz)

Figure 3. VOR Suppression Experiment Protocol.

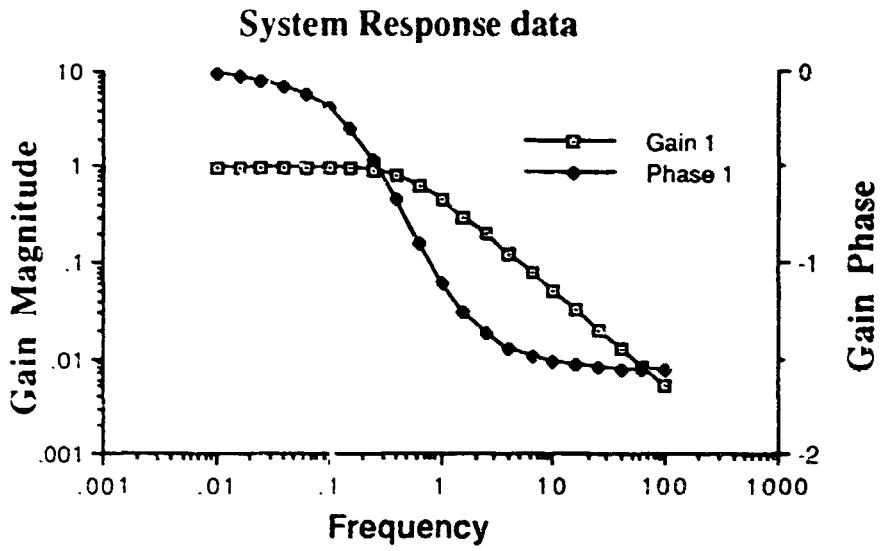

Figure 4. View of a gain-phase system analysis.

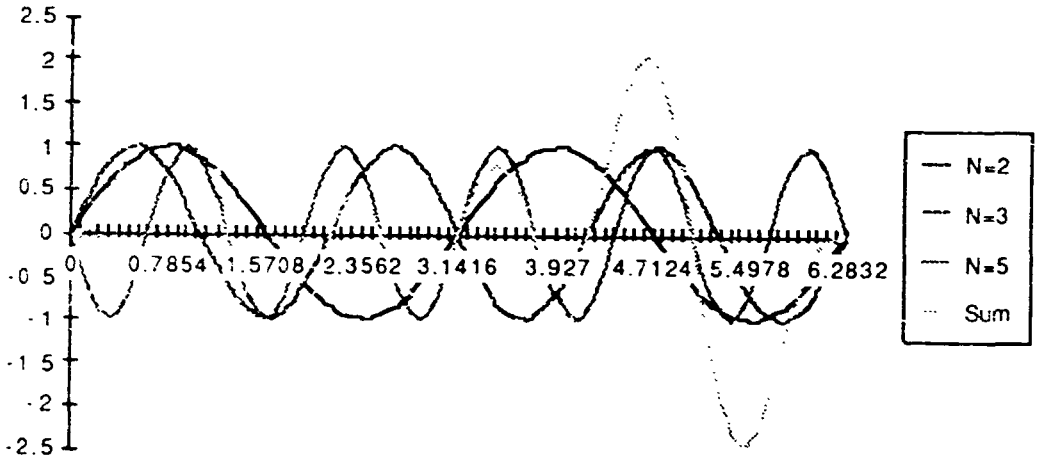

Figure 5. Ilustration of a Sum-of-Sines Plot.

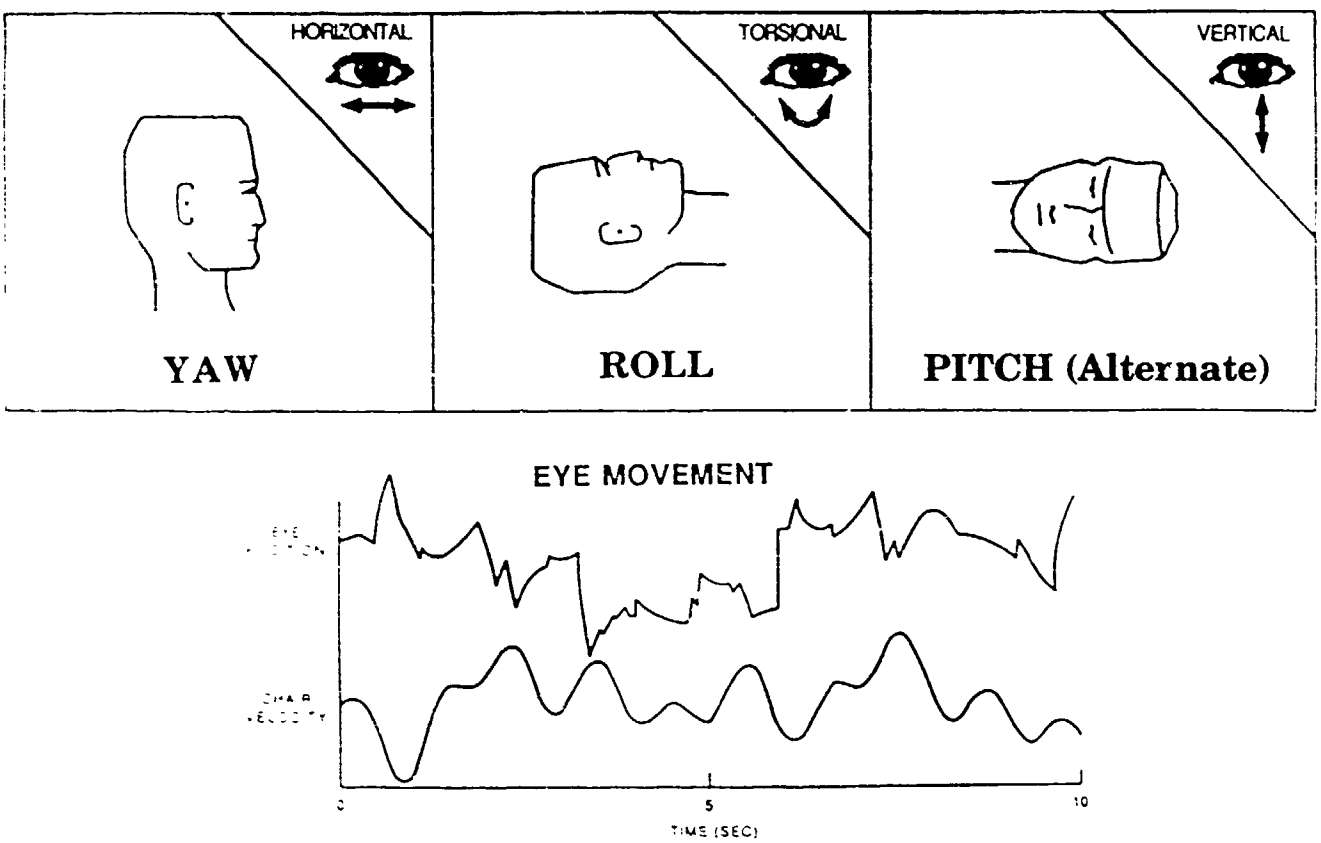

Figure 6. Semicircular Canal Dynamic Experiment Protocol.

ROTATIONAL AXES

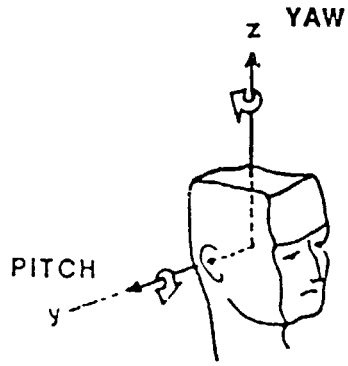

STIMULUS CONDITIONS

Optokinetic Stimulus	Rotator Profile
± 40 °/sec	Static
OFF	Sinusoid (0.2 & 0.8 Hz)
± 40 °/sec	Sinusoid (0.2 & 0.8 Hz)

EYE MOVEMENT RESPONSES

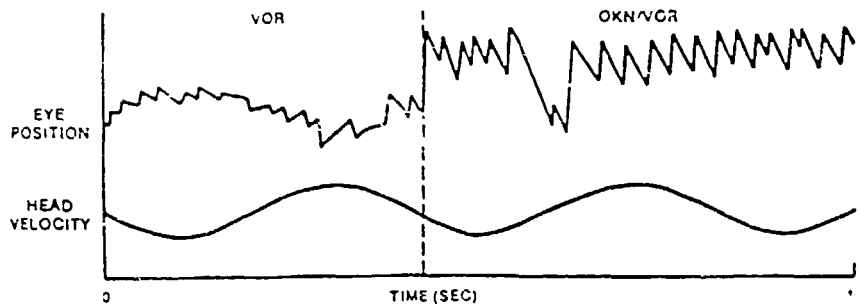

Figure 7. VOR Suppression Experiment Protocol.

ONE-DIMENSIONAL

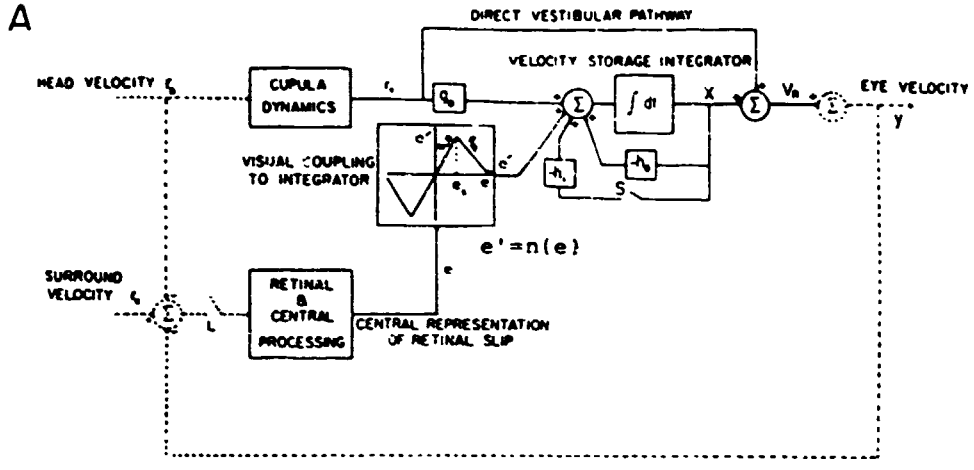

THREE-DIMENSIONAL

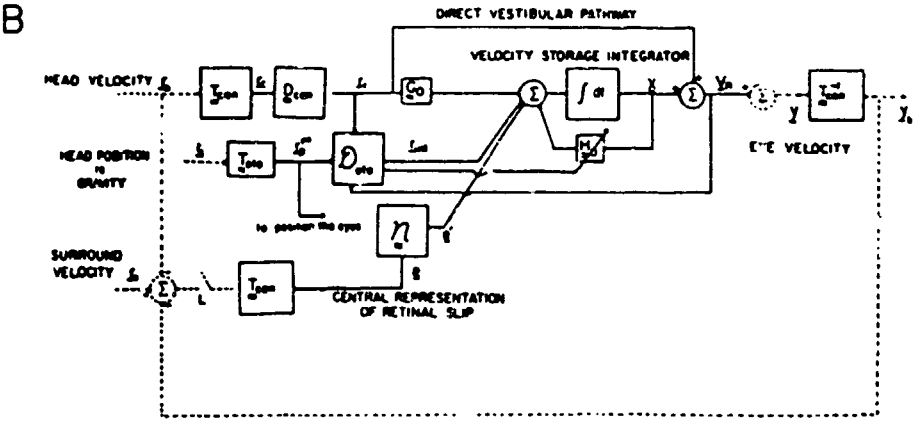

(From Raphan & Cohen: Velocity Storage, 1988)

Figure 8. Velocity Storage Models.

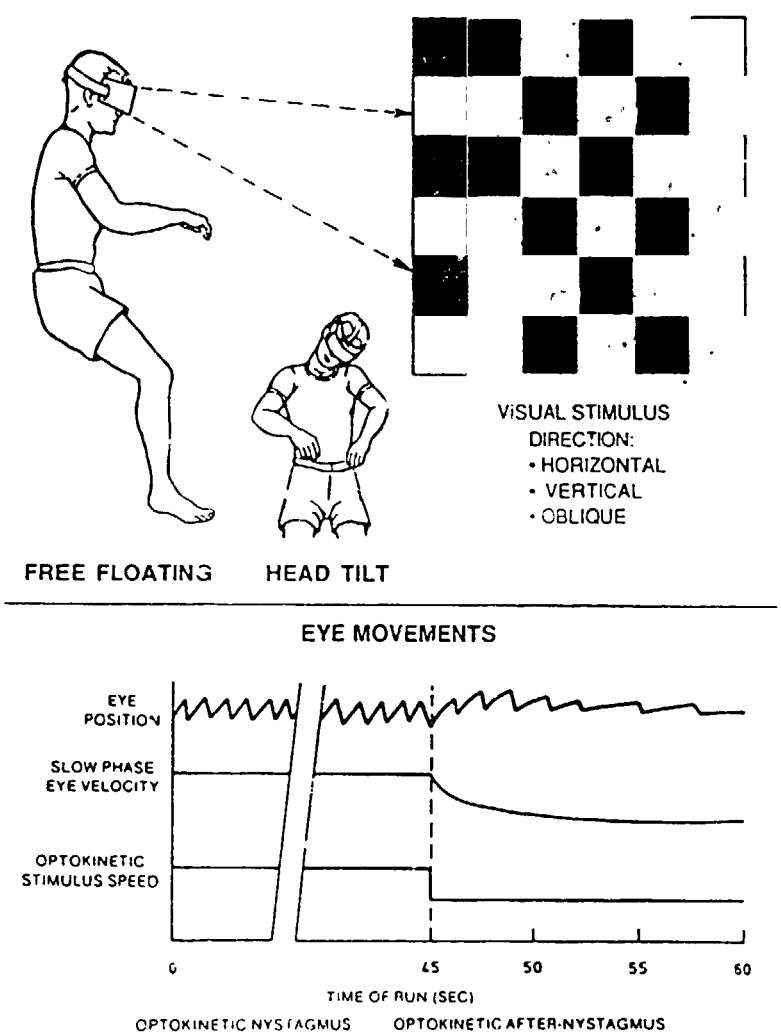

Figure 9. Optokinetic Responses Experiment Protocol.

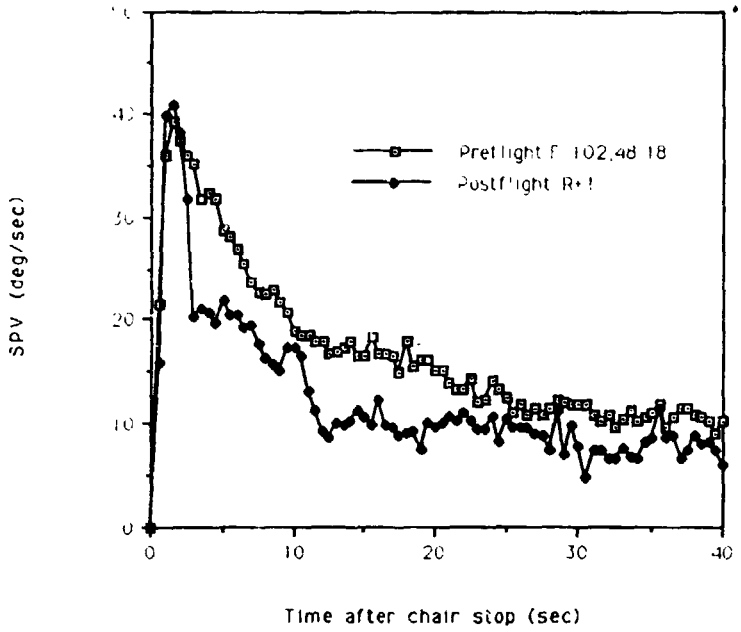

Figure 10. Preflight vs Postflight PRN Responses.

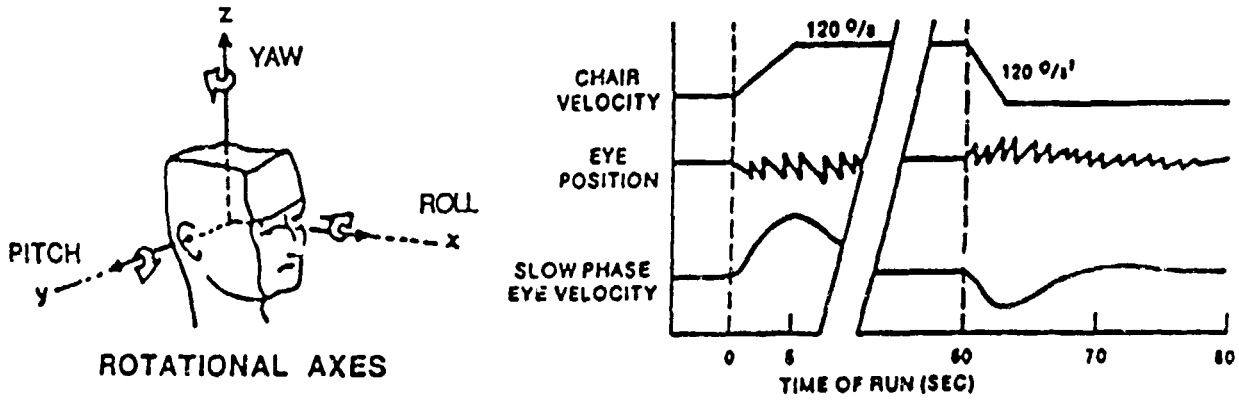

Figure 11. PRN Experiment Protocol.

DIRECTIONS x = symptoms you have experienced any time during the shift
+ = symptoms you have at the present time

MET time of reports (D/HH MM)								
Sweat (slight) "mild clammy feeling"								
Sweat (moderate) "small beads of sweat"								
Sweat (intense) "profuse whole body"								
Pallor (slight) "limited to mouth, earlobes"								
Pallor (moderate) "involves face, torso"								
Pallor (intense) "white as a ghost, ashen"								
Subject warmth								
Flushing								
Dry lips/mouth								
Salivation (moderate) "swallowing more frequently"								
Salivation (intense) "copious amounts"								
Yawning								
Puffy face/stuffed nose								
Distorted smell/taste								
Back pain								
Lethargy								
Headache (slight) "intermittent, mild "								
Headache (moderate) "persistent"								
Headache (intense) "incapacitating"								
Dizziness (lightheadedness or vertigo)								
Disorientation								
Drowsiness (slight) "decr. mental alertness"								
Drowsiness (moderate) "feel like falling asleep"								
Drowsiness (intense) "literaly falling asleep"								
Apathy								
Concentration impaired								
Appetite loss								
Belching								
Epigastric awareness - intermittent, mild sensation (not uncomfortable)								
Epigastric discomfort - persistent and uncomfortable								
Nausea (slight), more intense and unpleasant								
Nausea (mod), feel like "reaching for the bag"								
Nausea (intense)								
Vomiting								
Sudden vomit								
MS medication effective								
Feeling Fine								

Figures 12. MVI Daily Motion Sickness Symptom Checklist.

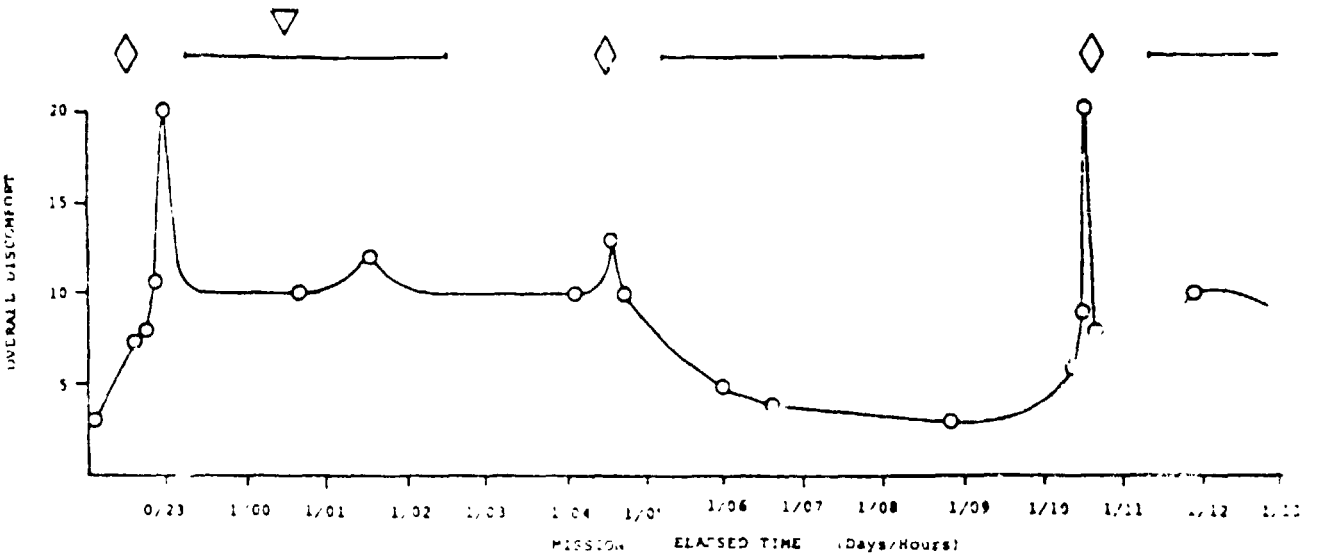

Figure 13. Subjective Comfort vs. Time for Subject B, Spacelab 1, Second day of orbit (Oman, et al., 1984).

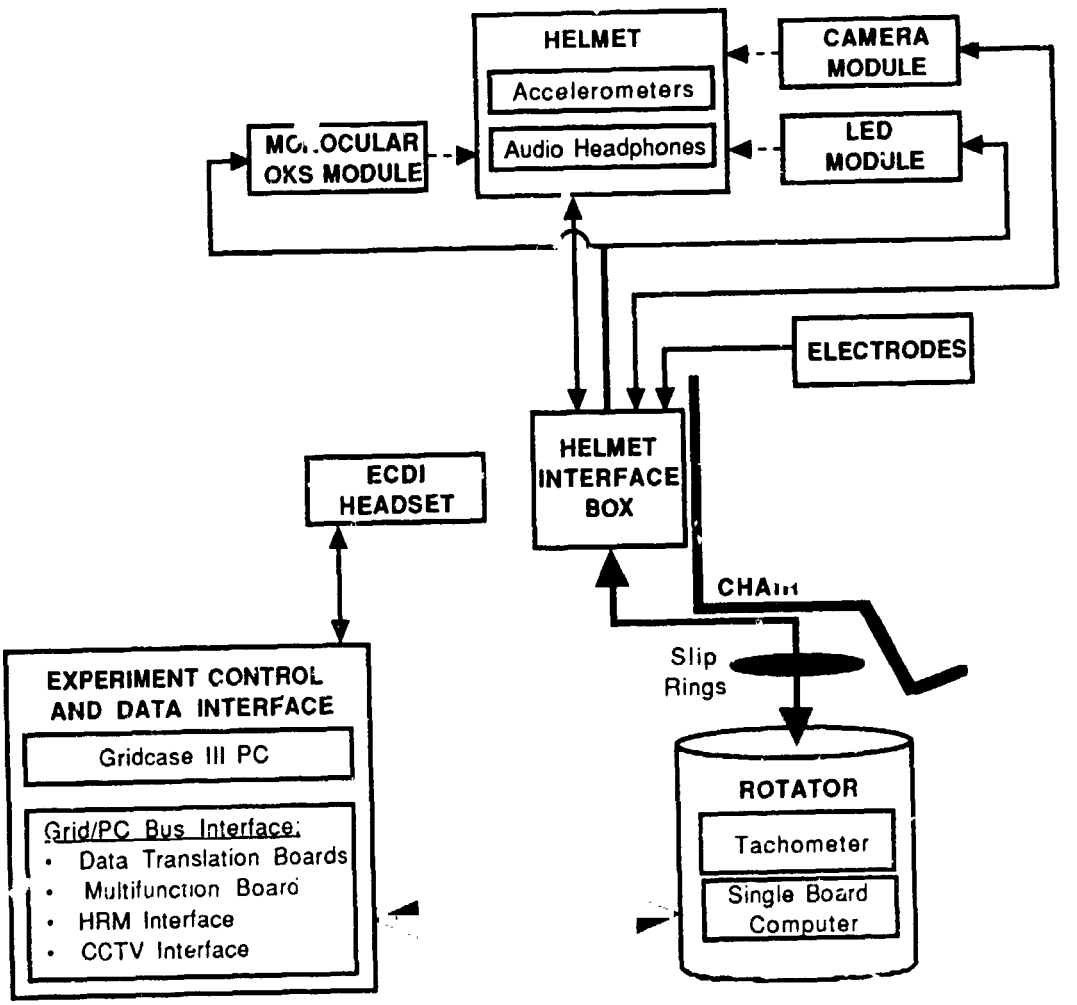

Figure 14. MVI Flight Hardware Block Diagram.

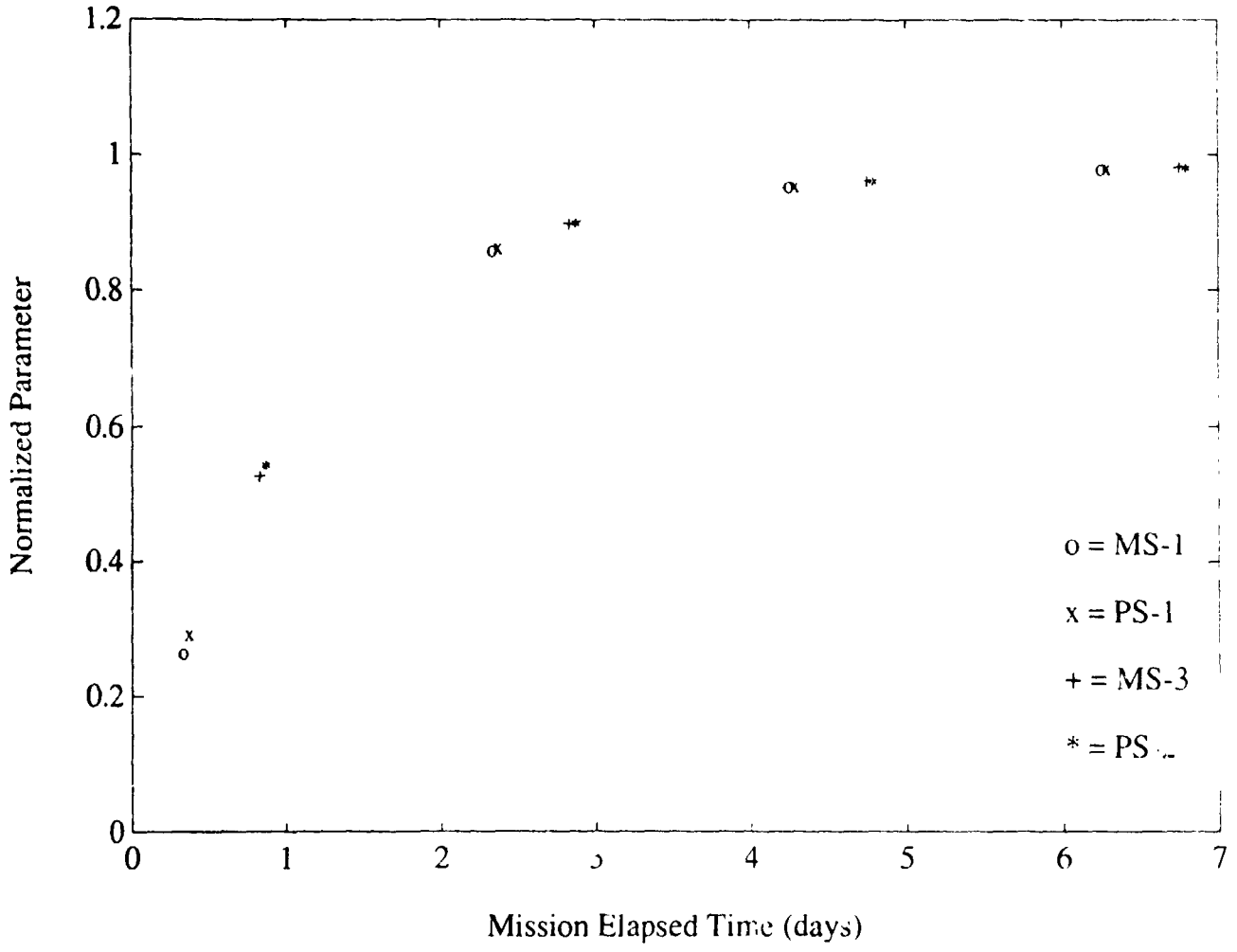

Figure 15. MVI Measurements in Pitch Relative to Theoretical Response Adaptation Curves.

N92-23527

BIOSTACK
(14-IML-1)

H. Bücker
Institute for Aerospace Medicine, DLR
Cologne, Germany

Orbiting spacecrafts are embedded in a complex environment consisting of electromagnetic radiation and of charged particles of solar and galactic origin, as well a of charged particles of the radiation belts and neutrons which result as an intraction production of the galactic radiation with the Earth's atmosphere.

The Biostack experiments address especially the biological effects of the galactic particles of high atomic number and high energy, called HZE particles. The objective of the experiments is to substantiate the assessment of spaceflight radiation hazard especially regarding these particles.

Experiments conducted during Apollo 16 and 17, Apollo-Soyuz, and Spacelab 1 misions demonstrated that the very high local concentration of absorbed energy delivered by single particles can have serious biological effects on an organism and that the seriousness of that damage is related to the organism's ability to repair or replace affected cells. The IML-1 Biostack investigation builds on the results of these earlier investigations, using advanced methods of dosimetry and exposing new biological samples and detectors.

Proper biological dosimetry of cosmic HZE particles is necessary to determine the effects of single heavy ions on individual biological test organisms. This is achieved by suitable combinations of physical visual particle detectors to which test organisms are attached in monolayers by various established techniques so that the spatial relation between the particles' trajectories and the affected cells can be read together with the biological response to the particles' passage. Radiation detectors to be utilized are nuclear emulsion and plastic detectors. Multiple detector sheets and biological monolayers are arranged in a sandwich-like manner. The resulting stacks are housed in hermetically-sealed cylindrical aluminum boxes. The biological test systems are Bacillus subtilis, Saccharomyces cerevisiae and Sordaria fimicula spores, Arabidopsis thaliana seeds, and Artemia salina eggs. Biological effects under investigation are inactivation, mutation induction, repair deficiencies, and developmental studies. Three boxes are located in two Spacelab racks, and one is under the floor to measure radiation doses in different areas of the laboratory.

Postflight processing of the particle detectors will reveal the particles' tracks and the biological response of the affected cells by various established techniques adapted to a given detector/cell combination.

The Biostack data will be ued to calculate the potential hazards of cosmic rays to humans and biological experiments during spaceflight. Parts of the shuttle that are particularly vulnerable to radiation will be identified so that better radiation protection can be developed for those areas. Additionally, the science of radiation biology will benefit from a better understanding of the action of these particles on biological matter.

N92-23628

MENTAL WORKLOAD AND PERFORMANCE EXPERIMENT (15-IML-1)

Harold L. Alexander
Massachusetts Institute of Technology
Cambridge, MA USA

Whether on Earth or in space, people tend to work more productively in settings designed for efficiency and comfort. Because comfortable and stress-free working environments enhance performance and contribute to congenial relationships among co-workers, the living and working arrangements for spacecraft to be used for missions lasting months or years assume particular importance. The Mental Workload and Performance Experiment (MWPE), in part, examines the appropriate design of workstations for performance of various tasks in microgravity, by providing a variable-configuration workstation that may be adjusted by the astronauts

The workload and stress associated with space flight, along with direct effects of microgravity and adaptation, may also act to reduce the on-orbit performance of astronauts. It is important to quantify any such effects for the sake of planning and scheduling on-orbit astronaut activities. Since Space Station crew operations will require a great deal of computer interaction, MWPE includes an interactive experiment to be performed on a GRiD 1530 portable microcomputer by each of four astronauts. The experimental task is designed to test both cognitive and motor performance through a combination of accepted Fitts and Sternberg tasks. On-orbit performance will be compared to baseline performance measured during pre-flight and post-flight experiment sessions.

The importance of microgravity workstation design is due to the effect of weightlessness of body dynamics and neuromuscular control. Several experiments have indicated (Watt et al., 1985) that equilibrium limb positions are determine by balanced action of agonist-antagonist muscle pairs. A relaxed body position therefore corresponds to the balance of muscle pairs in a relaxed condition: on Earth this position is further influenced by the participation of gravitational forces in the balance. The upright, standing Earth-based posture, for example, is aided by a forward moment induced by gravity about the ankle joints, that helps resist the substantial moment that is imposed by the strong extensor muscles in the calf even when relaxed. Similar gravitational effects help straighten the knees and waist. Earth-based workstations, and the Spacelab, are designed to accommodate the upright, one-gravity posture.

In microgravity, by contrast, the strong calf and thigh muscles tend to keep the toes somewhat pointed and the knees and waist flexed (see Figure 1). With the feet planted on the floor adjacent to an equipment rack, therefore, a relaxed posture tilts the entire body well away from the rack, out of reach of controls and indicators. In order to work at a vertical rack in microgravity, therefore, an astronaut must strongly tense the ankle flexor, knee extensor, and

back muscles in order to resist their strong antagonists and achieve an upright posture. This is very fatiguing over a long time.

The MWPE anthropometric experiments are conducted by having the astronauts use an adjustable workstation for a variety of on-orbit activities. The anthropometric workstation is attached to the Spacelab vertical handrails using a pair of articulated two-link arms that may be made rigid by hand-tightening a screw. The astronaut works at the workstation with his/her feet secured in foot loops, and positions and orients the anthropometric workstation in a way that is comfortable for the current task. Tasks to be performed at the anthropometric workstation are daily planning, a paperwork task; seed planting for the GPPF experiment, a characteristic hand-work task; and the MWPE computer interaction task. By observing the favored geometric relationships between the foot loops and the work surface of the anthropometric workstation, workstation design parameters may be determined for each type of task.

The MWPE interactive task combines memorization, short-term recall, and computer-screen target selection. The memory portion corresponds to the accepted Sternberg short-term memory task: it requires memorizing a set of one, two, four, or seven letters that are presented on the computer screen (see Figure 2). Once the subject has memorized the letters, he/she continues by striking the return key at the computer keyboard. A circular array of eight targets then appears on the screen, each target labeled with a single letter (Figure 3). Exactly one of these letters belongs to the memory set, and the subject is required to find the target labeled with that letter: the time required to do so is called the reaction time. Finding the target completes the Sternberg portion of the task.

The variety of memory set sizes (one, two. four, seven) presents the subject with a variety of levels of difficulty in the Sternberg position of the task. The subject's reaction time is taken as a measure of basic cognitive performance under the prevailing conditions. The Sternberg data-analysis paradigm models the reaction time as consisting of a constant delay time, plus a component proportional to the index of difficulty which equals the log to the base two of the memory set size. This paradigm provides a convenient parameterization for analyzing reaction time that is well founded in performance-measurement literature. The varying cognitive challenges also offer the chance to detect and characterize any patterns of performance degradation on orbit.

The Fitts task focuses on motor control, or the speed with which the subject is able to move and control an on-screen cursor. The cursor must be moved to the target selected during the Sternberg task, using one of three computer input devices: it is the beginning of this motion that marks the end of the reaction-time period. The Fittts movement time is recorded from the first cursor motion until the cursor is settled within the correct target square.

The cursor positioning motor-control challenge to the subject is varied by changing target arrangements, input devices, and motion directions. Both the target size and the distance to travel to the target vary. In addition, the difficulty of traveling to a particular target depends on the direction of travel. Most significantly, the input devices themselves vary in difficulty of use:

the joystick is a rate-controlling device and is rather more difficult to control than the position-controlling trackball. The keyboard provides a third control mode, using arrow keys to move the cursor about on the screen. As motor control and hand-eye coordination may be influenced by the on-orbit environment, either indirectly through fatigue and disorientation or directly through adaptation to microgravity, the cursor-control component provides a means of detecting such effects.

Experimental data collection for the anthropometric portion of the Mental Workload and Performance Experiment will be by analysis of videotapes of astronauts using the MWPE workstation on orbit. By comparing on-orbit video images of the workstation with images taken on the ground of the workstation surroundings, it will be possible to determine the selected configurations and to correlate them to the corresponding tasks. Astronaut comments will be useful as well in assessing the relative comfort and usefulness of workstation configurations.

The software used for the GRiD computer interaction experiments places the resulting data on computer diskettes for return to the ground for processing. In addition to reaction and movement times the software records the time required for the subject to memorize each data set, the time required for the subject to settle on the correct target, and the initial motion direction of the target cursor. These quantities allow additional flexibility of analysis of subject performance.

The results of the MWPE experiment are intended to be useful to Space Station Freedom designers and planners in creating effective, comfortable work environments for the crew members and in anticipating and planning for astronaut productivity on orbit. It is very important to understand astronaut on-orbit performance, so that systems and procedures may be developed that are realistic and that do not overload or under-utilize crew members. MWPE also gives researchers a start at investigating fundamental effects of microgravity and microgravity adaptation of crew members on cognitive and motor performance.

References

Watt, D.G.D., Money, K. E., Bondar, E. L., Thirsk, R. B., Garneau, M., Scully-Power, P. (1985), Canadian medical experiments on shuttle flight 41-G, Canad Aeronautics Space J 31:215-226.

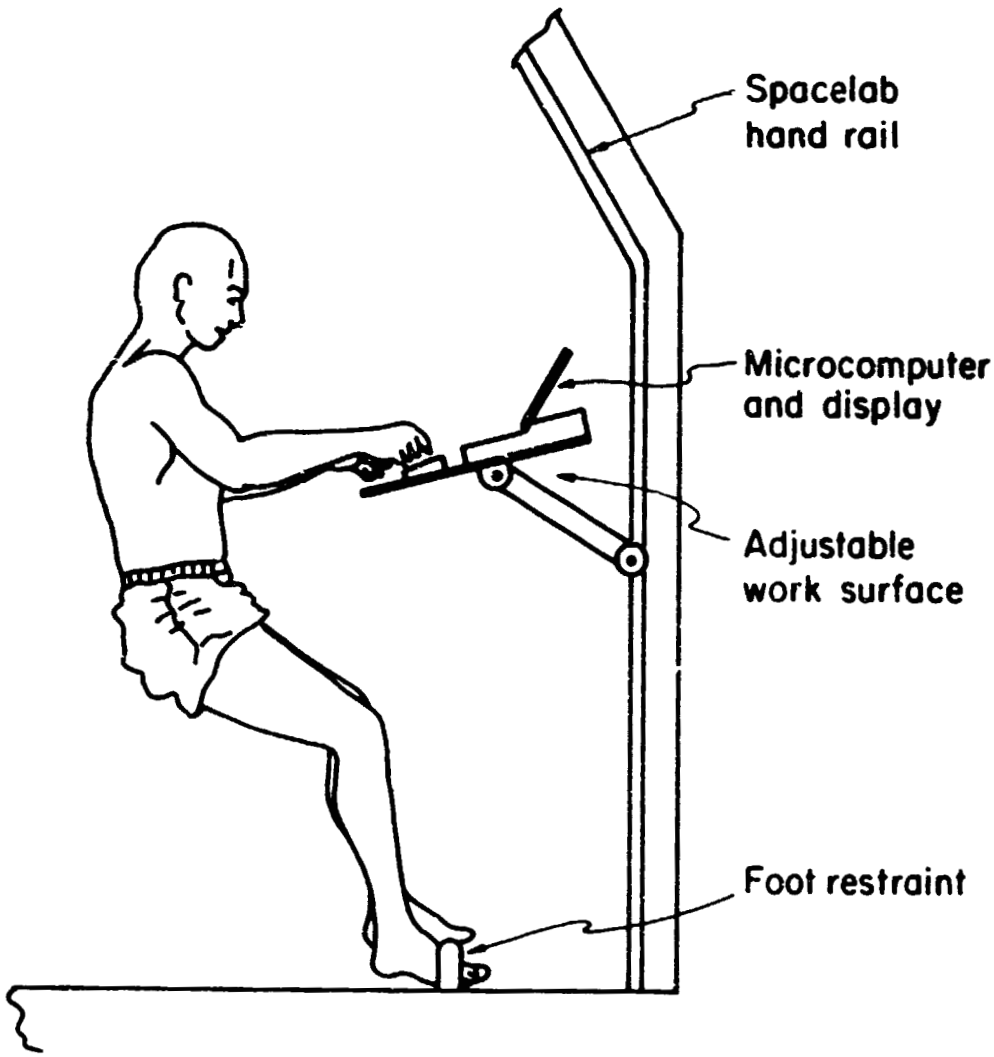

Figure 1. MWPE Deployed in Spacelab.

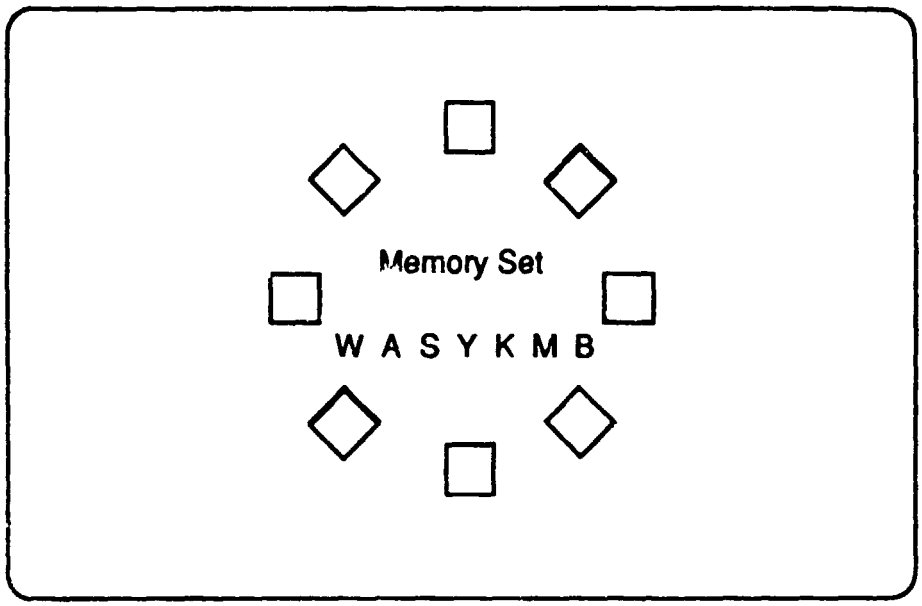

Display 1: Memory set display on computer screen.

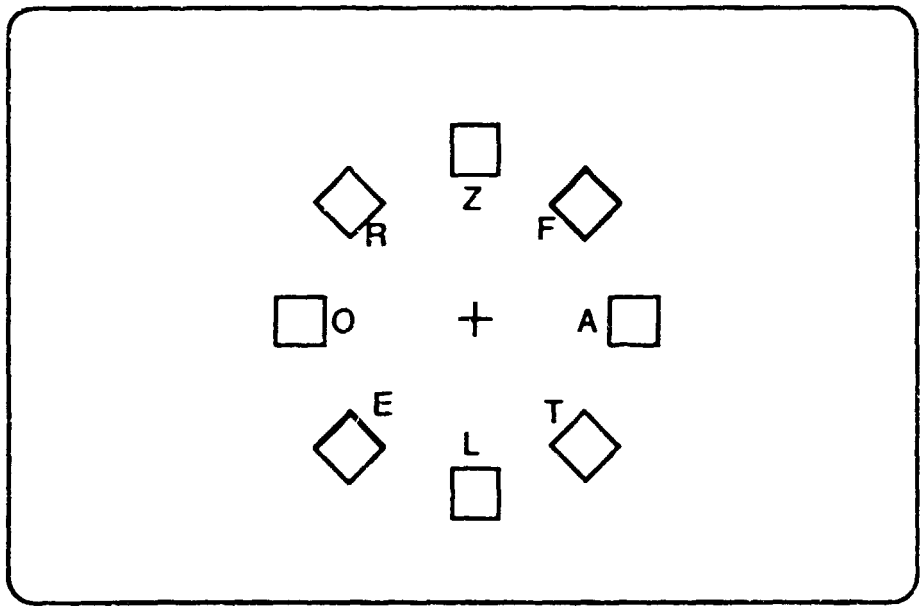

Display 2: Target acquisiton display on computer screen.

Figure 2. Computer Screen Displays for the Mental Workload and Performance Experiment.

N92-23329

RADIATION MONITORING CONTAINER DEVICE
(16-IML-1)

S. Nagaoka
National Space Development Agency of Japan (NASDA)
Tokyo, Japan

As the era of Space Station Freedom and solar system travel approaches, it becomes increasingly important to develop radiation protection for the people who will live and work in space for long durations. As we know, the Earth's atmosphere, a dense blanket of air, effectively protects us from most of the space radiation, particularly against the high-energy radiation at levels lethal to most living species. Beyond the Earth's atmosphere, what can protect life from such damaging radiation? This experiment with the Radiation Monitoring Container Device is designed by NASDA to give a preliminary answer to this question. The investigation measures the radiation levels inside the space transportation systems like shuttle and looks at basic effects from the aspect of radiation biology. The data gathered will be analyzed to understand any interrelation between the physical properties of the radiation and its biological effects and used to develop a sensitive solid-state nuclear track detector for future space systems.

In this experiment, layers of the radiation detectors and biological specimens, bacterial spores (Bacillus subtilis), shrimp eggs (Altemia salina), and maize seeds (Zea mays) are sandwiched together in the Radiation Monitoring Container. The detectors, sheets of plastic materials (TS-16 and CR-39), record the nuclear track of cosmic radiation. The dosimeter package contains conventional detectors made of materials such as lithium fluoride or magnesium-silica-terbium. These thermoluminescent materials (TLD) will, when moderately heated, emit luminescent photons linearly depending upon the dose of radiation received. The experiment, enclosed in a box-like container, is mounted on the aft end cone of the Spacelab, the area where the shielding is somewhat less than other locations.

Each plastic detector in the device can register individual nuclear tracks in three dimensions while the TLD accumulates radiation energy. The biological specimens in the device are exposed to cosmic radiation for approximately 6 days during the mission. All specimens and radiation detectors are analyzed after the mission to correlate the radiation characteristics and biological effects. The plastic detectors are etched chemically to visualize the radiation tracks called "etch pits". The geometric properties of the etch pit can reveal the physical characteristics of the radiation, such as incident angle, energy, and nucleon type. Three-dimensional trajectories are analyzed by a computerized microscopic image handler with a three-dimensional stage controller, and reconstructed through the piled detector sheets in relation to the positions of the biological specimens. The specimens will be evaluated for radiation effects by biological and biochemical methods using such intrinsic characteristics as the processes of development, sporulation, hatching, and germination. Primary genetic studies will also be carried out at the cellular, organ, and individual levels.

SECTION II

MICROGRAVITY SCIENCE

N92-23630

A STUDY OF SOLUTION CRYSTAL GROWTH IN LOW-g (2-IML-1)

Ravindra B. Lal
Alabama A&M University
Huntsville, AL USA

I. INTRODUCTION

During the International Microgravity Laboratory-1 (IML-1) mission it is planned to grow triglycine sulfate (TGS) crystals from aqueous solution using the modified Fluids Experiment System (FES). A special cooled sting technique[1] will be used for solution crystal growth. The objectives of the experiment are: (a) to grow crystals of TGS using modified fluids experiment system, (b) to perform holographic interferometric tomography of the fluid field in three dimensions, (c) to study the fluid motion due to g-jitter by multiple exposure holography of tracer particles, and (d) to study the influence of g-jitter on the growth rate.

TGS cystals have technological interest as a pyroelectric infrared detector that can be used with no cooling devices. There are many applications for improved infrared detectors in military systems, astronomical telescopes, Earth observation cameras, and environmental analysis monitors. When grown to useful sizes on Earth, the crystals develop defects that limit their performance.

II. EXPERIMENT

During the IML-1 mission it is planned to have two experiment runs.

1. TGS-1 run (Isothermal) Sting and fluid temperature same and near saturation temperature. (010) oriented polyhedral seed (Figure 1).

2. TGS-2 run (Polynomial) The sting follows a predetermined polynomial. (001) oriented polyhedral seed (Figure 1).

A. Short Description of the Two Experiments

These experiments will be performed in the Fluids Experiment System (FES). The details of the FES are given elsewhere.[2] The FES is a windowed and instrumented crystal growth research cell designed to allow a variety of holographic diagnostics and schlieren viewing of the crystal and surrounding fluid as the crystal grows in space. Two types of images are recorded: schlieren images (transmitted on down-link as black and white video that reveals flow patterns and variations in fluid density) and holograms (recordings of three dimensional images that lead to quantitative determination of the concentration of the solution surrounding the crystal). TGS solution is nearly transparent, so it is possible to record holographic images

through the fluid around a growing crystal. Using holographic interferometry, temperature and concentration gradients in the fluid and their motion can be monitored to determine how they are reduced in space and to determine how the crystal growth takes place in a low gravity environment. The FES has been slightly modified since the Spacelab 3 mission in 1985. The following modifications have been made to the FES. The knife edge has been realigned to avoid blackout at certain angles; holographic optical elements (HOE) have been added to the test cell windows for three-dimensional reconstruction of concentration gradients; a new software has been added; a viewing window has been added to view the test cell without opening the doors of the test cell enclosure; test cell bladder in the cap assembly has been reworked; a gold coated stainless steel pump has been replaced by a titanium pump; and the inside of the test cells has been coated with silicone RTV to reduce metallic contamination of TGS solutions.

The FES optical diagnostic system was modified for IML-1 after its last use in Spacelab 3 to incorporate holographic tomography (the ability to take optical data through the cell at multiple angles) as shown in Figure 2. Specially designed holographic optical elements (HOEs) have been added to the main test cell windows to provide a capability to illuminate and view the crystal at three different angles. The straight through view remains unchanged and two views at 23.5° are made possible by the HOEs. The schlieren system operation remains essentially the same while the hologram now records all three views on a single frame in a manner that allows them to be separated later back on Earth. The availability of the three views will lead to a more accurate quantitative understanding of the solution concentration and crystal growth.

Holograms and video data will be recorded during mechanical operations and critical phases of the crystal growth. Acceleration of the seed particles can be observed in real time on the video down link and will be determined accurately from the analysis of the holography data. During the experiment, the principal investigator and his team will monitor the down link video of the crystal and the growth solution and may instruct the crew to adjust some growth parameters.

In the first experiment a TGS crystal oriented in (010) direction will be grown for approximately 23 hours. The (010) face is the fastest growing face in TGS and is also the face required for detector fabrication. The growing face is uncut and unpolished and is about 1 cm x 1 cm in size. The solution of TGS will be seeded with buoyant particles of three different sizes (300 μm, 400 μm, and 600 μm). The main objective for this experiment run is to determine the effects of g-jitter and other g-variations on the fluid flow. Holograms will be taken at a programmed rate especially during any crew activities, and other Microgravity Vestibular Investigation (MVI) activities.

The second experiment run is basically a crystal growth run. The time allotted for this run is about 43 hours. No particles will be added to the TGS solution. The seed crystal will be (001) oriented polyhedral crystal which is uncut and unpolished on the growing side. This seed is about 1.5 cm x 1.5 cm in size. The experiment will follow a predetermined polynomial[3], but depending upon actual space conditions, the growth rate can be modified by changing the

constants in the polynomial by crew interface. After the growth, the sting and the grown crystal will be removed from the test cell and will be stored in a specially designed container.

The payload crew will begin each run by placing a pre-stored sting with attached TGS seed crystal in a test cell filled with about 1.0 liter of TGS solution. The seed and the fluid will be separated by a cap assembly that will be retracted when the experiment begins. To dissolve all crystallites that will have formed in the solution at room temperature, the test cell will be preheated to a temperature of 70 °C on the optical bench, while keeping the sting temperature at 42 °C. The cell and the optical bench will then be cooled while the sting is heated to an appropriate temperature to bring the sting and the fluid to around 46 °C. At this temperature the cap will be retracted. A part of the seed will be dissolved to remove any surface imperfections and spurious nuclei. After that the experiment will follow a predetermined schedule. A typical time line profile is given in Figure 3. At the end of the run the cap will again be closed, the test cell removed from the optical bench, and the sting removed from the cell and stored in a specially designed container such that the crystal cools slowly to room temperature.

After the mission, the crystals will be returned to our laboratory for extensive investigations for their structural and electrical properties, including their capability for infrared detection. The space grown crystals will be compared with the laboratory grown crystals. Holograms taken during the mission will be reconstructed on ground for detailed optical analysis of fluid behavior. Data on the particle studies will be analyzed and correlated with "g" measurements on the shuttle.

On the IML-1 mission, accelerations that may cause convection and disturb the crystal growth will be carefully monitored. In addition to an internal FES accelerometer that will measure acceleration above 5 Hz, the Space Acceleration Monitoring System (SAMS) has two accelerometers located in the FES rack and one mounted in the Spacelab aisles. The special set of accelerometers are expected to provide information on low frequency (0 to 5 Hz) vibrations. Because the effects of g-jitter are believed to be extremely important in the crystal growth experiment we chose to incorporate optical techniques to monitor these effects directly.

III. UNDERLYING SCIENCE FOR THE GROWTH OF TGS CRYSTAL

A. Growth of TGS Crystals

The dielectric loss in TGS is due to the following: domain relaxation, microscopic solution and air inclusions incorporated during growth, and dislocations/strain centers which pin the domains. In space grown crystals we expect the growth to be mainly diffusion controlled and so we expect ordered deposition, fewer microscopic solution and air inclusions (solution is degassed before filling) and less strain centers and so domains will be more mobile. So we expect low dielectric loss (ε'') and improved figure of merit.

The ultimate use of these crystals is for IR detectors for 8 μm-14 μm range. The detectors will be fabricated at EDO/Barnes Engineering Division in Shelton, CT. All other electrical

properties will be measured in our laboratory at Alabama A & M University. A section of both crystals will be analyzed by high resolution synchrotron X-radiation diffraction imaging at Brookhaven National Laboratory with the help of NIST.

A study of the effects of microgravity on TGS crystal growth in space by computer simulation is underway to help in the design of control parameters of spaceflight experiments.

A mathematical model of TGS crystal growth in space has been established including the field model, the interface model, and various boundary conditions.[4] The behaviors of the TGS aqueous solution follow the basic conservation laws of continuity, momentum, energy and concentration which are time dependent. The liquid-solid interface follows the growth kinetics and the mass balance. A finite volume code called COM-MIX has been employed and extensively modified to implement the simulation.

A series of two-dimensional cases are tested with different steady background g level ($10^{-1} \sim 10^{-4}$ g_0) and different orientations (horizontal and vertical). Some cases of g-jitter are also simulated. Alternative boundary conditions are being tested. The results will be compared with the flight data.

B. Experiment with Seed Particles in the FES

Seed particles of three different monodisperse sizes will be added to the fluid in the FES. These will be observed on TV downlink in real time (only the largest particles are expected to show up clearly on the TV image). Their positions will be noted during each downlink and compared with later values to give us preliminary information on fluid and particle motion. The TV image will provide limited resolution and accuracy. Image processing will be done on line on the downlink image to help improve this. Holograms of the particle distribution will be made at preselected times during the experiments to later allow an accurate three-dimensional location on the particles as a function of time. Preliminary ground based results of particles image displacement velocity experiments were presented by Trolinger et al.[5]

1. Primary Science Objective

The primary science objective is to observe and quantify minute convection currents in the vicinity of the crystal and to correlate these with crystal growth processes. We will attempt to observe, isolate, and quantify the following components of fluid convection:

(a) Growth driven convection
(b) Convection due to g-jitter-random forces
(c) Convection due to other quasi-steady state acceleration forces - water dumps, etc.
(d) Convection due to residual microgravity - air drag, gravity gradient, etc.

The use of different particle sizes should allow us to make these measurements accurately and

with high spatial resolution. The diffusion coefficient in g-jitter varies as the fourth power of radius, while terminal velocity varies as second power of radius.

We should be able to correlate the presence of convection with crystal growth anomalies and processes, and we should be able to correlate the presence of convection with other events. Namely, we should be able to more accurately characterize the space shuttle environment, how energy is coupled to an experiment, and its effect on crystal growth.

An accurate measurement of convection will be made in a regime never measured before. This will allow the validation of both theory and CFD codes.

2. Secondary Science Objectives

The dynamics of three ensembles of monodisperse particles in suspension will be observed in microgravity. This will provide important basic scientific information about inertial random walk, two phase flow, particle dynamics, and residual gravitational field in the Spacelab.

Testing the theory of intertial random walk - Inertial random walk, a novel type of diffusion, has been predicted by Regel et al.[6] to exist in microgravity, but has never been observed. It may have a significant effect on certain types of materials processing in space. It has been simulated (in one dimension) in ground experiments but only when measured in space will the theory truly be tested. Our particle experiments are almost ideal for testing the theory of inertial random walk. Requirements of particle sizes and types are fortunately similar for both the primary science objective and this objective, allowing us to pursue this objective with no added cost.

Testing two-phase flow and particle dynamics theory - Two phase flow has been studied very little in microgravity. The general equations of two phase flow are surprisingly untested because of the difficulty of testing many regimes. The microgravity environment will allow us to examine two phase flow in an extremely low Reynolds number regime where convection would normally dominate the results. The use of multiple particle sizes will allow us to test a variety of two phase flow effects.

Materials processing which involves free-floating particles depends heavily on particle dynamics and interaction. The statistics of particle diffusion and collision rates have been developed but have not been tested in microgravity. Although our selected particle number density is somewhat low, the study of particle dynamics and interaction should be enhanced by the tracking of all particles in three-dimensions in microgravity.

Residual gravitational field in Spacelab - The equations of motion of the particles lead us to the conclusion that we will be able to accurately measure the residual gravitational field on the Spacelab by tracking these suspended particles. The selection of the size and density range has increased the accuracy of the measurement. We should also be able to measure relatively low frequency changes in g. High frequency changes in g will be filtered out of our measure-

ment. The measurement will be correlated with other recorded events in the IML-1 mission. This should provide a significantly improved characterization of the Spacelab environment.

C. Holographic Optical Elements (HOEs, holograms that emulate optical components)

First space application of HOEs - HOEs expand the FES optical system capability from a single angle of view to three angles of view without any significant weight or volume changes in the FES. The HOEs, thin materials which are attached to the FES windows, split the input light beam into three beams traversing the crystal surface at three angles. This is important to resolve any non-axially symmetric diffusion fronts. The HOE on the output window collects the three beams and bends them back to allow their collection in the same recording camera. To achieve the same thing with conventional optics would have required a major redesign and configuration change in the FES and would have added considerable weight and volume. The concept is likely to find application in other optical diagnostics requirements for space experiments where weight and volume are critical parameters, and where a wider angle of view is needed for viewing.

ACKNOWLEDGEMENTS

Help given by Rudolph Ruff, Todd MacLeod, David Johnston, and David McIntosh of NASA/MSFC and other Teledyne Brown Engineering company personnel during development of this experiment is gratefully acknowledged.

References

1. Lal, R. B., Aggarwal, M. D., Kroes, R. L., and Wilcox, W. R., Phys. Stat. Sol (a) 80, 547 (1983).

2. Materials Processing in Spacelab 3-Fluid Experiment System, Vapor Crystal Growth System, Applications Payload Projects, NASA/MSFC, Code JA84, Marshall Space Flight Center, AL 35812.

3. Liu, L. C., Wilcox, W. R., Kroes, R. L. and Lal, R. B., Proc. Mat. Res. Soc., Vol. 9, p. 339 (Ed., Guy E. Rindone) North Holland, NY (1982).

4. Sun, J., Carlson, F. M., and Wilcox, W. R., 42nd Congress of the International Astronautical Federation, October 5-11, 1991, Montreal, Canada.

5. Trolinger, J. D., McIntosh, D., Witherow, W. K., Lal, R. B., and Batra, A. K., Proc. SPIE, 1557 (1990).

6. Regel, L. L., Vedernikov, A. A., Ilinski, R. V., and Melikhov, I. M., Proc. 6th European Symposium on Materials Sciences Under Microgravity Conditions, Bordeaux, France, December 2-5. 1986.

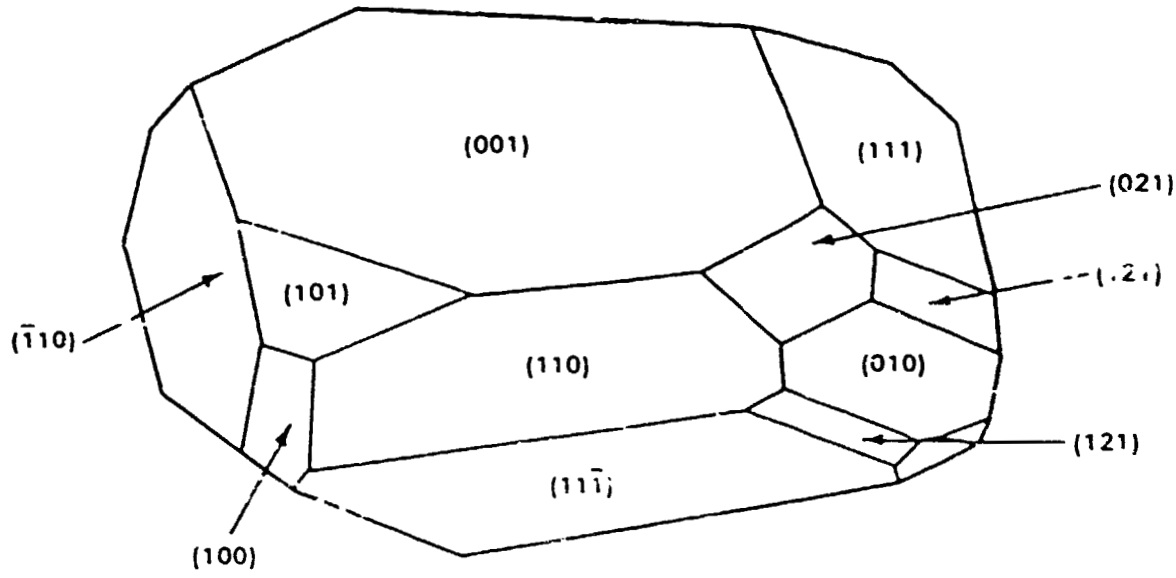

CRYSTALLOGRAPHIC FACES OF TGS CRYSTAL

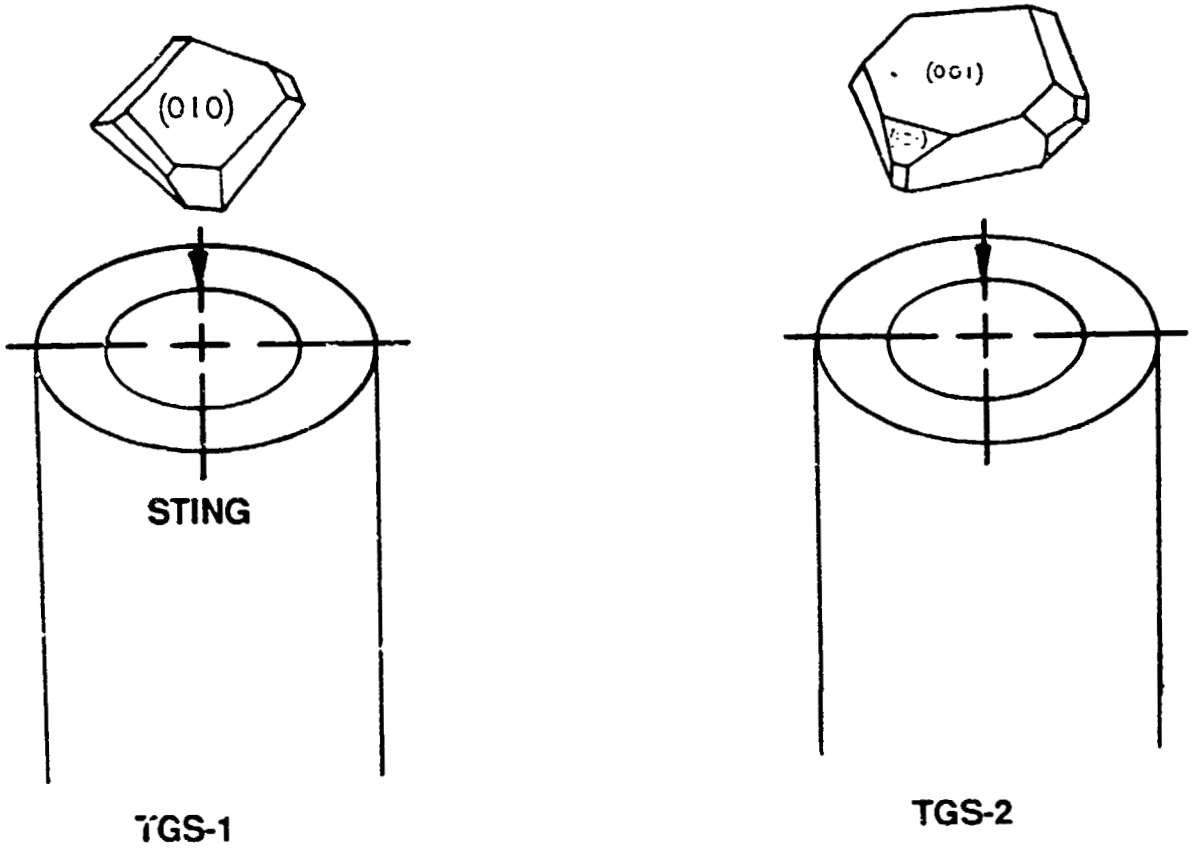

Figure 1. Triglycine Sulfate Growth Runs on the IML-1 Mission.

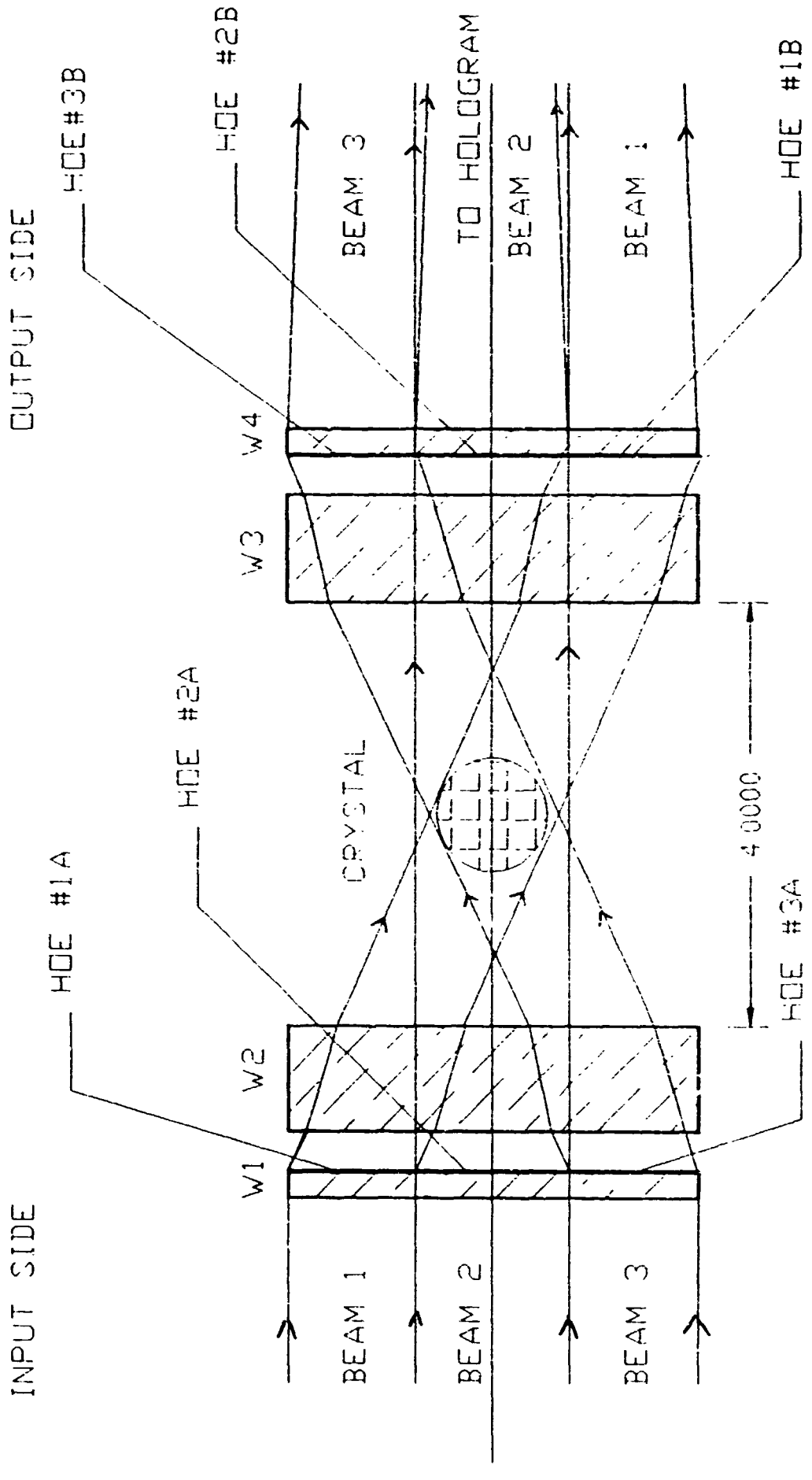

Figure 2. FES Optical Diagnostic System.

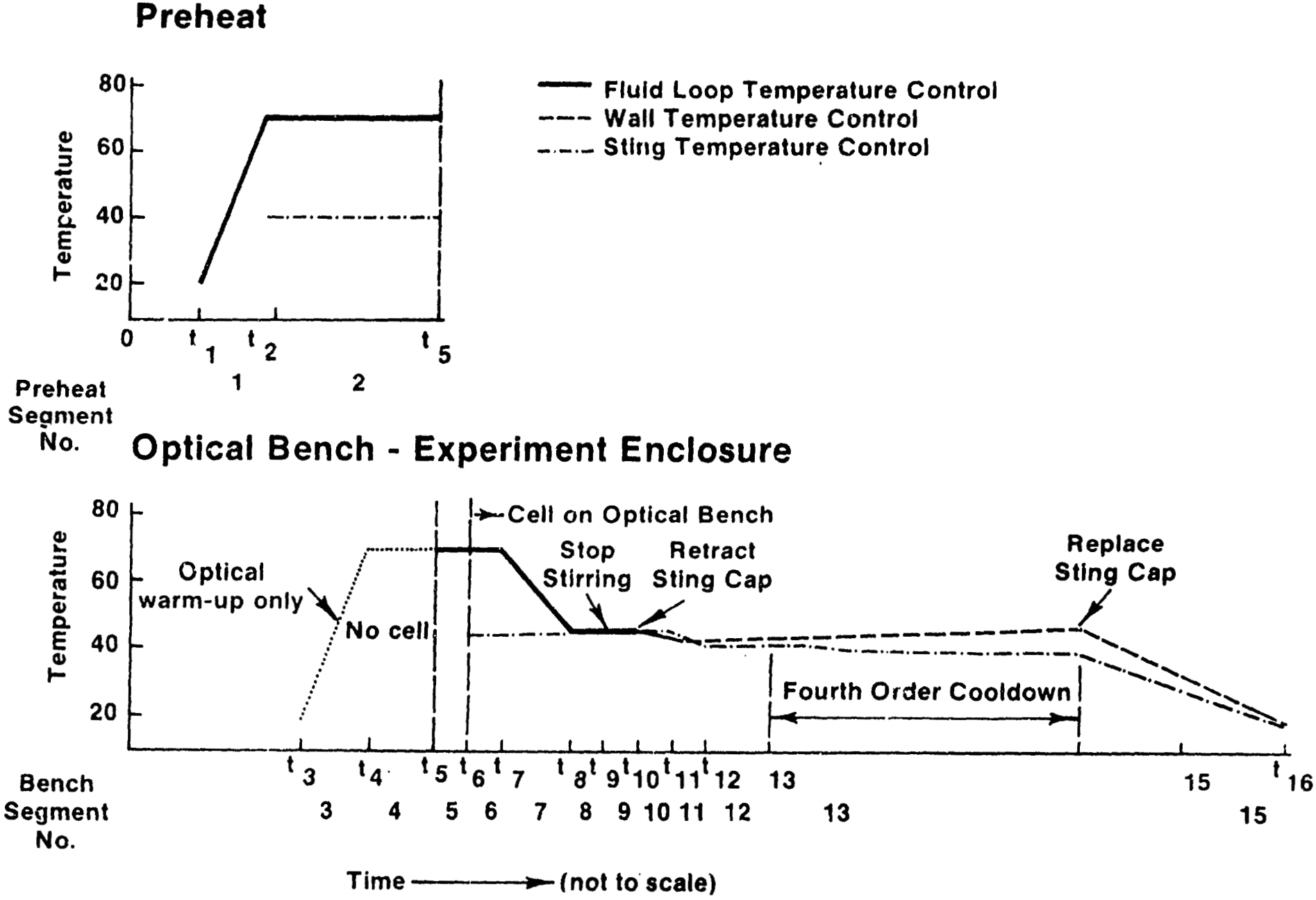

Figure 3. FES Timeline.

N92-23631

AN OPTICAL STUDY OF GRAIN FORMATION: CASTING AND SOLIDIFICATION TECHNOLOGY (2-IML-1)

Mary H. McCay
University of Tennessee Space Institute
Tullahoma, TN USA

This investigation is directed at characterizing alloy solidification by studying the unidirectional growth of a metal-model material in microgravity. Using holograms and supporting temperature measurements obtained during processing in the Fluids Experiment System (FES), the solute and thermal fields associated with the dendrite growth front and extraneous nucleation will be measured and compared to a theoretical (computational) model. Ground based supporting experiments include particle tracking to measure the velocity fields, and optical phase shift techniques (e.g., confocal optical signal processing, interferometery, and Schlieren) to study thermal and solutal fields.

It is planned to utilize three cells, or CAST science modules (CSM), on Spacelab. In two CSMs a matrix of temperature gradients and growth rates will produce a variety of desired solidification conditions such as thermal undercooling, constitutional supercooling and fluid motion. In the third CSM, a dilute control (nonsolidifying) solution will be processed under two of the previous conditions. When the solidification process has been adequately characterized and compared with the model, a second series of follow-on experiments will be proposed for a future flight in which a magnified image will be used to study coarsening effects with forced fluid motion used to artificially create perturbing crystallites ahead of the interface.

The accumulation of metal model data on constitutional and thermal effects during unidirectional solidification of an alloy material is intended to enhance and then validate theoretical models of the solidification process. The microgravity data will permit the metallurgical aspects of the model to be independently verified by minimizing the overwhelming effect of convection at significant gravity levels. The validated computational models will be subsequently applied to metal systems in both environments.

A science team has been assembled that supplies expertise in the areas of microgravity solidification, fluid flow, and heat transfer, dendrite analysis, applied optics, image analysis, and the FES. Using the capabilities of this group, both the design and analysis of the experimental results will be optimized.

Background

Constitutional Supercooling

In recent years a series of Space Processing Applications Rocket (SPAR) and KC-135 aircraft experiments have been flown to study the effects of gravity on the solidification of first, a metal-model (28 NH_4Cl-H_2O)[1,2] and then metal alloys (Sn-15Pb, Sn- 3Bi, Al-4.5Cu, MAR-M246, and PWA 1480).[3-6] In the first metal-model experiment (bi-directional solidification) four [110] dendrite arrays nucleated and grew outward from the container walls filling the entire crucible. No crystallite appeared ahead of the interface, implying that in the absence of gravity, the forces were not present that would cause dendrite fragmentation and movement in the liquid. The second (unidirectional solidification) experiment also began [110] growth at the cooled wall, but several [100] crystallites appeared and grew ahead of the interface. In each instance the low-gravity arrays grew significantly slower than one-g ground runs. In the two metal-model experiments, the growth rates were the same, but the temperature gradients differed by a factor of 7 (70 °C/cm for flight one and 10 °C/cm for flight two). This gives constitutionally supercooled regions of 0.5 cm and 3.8 cm, respectively. Based on theories of the columar to equiaxed transition in castings,[7-9] several interpretations can be made from these results, the principal two being that gravity driven fluid flow is responsible for the melting off of dendrite arms and their transport into the melt, or a non-convective related phenomena encourages nucleation ahead of the interface. Rather than distinguishing between the two possibilities as was intended, the SPAR experiments were inconclusive.

A third explanation was the occurrence of residual flow from the de-spin of the sounding rocket. If these were still present when the second experiment began freezing, they could account for crystallites moving into the fluid. This hypothesis was tested in KC-135 and F104 low gravity aircraft experiments[10,11] using shadowgraph, interferometry, and Schlieren techniques. These optical techniques enabled the experimenters to observe both the diffusion layer adjacent to the growth interface and the presence of convection plumes. The flight profile of the KC-135 causes a sample to experience 1 to 2 g's before entering a 20 sec period of low gravity. During unidirectional solidification studies growth plumes were established during the initial high g and flow rates on the order of a 1 cm/min were seen prior to inception of the low (.01 g) gravity period. These plumes dampened and began to diffuse 10 sec after entry into low gravity, indicating that the predicted[12] damping times for these experimental cases must have been inaccurate. Further thermal data from F104 flights support the concept that damping times in these materials are rapid. It, therefore, is implausible that the nuclei were carried ahead of the interface by residual flows.

Experiments with metal systems on SPAR produced similar results.[3,4] The Sn-15 Pb alloy solidified with large equiaxed grains in contrast to the more columnar plus small equiaxed grains obtained from 1-g and centrifuge solidification. The Sn-3Bi alloy also solidified initially with large grains on SPAR but the final region surrounding the shrinkage cavity froze with small equiaxed grains. It is not known if these small grains formed due to constitutional supercooling nucleation, a gravity independent flow as a result of the shrinkage cavity, or gravity driven

convection due to the sounding rocket leaving the low-gravity conditions. The controversy remains concerning the formation of grains ahead of an interface.

These investigators feel that this controversy can be resolved by a more thorough study of solidification in microgravity. The extended times available on Spacelab will allow experiment conditions that cover a range of growth rates, temperature gradients, and hence, constitutionally supercooled regions without the confusing presence of gravity driven fluid flow. The solutal and thermal fields associated with the dendrite growth front will be measured and compared to a theoretical (computational) model.

Freckling

The ammonium cloride-water system is used to study the occurrence of thermalsolutal convection and pluming as it would occur in metal systems such as steel castings,[13,14] the superalloys,[15] or others[16,17] since it has an inverted diffusion layer at the interface due to rejection of water-rich solute. The pluming phenomena which occurs when the inverted layer becomes unstable is often called freckling and tends to limit the range of compositions for many alloys processed on Earth due to the resultant localized segregation and small equiaxed grains in the final casting. The plumes contain cooler liquid with a different composition from the surrounding region. As they traverse the dendrite forest, they carry dendrite fragments which appear as trails of equiaxed grains in the final ingot. The region of the freckles, therefore, has a different composition (and melting point) and crystalline morphology from the remainder of the ingot.

Freckling was first studied systematically in the metal-model NH_4Cl-H_2O[15] and found to depend on thermal diffusivity, solid/liquid density ratio, solid solute solubility, solute diffusivity, and viscosity. Several investigators[15,16] have attempted to define criteria for the convective instabilities produced by the inverted layer based on either thermal properties or concentration effects. Since such criteria do not include both the effect of latent heat and segregation simultaneously, they grossly underestimate the solidification conditions (growth rate and temperature gradient) that are necessary to eliminate freckling. The presence of latent heat increases the size of the inverted layer at a critical growth rate and consideration of the combined effects decreases the growth rate for stability in NH_4Cl-H_2O by 2 orders of magnitude.[18] Freckling has generally been thought to begin within the mushy zone below the dendrite tips but recent work[17] confirmed by the author also on NH_4Cl-H_2O, suggests that the channels for freckling originate at the dendrite front and spread.

Using confocal laser optical signal processing and neutrally buoyant particle laser tracking techniques, the CAST investigators studied the formation and breakdown of the inverted density layer at the dendrite front.[19,20] The convective pluming was shown not to be a natural occurrence resulting from a fundamental (Rayleigh-Benard) fluid dynamic instability at the density inversion interface. The nature of the breakdown was vortical, bounded by the dendritic interface on the bottom and the thermally lightened fluid on top (Figure 1). The significant

variation with previous thinking, however, was the observation of a vortical front which serves to replenish solute without significant disturbance to the bulk liquid.

In the proposed flight experiment, the size and characteristics of the inverted layer as a function of growth condition will be measured from reconstructed holograms and compared with theoretical expectations. For the minimum experimental temperature gradient (2 °C/cm) the layer will decrease with increasing growth rate (R) until a critical R is reached upon which the layer will increase due to latent heat effects. For the maximum temperature gradient (28 °C/cm), the layer will decrease monotonically with increasing R since the critical R cannot be reached due to FES limitations.

Since optical techniques such as Schlieren and interferometry easily delineate organized convective motions, the FES system is a powerful tool for studying this phenomena. The size of a stable inverted density layer can be as large as 1 cm under the proposed experiment's low temperature gradient and growth condition. In ground based experiments the layer becomes unstable long before it reaches its maximum size with the result that events (such as equiaxed growth) within the layer are difficult to study. During the IML flight the layer can reach a large enough size that such characteristics can be resolved.

Dendrite Coarsening and Tip Concentration

Dendrite coarsening is a phenomena that occurs on the micro-scale and is primarily responsible for final dendrite arm spacings by causing the dissolution and shrinkage of smaller arms and the growth of larger arms. It is a function of local solidification time and the gradients of temperature and concentration.

The SPAR experiments[1-4] and KC-135 flights[5-6] have shown a gravity-related coarsening effect on the secondary dendrite arms. Each alloy system showed greater arm spacings for the low-gravity solidification. In the instance of KC-135 flights, the arm spacings increased in low-g, decreased in high-g, and then increased again when the next low-g parabola was flown. Theories on dendrite structure[21,22] suggest that by changing the surrounding concentration field and effective diffusion length, the perturbation frequency and, hence, the dendrite arm spacing is affected. In the case of low gravity, the diffusion length and therefore the arm spacings would increase. A more recent KC-135 experiment[5] on the superalloy PWA 1480 has shown the same physical results for the primary arm spacings (e.g., spacing increases as gravity level decreases). Current theories[23-25] suggest that these spacings are related to temperature gradient and growth rate or concentration gradient. This was the first study of low-gravity primary arm spacings, and it suggests that data at significantly increased low-gravity time periods are needed.

The present resolution of FES precludes secondary arm spacing measurements until late in the solidification runs. Hence it is planned that first the solidification process itself will be modeled for the microgravity environment, then the coarsening of the dendrite arms will be

studied. The analysis of coarsening will be accomplished using a magnification lens attachment to the FES in an experiment is proposed for a subsequent flight.

Method and Approach

A two component system is required in order to model alloy solidification and investigate freckling phenomena. Since NH_4Cl-H_2O has been extensively used for similar studies, it has been chosen for these experiments. The present investigator has characterized NH_4Cl-H_2O optically in addition to accummulating other significant property data. Compared to other available metal models (e.g., succinonitrile with solute), NH_4Cl-H_2O is the superior medium available.

The CAST experiment will proceed systematically with a matrix of nine temperature gradients and growth rate conditions that will encompass a range of inverted density layer sizes and constitutionally supercooled region sizes. Based on earlier KC-135 results, the temperature gradients are expected to be different in low gravity for the same test parameters, so two non-solidifying control samples will be run at identical conditions to two of the primary runs to evaluate those differences. To produce more rapid solidification fronts, two runs will be processed in which the fluid is cooled below its freezing point and solidification initiated by thermal shock.

Holograms will be taken at repeated intervals during the growth runs. In this way, various optical techniques can be used through post-flight reconstructions to determine concentration and thermal profiles, observe perturbations in the inverted layer, and distinguish nuclei that form ahead of the interface. The techniques for reconstruction and optical analysis have been developed in support of the holographic measurements.[26-27]

References

1. Johnston, M. H., and Griner, C. A.: 1977, Met. Trans. A 8(A), 77.
2. Johnston, M. H., Griner, C. S Parr, R. A., and Robertson, S. J.: 1980, J. Crystal Growth 50, 831.
3. Johnston, M. H., and Parr, R. A.: 1982, Met. Trans. 13B 85.
4. Johnston, M. H., and Parr, R. A.: 1982, Proceedings, Materials Research Society, Materials Processing in the Reduced Gravity Environment of Space, G. E. Rindone, Editor, Elsevier Science Publishing Co., Inc., p. 651.
5. McCay, M. H., Lee, J. E., and Curreri, P. A.: 1986, Met. Trans. 17A, 2301-2302.
6. Johnston, M. H., Curreri, P. A., Parr, R. A., and Alter, W. S.: 1985, Met. Trans. 16A, 1683-1686.
7. Wingard, W. C., and Chalmers, B.: 1954, Trans. Am. Soc. Metals 46.

8. Jackson, A. K., Hund, J. D., Uhlmann, D. R., and Steward, III, T. P.: 1966, Trans. Met. Soc. AIME 236, 149.
9. Doherty, R. D., Cooper, P. D., Bradbury, M. H., and Honey, F. J.: 1977, Met Trans. A 8(A), 397.
10. Johnston, M. H., and Owen, R. B.: 1983, Met. Trans. A 14(A), 2163.
11. Owen, R. B., and Johnston, M. H.: 1981, Optics and Lasers in Engineering 2, 129.
12. Owen, R. B., and Johnston, M. H.: 1984, Optics and Lasers in Engineering 5, 95.
13. McDonald, R. J., and Hunt, J. D.: 1969, Trans. AIME 245, 1993-1997.
14. McDonald, R. J., and Hunt, J. D.: 1970, Met. Trans. 1, 1987-1988.
15. Copley, S. M., Giamei, A. F., Johnson, S. M., and Hornbecker, M. F.: 1970, Met. Trans. 1, 2193-2204.
16. Sharp, R. M., and Hellawell, A.: 1972, J. Crystal Growth 12, 261-262.
17. Sample, A. K., and Hellawell, A.: 1984, Met. Trans. 15(A), 2153-2173.
18. McCay, T. D., and McCay, M. H., submitted to J. Crystal Growth.
19. McCay, T. D., McCay, M. H., and Gray, P. A.: 1989, "Experimental Observation of Convective Breakdown During Directional Solidification," Phys. Review Letters, 2060-2063.
20. McCay, T. D., McCay, M. H., Lowry, S. A., and Smith, L. M., "Convective Instabilities During Directional Solidification," 1989, J. of Thermophysics and Heat Transfer 3, 345-350.
21. Glicksman, M. E., Singh, N. B., and Chopra, M.: 1982, Materials Processing in the Reduced Gravity Environment of Space, Guy E. Rindone, Editor, Elsevier Science Publishing Co., Inc., p. 461.
22. Glicksman, M. E., and Voorhees, P. W.: 1984, Met. Trans. A 15(A), 995.
23. Hunt, J. D.: 1979, "Solidification and Casting of Metals," The Metals Society Book 192, London, pp. 3-9.
24. Kurz, W., and Fisher, D. J.: 1984, Metal. Trans. A 15(A), 967-975.
25. Somboonsuk, K., Mason, J. T., and Trivedi, R.: 1984, Met. Trans. A 15(A), 967-975.
26. McCay, M. H., McCay, T. D., and Smith, L. M.: 1990, "Solidification Studies Using a Confocal Optical Signal Processor," J. Applied Optics 29 699-703.
27. Yesko, M. E., "An Automated System for Holographic Reconstruction and Interferometric Analysis of Solutal Gradients," U.T.S.I. Master of Science Thesis, Tullahoma, TN, August 1991.

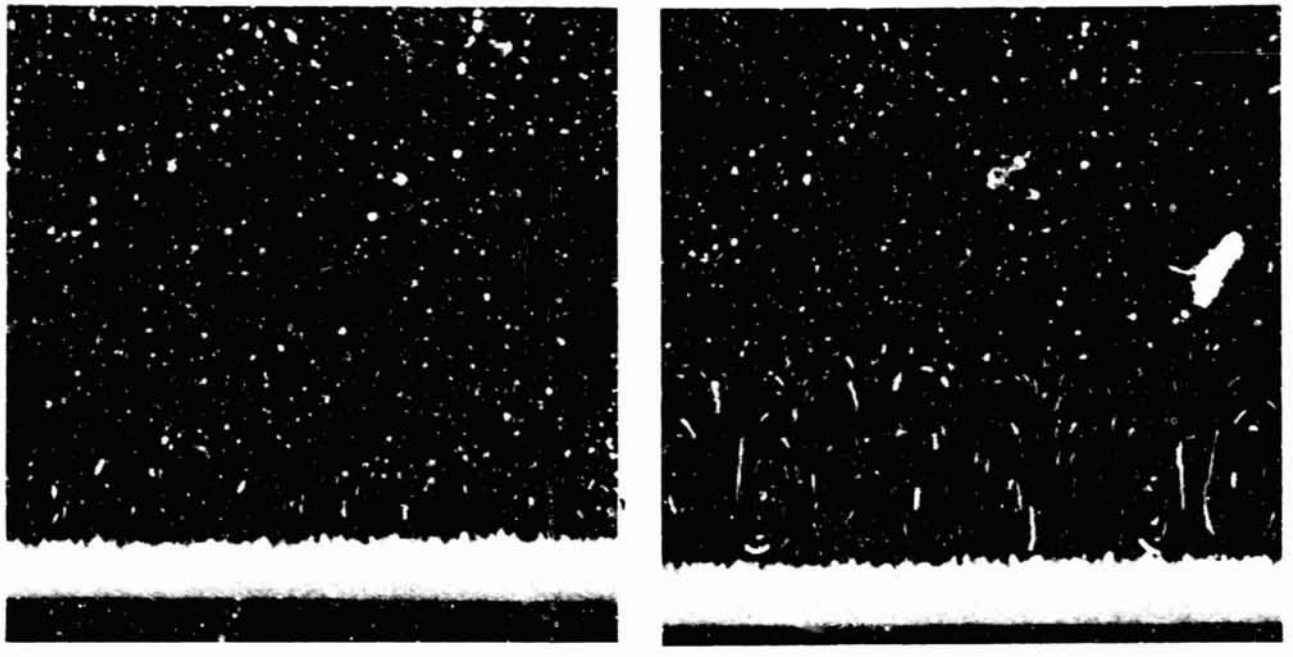

(a) (b)

Figure 1. Particle tracking optical system image of the flow geometry of a directionally solidified NH_4Cl-H_2O solution at (a) breakdown and (b) 30 seconds later.

N92-23632

VAPOR CRYSTAL GROWTH STUDIES OF SINGLE CRYSTALS OF MERCURIC IODIDE (3-.. iL-1)

Lodewijk van den Berg
EG&G Energy Measurements, Inc.
Santa Barbara Operations
Goleta, California USA

BACKGROUND

A single crystal of mercuric iodide (HgI_2) will be grown during the IML-1 mission. The crystal growth process takes place by sublimation of HgI_2 from an aggregate of purified material (the source), transport of the molecules in the vapor from the source to the crystal, and condensation on the crystal surface.

The equipment used is the Vapor Crystal Growth System (VCGS), primarily consisting of an experiment enclosure in which the furnace and growth ampoule are installed, a temperature control system, an air circulation system to provide the proper amount of cooling and a microscope to observe the growing crystal. The system is installed in a half-rack of the Spacelab.

The objectives of the experiment are:

a. To grow a high-quality crystal of HgI_2 of sufficient size so that its properties can be extensively analyzed; and

b. To study the vapor transport process, specifically the rate of diffusion transport at greatly reduced gravity where convection is minimized.

Single crystals of HgI_2 have technological applications as the critical sensing elements in x-ray and gamma ray detection systems. The radiation creates electronic charges in the detectors, and measurement of these charges makes it possible to determine the intensity and the energy of the radiation. The material has a very high resistivity at ambient temperatures so that cooling of the systems is not required and power consumption is minimal.

These systems can be used in environmental and personal monitoring, manufacturing operations, nuclear medicine, focal plane arrays for x-ray and gamma ray telescopes, and elemental analysis systems using x-ray fluorescence.

EXPERIMENT

The time-line of the IML-1 mission provides for the growth of one crystal.

In order to avoid the difficult and time-consuming process of seed initiation and selection during the space flight, a seed crystal has been grown pre-flight inside the ampoule using a prototype flight furnace. This activity at the same time provided the temperature parameters for continuation of the crystal growth during the flight.

At the start of the experiment the payload specialist will install the ampoule/furnace combination in the experiment enclosure and will initiate the growth procedure. The pre-programmed time-temperature sequence of the experiment is shown in Figure 1. The sequence exists of three phases: heat-up, growth, and cool-down. The software which controls the experiment is interactive, in the sense that the nominal times and temperatures preset in the software can be adjusted by the crew member to optimize the growth conditions. The growing crystal can be viewed through the microscope, and the observations and judgements of the crew member, in consultation with the P.I. team on the ground, are critical for a successful completion of the experiment.

The results of the experiment on Spacelab 3 showed that the system used to grow a crystal in microgravity makes it possible to produce a crystal of a structural quality never before observed and with electronic properties which had been thought unattainable. The experiment on IML-1 will be performed to validate these results while the crystal growth procedures are optimized based on the Spacelab 3 experience.

After the flight the whole crystal will be analyzed for structural quality and homogeneity by means of gamma ray diffraction rocking curves. The crystal subsequently will be processed into detector structures so that the transport properties of the electronic charge carriers can be measured. In addition, thin sections will be provided to NTIS for evaluation of the microscopic defect structure using a cyclotron-generated x-ray beam.

ACKNOWLEDGEMENTS

The engineering work of R. Ruff, T. McLeod, and E. Smith of NASA, Marshall Space Flight Center, has been a critical contribution to the development of this experiment.

References

1. L. van den Berg and W. F. Schnepple, "Growth of Single Crystals of Mercuric Iodide in Spacelab 3," in Materials Processing in the Reduced Gravity Environment of Space, Materials Research Society Symposium Proceedings, Volume 9, 439 (1982), G. Rindone, Editor.

2. L. van den Berg and W. F. Schnepple, "Mercuric Iodide Crystal Growth in Space," Nucl. Inst. Meth. A 283 335 (1989).

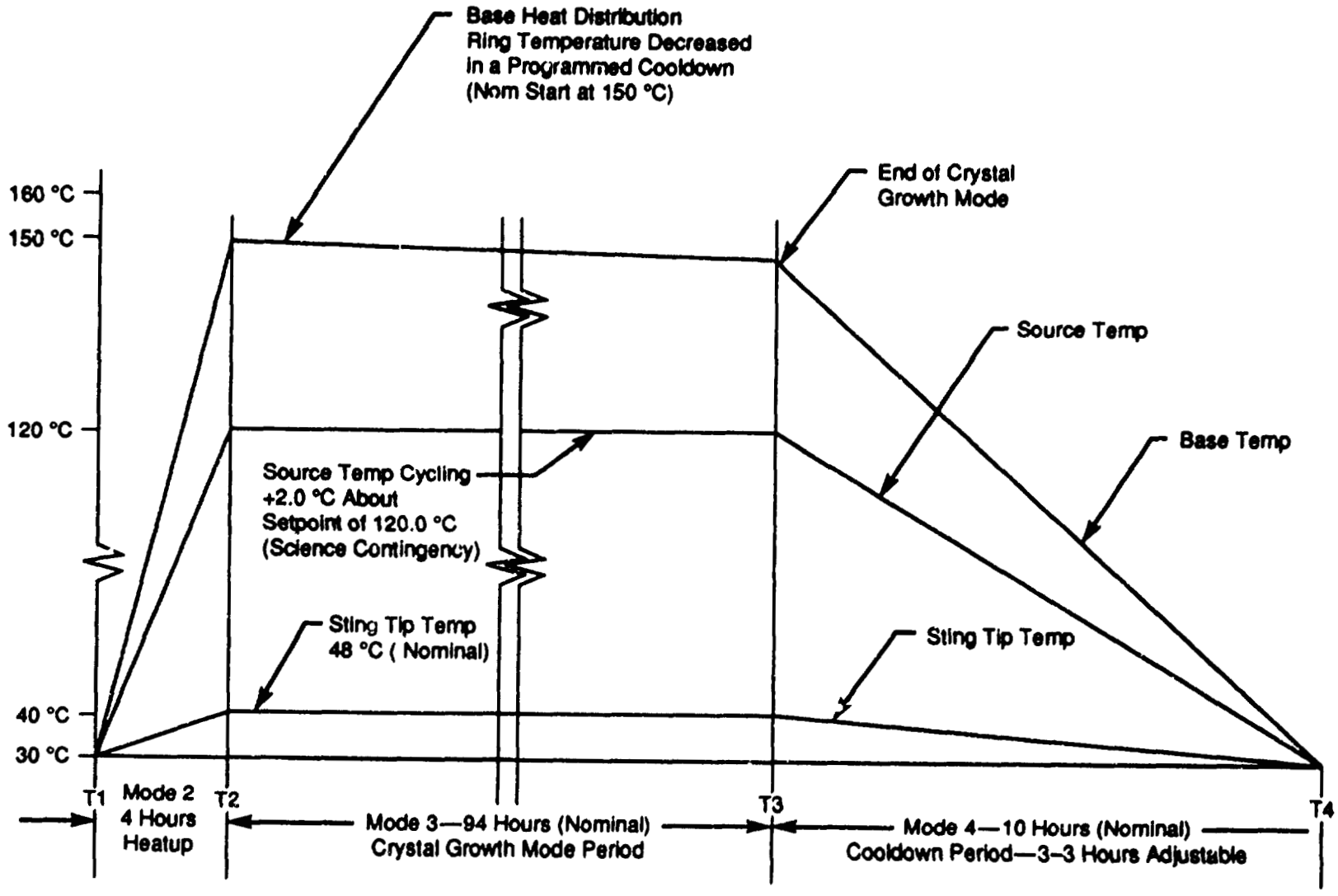

Figure 1. The Pre-Programmed Time-Temperature Sequence of the VCGS Experiment.

N92-23633

MERCURY IODIDE NUCLEATION AND CRYSTAL GROWTH IN VAPOR PHASE (4-IML-1)

Robert Cadoret
University of Clermont-Ferrand
Aubiere, France

The objectives of this experiment are to grow simultaneously three single crystals of Mercuric Iodide (HgI_2) in an imposed temperature profile and to assess the advantages of growth in microgravity on the HgI_2 crystal quality.

Similar experiments conducted on Spacelab 1 and Spacelab 3 demonstrated that it was possible to nucleate and grow monocrystals of HgI_2 using the forced flux method. However the nucleation phase was found to be extremely sensitive to slight fluctuations in HgI_2 concentrations and much more difficult to control than the growth phase of the crystallization process. Growth in microgravity should reduce fluctuations in HgI_2 concentrations and thus decrease the resultant crystal defects. In order to test this hypothesis, a seeded growth of HgI_2 crystals will be performed on IML-1. As shown in Figure 1, the primary equipment used in this experiment is an insulated furnace which contains the samples in three stainless steel cartridges that surround the heating element. Each stainless steel cartridge houses a glass ampoule containing the raw crystals of HgI_2. This arrangement allows three crystal growth experiments to occur simultaneously. The temperature of the source and the temperature of the crystal zone are precisely controlled (±0.1 °C) by the use of two water heat pipes. The outside walls of the glass ampoules are chemically polished in order to get a perfect contact with the cartridges. The sublimation flux is supplied by a HgI_2 source located at one end of each ampoule in a constant temperature zone (Figure 2). Each ampoule has an internal pressure controlled by the introduction of a small amount of Nitrogen (0.3 torr to 1 torr). The ampoules contain Mercury Diodide from different origins (France or USA) and have different vacuum pressures inside. Ampoules used in the second run will have lower pressures than those used in the first run. A total of 6 ampoules will be used. The process is initiated by heating the source material to a temperature of about 100 °C. This results in the source material subliming. Condensation occurs on a 2 mm HgI_2 seed crystal located on a long pedestal or the mid position of the ampoule, in the temperature gradient zone imposed by the heat sink and the operating temperature of the heat pipe furnace. Thus crystal growth is performed in a temperature gradient by physical vapor transport from the source material to the seed crystal. The well-defined temperature profile should allow nucleation and growth of single crystals at low supersaturation. Low supersaturation is required to reduce the probability of defect nucleation at its lowest value. In such a quasi-equilibrium conditions of growth the microgravity environment can prevent defects caused by local gravity induced concentration fluctuations.

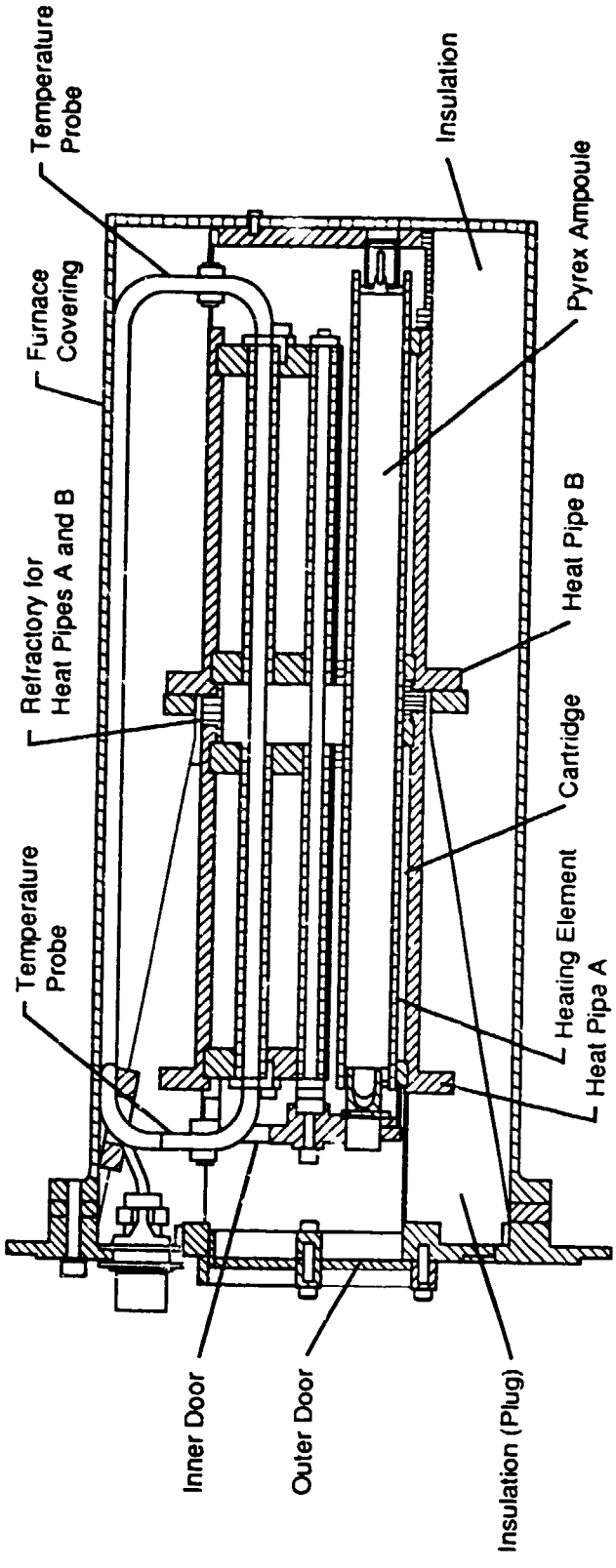

Figure 1. Mercury Iodide Crystal Growth Furnace.

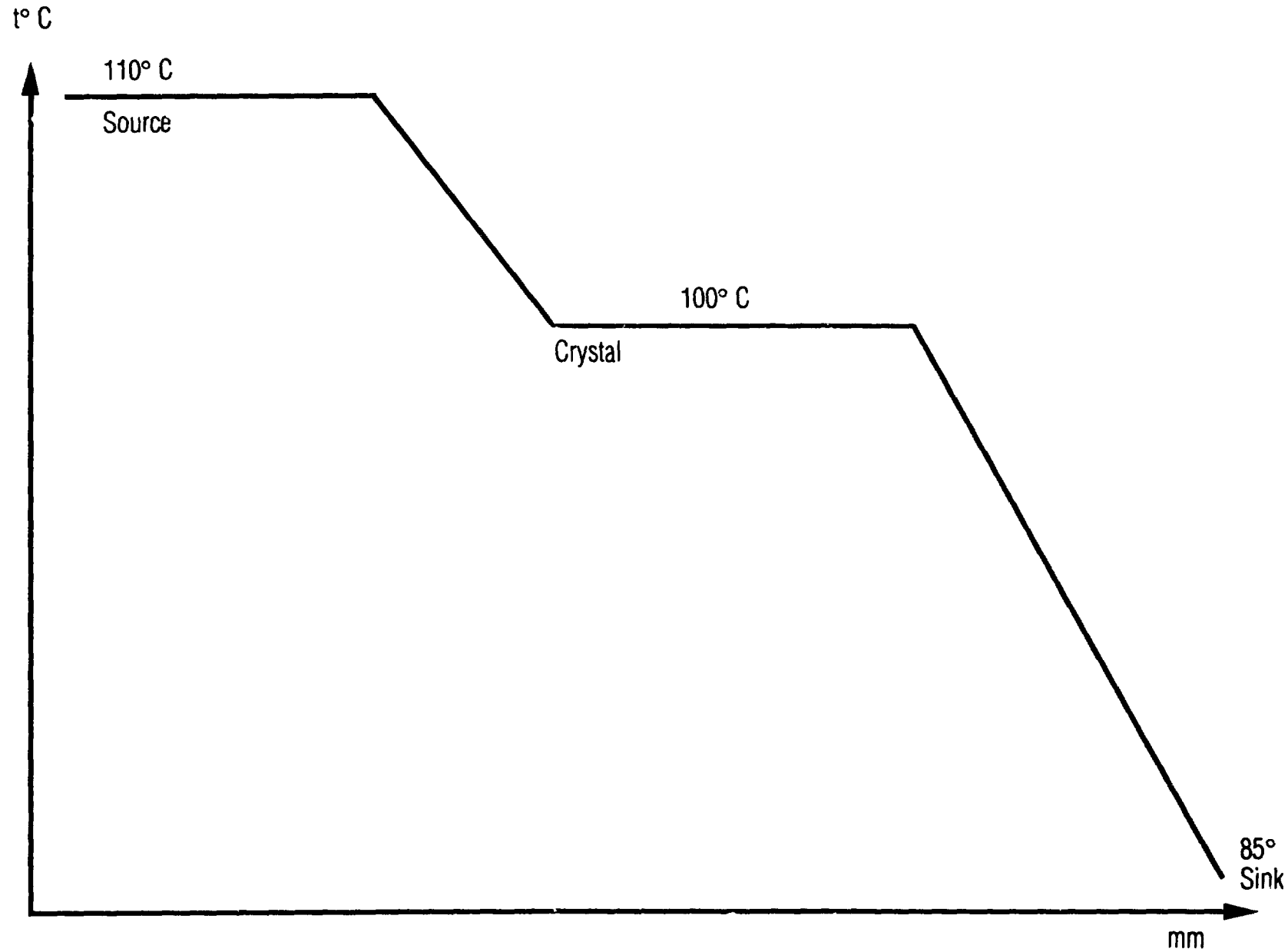

Figure 2. Temperature Profile of the Mercury Iodide Crystal Growth Experiment.

N92-23634

PROTEIN CRYSTAL GROWTH
(5-IML-1)

Charles E. Bugg
University of Alabama at Birmingham
Birmingham, AL USA

Proteins (enzymes, hormones, immunoglobulins, and numerous other types) account for 50% or more of the dry weight of most living systems and play a crucial role in virtually all biological processes. Since the specific functions of essentially all biological molecules are determined by their three-dimensional structures, it is obvious that a detailed understanding of the structural makeup of a protein is essential to any systematic research pertaining to it. At the present time, protein crystallography has no substitute: It is the only technique available for elucidating the atomic arrangements within complicated biological molecules.

Most macromolecules are extremely difficult to crystallize, and many otherwise exciting and promising projects have terminated at the crystal growth stage. Single crystals that have dimensions of 0.2-1.0 mm on a side are generally required for x-ray crystallographic analyses of macromolecular structures, and much larger crystals are required for neutron diffraction analyses. Proteins and other biological macromolecules often yield small micro-crystals readily, but it might then take several years of trial and error experimentation before these micro-crystals can be induced to grow large enough for a complete structural analysis. Even when large crystals are obtained, the crystals of essentially all biological macromolecules diffract rather poorly due to internal disorder. Thus, there is a pressing need to better understand protein crystal growth, and to develop new techniques that can be used to enhance the size and quality of protein crystals.

In principle, there are several aspects of microgravity that might be exploited to enhance protein crystal growth. According to theoretical considerations and experiment results, the major factor that might be expected to alter crystal growth processes in space is the elimination of density-driven convective flow. Convection in solution growth is caused by density gradients that occur when solute is depleted from the solution at the growing crystal surfaces. The density-dependent convection might be expected to affect protein crystal growth from aqueous solutions in several different ways. Convection will force solution to flow past the crystal, thus bringing material to the growing crystal surfaces at a rate that is significantly different from the steady-state diffusion rate that would be predominant in quiescent solutions. The flow patterns may generate significant variation in concentration at different parts of a crystal, thus leading to non-uniform growth rates. Also, convection may lead to significant physical stirring of growth solutions; in general, it is expected that such stirring effects might alter nucleation in growth processes.

Another factor that can be readily controlled in the absence of gravity is the sedimentation of growing crystals in a gravitational field. When a protein crystal grows from

aqueous solution on Earth, it generally migrates to the top or the bottom of the crystallization vessel (depending on whether its density is greater or less than the density of the solution). Therefore, protein crystals often grow from solution at an interface where all sides of the crystal are not equally accessible to the crystallizing solution. (In most cases, sedimentation causes proteins to crystallize as fused masses that contain highly disordered crystalline arrays.) Under microgravity conditions, it is expected that protein crystals will not display this tendencey to migrate away from initial nucleation sites, and can thus grow in isotonic environments, forming discrete, independent nucleation in sites.

Another potential advantage of microgravity for protein crystal growth is the option of doing containerless crystal growth. Contacts with vessel walls often lead to heterogeneous nucleation in crystal growth solutions. In the microgravity environment, it may be possible to form stable spherical droplets of crystallizing materials, which might be suspended by acoustical levitation or other methods. It is definitely possible to form relatively large stable droplets of protein solutions by extruding solutions from a pipette or a syringe; thus, protein crystals might be grown under microgravity conditions in relative large droplets adhering to syringe tips, without the extensive wall effects that generally accompany crystallization experiments on Earth.

As a result of the above theories and facts, one can readily understand why the microgravity environment established by Earth-orbiting vehicles is perceived to offer unique opportunities for the protein crystallographer. This perception led to the establishment of the Protein Crystal Growth in a Microgravity Environment (PCG/ME) project that continues today under NASA sponsorship. This project has advanced from simple hand-held devices (containing only a few protein solutions) to a more complex system involving 60 or more individual protein experiments in a thermally conditioned environment. The results of experiments already performed during STS missions have in many cases resulted in protein crystals being growth that are significantly larger and more structurally correct that the best specimens produced one earth. Thusly, the near-term objective of the PCG/ME project is to continue to improve the techniques, procedures, and hardware systems used to grow protein crystals in Earth orbit. A large number of industrial guest investigators and co-investigators are involved in the project (reference Attachment A) and multiple flight opportunities are obviously required to accomplish the referenced objectives.

The hardware complement currently in use consists of a Refrigerator/Incubator Module (R/IM) that provides protection and a controlled thermal environment (Figure 1), a Vapor Diffusion Apparatus (VDA) designed to manipulate and process the protein samples (reference Fig. 2). The VDA tray consists of 20 chamber assemblies, gang-operated dual cylinder syringes, and gang-operated plug mechanisms. The overall assemly is mounted between two aluminum/Plexiglas windows with a soft silicon rubber (35 to 65 durometer) gaskets providing sealing of the overall assembly to prevent external leakage and chamber to chamber leakage.

The dual-cylinder syringe is made of polysulfone and is operated by a ganged piston assembly. Each cylinder of the syringe contains a maximum of 40 µl of either precipitant or protein solution. When the wheel that operates the ganged pistons is rotated, the solutions are

either forced onto the syringe tip or withdrawn into the syringe cylinders, depending upon the direction of the rotation. The drive assembly is designed such that from the launch configuration of the syringe piston, eight to nine revolutions of the wheel are required to push solutions in the cylinder to the tip of the syringe to form a drop. Several peripheral items of equipment such as a temperature logging device and photographic equipment are also utilized. The current system was first flown on STS-26 in September 1988, and was subsequently reflown on STS-29 in April 1989.

The STS-26 orbiter middeck experiment was the first temperature controlled or systematic investigation to grow useful crystals by vapor diffusion in microgravity. Results from this experiment were very encouraging, since high quality crystals were obtained from most of the protein and enzyme samples flown and four samples grew crystals of exceptional size and quality. The STS-29 results were not quite as promising as those from STS- 26 due to several hardware/procedural problems. However, crystals of greater size and uniformity than those grown on Earth were still produced. The knowledge gleaned from these flights is being applied to follow-on PCG flights, in order to help define the flight and post-flight techniques and analytical methods and procedures used.

The IML-1 mission will accommodate two R/IMs (4 °C and 22 °C). (Each R/IM replaces one standard middeck locker, and uses Orbiter-provided 28 Vdc power from a standard outlet in the ceiling of the middeck.) The samples being grown will utilize seeding crystals in the growth process. The seeding crystal is inserted through a small opening in the top of the VDA window using a drop dispenser. The drop dispensers are stowed in the R/IM during the mission. The seed crystal is contained in a drop of stabilizing solution that is planted by allowing the stabilizing solution drop to come into contact with the protein drop. The PCG experiment is nominally activated during flight Day 1 activities. During activation, the PCG photo TV setup is performed, the R/IM door is removed, and the solutions in the syringes are mixed by attaching a handwheel to a syringe piston ganging mechanism and rotating it alternately clockwise and counter-clockwise and then again clockwise to deploy the droplets from the tips of the syringes. Once the droplets are deployed, the PCG photo session begins. During the photo sessions, a 35 mm camera is used to photograph the droplets on the tips of the syringes. The seed crystals are planted 12 to 36 hours after activation. After completion of the seeding session the PCG unit is left untouched until deactivation in the R/IM.

Disturbances during critical times such as activation plus 12 hours to activation plus 36 hours could cause premature nucleation. These disturbances could be caused by treadmill activity or RCS firings. A showering effect results when crystal formation is disturbed, thus resulting in many little crystals. These vibrational forces should be kept to a minimum for maximum scientific results from the experiment.

PCG is deactivated on the last flight day prior to deorbit, at the latest possible time. The deactivation process involves completing the final photo session, which is taking photographs of the crystals formed on the tips of the syringes. Once the photo session is completed, the droplets

are retracted back into the syringes, the R/IM door is closed, and the PCG unit is ready to return to the landing site.

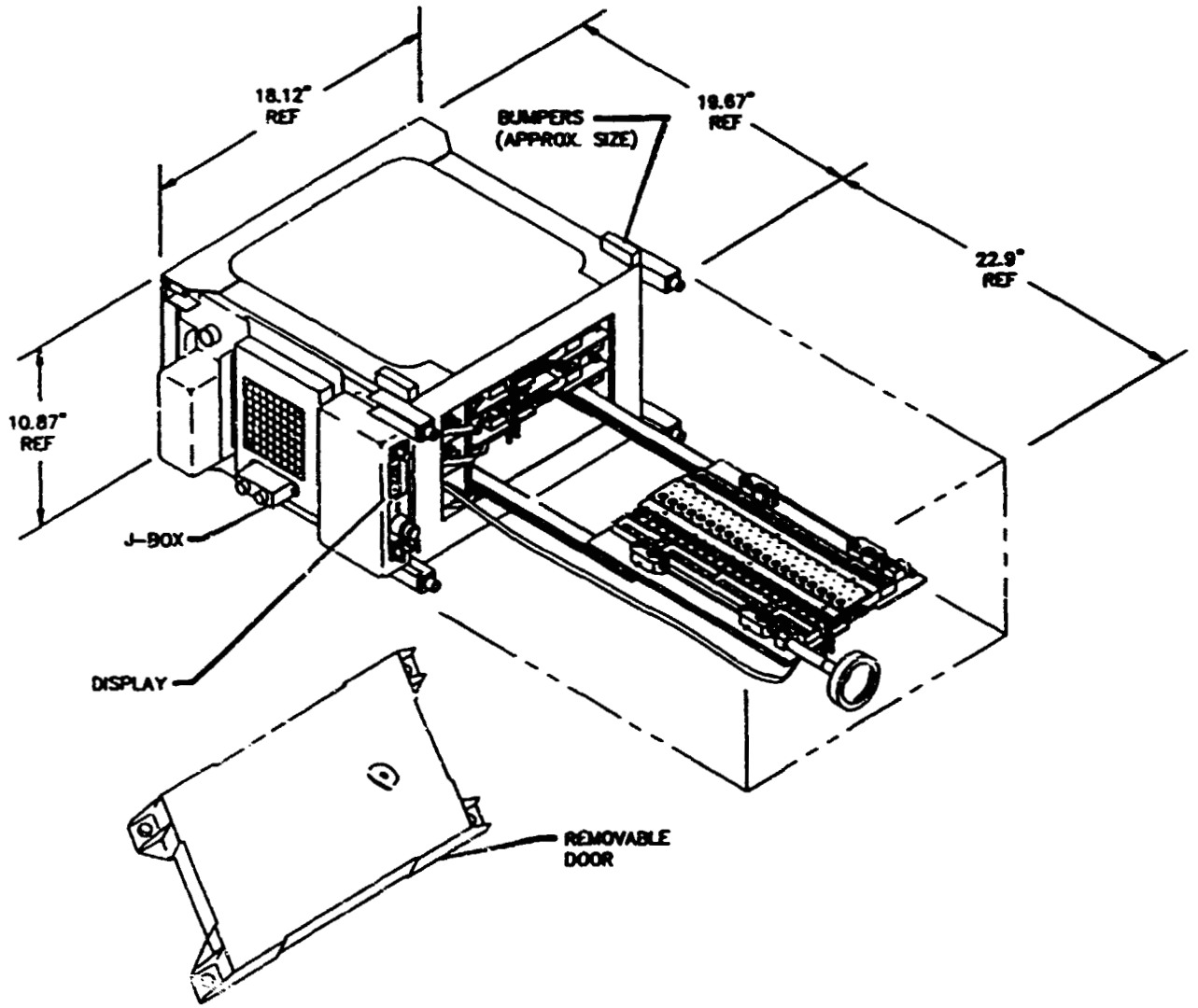

Figure 1. Refrigerator/Incubator Module (R/IM).

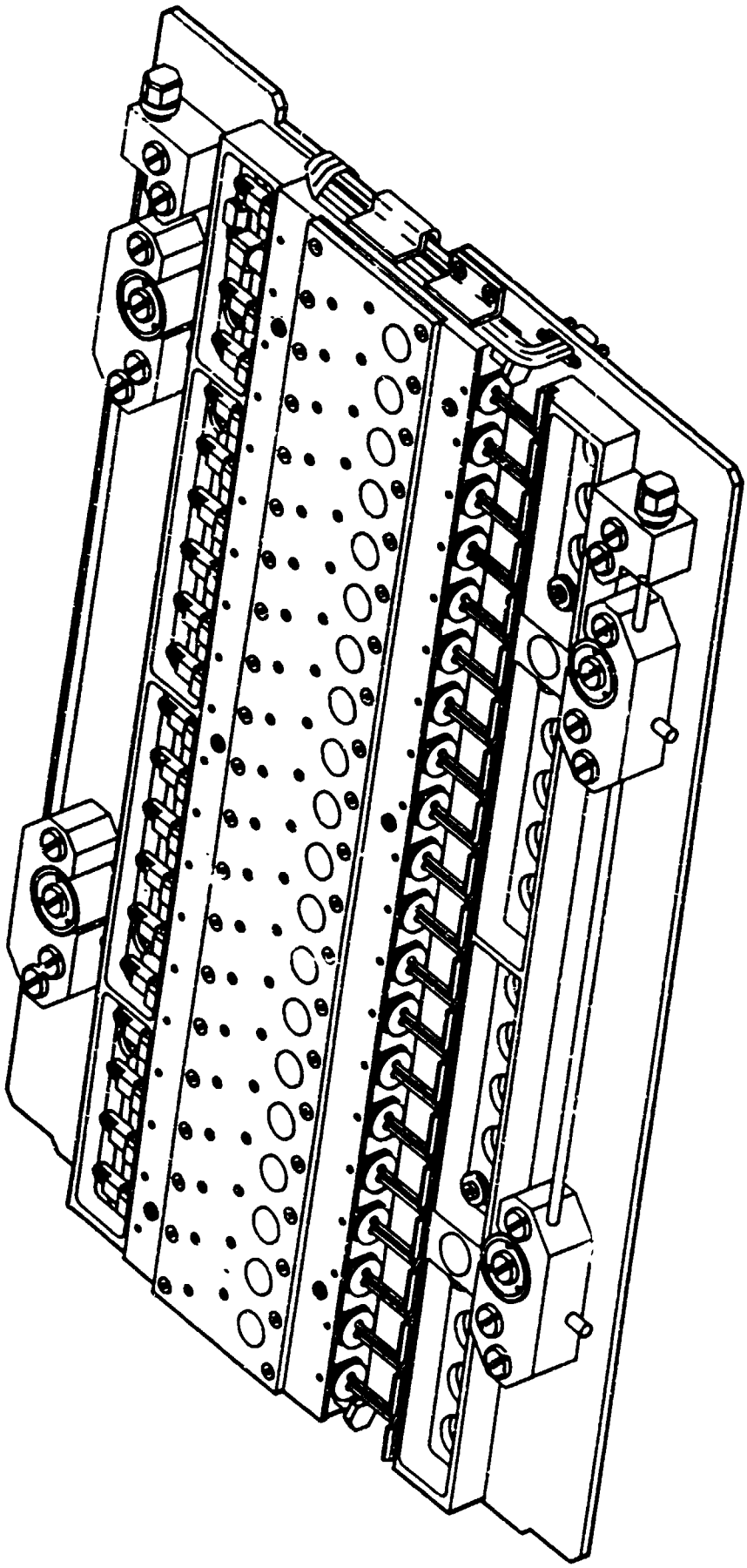

Figure 2. Vapor Diffusion Apparatus (VDA).

N92-23635

ORGANIC CRYSTAL GROWTH EXPERIMENT FACILITY
(13-IML-1)

Akio Kanbayashi
National Space Development Agency of Japan
Tokyo, Japan

The interesting nature of metal-like organic compounds composed of charge transfer complexes has been recently realized. Crystals of these complexes can usually be grown by the solution crystallization method. Some pure crystals of such organic metal-conductors behave as organic superconductors at cryogenic temperatures where they have unique physical properties, for instance, anisotropic electronic conduction. Their low dimensional metallic conductivity seems to depend largely on their singularity of the crystal structure. In order to investigate the properties of metallic conduction, it is necessary to grow large, defect-free single crystals from the charge transfer complexes. It is difficult to grow such organic single crystals on Earth, especially from the chemical reactions through diffusion-controlled process in the solutions, because of gravitational disturbances, or sedimentation. The difficulty primarily arises from the density differences between the two reactant solutions, the donor and the accepter, and between the crystals formed and the solutions. Typical ground-grown crystals for the charge transfer complex, TTF $\{Ni(dmit)_2\}_2$, a compound which could exhibit superconductivity below a critical temperature (T_c), are small needle-like fragments (2 mm x 0.1 mm). The crystal size obtained in ground experiments is never large enough to determine the physical properties, such as anisotropic superconductivity.

The IML-1 Organic Crystal Growth with G-Gitter Preventative Measure (OCGP) experiment is expected to grow a single crystal large enough to allow its intrinsic physical properties to be measured and its detailed crystal structure to be determined. This experiment also attempts to assess the experimental conditions including the microgravity environment for further investigation of the fundamental process of solution crystallization, nucleation, and growth from supersaturated phases including chemical reactions. Microgravity disturbances, G-jitter, may be an important environmental factor in the experimental method to assess.

The Organic Crystal Growth Facility (OCGF), the major hardware component of the OCGP experiment, consists of two independent crystallization chambers (OCCs) and a mounting structure. Two identical experiments will be carried out in the facility. One of the OCCs is mounted on a vibration damping structure, the other is mounted directly to the Spacelab rack without any damping. The vibration damping effect on organic crystal growth can then be carefully studied by comparing the crystals formed in the two OCC's. OCGF is illustrated in Figure 1. The OCC is illustrated in Figures 2(a) and 2(b).

TECHNICAL DATA FOR THE OCGF

- OCGF
  dimension: 440W x 266H x 360D (mm)
  weight: <12 (kg)

- OCC
  dimension: 80W x 130H x 301D (mm)
  capacity: 75 (cm^3) (central reaction cell)
  73 (cm^3) (each of two side cells)

- VIBRATION DAMPING MATERIAL: Epoxy-based polymer

The OCC is made of quartz glass and is divided into three rectangular cells filled with organic solvent and reaction compounds. The glass chamber is entirely covered by an aluminum housing. The reaction will be initiated manually by opening holes of the two partitions between the cells. For this manual operation, a rotary handle is located in front of the outer housing. The reaction and crystal formation occur in the central cells of the OCCs. The acceptor and donor reactants will meet there by diffusion. The crystal growth is a slow process and usually requires more than 1 week to complete. The two reactants, used as solutes in this experiment, are the organic compounds $(TTF)_3(BF_4)_2$ and $(Bu_4N)\{Ni(dmit)_2\}$. Acetone is used as the solvent. The amounts of these materials per each OCC cell are as follows:

$(TTF)_3(BF_4)_2$, Tris-tetrathiafulvalene-bis-tetrafluoro borate: 47 mg

$(Bu_4N)\{Ni(dmit)_2\}$, Tetrabuthylammonium-nickel-bis-dmit: 166 mg

$(CH_3)_2CO$, Acetone: 221 cm^3

The reaction forms the insoluble charge transfer complex TTF $\{Ni(dmit)_2\}_2$ or TTF-bNbD (Tetrathiafulvalene-bis-nickel-bis-dmit) for brevity, where "dmit" stands for [4,5 dimer. . to-1,3 dithiol-2 thione], or (C_3S_5), or isotrithione-dithiolate.

Experiment deactivation is accomplished when the crew rotates the handle of each OCC on board, thus closing the holes in the partitions. After the mission, space-grown crystals will be carefully analyzed, focusing on the difference in crystal structure and its morphology, electrical and magnetic properties, superconductivity and other important properties which are due to microgravity effects.

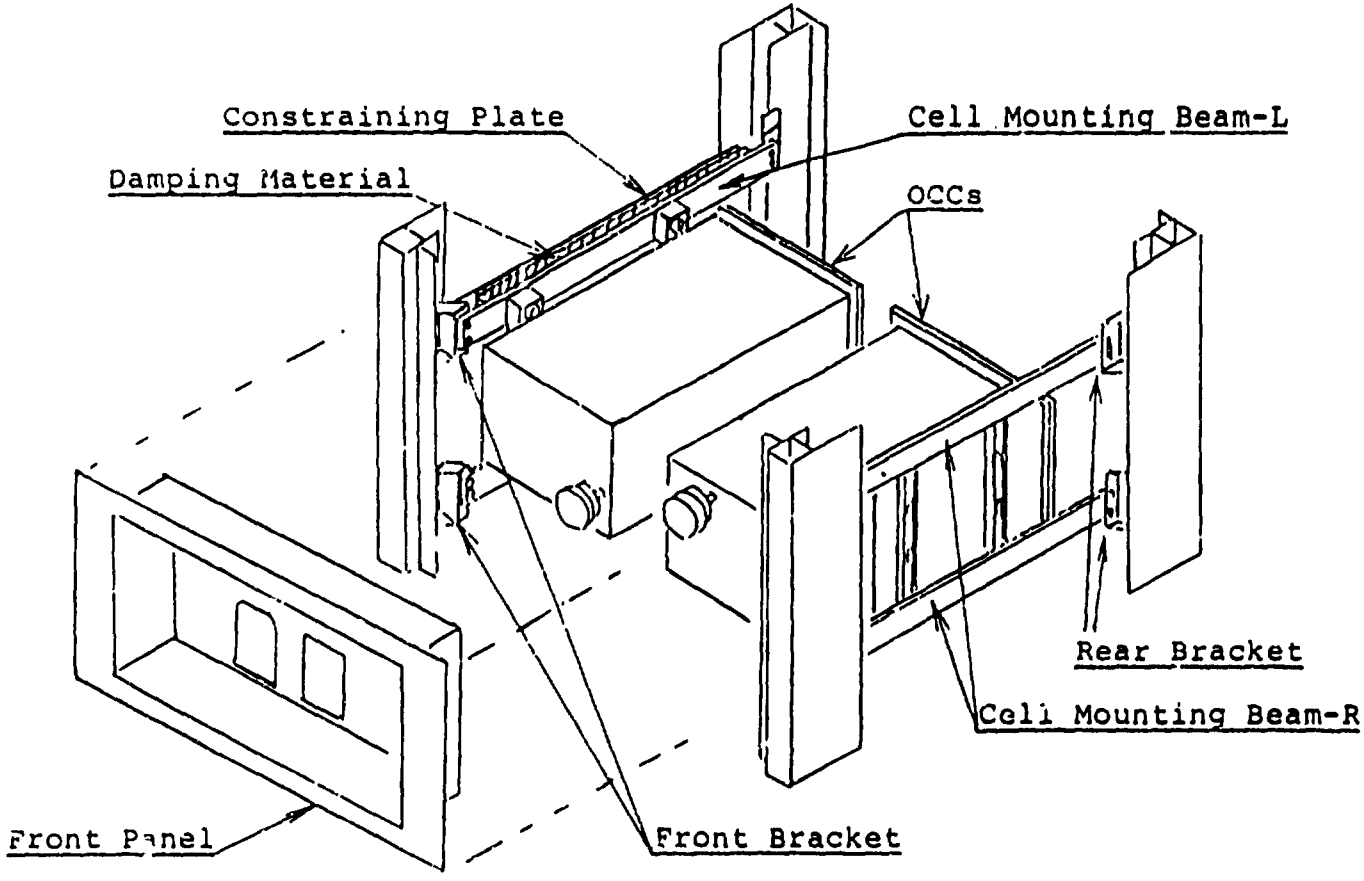

Figure 1. Organic Crystal Growth Facility Concept.

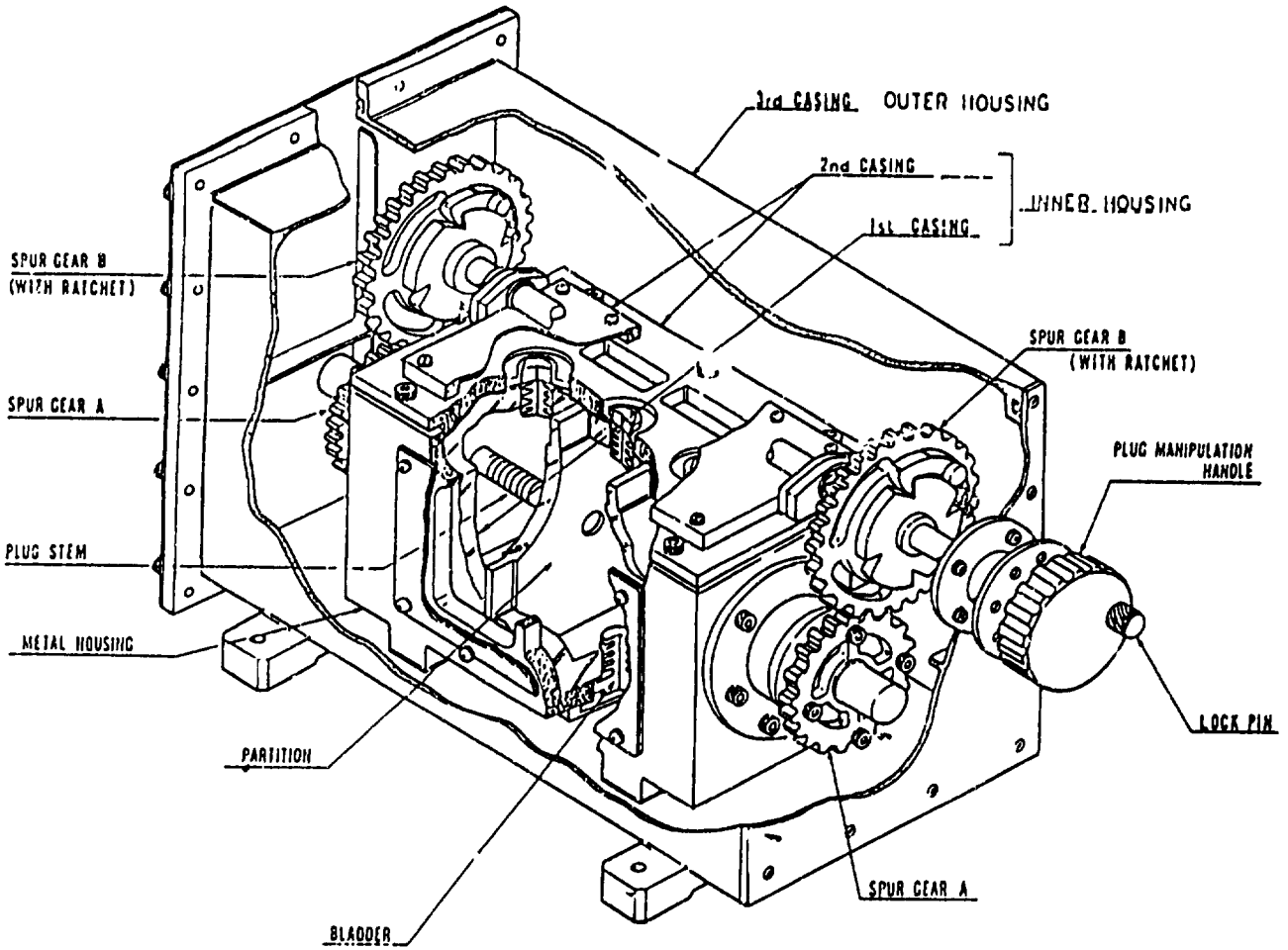

Figure 2a. Organic Crystal Growth Cell Concept.

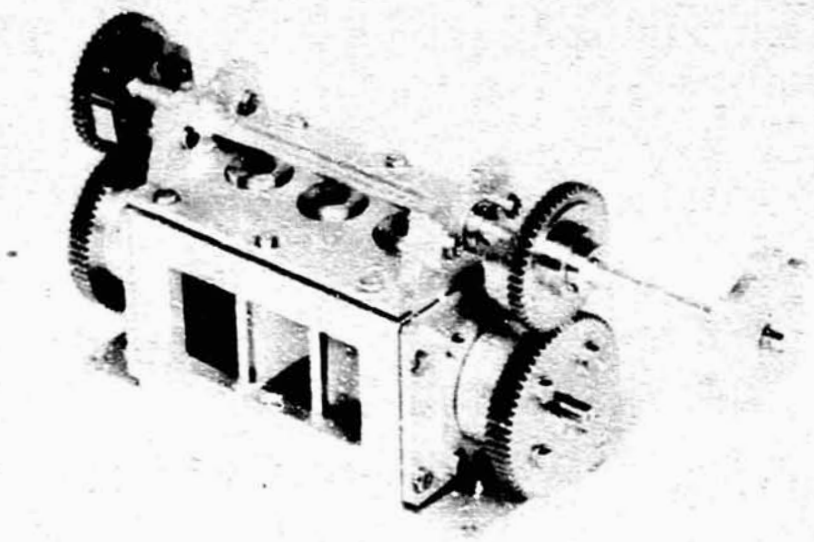

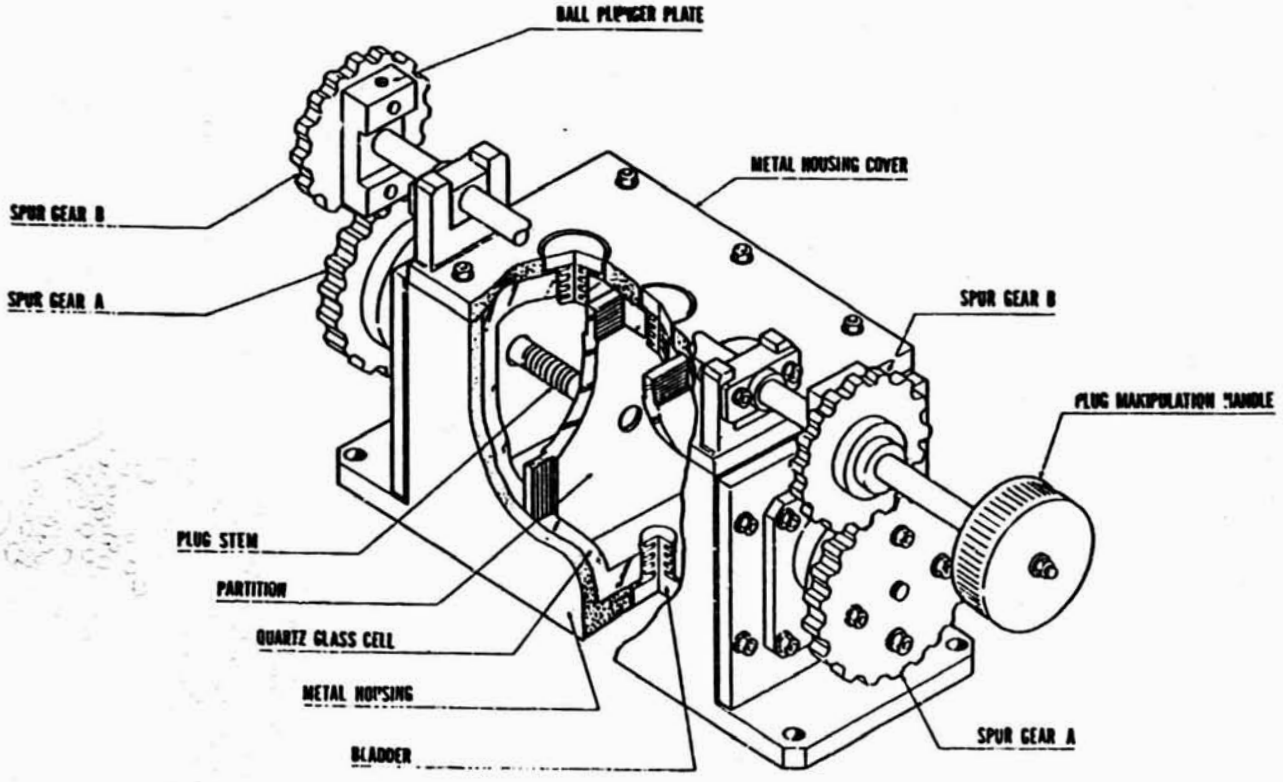

Figure 2b. Organic Crystal Growth Cell Flight Model.

N92-23636

CRYOSTAT
18-IML-1

DARA, GmbH Germany

Hardware

The Facility

The CRYOSTAT is an autonomously working rack-mounted equipment (Fig. 1). It provides two thermostat chambers, independently controlled by a processor via on/off switching of the current through peltier elements.

The temperature profiles of the freezer and stabilizer are subdivided in a common number of steps, each one with a preprogrammable temperature gradient or at constant temperature. Core parameters can be reprogrammed by crew interaction in case of rescheduling the CRYOSTAT operation time due to changed mission requirements or contingency.

Actions of the CRYOSTAT (e.g., opening the slide), the steps, actual temperature of the thermostat chambers, experiment time, and the housekeeping data are recorded on a built-in RAM and a tape.

In each thermostat chamber a specific sample container can be inserted which consists of a transparent Plexiglas block accommodating seven crystallization experiments.

The Sample Container

A schematic cross section of a sample container (Figs. 2a and 2b) demonstrates the operational principle:

In the non-operation mode each of the cylindrical crystallization volumes arranged in parallel in the sample container is divided by a slide to separate the protein and the salt solutions. Sealing of the reservoirs against each other and against the other experiments is achieved by a set of O-rings. For initiating the crystallization process the slide has to be pushed in by a slide drive mechanism and assigned holes in the slide filled with buffer solution will establish the contact between these solutions.

The volumes per experiment for protein, salt and buffer solutions are 0.57 ml, 0.84 ml, and 0.67 ml, respectively.

The Operation

The Cryostat Stowage Container, a dewar (Fig. 3), containing the two sample containers is loaded in the middeck about 17 hours before launch. Once in space, the crew activates the CRYOSTAT. After facility conditioning the samples are inserted in the thermostat chambers. The crystallization process starts automatically if the initial temperature for the samples is reached. The operational/temperature profile for the IML-1 samples is shown in Fig. 4. When the experiment ends, the crew remove the samples, put them back in the Middeck stowage for early retrieval, and deactivate the facility.

After the flight, the crystals are analyzed by x-ray crystallography and compared to terrestrially grown crystals.

Technical Data of CRYOSTAT:

Operating Temperature Range:	
Stabilizer:	+ 15 °C to + 25 °C
Freezer:	- 4 °C to + 20 °C
Accuracy:	± 0.5 °C
Chamber Volumes for Sample Container	54 mm x 54 mm x 182 mm
Data Storage Capacity	240 kB in buffered RAM 10 MB on tape recorder
Cryostat Stowage Container, Holding Time (20 °C amb. temp.)	65 hours

---

The Experiments

Single Crystal Growth of Beta-Galactosidase and Beta-Galactosidase/Inhibitor-Complex

Principal Investigator:

Dr. W. Littke, University of Freiburg, Chemical Laboratories, Freiburg, Germany

For this investigation the CRYOSTAT is used in the freezer mode. Temperature starts at -4 °C and gradually increases to 20 °C. The total concentration of the salt (ammonium sulfate) in each chamber system is constant.

The proteir to be crystallized β-galactosidase and β-galactosidase/inhibitor-complex, respectively.

β-galactosidase is an enzyme that hydrolyzes lactose (glucose-4-β-D-galactoside), and is found in intestines of babies and baby animals as well as in E. coli. It is the key enzyme of modern genetics and therefore one would like to determine the three-dimensional molecular structure of the compound to find out the interaction mechanism between function and structure.

The high molecular substance (465.000 D) is the first protein of space history crystallized in space in 1983 on Spacelab 1 using the CRYOSTAT. The crystals were several times larger and more perfect than those produced under terrestrial conditions. Because of limited quantity available, x-ray studies with the crystals could not be finished.

Crystal Growth of the Electrogenic Membrane Protein Bacteriorhodospin

Principal Investigator:

Professor Dr. G. Wagner, University of Giessen, Botanical Institute 1, Giessen, Germany

This experiment uses the stabilizer mode. In this mode the temperature remains stable at 20 °C, but the concentrations of the salt and the buffer solutions are varied from sample to sample, so investigators can determine which concentration promotes the growth of better, larger crystals.

The protein to be crystallized is bacteriorhodospin, a well-known membrane protein that converts light energy to voltages in the membranes of photosynthetic archaebacteria.

Microbiologists are interested in this system because bacteriorhodopsin represents an almost ideal system to study light-energy-driven vectorial membrane transport developed in Earth's early environment.

Many ground-based experiments have been done with bacteriorhodopsin, that forms two-dimensional crystals on high salt concentrations. However, resolution of the three-dimensional structure, which will help biologists understand how bacteriorhodopsin works, depends on the availability of isometrically large, highly ordered crystals. Hitherto, high-quality crystals have not been grown under terrestrial conditions.

Crystallization of Proteins and Viruses in Microgravity by Liquid-Liquid Diffusion

Principal Investigator:

Dr. A. McPherson, Department of Biochemistry, University of California at Riverside, USA,

Canavalin:

Canavalin is a representative of a highly homologous class of plant proteins classically known as vicillins. These are the major storage proteins of leguminous seeds such as kidney beans, green beans, garden peas, and most other edible beans and seeds. Thus, this plant seed protein is among the largest sources of nutritional protein available to man for his own consumption and that of his agriculturally important animals. It is a crucial component of the world's diet, particularly in the developing countries. Its improvement by genetic means to enhance its nutritional properties is, therefore, a major objective of protein engineering as applied to the agricultural sphere. Success in enhancing its nutritional properties, its viability and its abundance could contribute substantially to the alleviation of world hunger and famine.

The protein itself is of appreciable interest as well to the biochemist and molecular biologist. Its structure at the atomic level has now been determined by three-dimensional x-ray diffraction analysis, and the gene coding for its expression has been cloned. Thus, all the elements are in place for the systematic and rational application of automated computer graphics analysis, site directed mutagenesis and recombinant DNA technology to the modification of its physical and chemical character. It represents one of the few clear examples where this is true.

The protein is a trimeric molecule of 150,000 daltons, composed of three identical subunits. X-ray and genetic analyses have shown the 50,000 dalton subunit to be internally redundant in terms of both amino acid sequence and three-dimensional structure, thus, the gene which codes for this protein must be a tandem duplicate. This is one of the few proven examples of such a case. The oligomer possesses a perfect threefold axis of symmetry relating it subunits and each subunit, in turn, contains an internal pseudo dyad axis of symmetry.

The protein, canavalin, can be isolated in very large amounts from Jack Beans (Canavalis ensiformis), a useful cattle feed, by traditional biochemical techniques and is crystallized from

1% NaCl buffered with phosphate at pH 7.2. It was first isolated by the famous biochemist, J. B. Sumner, in 1917 and crystallized by him in 1934. It was, in fact, one of the earlist proteins ever crystallized.

Satellite Tobacco Mosaic Virus:

Satellite tobacco mosaic virus (STMV) is a T=1 icosahedral virus that, along with its master virus tobacco mosaic virus, (TMV), infects tobacco and a variety of other plants. STMV is one of the few known cases of a spherical satellite virus that requires coinfection by a fillimentous virus (TMV). STMV has a molecular weight of about 1.5 x 10^6 daltons and is composed of 60 copies of a coat protein of molecular weight 17,500 daltons each and a single stranded RNA genome of 1066 nucleotides. The genome codes only for the coat protein, no other product is made.

STMV is the smallest virus ever crystallized and it is under active study by x-ray diffraction analysis to determine its detailed three-dimensional atomic structure. Crystals can be reproducibly grown from ammonium sulfate solutions, from polythylene glycol, and over a broad range of pH values.

Because STMV is such a large particle it offers a number of unique advantages for the study of macromolecular crystal growth. It is the subject of quasi elastic light scattering investigations to delineate nucleation mechanisms, and it provides crystals ideally suited for electon microscopy studies as well.

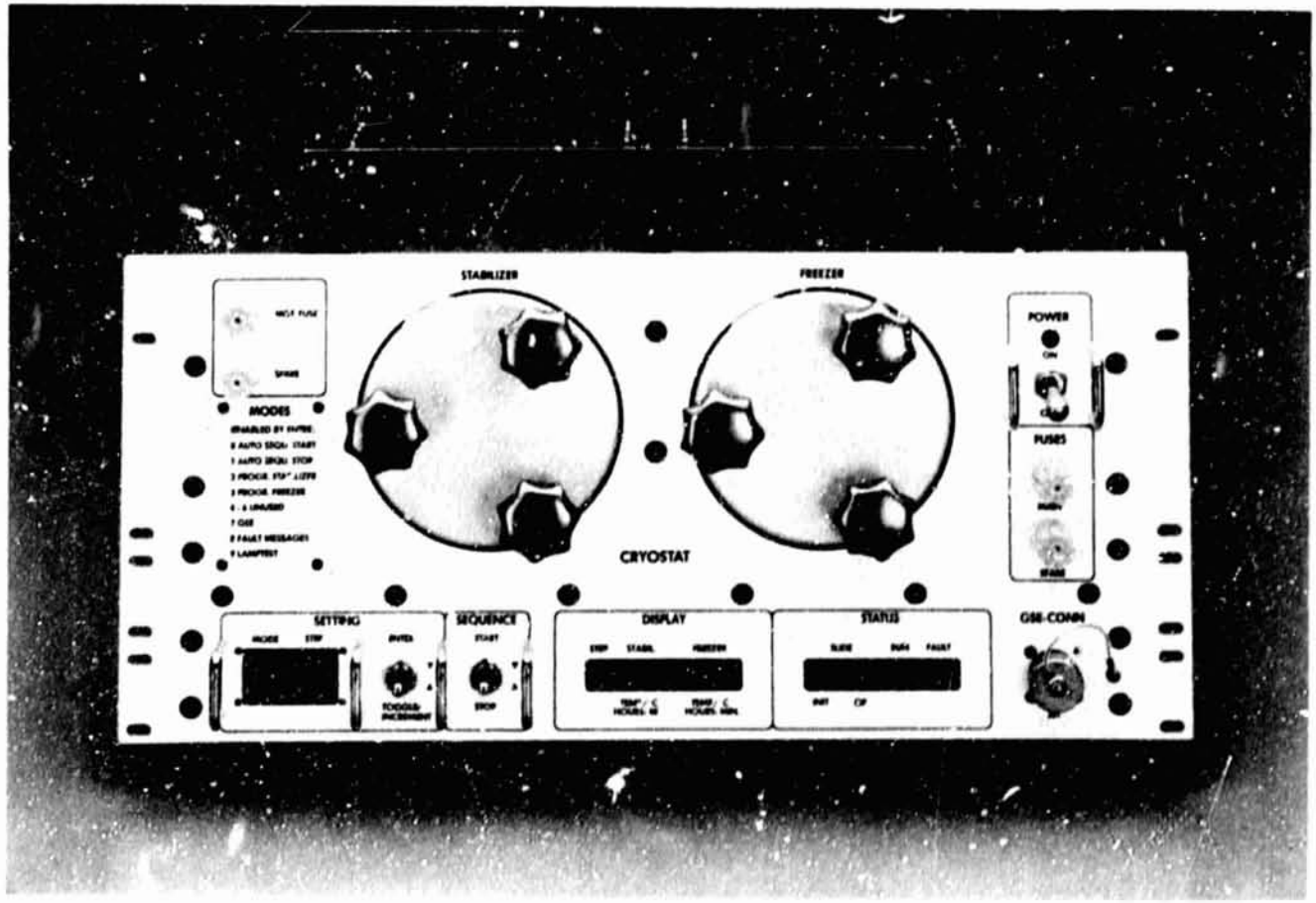

Figure 1. Cryostat front panel.

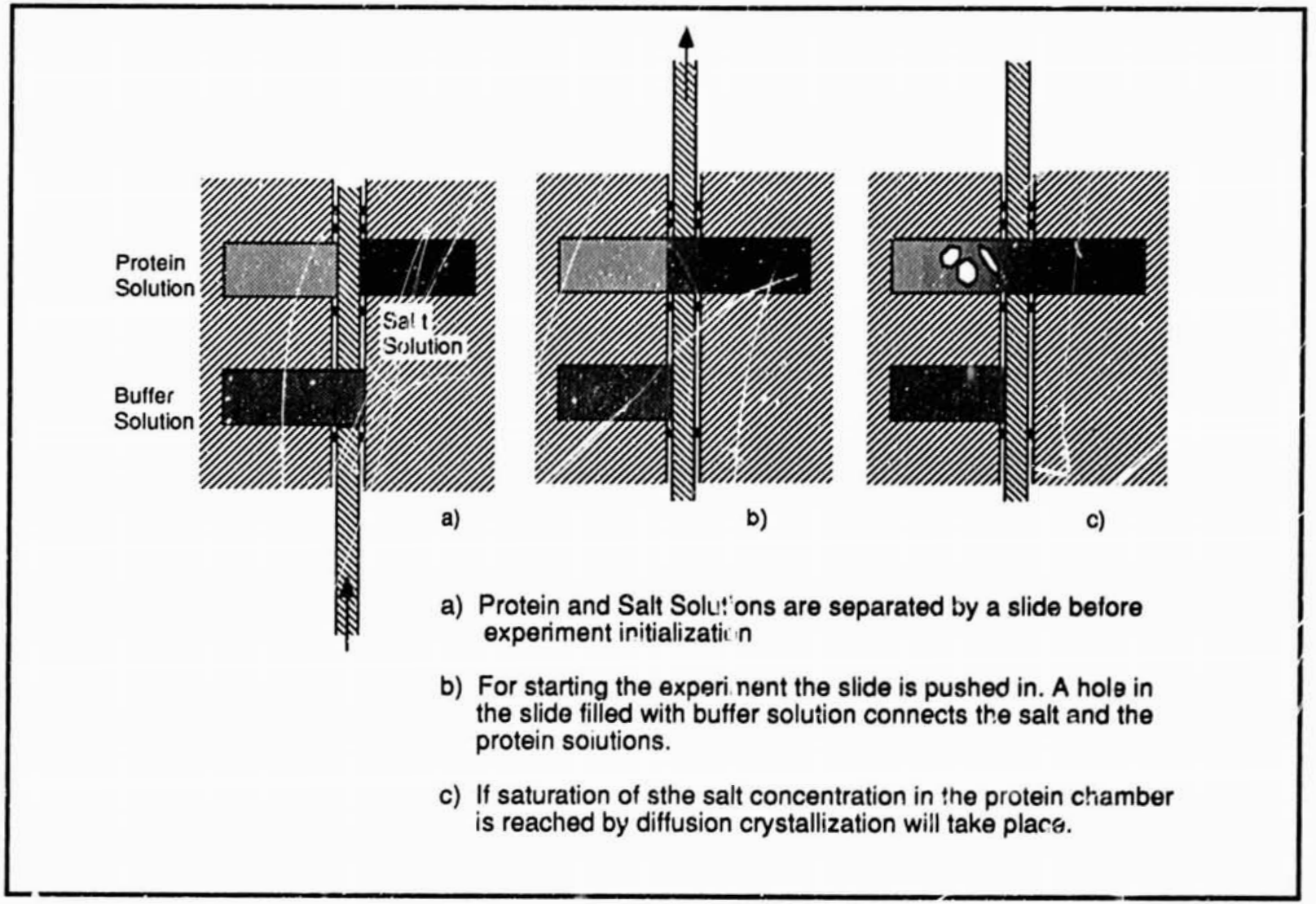

Figure 2a. Cryostat crystallization principle.

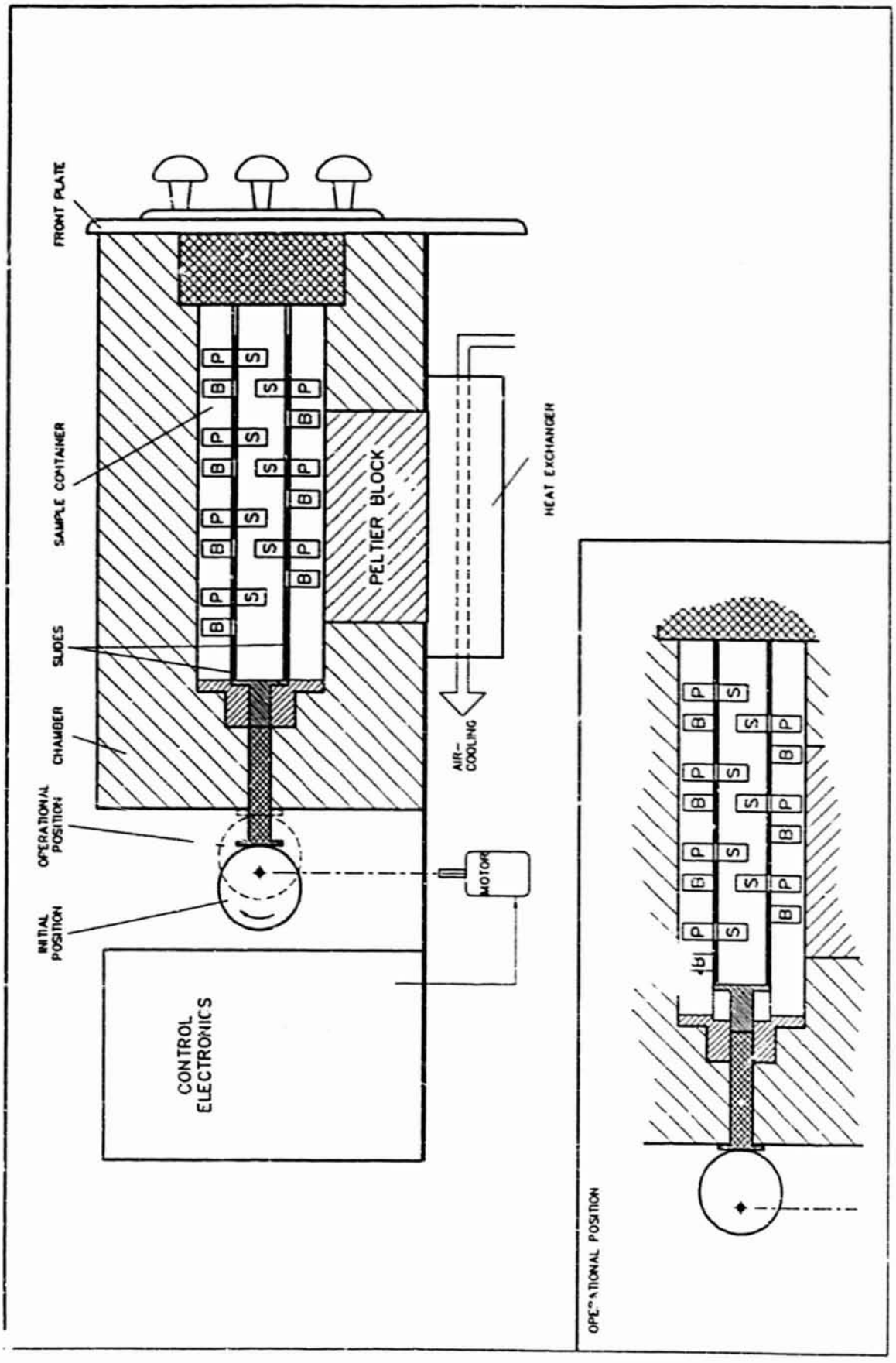

Figure 2b. Cryostat operating schematic.

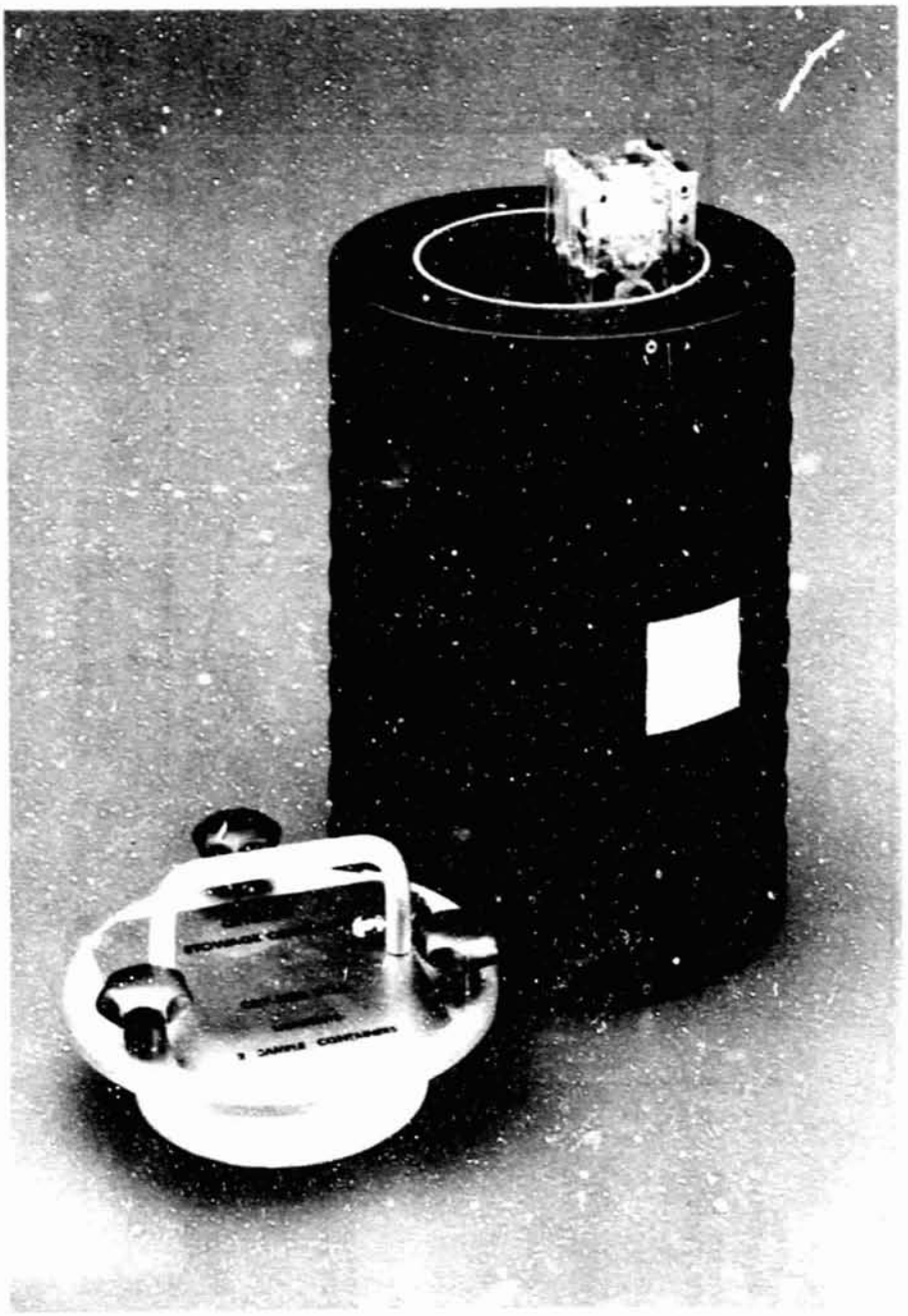

Figure 3. Cryostat sample stowage container.

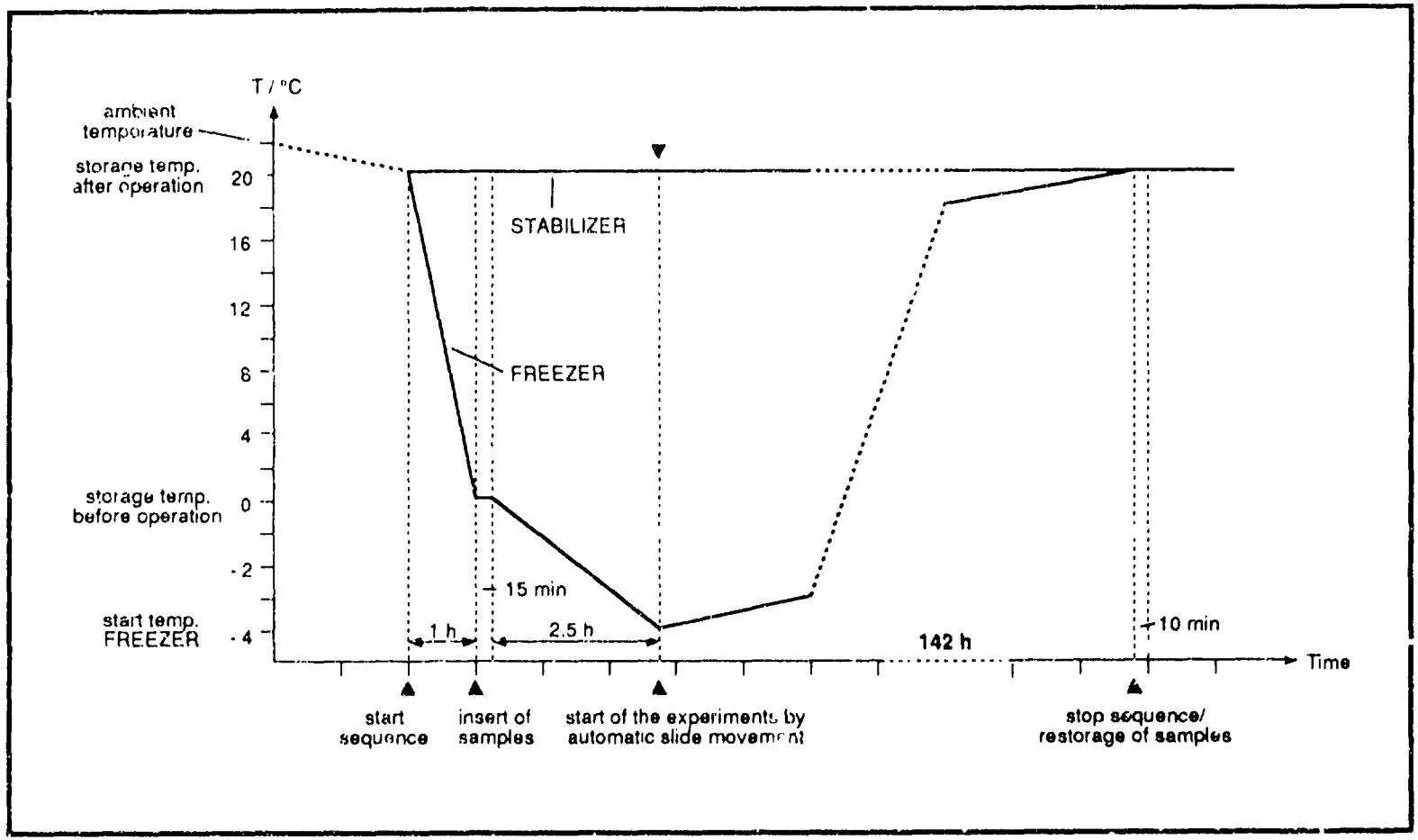

Figure 4. Cryostat experiment temperature/time profile.

N92-23637

THE CRITICAL POINT FACILITY (CPF)

The Critical Point Facility (CPF) is an ESA multi-user facility designed for microgravity research onboard Spacelab. It has been conceived and built to offer investigators opportunities to conduct research on critical point phenomena in microgravity. This facility provides the high precision and stability temperature standards required in this field of research. It has been primarily designed for the purpose of optical investigations of transparent fluids. During a Spacelab mission, the CPF automatically processes several thermostats sequentially, each thermostat corresponding to an experiment. The CPF is now integrated in Spacelab at Kennedy Space Center, in preparation for the IML-1 mission.

Scientific Objectives

Pure fluids near the gas-liquid transition and binary mixtures may undergo a phase separation. Their miscibility or coexistence curve exhibits the general features shown in Figure 1. At high temperatures, the system is formed as a single phase. When the temperature is lowered and the coexistence curve reached, instability sets in: a phase separation is initiated in the form of density fluctuations, until two distinct equilibrium phases, located on the coexistence curve, are formed. The peak of this curve is the critical point.

The CPF has been designed to submit transparent fluids to an adequate, user-defined thermal scenario, and to monitor their behavior by using thermal and optical means. For instance, the density fluctuations mentioned above may produce scattered light which can be monitored by two of the CPF diagnostics. In addition, variations of the index of refraction (related to temperature or density inhomogeneities) can be analyzed with an interferometer.

Because they are strongly affected by gravity, a good understanding of critical phenomena in fluids can only be gained in low gravity conditions. First, fluids at the critical point become compressed under their own weight because their isothermal compressibility diverges at that point. As a consequence, fluids cannot be maintained in a critical state under gravity conditions. Secondly, the role played by gravity in the formation of interfaces between distinct phases is not clearly understood. Hence, the microgravity environment of Spacelab is very appropriate for this type of experiment.

CPF Design

The CPF has been designed for installation in a Spacelab rack. It is composed of two interconnected drawers: the experiment and the electronic drawers (Figs. 2 & 3). The electronic drawer provides the power supply, the electronics, and the data handling capabilities, whereas the experiment drawer contains the complete optical diagnostic system which surrounds the exchangeable thermostat. The thermostat houses the test cell which contains the fluid to be investigated and provides interfaces for the stimuli (thermal, acoustic, or magnetic mixer) and for the diagnostic devices (thermal, optical).

The CPF is fully automated: it runs experiments according to a pre-recorded timeline, defined by the investigator, and which can be modified in real-time at the investigator's request during the experiment run. This method, which requires minimum crew involvement, is particularly adapted to the very long experiment durations typical of this field of research.

The thermostat (Fig. 4) provides an excellent thermal control of the test fluid, with an accuracy of one thousandth of a degree (0.001 °C). This is achieved by using three co-axial cylinders, the second of which is surrounded by Joule heating wires and by torus-shaped Peltier elements at the top and bottom. The thermostat control electronics are also temperature controlled. Besides its thermal role, the thermostat has optical and electrical interfaces to enable stimuli and diagnostics to interact with the test fluid. It has a built-in identification number which ensures it will be processed in conjunction with the proper pre-recorded timeline.

The thermal capabilities provided by the thermostat within the test fluid are given below:

- temperature controlled between 30 °C and 70 °C
- heating and cooling with minimum step size of 1 mK
- maximum heating/cooling rate: 36 K/hr/10 K/hr
- temperature stability: 0.1 mK/hr
- temperature gradients within fluid: <0.1 mK/cm
- quenching rate: up to 25 mK/sec
- quenching step size: between 4 and 100 mK

An acoustic mixer at 1.7 MHz or a magnetically-driven mixing bar can be activated to eliminate any fluid density or concentration inhomogeneity.

The temperature of the test fluid is monitored with a precision of 0.1 mK relative to the critical temperature (T_c), which is determined beforehand but can be updated during the experiment onboard Spacelab.

The optical diagnostic methods are:

- direct visualization (transmission of collimated light)
- small angle scattering between 0 °C and 30 °C
- wide angle scattering between -38 °C and 90 °C
- interferometry (Twyman-Green type)
- beam attenuation in transmission
- monitoring of the intensity of the input laser beam

The performance of these diagnostics is described in detail in Table 1, and their geometry with regard to the thermostat are shown in Fig. 5. The direct visualization and the interferometric images can be acquired simultaneously by a CCD and by a photocamera in any combination controlled by the automatic program which runs the CPF.

Operations

During the CPF experiments onboard Spacelab, the investigator on the ground is fully aware of the way his experiment is running thanks to the following:

- the CPF housekeeping and scientific data are displayed in real time
- the CCD images from CPF are displayed in real time, at TV rate (30 fps) during short, preselected periods and continuously at a reduced rate of 1 image every 6 sec
- voice contact is foreseen when a crew member is working on CPF

The investigator can also modify the automatic program running his experiment at any stage.

All data sent to the ground are recorded and made available to the investigator after the mission, together with the photocamera pictures.

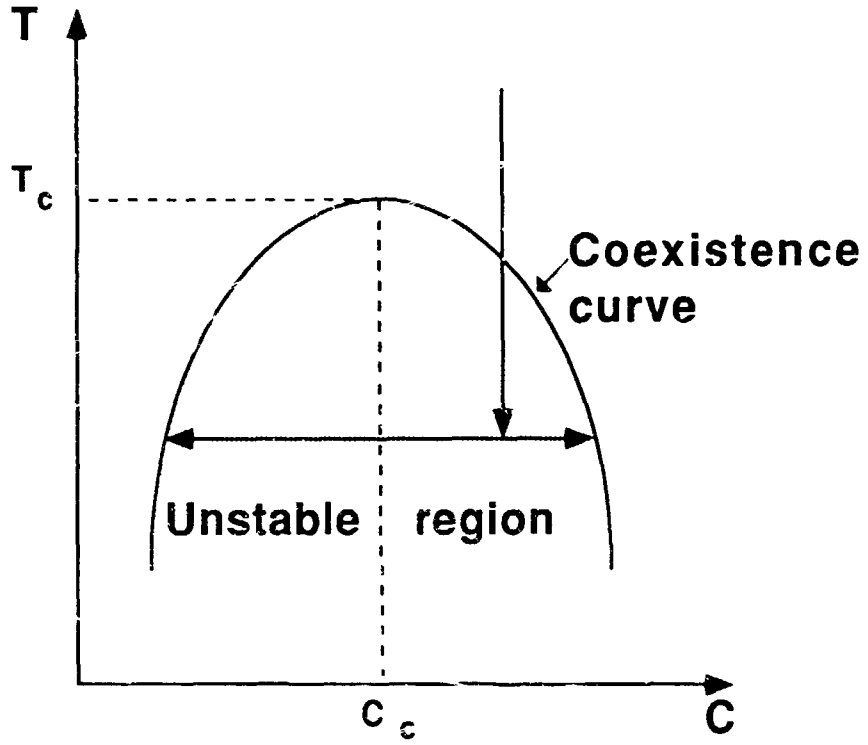

T : temperature
C : concentration

Figure 1. Coexistence curve.

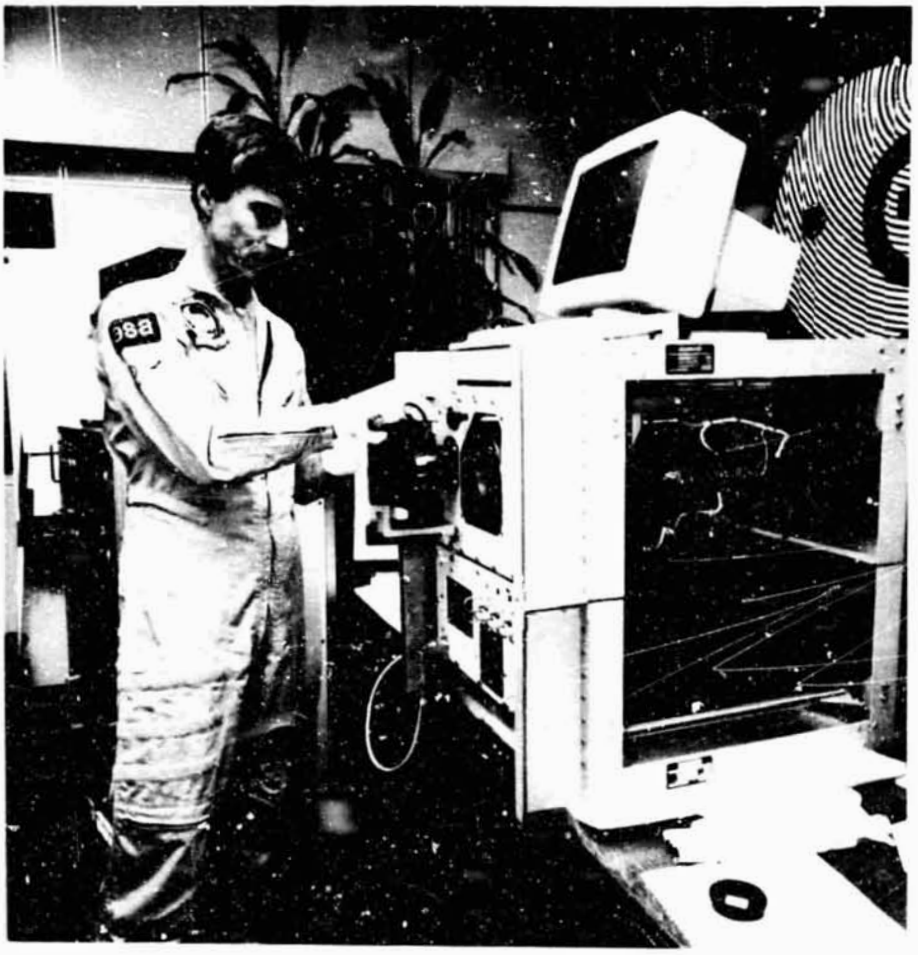

Figure 2. ESA's scientist astronaut Ulf Merbold, who has been nominated Payload Specialist for the IML-1 mission, training on the CPF

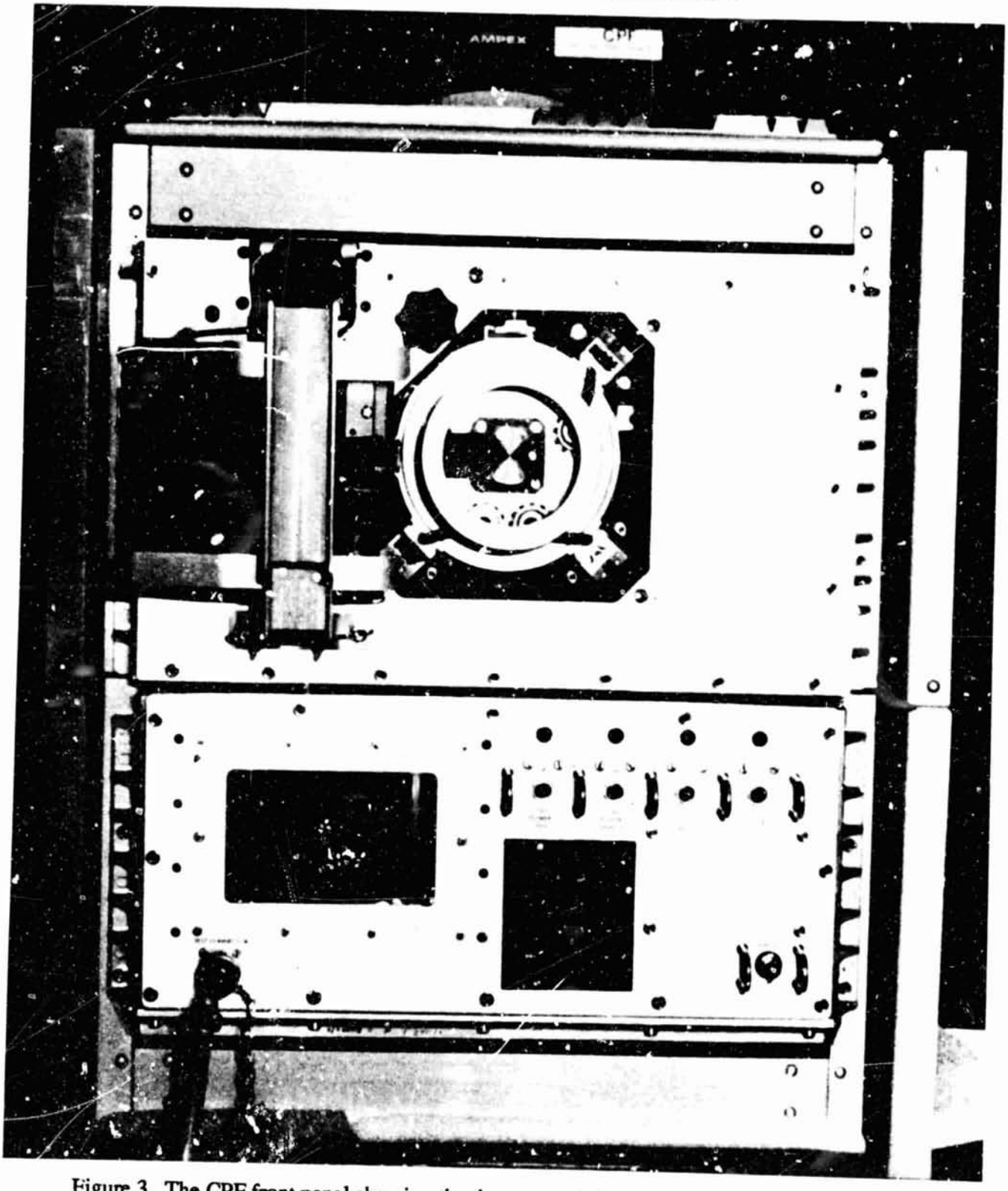

Figure 3. The CPF front panel showing the thermostat (with the protective cover plate removed) in the center of the upper (experiment) drawer. The photocamera can be seen to the left of the thermostat. On the left-hand side of the lower (electronics) drawer, the display panel can be seen with the keypad to its right. The overall dimensions are: height: 49 cm, width: 48 cm, depth: 58 cm.

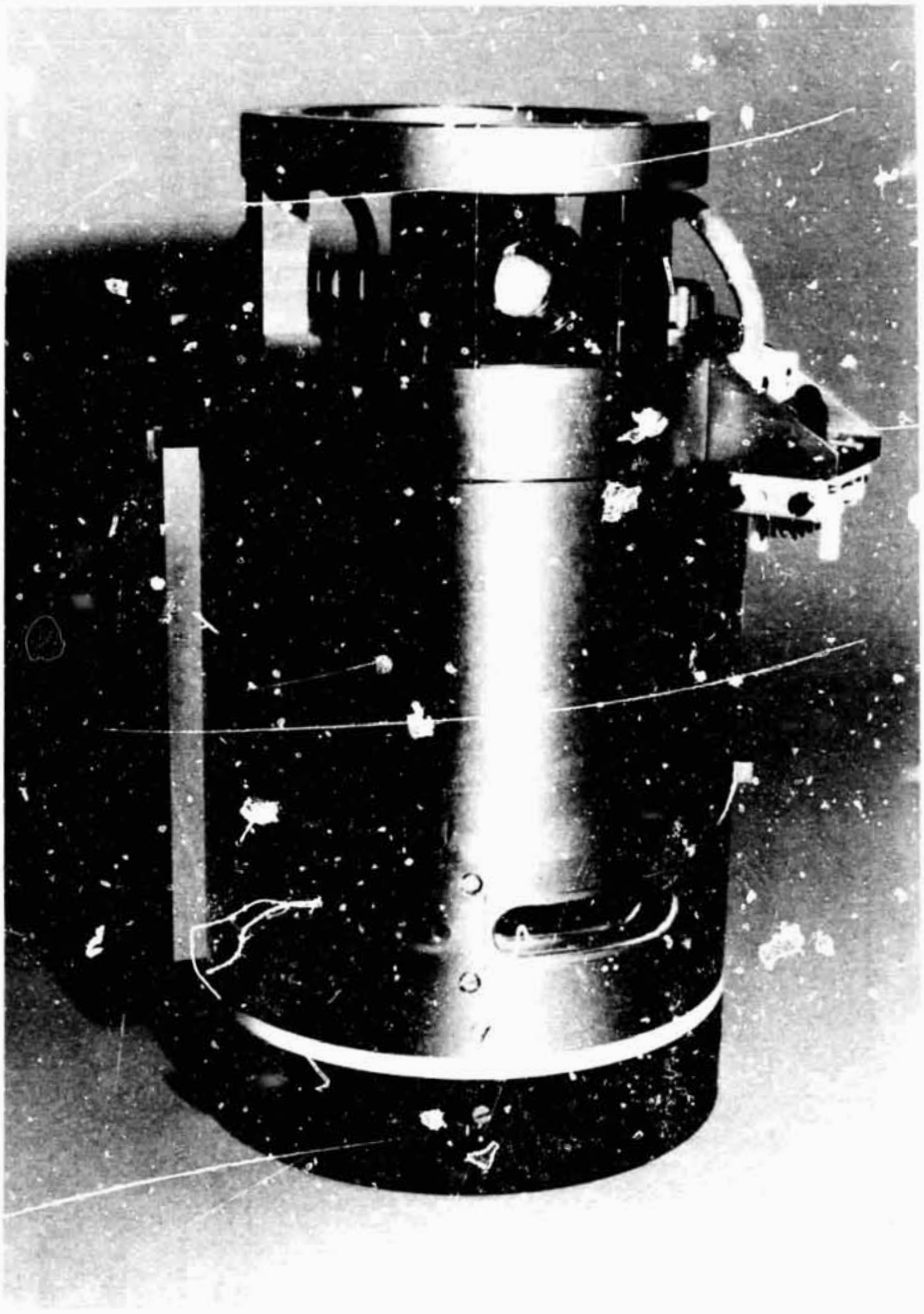

Figure 4. The CPF thermostat. The output of the interferometric channel is on top; the output of the SALS is on the bottom, the three holes on the side are used for wide angle scattering.

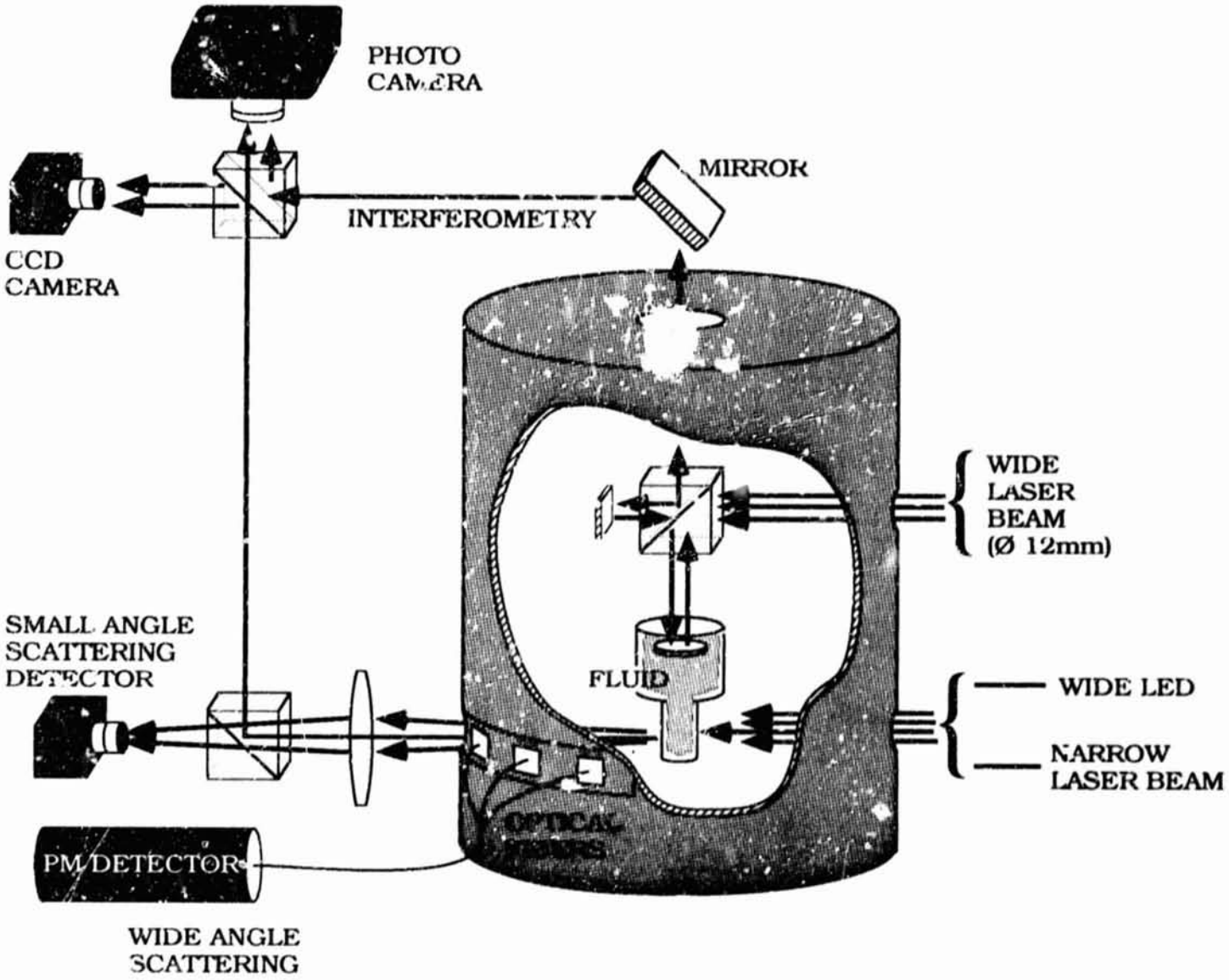

Figure 5. Schematic of the thermostat.

CPF : OPTICAL DIAGNOSTICS	VISUAL	ATTENUATION	INTERFEROMETRY (TWYMAN - GREEN)	SMALL ANGLE SCATTERING (SALS)	WIDE ANGLE SCATTERING (WALS)
SOURCE	LED light collimated .6 & 1.5 micro W (selectable)	He-Ne laser 1.0 mW	He-Ne laser .06 mw	He-Ne laser 1.0 mW .6 mm diam	He-Ne laser 1.0 mW .6mm diam
FIELD OF VIEW AT OBJECT	12 mm diameter	.6 mm diameter	12 mm diameter		1°
DETECTION : •DETECTOR	CCD camera photo camera	16 pixels of SALS CCD	CCD camera photo camera	linear CCD 512 pixels	Photomultiplier
•ANGLES	NA	NA	NA	0° -> 30°	-22°, -30°, -38,° 66°, 74°, 82°, 90°; laser input ref. , dark signal
•SENSITIVITY		10^{-4} -> 10^{-6} W		4 10^{-7} -> 10^{-9} W	10^{-8} -> 10^{-12} W
•INTENSITY RESOLUT.	6 bits/pixel for CCD	6 bits	6 bits/pixel for CCD	6 bits (linear)	12 bits (linear)
•AQUISITION RATE	30 fps	1 Hz	30 fps	1 Hz or 0.1 Hz	5 cycles/minute
RESOLUTION AT OBJECT:					
•SPATIAL	25 µm with CCD	NA	fringe density: 25 mm^{-1} with camera 10 mm^{-1} with CCD	NA	NA
•ANGULAR	NA	NA	NA	.25°	2°

Table 1. CPF Optical Diagnostics.

N92-23638

NEAR-CRITICAL POINT PHENOMENA IN FLUIDS
(19-IML-1)

D. Beysens
Service de Physique de l'Etat Condense´ - Centre d'Etudes de Saclay
91191 Gif sur Yvette Cedex
France

Understanding the effects of gravity is essential if we are to predict the behavior of fluids in spacecraft and orbital stations, and, more generally, to give us a better knowledge of the hydrodynamics in these systems. This is the general goal of our study, namely, to understand the behavior of fluids in space. In order to get more general results, we use fluids near their critical point.

What is the critical point?

The simplest way to describe the critical point is to consider the different states of matter: solid, liquid, and gas (Figure 1). These states are delimited by transition lines. It is well known that these lines meet at the 'triple point' where the three phases -- solid, liquid, and gas -- coexist. There is, however, another situation which occurs when liquid and vapor phases coexist. If the temperature and pressure are increased to a high enough level, a point beyond which both liquid and gas phases become indistinguishable is reached. This is the "critical point" where the meniscus between the two phases vanishes. The critical point is located at a particular value of pressure, temperature and density in different substances. The critical point of water, for example, is at a high temperature and pressure (370 °C and 220 bar); it is near room temperature in other substance like carbon dioxide CO_2 (31 °C and 74 bar) or sulphur hexafluoride SF_6 (45 °C and 38 bar).

Universality of critical point behavior

The behavior of all fluids near their critical point becomes the same and is very unusual. The fluid becomes very compressible, fluctuations of density are very large, leading to large fluctuations in the refractive index which means that the system scatters light very much. Fluids look milky, this is the so-called 'critical opalescence' phenomenon.

There is a general reason for these very large fluctuations: the system is so close to the transition point that it "hesitates" between the two equally possible states. The notion of a critical point applies, in fact, to a whole class of systems, where the same kind of behavior can be observed. This applies to all mixtures of partially miscible liquids whose miscibility curve ends in a critical point: mixtures of two simple liquids like water and phenol, or cyclohexane and methanol, micellar solutions (mixtures of water and soap), micro-emulsions (mixtures of water, oil, and soap) and mixtures of molten metals (alloys), as well as to many other fluid systems. In

fact all these systems belong to the same 'universal class' whose representative is...a magnet, which undergoes a critical-point transition at the Curie point (the point at which its magnetisation becomes zero). The relevant model is the well known three-dimensional 'Ising model'. All these systems present very close analogies, and the same universal laws apply to their behavior which ultimately depends on the dimensionality of space.

It is important to note that the critical behavior of fluids is not restricted to the immediate vicinity of the critical point. The behavior of fluids can be described in terms of the critical point within a range of more than 100 °C in most of the systems cited above. This is why their study is of interest to many areas, including thermodynamic and transport properties (especially heat and mass transport), and hydrodynamics. The technical implications of these studies are numerous. For example, heat exchangers, oil recovery, the solvent industry, hydrodynamics of two-phase flows, and the processing of polymers, metals and glass, a all dependent on critical point phenomena.

Gravity-sensitive behavior

It is at this point that the experiments in zero-gravity become meaningful. Critical fluids and liquid mixtures are not only critical systems, they are also fluids. And the behavior of fluids on Earth is quite often dictated by gravity. The particularity of critical fluids is that the influence of gravity appears to be very important. This is because some key parameters exhibit extreme values near the critical point:

- compressibility, which makes a pure fluid compressed under its own weight;
- capillary length, where the Earth-bound study of the kinetics of phase separation is governed by gravity flows;
- heat transport, which is slowed down in pure fluids, and mass transport, which also decreases in mixtures of liquids. In pure fluids, the diffusion of heat is so slow that it is the motion of the fluid due to convection that ensures heat transport on Earth.

The liquid mixtures experiment (BEM1) on the IML1 mission

The IML-1 mission offers our team an excellent opportunity to continue our research in this field. We have improved the properties of a naturally near density-matched mixture (cyclohexane and methanol) by partial deuteration of one of the components (cyclohexane) in order to adjust the densities very finely. In this liquid mixture, the critical point is a point of miscibility and the diffusion of the two species is considerably slowed down. Two sounding rocket flights (Texus 11 in 1985 and Texus 13 in 1986) demonstrated that the suppression of gravity effects was effective, at least for the study of the phase separation process by spinodal decomposition (a common process in metallurgy and glass processing). This process occurs in liquid mixtures in the immediate vicinity of the critical point. Thanks to these results, we have been able to carry out a number of ground-based experiments to predict the behavior of phase separating critical mixtures in the absence of gravity. The following areas have in particular been successfully addressed: growth kinetics, the efficiency of partitioning, the effects of capillary and wetting effects by the wall, the influence of a concentration gradient.

For the spinodal decomposition process, the six minutes of microgravity obtained by the use of the Texus rockets were sufficient. However, if the above study is to be extended to the phase separation process in off-critical fluids (nucleation), the kinetics of evolution become much slower and sounding rockets can no longer be used. The aim of the first experiment (BEM1) on IML-1 is, therefore, to check whether the slow growth that is currently observed in the above density-matched system on Earth is due to remaining gravity flows or to a real growth process. For this purpose, a differential experiment will be performed, where the behavior of a slightly off-critical sample of the density-matched mixture of cyclohexane and methanol will be compared with Earth-bound control experiments. For quantitative comparison, the light scattering facility of the CPF will be used in conjunction with the LED illumination (direct observation) and further image analysis. The scenario of the experiment is simple: heat the liquid mixture above its critical temperature (Tc), homogenise it by means of ultrasounds (see Figure 2), lower the temperature to check the value of the critical temperature, and quench the system a few millidegrees below Tc in the unstable region where its phase separates. Then wait to determine the growth kinetics of the two new phases.

The pure fluids experiment (BEM2) on the IML-1 mission

When dealing with pure fluid systems, it is impossible to use the partial deuteration tactic mentioned above since both vapor and liquid are of the same chemical species. Only zero-gravity experiments can remove the effects of gravity. As already noted above, in contrast to liquid mixtures, the liquid-vapor system near its critical point displays a very large anomaly in the heat transport. This anomaly results in very long equilibrium times that are not seen on Earth because heat transport causes very strong convection in the system. The temperature homogenisation of such a system is therefore very important in zero gravity. In order to understand this problem better, we have made a numerical simulation of the hydrodynamic behavior. In this case, our results show that, surprisingly, heat transport is accelerated near the critical point thanks to a phenomenon that we have called the 'Piston Effect'. Our simulation shows that, when heating a fluid to a boundary, only a small layer warms up which expands in the same way as a 'piston'. This 'piston' travels back and forth in the sample cell and converts its energy into heat. Convections accompany this phenomenon and equilibration can be achieved quite rapidly. We have qualitatively demonstrated this effect in an experiment on Texus 25 where thermalisation of a CO_2 sample took less than 10 seconds whereas heat diffusion alone was expected to take 10 days. During the same experiment, we were also able to demonstrate that the kinetics of phase separation of pure fluids, according to the 'spinodal decomposition' process, was the same as that of binary mixtures. No special compressibility effects occurred. It can, therefore, be concluded that all the studies performed with critical density-matched mixtures (see above) can also be applied to pure fluids.

Due to the short duration time of the Texus 25 experiment, valuable information on the long-term homogenization in pure fluids could not be obtained. Moreover, the phase separation of off-critical pure fluids takes too long for investigations to be carried out in sounding rockets. The experiment BEM2 on IML-1 is aimed at investigating these two problems in two samples placed in the same thermostat. The first is filled at a slightly off-critical density with SF_6 for the

study of the kinetics of phase separation in off-critical conditions, as in BEM1 but with a pure fluid, and the other is filled with SF_6 at exactly its critical density to study the thermalisation and relaxation of the density inhomogeneities. All samples have a gold thread set inside the cell. This thread is thermally coupled with the thermostat in order to separate the effects in the bulk, around the thread, from the effects of the surface of the window cell. As for the BEM1 experiment, the CPF's light scattering and LED direct observation possibilities will be used with the first cell. Interferometry will be used to measure the density variations in the second cell. In both cases, the scenario will be the same: heating above Tc, waiting until homogenization occurs, stepping down to Tc while studying the relaxation of the density by interferometry, quenching below Tc, and determination, as for the BEM1 experiment, of the kinetics of phase separation.

General results expected from IML-1

What should emerge from the IML-1 mission is a better understanding of the kinetics of growth in off-critical conditions, in both liquid mixtures and pure fluids. This complex phenomenon is the object of intensive investigation in physics and materials sciences area. We also expect that the IML-1 flight will procure key results to provide us with a better understanding of v a pure fluid can be homogenized without gravity-induced convections, and to what extent ıe 'Piston Effect' is effective in thermalizing the compressible fluids. Ultimately we should be a ble to decide whether this effect is also responsible for the acceleration of the heat transport on Earth in place of the commonly admitted convection effects.

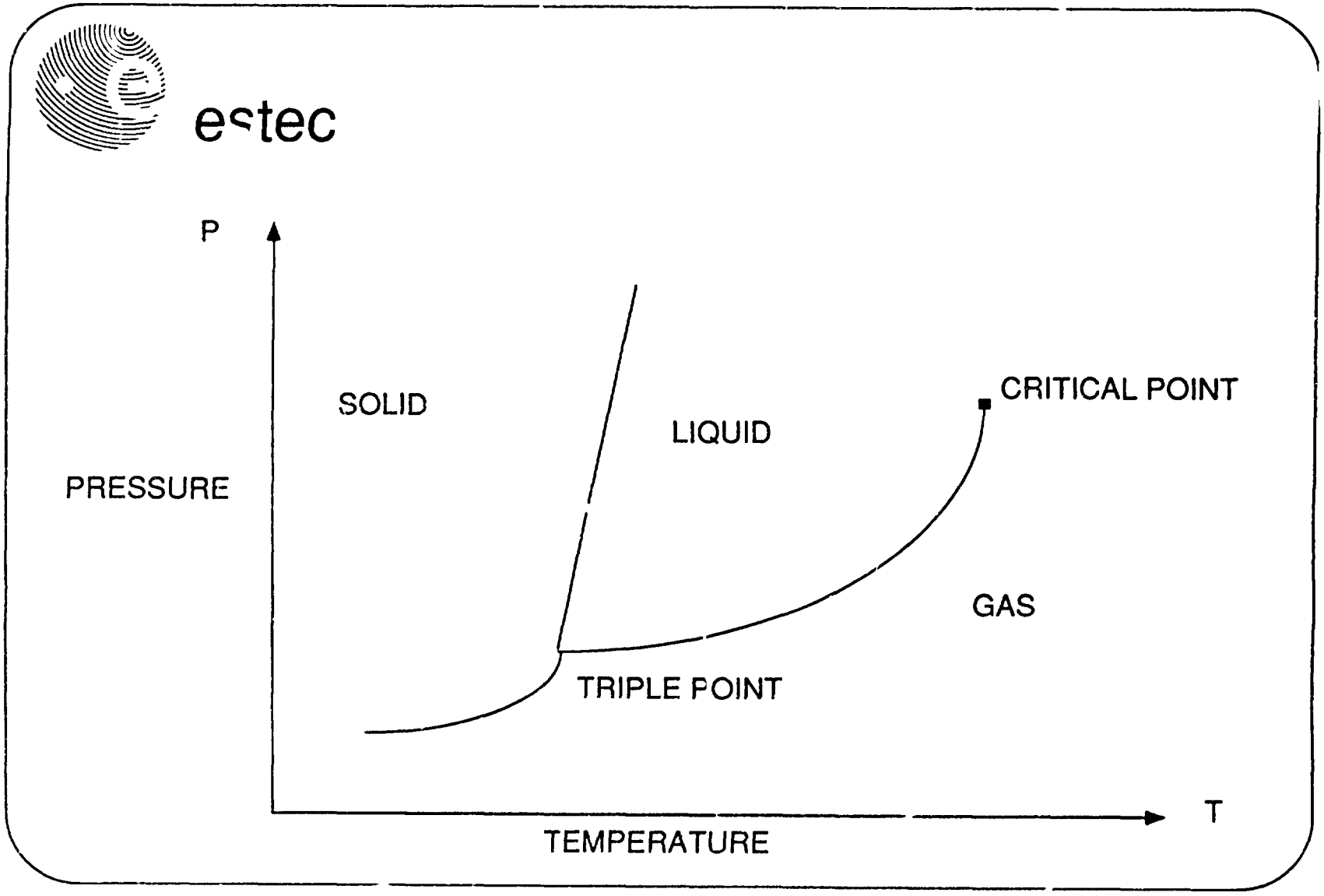

Figure 1. Phase diagram of a pure substance, C.P. = critical point; T.P. = triple point.

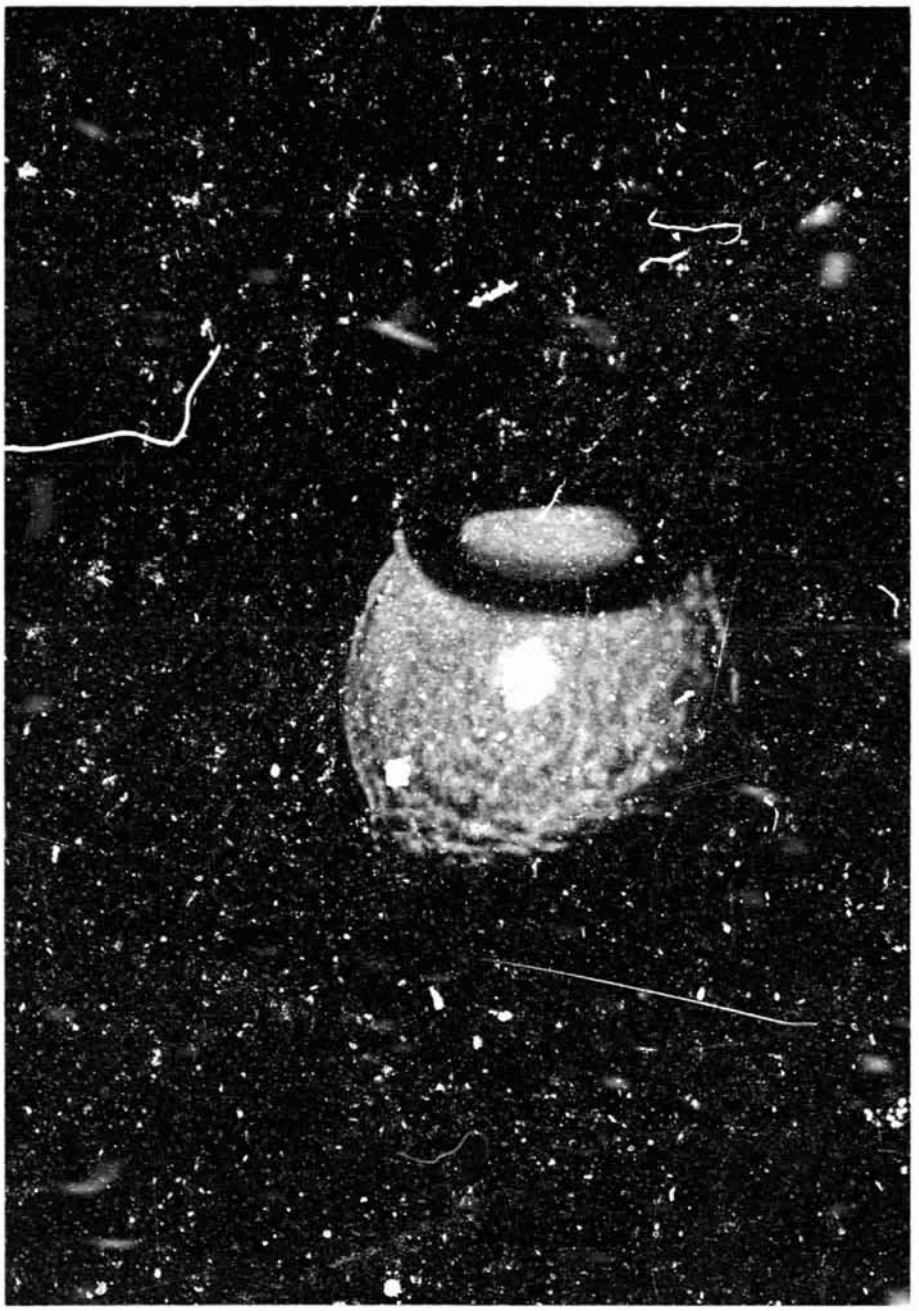

Figure 2. Binary fluid mixture of methanol-deuterated cyclohexane being mixed by ultrasounds with the CPF during ground tests. An air bubble can be seen at the top. The white dot in the middle is the thin laser beam used for scattering diagnostics.

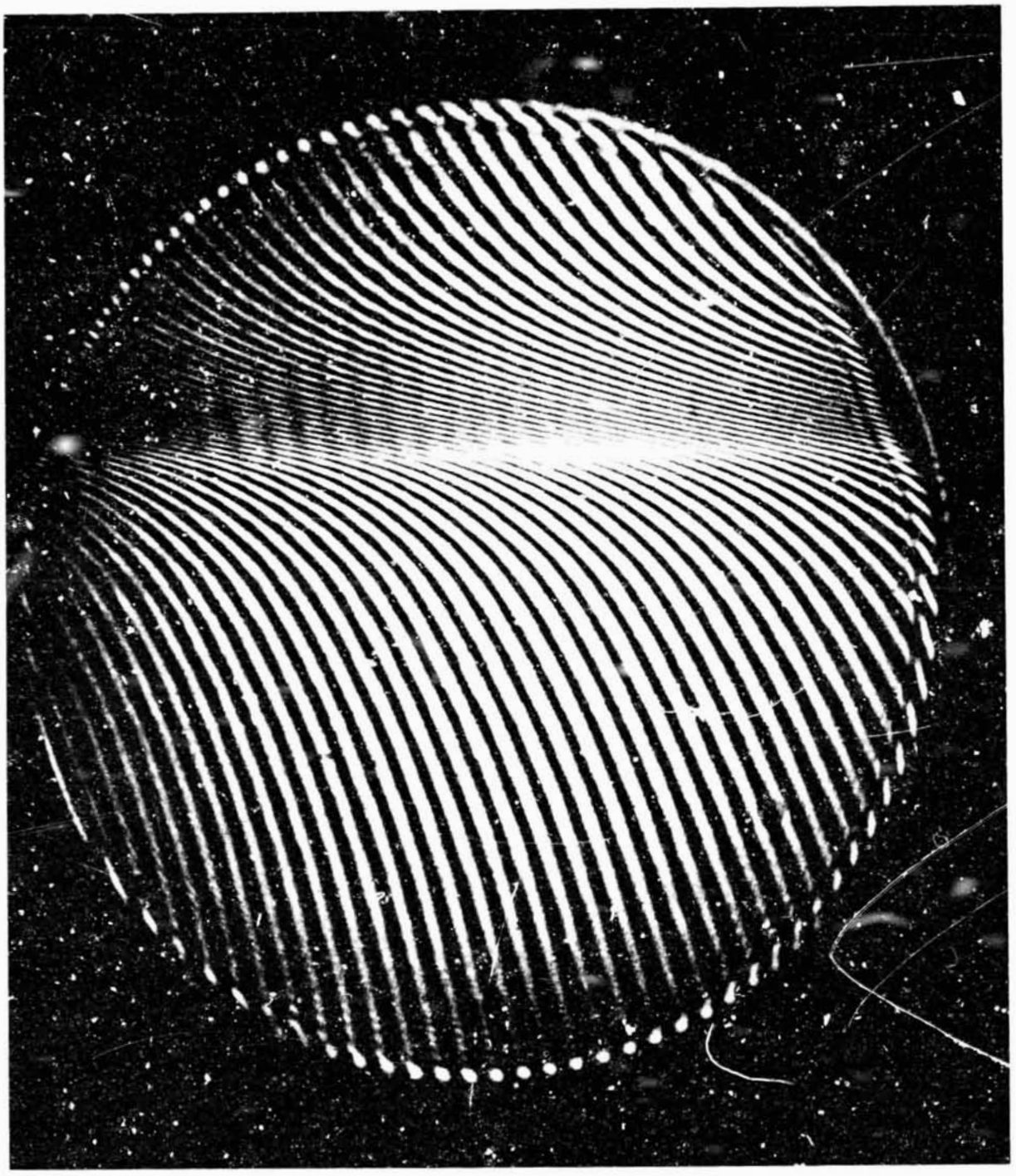

Figure 3. Interferometric pattern of SF_6 just above the critical point showing the fluid compressed by its own weight.

N92-23639

STUDY OF DENSITY DISTRIBUTION IN A NEAR-CRITICAL SIMPLE FLUID (19-IML-1)

Teun Michels
Van der Waals Laboratory
Amsterdam, The Netherlands

This 60 hour experiment uses visual observation, interferometry, and light scattering techniques to observe and analyze the density distribution in SF_6 above and below the critical tempertue. Below the critical temperature (T_c = 45.6 °C) the fluid system is split up into two coexisting phases, liquid and vapour. The spatial separation of these phases on earth - liquid below and vapour above - is not an intrinsic property of the fluid system; it is merely an effect of the action of the gravity field. At a fixed temperature the density of each of the coexisting phases is in principle fixed. However, near T_c, where the fluid is strongly compressible, gravity induced hydrostatic forces will result in a gradual decrease in density with increasing height in the sample container. This hydrostatic density profile is even more pronounced in the one-phase fluid at tempertures slightly above T_c.

The gravity-induced density distributions can be visualized and analyzed using an interference technique. This is shown in the three photographic recordings: density profiles are characterized by the horizontal shift of the essentially straight fringes; the density value can be calculated from the distance between these fringes.

It can hence be seen that the gravity induced gradient predominates the intrinsic density distribution of the critical sample. It will be understood that it also largely determines the rate at which, after a change in temperature, the near- critical system evolves towards its equilibrium density distribution.

The proposed experiment is set up to investigate the intrinsic density distributions and equilibration rates of a critical sample in a small container. Within this scope it will also be of interest to analyse in the absence of strong gravitational forces, the influence of the much weaker adhesive surface forces near the container walls as well as of those at the interface between coexisting phases. Interferometer patterns will be used to determine local density and thickness of surface and interface layers. The light scattering data will reveal the s of the density fluctuations on a microscopic scale, which play a fundamental role in the theoretical understanding of critical behaviour. The visual observation system is used to keep track of the sample behaviour, so as to optimize the timeline of the experiment during execution.

In the experiment timeline the sample is first to be homogenized at a temperature well above T_c. Next it will undergo a sequence of temperature steps covering a range of a few degrees around T_c. Since the critical properties of the system depend exponentially on $T-T_c$, the

temperature distance to T_c, the stepsizes range from above 1 °C at $T-T_c = 5$ °C to 1 millidegree very close to T_c; waiting times required to study the equilibration rate will, accordingly, vary from 20 min. well away from T_c to as much as six hours within millidegrees from this temperature. In order to observe "memory" effects three runs have to be executed: one cooling down from 3 °C above the critical temperature to about 1 °C below, one heating up over the same range and a third cooling down again.

N92-23640

CRITICAL FLUID THERMAL EQUILIBRATION EXPERIMENT (19-IML-1)

R. Allen Wilkinson
NASA Lewis Research Center
Cleveland, OH USA

Gravity sometimes obscures interesting physical phenomena or, in some cases, blocks all experimental techniques of making a desired measurement. It is the later case that drives low-gravity experiments in critical point fluid systems. The feverish activity in fluid critical phenomena of the 70's slowed to a near standstill in part due to gravitational limitation on acquiring further experimental data closer to the critical temperature. The availability of low-gravity on longer and longer duration space missions has brought back to life experimental effort. A recent international workshop sponsored by NASA and NIST concluded that unexpected behavior of near critical fluids in low-gravity brings to the fore equilibration dynamics as a frontier in critical phenomena research. How long does it take for a fluid sample to relax to equilibrium after a temperature step near the critical point?

Any pure fluid possesses a liquid-vapor critical point. It is uniquely defined by a temperature, pressure, and density state in thermodynamics. For states with either temperature, pressure, or density greater than the critical values; liquid and vapor are no longer distinguishable. At the critical point a fluid fluctuates spatially and temporally in small domains between liquid and vapor. The consequence is that the fluid is infinitely compressible.

Such compressibility is the root of the troubles caused by gravity. A constant volume sample loaded on average to the critical density can not maintain a large portion of the sample at the critical point because the weight of the fluid is enough to compress half of the sample to a density above the critical density, leaving the other half below the critical density. There then remains a thin portion between the two halves that is at the critical density. However, the closer to the critical temperature, the more compressible the fluid, and the thinner is the critical zone. At some temperature the zone is too small to use any known experimental probe to measure thermodynamic properties. Low- gravity reduces the weight of the fluid on itself and widens the critical zone for a given temperature. Or best of all allows one to go closer to the critical temperature before experimental probe dimension limits are reached.

The crucial issue that this experiment attempts to understand is the time it takes for a sample to reach temperature and density equilibrium as the critical point is approached; is it infinity due to mass and thermal diffusion, or do pressure waves speed up energy transport while mass is still under diffusion control? The time scales involved (tens of hours to days) necessitate long duration experiments in space.

The experiment being developed involves a small (0.078 cm^3) constant volume sample of sulfur-hexaflouride thermostated with milli-Kelvin control near its critical temperature of 45.54 °C and observed via interferometry, visualization, and light attenuation. One sample cell supports interferometry and another cell supports visualization. The two cells are integrated into a precision thermostat before launch. The thermostat is inserted into the experiment facility (Critical Point Facility) while on orbit at the initiation of the 60 hour experiment window. Video recording will occur for one or the other cells at all times. Such recording of long duration low gravity spatially and temporally varying compressible fluid dynamics has not been seen before. To respond to the unexpected, telescience will be exploited to the limits available on a Space Lab.

The science objectives are to observe: (1) large phase domain homogenization without and with stirring, (2) time evolution of heat and mass after a temperature step is applied to a one-phase equilibrium sample, (3) phase evolution and configuration upon going two-phase from a one-phase equilibrium state, (4) effects of stirring on a low-g two-phase configuration, (5) two-phase to one-phase healing dynamics starting from a two-phase low-g configuration, (6) effects of shuttle acceleration events on spatially and temporally varying compressibile critical fluid dynamics, and (7) quantifying the mass and thermal homogenization time constant of a one-phase system under logarithmic temperature steps.

Bibliography

M. R. Moldover, et al.: Gravity Effects in Fluids Near the Gas- Liquid Critical Point. Rev. Mod. Phys. vol. 51, no. 1, January 1979, pp. 79-99.

CRITICAL FLUID THERMAL EQUILIBRATION

The LeRC Critical Fluid Thermal Equilibration cell will fly on the Shuttle in the European Space Agency's Critical Point Facility. CFTE will examine the thermal relaxation and the fluid density profile as a function of time after a temperature perturbation of sulfur hexafluoride near its liquid-vapor critical point in the low-gravity environment of the Shuttle.

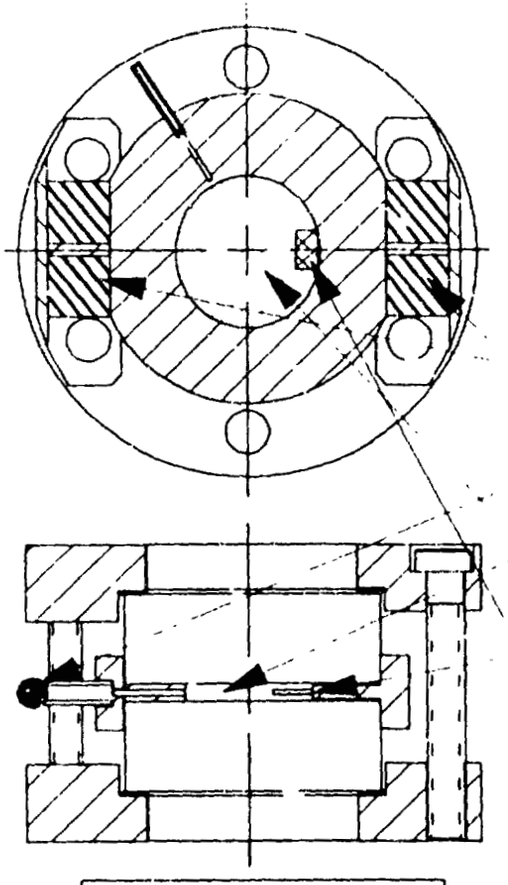

ELECTROMAGNETIC COILS TO ACTIVATE STIRRER

SEALED FILL TUBE

FLUID VOLUME
10mm DIAMETER X 1mm THICK

STIR BAR

THERMOSTAT CONTAINING LeRC CFTE CELL

VIDEO DISPLAY MONITOR

LeRC CFTE CELL

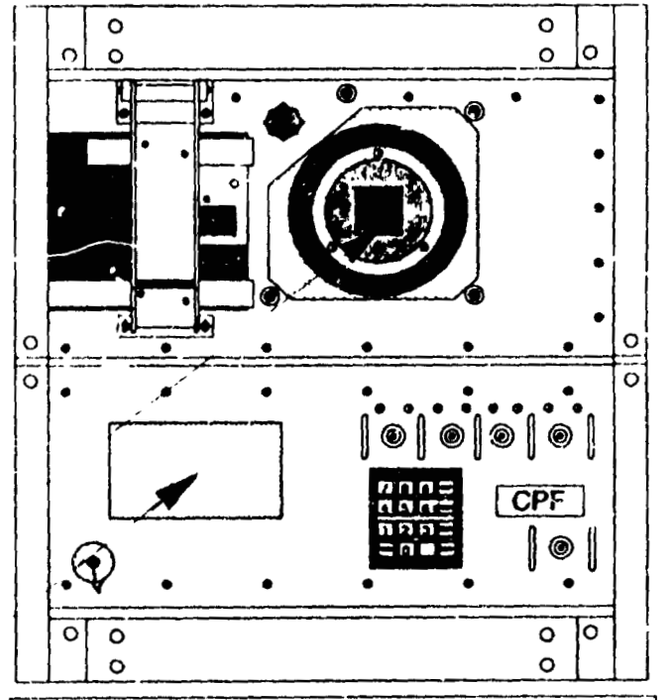

ESA CRITICAL POINT FACILITY

Figure 1. Critical fluid equilibration.

N92-23641

IMAX CAMERA
(12-IML-1)

IMAX Space Technology, Inc.
Houston, TX USA

The IMAX camera system is used to record on-orbit activities of interest to the public. Because of the extremely high resolution of the IMAX camera, projector, and audio systems, the audience is afforded a motion picture experience unlike any other. IMAX films have been said to be the next best thing to actually being there. For this reason, IMAX is the perfect medium to bring the space experience down to Earth.

IMAX and OMNIMAX motion picture systems were designed to create motion picture images of superior quality and audience impact. These "high-fidelity" images, accompanied by superior quality multi-channel sound, involve the viewers in the motion picture. A strong sense of reality is achieved by reducing or eliminating the various "clues" which normally remind the audience that they are watching a motion picture.

The IMAX system presents motion pictures on a screen which is flat or just slightly curved and rectangular (1.34 to 1 aspect ratio). The image occupies a 60 to 120 degree lateral field of view and a 40 to 80 degree vertical field of view.

The OMNIMAX system presents motion pictures on a dome screen, typically using about 80 percent of a hemisphere. In this type of theater, the image occupies a lateral field of view averaging 180 degrees and a vertical field of view averaging 125 degrees.

Features of the IMAX/OMNIMAX system and theater design include:

A screen-to-audience relationship that provides every viewer a virtually unobstructed, very wide field of view. The edges of the picture are not within the recognition field of view.

The bottom edge of the screen is placed so that audience can look down as well as up and to the sides. This allows the horizon to be in a natural position for most viewers.

IMAX/OMNIMAX is the largest motion picture format in the world (10 times larger than the usual 35 mm format). This large format records images with more "information" thereby producing a virtually grain-free, sharply defined image.

The specially designed IMAX/OMNIMAX rolling loop projector handles the large format film with outstanding image stability. Special attention to the illumination system and screen design results in excellent picture contrast and brightness.

The IMAX Sound System by SONICS is a six-channel high fidelity system that has been developed specifically for use in these theaters. The system includes six specially designed loudspeakers located behind the screen and around the audience, and a central sub-bass (or sub-woofer) loudspeaker array.

In order to provide the desired frequency response, dynamic range, and acoustic output capability, the system utilizes essentially a 5-way loudspeaker/amplification scheme. That is, the audible frequency spectrum is divided into five bands of approximately two octaves each. Each of these bands is then amplified separately, with a total amplifier output capability of approximately 14,000 watts.

Each of the six main loudspeaker channels reproduces approximately eight octaves, with the bottom two octaves of all channels reproduced by a single sub-bass loudspeaker array located at the center of the screen.

In IMAX, the sound is not recorded on the film as in conventional 35 mm optical or 70 mm magnetic, but on a separate sound reproducer synchronized with the projector. This separate sound reproducer has traditionally been a six-track. 35 mm sprocketed tape reproducer called a "Dubber".

THE IMAX CAMERA SYSTEM

The IMAX camera is a 65 mm, single lens, reflex viewing design with a 15 perforation per frame horizontal pull-across. The frame size is 2.06 by 2.77 inches film travels through the camera at a rate of 336 feet per minute (5.6 feet per second) when the camera is running at the standard 24 frames per second. The film magazines hold 1100 feet of Estar base 65 mm color negative film. This yields between 3 min. to 3 min. 15 sec of filming time per load.

Film used is Eastman Kodak color negative. 5245 (estar base) is used for exterior filming and 5296 (Estar base) is used for interior and low light level filming. In a normal four locker configuration, seven rolls of film are flown, two loaded in the magazines and five in metal film cans.

The camera has a rotating shutter with a 155° opening which yields an exposure time of about 1/60th of a second. The camera runs on a 30 V dc motor. The frame rate is variable from 6 to 36 frames per second. The electronically controlled motor maintains speed with ±0.3 fps. Two independent thermal circuit breakers protect the camera electronics.

A specially designed power panel supplies power to the camera. The panel includes filters for EMI/EMC, power switch, and a 20 amp magnetic circuit breaker. When installed on the Aft Flight Deck the panel receives its power from Cabin Payload

bus A or B. The camera draws between 300 and 400 watts of power under normal operating conditions.

The viewing system is a through-the-lens type using a beam splitter (a partial mirror) in the light path to reflect light into the viewfinder. The beam splitter reduces the amount of light reaching the film by two-thirds of a stop. This is taken into consideration when determining the ISO rating of the film used.

The viewfinder has diopter adjustment which can be varied to compensate for differences in individual eyesight. A magnifier is provided for critical adjustment of the diopter and lens focus. A manual light trap can be closed to prevent spurious light from entering the viewfinder which could cause unwanted exposure of the film. A silicone rubber eyecup provides a light seal between the cameraperson's eye and the viewfinder.

Camera controls include a fixed and variable frame rate adjustment system, electronic and mechanical footage counters, electronic and mechanical tachometers (frame rate indicators), pilot light, and on-off switch. Exterior controls are connected to the camera via special mil-spec electrical connectors. Switches in the camera film compartment prevent the camera from running when the lid is open, if there is not film present or if there is a film jam.

Depending on configuration, the camera weights between 85 and 95 pounds with a full load of film.

IMAX uses modified Zeiss medium format lenses. The lenses have IMAX heavy duty bayonet mounts and front element support cages to improve lens mount stiffness and eliminate image shake. Levers are provided on the focus rings to facilitate focusing. Custom ultraviolet filters are used on all lenses. Lens selection varies depending on flight requirements. The following lenses are available for flight use:

30 mm f:3.5 fisheye - 48.4° horizontal by 96° vertical field of view for IMAX and 148.4° horizontal by 74.2° vertically up and 31.5° vertically down for OMNIMAX. The 30 mm is the standard OMNIMAX lens.

40 mm f:4, this lens gives the truest representation of real life on the IMAX screen. Field of view is 82° horizontal by 62.5° vertical.

50 mm f:2.8 - 70° horizontal by 52° vertical field of view

60 mm f:3.5 - 80.2° horizontal by 44° vertical field of view.

100 mm f:3.5 - 38.4° horizontal by 27.3° vertical field of view.

110 mm f:2 - 35.1° horizontal by 24.9° vertical field of view.

250 mm f:6.6 - 15.8° horizontal by 11.1° vertical field of view.

The 30 mm, 50 mm, and 110 mm will be aboard IML-1.

Accessories for the IMAX camera include a gimballed mount, overhead window bracket, camera handle, audio cassette recorder, emergency speed control and photoflood light (cage light).

The gimballed mount is used for filming out the Orbiter aft flight deck windows. The mount is attached to the camera and then held in place in the windows via a Velcro interface. A small shroud (black cloth) is used with this mount to reduce the chance of reflections from the glass ruining the image. To maintain the proper lens to window clearances the gimballed bracket has two operating configurations. The short configuration is for use with the 30 mm lens. The long configuration is used for all other lenses. Inhibit rings on the lenses prevent lens mounting if the bracket is in the wrong configuration.

The gimballed mount is also used with the overhead window bracket for filming out the overhead windows. The gimballed mount is attached to the overhead bracket via a Velcro interface like that of the aft window.

There are two configurations for the overhead window bracket as well. The stowed position, the configuration in which the bracket is launched, and the extended position. The overhead window bracket is held in place by the window shade latches. There is also a shroud for use with the overhead window bracket. The shrouds are held in place by Velcro.

During in cabin filming the camera handle may be attached to facilitate movement of the camera. The handle consists of two hand grips (one on each side of the camera) and an electrical interface with a thumb switch on each hand grip. Electrical connection is made through the cameras remote interlock plug on the right side of the camera. Once the electrical connection has been made the camera switch must be turned on to arm the thumb switches.

An audio cassette stereo recorder is flown to record dialogue during in cabin filming, crew comments and camera technical information. Twelve, 60-minute cassettes are provided along with an extra set of batteries for the recorder. The recorder has two microphones for stereo recording.

An emergency speed control (ESC) is provided for use should the internal speed control electronics fail. The ESC is connected to the camera via the remote interlock plug. Use of the ESC precludes use of the handle as they attach to the same connector. The camera will not run as steadily as when the normal internal circuitry is functioning. Camera speed (frames per second) should be monitored during filming. Speed adjustments should be made while the camera is running if the camera speed varies more than ±2 frames per second.

Three, 150-watt photoflood lights are flown for in-cabin filming. The light level on the mid-deck or in the module is not sufficient for IMAX photography; therefore, supplemental light must be supplied. The photoflood runs off the Orbiter 400 hz 110 volt power system.

Other support items include a film changing bag, cleaning tool, lens tissue, spare film core, "Exposed Film" tape roll and spare black film sacks.

The film changing bag is used to load and unload the film magazines, as total darkness is required for this operation.

Certain areas in the camera movement require cleaning after each roll of film is shot. The cleaning tool is used to scrape away the film residue which builds up due to the high speed at which the film moves through the camera.

Lens tissue is used to clean the lenses and other optical elements of the camera should the need arise.

The spare film core is used if a roll of film breaks in the middle and cannot be recovered using normal malfunction procedures.

The "Exposed Film" tape is used to secure the film cans. This is to make it easier for the crew to differentiate between exposed and unexposed film.

The spare black film sacks are used with the spare film core if a film break cannot be recovered using normal malfunction procedures.

The following is a list of the IMAX-IML-1 flight package:

IMAX Camera
Three Lenses, 30 mm, 50 mm, 110 mm
(two lenses flight dependent)
Gimballed Mount
Overhead Window Bracket
Two Power Cables (20' ea.)
Power Cable Connector
Audio Recorder and Microphone
Film Changing Bag
Cleaning Tool
"EXPOSED FILM" Tape
Twelve Audio Cassettes
Spare Black Film Sacks
Three Film Magazines
Twelve Rolls of Film
Emergency Speed Control
Gimballed Shroud
Overhead Window Shroud
Three Photoflood Lights
Multi-Photo Flood Adapter Cable
Camera Handle
Spare Film Can
Lens Tissue
Spare Film Core
Spare Recorder Batteries
Camera Belt Guard

N92-23642

MICROGRAVITY ACCELERATION MEASUREMENT AND ENVIRONMENT CHARACTERIZATION SCIENCE (17-IML-1)

Science

The Space Acceleration Measurement System (SAMS) is a general purpose instrumentation system designed to measure the accelerations onboard the Shuttle Orbiter and Shuttle/Spacelab vehicles (see Figure 1). These measurements are used to support microgravity experiments and investigations into the microgravity environment of the vehicle. Acceleration measurements can be made at locations remote from the SAMS main instrumentation unit by the use of up to three remote triaxial sensor heads. The SAMS was developed by NASA's Lewis Research Center (LeRC) in support of NASA's microgravity science programs.

The prime objective for SAMS on the IML-1 mission will be to measure the accelerations experienced by the Fluid Experiment System (FES). The SAMS acceleration measurements for FES will be complemented by low-level, low-frequency acceleration measurements made by the Orbital Acceleration Research Experiment (OARE) installed on the shuttle. Secondary objectives for SAMS will be to measure accelerations at several specific locations to enable the acceleration transfer function of the Spacelab module to be analyzed. This analysis effort will be in conjunction with similar measurements analyses on other Spacelab missions.

In the past, numerous acceleration measurement systems have flown on various space missions. These systems were tailored to measure accelerations for a narrow set of requirements and were limited in bandwidth, dynamic range, and recording capability. In addition, these systems were mission peculiar and not easily modified for other applications. The result has been an inability to accurately assess the expected microgravity environment prior to a mission for a particular experiment and/or location.

SAMS configurations are under development for the Orbiter Middeck locker area, Spacelab SMIDEX rack and Spacelab center aisle and under development for the Orbiter cargo bay, enabling microgravity measurements at nearly any desired payload location.

SAMS units are currently manifested on the SLS-1, IML-1, SL-J, USML-1, USMP-1 and IML-2 missions. There will be eight flight units fabricated to support the expected flight rate of microgravity science missions (e.g., IML-3, USML-2, USMP-2).

Instrument

A SAMS unit consists of a main unit (shown in Figure 2 with one triaxial sensor head) and up to three remote triaxial sensor heads. The main unit is comprised of the crew interface, optical disk data storage devices, and control and processing electronics. The remote triaxial

sensor heads are comprised of three single axis acceleration sensors, preamplifiers and filters. Each head is connected to the main unit by an umbilical cable which has a maximum length of 20 feet.

The low-pass bandwidth for a triaxial sensor head is independent of the bandwidth of the other two heads and is chosen to match the requirements of the supported experiment. Standard choices for the low-pass bandwidth of a head are 0 to 2.5, 5, 10, 25, 50, and 100 Hz.

The standard SAMS triaxial sensor head employs the Sundstrant QA-2000 sensors, having a resolution of 1 μg. Two triaxial sensor heads utilizing Bell XI-79 sensors are also available having a resolution of 0.01 μg. The SAMS uses simultaneous sample and hold circuits to maintain phase coherence in the three axis measurements of a given triaxial sensor head. Similarly, the outputs of the three sensors of a given triaxial sensor head are digitized by the same 16 bit analog to digital converter. The signal processing for each triaxial sensor head has filtering characteristics matched to the data sampling rate for that triaxial sensor head. The preamplifier has four decade gain ranges and the capability for an electronic calibration mode.

The triaxial sensor head digitized data is formatted and transferred to optical disk. The optical disk drive enables crew-tended disk changes which allow nearly unlimited data storage during a mission. With 200 megabytes of storage per optical disk side, typical times between disk change operations are from hours to days, depending on the triaxial sensor head sampling rates.

To support the FES on IML-1, one SAMS head will be mounted on the FES optical bench in rack #10. This triaxial sensor head will utilize Sundstrang model QA1000 sensors and will be set for 100 hertz and 500 samples per second. This will result in measuring the acceleration environment experienced by the equipment mounted on the FES optical bench.

To measure the low-frequency accelerations experienced by the FES, the second head will be mounted toward the bottom of rack #10 and will be set for 2.5 hertz and 12.5 samples per second. This triaxial sensor head will utilize more sensitive Bell model XI-79 sensors and will be set for 2.5 hertz and 12.5 samples per second. Acceleration data (below 1 hertz) from the OARE will also be utilized to complement these low-frequency SAMS measurements. The OARE utilizes a MESA type of sensor which is particularly good (although expensive) for low-frequency, low magnitude measurements.

The third SAMS head will be mounted below the Spacelab module floor beneath the Microgravity Vestibular Investigations (MVI) rotating chair. This triaxial sensor head will utilize Sundstrand model QA2000 sensors and will be set for 100 hertz and 500 samples per second. This will characterize the MVI rotating chair as an acceleration source and will, in conjunction with the other two heads, allow characterization of the Spacelab module acceleration transfer function to be studied.

Data Processing and Analysis

Post mission processing of data by the SAMS project will be limited to data extraction, compensation, identification, format conversion, archival and dissemination. The processed data will be provided to the principal investigators involved with the particular mission and other interested organizations as required.

In conjunction with the SAMS project, researchers at The University of Alabama at Huntsville and The Charles Stark Draper Laboratories have initiated work to characterize the microgravity environment using the data obtained from the Spacelab-3 mission and the IML-1 mission.

The archival of SAMS data, combined with acceleration data from other sources (e.g., OARE, experiment accelerometers) will make possible the assessment of the microgravity environment of the Shuttle and Spacelab vehicles. This is an important step towards accommodating science experiments on these vehicles.

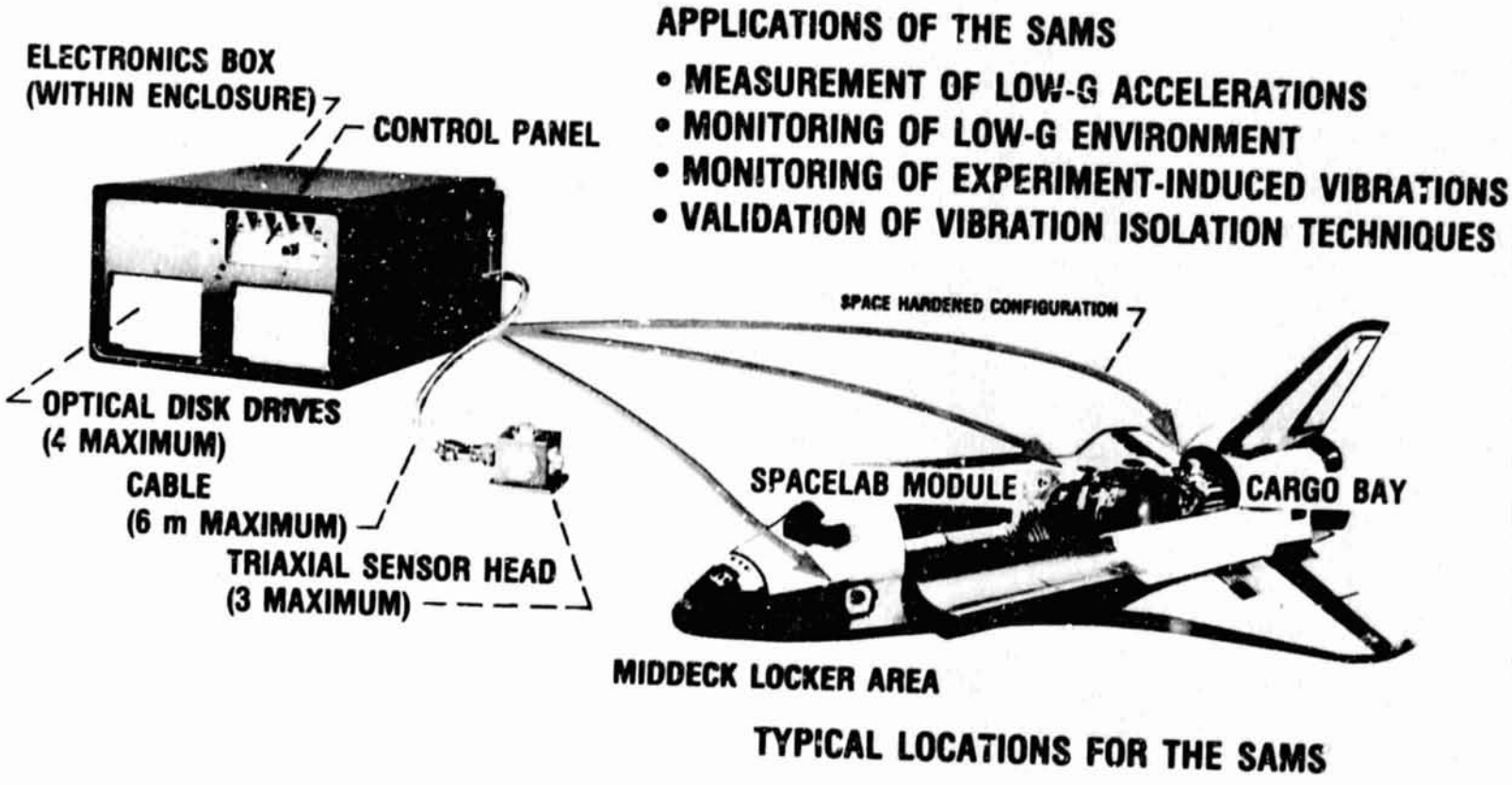

Figure 1. Space acceleration measurement system (SAMS).

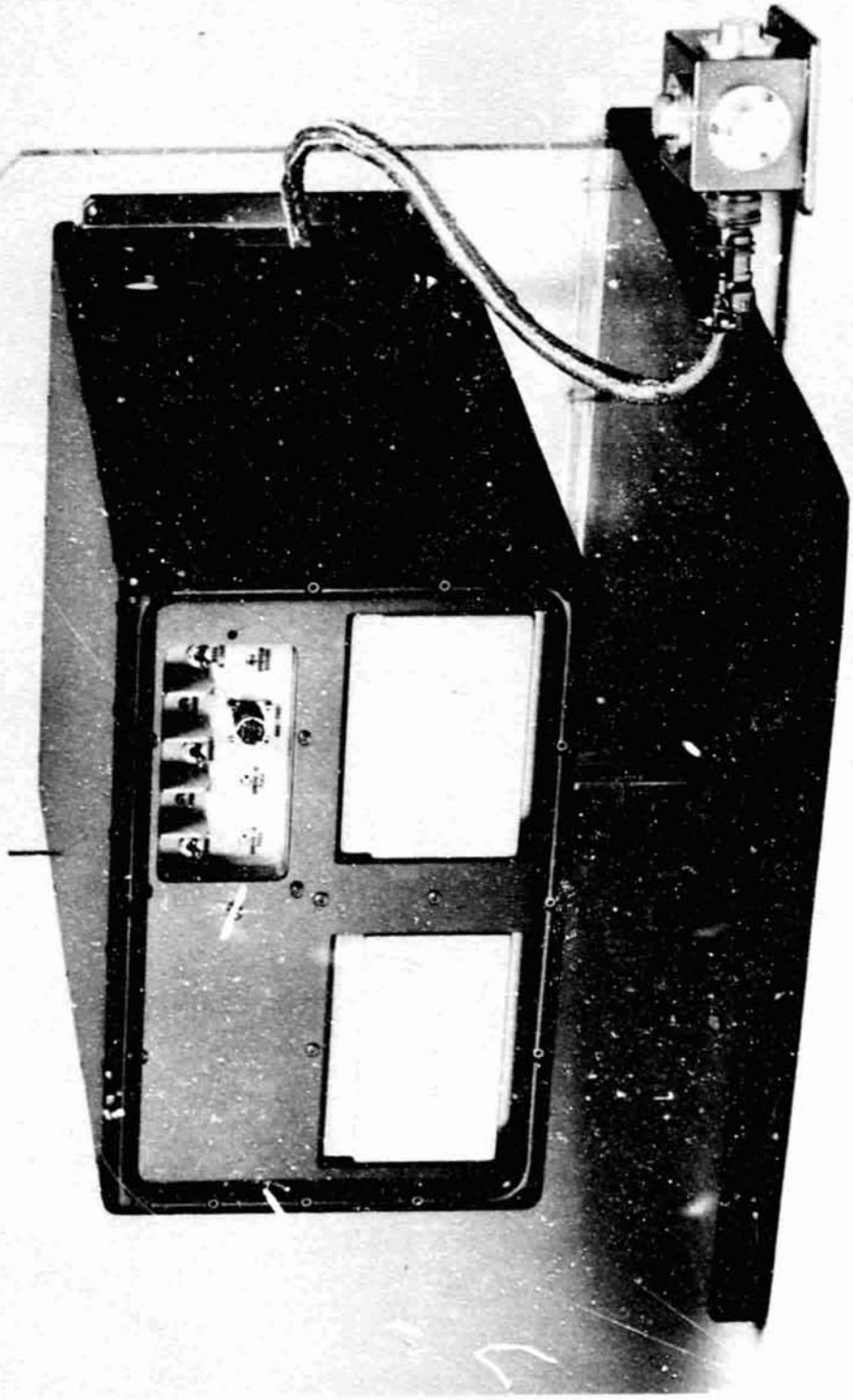

Figure 2. SAMS main unit with one triaxial sensor head.

APPENDIX

INTERNATIONAL MICROGRAVITY LABORATORY 1 CO-INVESTIGATORS AND GUEST INVESTIGATORS

Life Sciences

Gravitropic Responses of Plants in the Absence of a Complicating G-Force (6-IML-1)

A. Johnson
University of Trondheim
Norway

D. Heathcote
D. Chapman
Gravitational Plant Physiology Laboratory
USA

A Spaceflight Experiment to Investigate the Effects of a Range of Unilateral Blue Light Stimulations on the Movements of Wheat Coleoptiles (6-IML-1)

A. Brown
D. Chapman
Gravitational Plant Physiology Laboratory
USA

Genetic and Molecular Dosimetry of HZE Radiation (7-IML-1

E. Benton
University of San Francisco
USA

Chrondogenesis in Micromass Cultures of Embryonic Mouse Limb Mesenchymal Cells Exposed to Microgravity (7-IML-1)

T. Hewitt
The Johns Hopkins Unviersity and Hospitals
USA

Microgravitational Effects on Chromosome Behavior (7-IML-1)

J. Colasanti
East Carolina University School of Medicine
USA

Effects of Microgravity and Mechanical Stimulation on the In Vitro Mineralization and Resorption of Fetal Mouse Lone Bones (7-IML-1)

E. Burger
G. Kampen
ACTA Gree University de Boelelaan
The Netherlands

The Role of Gravity in the Establishment of the Dorsoventral Axis in the Amphibian Embryo (7-IML-1)

Effect of the Space Environment on the Development of Drosophila Melanogaster (7-IML-1)

T. Golzalez-Jurado
M. Maroto
UAM Institute of Biomedical Investigations
Spain

The Effect of Microgravity Environment on Cell Wall Generation, Cell Division, Growth and Differentiation of Plants From Protoplasts (7-IML-1)

T. Iverson
University of Trondheim
Norway

R. Wyndael
J. Christiansen
Institute of Molecular Biology and Plant Physiology
Denmark

Embryogenesis and Organogenesis of Carausius Morosus Under Spaceflight Conditions (7-IML-1)

R. Facius
G. Rei
Institute of Aerospace Medicine, DLR
Federal Republic of Germany

R. Beaujean
W. Enge
University of Kiel
Federal Republic of Germany

W. Heinrids
GH University of Siejen Adolf Reichwein
Federal Republic of Germany

E. Graul
W. Ructher
Univers. y of Marbury
Federal Republic of Germany

Dosimetric Mapping Inside Biorack (7-IML-1)

H. Buecker
R. Facius
M. Schaefer
DLR
Federal Republic of Germany

R. Beaujean
W. Enge
Universitat Kiel
Federal Republic of Germany

W. Heinrick
Universitat of Siegen
Federal Republic of Germany

Growth and Sporulation in Bacillus Subtilis Under Microgravity (7-IML-1)

M. Lange
B. Ernst
University of Frankfurt
Federal Republic of Germany

Friend Leukemia Virus Transformed Cells Exposed to Microgravity in the Presence of DMSO (7-IML-1)

O. Meuller
University of Berne
Switzerland

P. Bechler
M. Cogoli
Institut for Biotechnologie
Switzerland

Proliferation and Performance of Hybridoma Cells in Microgravity (7-IML-1)

P. Bechler
M. Cogoli
Institut for Biotechnologie
Switzerland

Dynamic Cell Culture (7-IML-1)

C. Nordau
University of Paris
France

F. Gmuender
Institut for Biotechnologie
Switzerland

The Genotypic Control of Graviresponse, Cell Polarity and Morphological Development of Arabidopsis Thaliana in a Microgravity Environment (7-IML-1)

Transmission of Gravistimulus in the Statocyte of the Lentil Root (7-IML-1)

D. Driss-Ecole
G. Salle
Pierre and Marie Curie University
France

K. Waldon
University of Glasglow
United Kingdom

Gravity Related Behavior of the Acellular Slime Mold Physarum Polycephalum (7-IML-1)

W. Briegleb
DLR
Federal Republic of Germany

K. Wohlfarth-Bottermann
University of Bonn
Federal Republic of Germany

Studies of Penetration of Antiobiotics in Bacterial Cells in Space Conditions (7-IML-1)

N. Moatti
L. Lapchine
G. Richoilley
J. Templier
J. Bes
G. Gasset
G. Farre
R. Eche
National Institute of Health and Medical Research
France

Energy Expenditure in Space Flight (8-IML-1)

M. Preshaw
H. Krouse
University of Calgary
Canada

J. Thirsk
Foothills Hospital, Calgary
Canada

Back Pain in Astronauts (8-IML-1)

R. Gagnon
L. Susak
F. Gagnon
I. Tsang
University of British Columbia
University Hospital (Shaughnessy Site)
Canada

Measurement of Change in Venous Compliance in Microgravity and Evaluation of an Experimental Antigravity Suit (8-IML-1)

L. Goodman
M Pecaric
K. Ackles
Defence and Civil Institute of Environmental Medicine
Canada

J. Bennett
J. Charles
Lyndon B. Johnson Space Center
USA

R. Aaslid
University of Berne, Inselspital
Switzerland

M. Kassam
P. Dunphy
Ryerson Polytechnical Institute
Canada

D. Leiski
P. Sullivan
R. Bondar
Canadian Space Agency
Canada

Space Adaptation Syndrome Experiments (8-IML-1)

G. Melville Jones
McGill University
Canada

J. Lackner
Brandeis University
USA

J. Landolt
Defense and Civil Institute of Environmental Medicine
Canada

M. Reschke
Lyndon B. Johnson Space Center
USA

L. Young
Massachusetts Institute of Technology
USA

A. Bensen
RAF Institute of Aviation Medicine
United Kingdom

F. Guedry
Naval Aerospace Medical Research Laboratory
USA

R. Jell
University of Manitoba
Canada

D. Parker
Miami University
USA

Phase Partitioning Experiment (8-IML-1)

J. Van Alstine
J. Harris
University of Alabama in Huntsville
USA

J. Boyce
University of British Columbia
Canada

Microgravity Vestibular Experiments (10-IML-1)

D. Anderson
University of Michigan
USA

A. Berthoz
CNRS
France

O. Black
Good Samaritan Hospital
USA

G. Clement
CNRS
France

B. Cohen
Mount Sinai Medical Center
USA

F. Guedry
Naval Aerospace Medical Research Laboratory
USA

J. Homick
Lyndon B. Johnson Space Center
USA

M. Igarashi
Baylor College of Medicine
USA

P. Dizio
R. Lackner
Brandeis University
USA

C. Oman
Massachusetts Institute of Technology
USA

D. Parker
Miami University of Ohio
USA

J. Vanderploeg
S. Wood
W. Poloski
KRUG International
USA

A. Benson
RAF Institute of Aviation Medicine
United Kingdom

R. Jell
University of Manitoba
Canada

D. Watt
McGill University
Canada

T. Raphan
O. Garriott
Teledyne Brown Engineering
USA

Biostack (14-IML-1)

R. Beaujean
W. Enge
Universitat Kiel
Federal Republic of Germany

E. Benton
University of San Francisco
USA

A. Kranz
U. Bork
Universitat Frankfurt
Federal Republic of Germany

R. Facius
G. Horneck
G. Reitz
M. Schaefer
J. Schott
DLR
Federal Republic of Germany

W. Ruether
O. Graul
Universitat Marburg
Federal Republic of Germany

W. Heinrich
Universitat Marburg
Federal Republic of Germany

J. Keifer
Strahlenzentrum
Federal Republic of Germany

A. Tallentire
University of Manchester
United Kingdom

S. Takaski
Japan Atomic Energy Research Institute
Japan

F. Masami
Institute of Space and Aeronautic Sciences
Japan

I. Ken-Ichic
University of Tokyo
Japan

T. Hirsohi
National Cancer Research Center
Japan

Mental Workload and Performance Evaluation (15-IML-1)

B. Lichtenberg
Payload Systems, Inc.
USA

Radiation Monitoring Container/Dosimeter (16-IML-1)

T. Doke
Waseda University
Japan

T. Takahashi
Institute for Physical and Chemical Research
Japan

T. Iwasaki
Science and Technology Agency
Japan

K. Ogura
Nihon University
Japan

Y Ishikawa
Tokyo University of Fisheries
Japan

M. Tkenaga
Institute of Radiation Biology
Japan

H. Watanabe
Japan Atomic Energy Research Institute
Japan

Microgravity Sciences

Study of Solution Crystal Growth in Low Gravity (2-IML-1)

W. Wilcox
Clarkson University
USA

J. Trolinger
Metrolaser
USA

A. Batra
Alabama A & M University
USA

Studying the Influence of Gravity on Fluid Flow and Nucleation During Casting Through Directional Solidification of a Transparent Metal Model Under Microgravity Conditions (2-IML-1)

L. Smith
T. McCay
S. Lowry
J. Hopkins
M. Vesko
University of Tennessee
USA

R. Porter
George C. Marshall Space Flight Center
USA

Vapor Crystal Growth Studies of Single Mercuric Iodide Crystals (3-IML-1)

C. Baccash
L. Frank
EG & G/EM, Inc.
USA

Mercury Iodide Nucleation and Crystal Growth in Vapor Phase (4-IML 1)

G. Le Lay
CNR
Marseille, France

L. Van den Berg
EG & G/EM, Inc.
USA

Protein Crystal Growth (5-IML-1)

Y. Babu
BioCryst Limited
USA

R. Naumann
E. Meehan
J. Baird
University of Alabama in Huntsville
USA

G. Birnbaum
National Research Council of Canada
Canada

C. Carter, Jr.
University of North Carolina
USA

D. Carter
R. Snyder
George C. Marshall Space Flight Center
USA

W. Rosenblum
L. DeLucas
S. Ealick
V. Senadhi
W. Cook
The University of Alabama at Birmingham
USA

E. Czerwinski
University of Texas Medical Branch
USA

D. Duchamp
H. Einspahr
B. Finzel
K. Watenpaugh
The Upjohn Company
USA

D. Eggleston
Smith Kline & French
USA

J. Camps
Laboratoire de Cristallographie et Cristallisation de
Macromoles Biologiques
France

N. Jones
Eli Lilly & Company
USA

T. Krenitsky
Burroughs-Wellcome Company
USA

W. Laver
The Australian Nation University
Australia

D. Voet
P. Lu
University of Fennsylvania
USA

A. McPherson
University of California at Riverside
USA

E. Meyer
Texas A & M University
USA

P. Trotta
T. Nagabhushan
Schering Corporation
USA

M. Navia
Merck, Sharpe & Dohme Research Labs
USA

W. Riley
The Dow-Elanco, Central Research, Biotechnology Labs
USA

M. Ross
Genentech, Inc.
USA

B. Rubin
Eastman Kodak Company
USA

F. Salemme
P. Weber
DuPont de Nemours and Company
USA

R. Sweet
B. Schoenborn
Brookhaven National Laboratory
USA

L. Sieker
University of Washington
USA

P. Sigler
Yale University
USA

F. Suddath
Georgia Institute of Technology
USA

K. Ward
Naval Research Laboratory
USA

A. Yonath
The Weizmann Institute of Science
Israel

Organic Crystal Growth with G-Jitter Preventative Measures (13-IML-1)

H. Anzai
M. Tokumoto
M. Keizo
K. Nobumori
Electrotechnical Laboratory
Japan

S. Yoda
National Space Development Agency of Japan
Japan

H. Kazumasa
Institute of Chemistry, NITI
Japan

I. Kurihide
Kyoto University
Japan

Cryostat (18-IML-1)

Critical Point Facility (18-IML-1)

P. Guenoun
F. Perrot
Service de Physique de l'Etat Condensé
CE Saclay
France

Y. Garrabos
B. Le Neindre
CNRS
France

R. Berg
M. Moldover
NIST
USA

R. Gammon
University of Maryland
USA

J. Straub
Tech. University Muenechan
Germany

H. van den Berg
C. Prins
B. van Deenen
H. Sa Konidou
T. van Lieshont
University of Amsterdam
The Netherlands

IMAX (12-IML-1)

Space Acceleration Measurement System (17-IML-1)

*U.S. GOVERNMENT PRINTING OFFICE: 1992 - 627-064/60023

REPORT DOCUMENTATION PAGE

Form Approved
OMB No 0704-0188

1. AGENCY USE ONLY (Leave blank)	2. REPORT DATE	3. REPORT TYPE AND DATES COVERED
	February 1992	Technical Memorandum

4. TITLE AND SUBTITLE
First International Microgravity Laboratory
Experiment Descriptions - First Edition

5. FUNDING NUMBERS

6. AUTHOR(S)
Teresa Y. Miller, Editor

7. PERFORMING ORGANIZATION NAME(S) AND ADDRESS(ES)
George C. Marshall Space Flight Center
Marshall Space Flight Center, AL 35812

8. PERFORMING ORGANIZATION REPORT NUMBER
M-681

9. SPONSORING/MONITORING AGENCY NAME(S) AND ADDRESS(ES)
National Aeronautics and Space Administration
Washington, D.C. 20546

10. SPONSORING/MONITORING AGENCY REPORT NUMBER
NASA TM-4353

11. SUPPLEMENTARY NOTES
Prepared by Space Science Laboratory

12a. DISTRIBUTION/AVAILABILITY STATEMENT
Unclassified--Unlimited
Subject Category: 29

12b. DISTRIBUTION CODE

13. ABSTRACT (Maximum 200 words)

This document contains brief descriptions of the experiments for the First International Microgravity Laboratory (IML-1) which is scheduled for launch from the Kennedy Space Center aboard the Orbiter Discovery in early 1992.

14. SUBJECT TERMS
Spacelab Missions, Life Sciences, Microgravity Science

15. NUMBER OF PAGES
312

16. PRICE CODE
A14

17. SECURITY CLASSIFICATION OF REPORT	18. SECURITY CLASSIFICATION OF THIS PAGE	19. SECURITY CLASSIFICATION OF ABSTRACT	20. LIMITATION OF ABSTRACT
Unclassified	Unclassified	Unclassified	Unlimited

NSN 7540-01-280-5500

Standard Form 298 (Rev 2-89)
Prescribed by ANSI Std 239-18
298-102